A SEISMIC REFRACTION STUDY OF THE CRUSTAL STRUCTURE OF NORTH WEST SCOTLAND AND ADJACENT CONTINENTAL MARGIN

by

A.R. Armour

A thesis submitted for the degree of
Doctor of Philosophy at the University of Durham

Graduate Society September, 1977

ABSTRACT

In the summer of 1975, the Department of Geological Sciences, University of Durham, carried out a long range refraction project using explosions fired in Rockall Trough and the Hebridean Shelf areas. Temporary recording stations were situated in the North-west Highlands and Islands of Scotland. The data was supplemented by recordings from the permanent networks of Scotland. Plus-minus, time-term, velocity filtering and particle motion processing methods were applied to the data. Wherever possible, results from gravity and magnetic studies and seismic reflection profiles were used to compliment the interpretations.

On the Hebridean Shelf, small sedimentary basins and lateral variations of basement velocity are shown which correlate with earlier gravity and magnetic interpretations. Low average crustal velocities on the shelf, west of the Hebrides, give crustal thicknesses of about 25 km but east of the Hebrides higher average crustal velocities give estimates of about 30 km. A mid-crustal refractor is not clearly observed but may be at a depth of about 18 km on the outer shelf. The Minch area shows large P_n time-terms but this does not necessarily signify thickened crust since they may be attributed to velocity anomalies within the crust.

Continental crustal thinning and transition to oceanic crust at the Rockall Trough margin takes place over a narrow zone of about 50 km width. Crustal thicknesses in Rockall Trough, at 58^{o} N, are between 7 and 12 km and further north, near Rosemary Bank, are between 12 and 24 km.

CONTENTS

LIST OF FIGURES

LIST OF TABLES

ACKNOWLEDGEMENTS

First of all I would like to thank Professor M.H.P. Bott for his help and guidance and provision of departmental facilities. Dr. R.E. Long, Mr. S. Armstrong and Mr. L. Arnold introduced me to the intricacies of seismic processing and they must be thanked for their patience and interest.

Thanks are due to the officers and crew of RRS Challenger and MV Charterer, to Mr. G. Wylie and Dr. G. Westbrook as senior scientists and to Commander C.C. Moore who fired the shots. The field recording work was a major collective effort by many staff, postgraduate and undergraduate students and technicians of Durham University. Without their care and cooperation this thesis would not have been possible.

I would like to thank Dr. C. Browitt, Mr. K. Chappell, Dr. B. Jacob, Dr. R.E. Long and Professor T. Murphy and the NERC for the provision of recording equipment and data. Discussion with many fellow students helped me maintain an even keel throughout this work.

Special thanks are due to Janine whose intelligent typing, reference checking (!) and general enthusiasm and encouragement did much to smooth the progress of this work.

The work for this thesis was carried out while I was in receipt of a Shell award and their financial support is gratefully acknowledged.

CHAPTER 1

INTRODUCTION

1.1 The region of study

In the summer of 1975 the Department of Geological Sciences, University of Durham carried out a long range seismic refraction project across the Scottish Mainland and the adjacent continental shelf west of the Hebrides into Rockall Trough. This will be referred to as the Hebridean Margin Seismic Project (HMSP). Rockall Trough is an area of deep water, with uncertain crustal type, separating the Rockall Plateau microcontinent from the main European continent. The origin of the Trough is linked with the processes of sea-floor spreading which probably began in early Mesozoic times and have split apart North America, Greenland, Europe and Africa. Part of the aim of the present work is to amplify and confirm some of the ideas concerning the development of Rockall Trough and its eastern margin by determining the crustal structure in the area. In addition, the crustal structure of the Caledonian fold belt and foreland region were investigated.

Figure 1.1 shows the main physiographic features of the area and illustrates how the region of the present study fits into the wider context of the north-east Atlantic. Continental areas are separated by areas of known oceanic crust in the Norwegian Sea, Labrador Sea, Reykjanes Basin, Bay of Biscay and the West European Basin of the North Atlantic. Rockall Plateau and the Faeroes Plateau are shallow water regions of

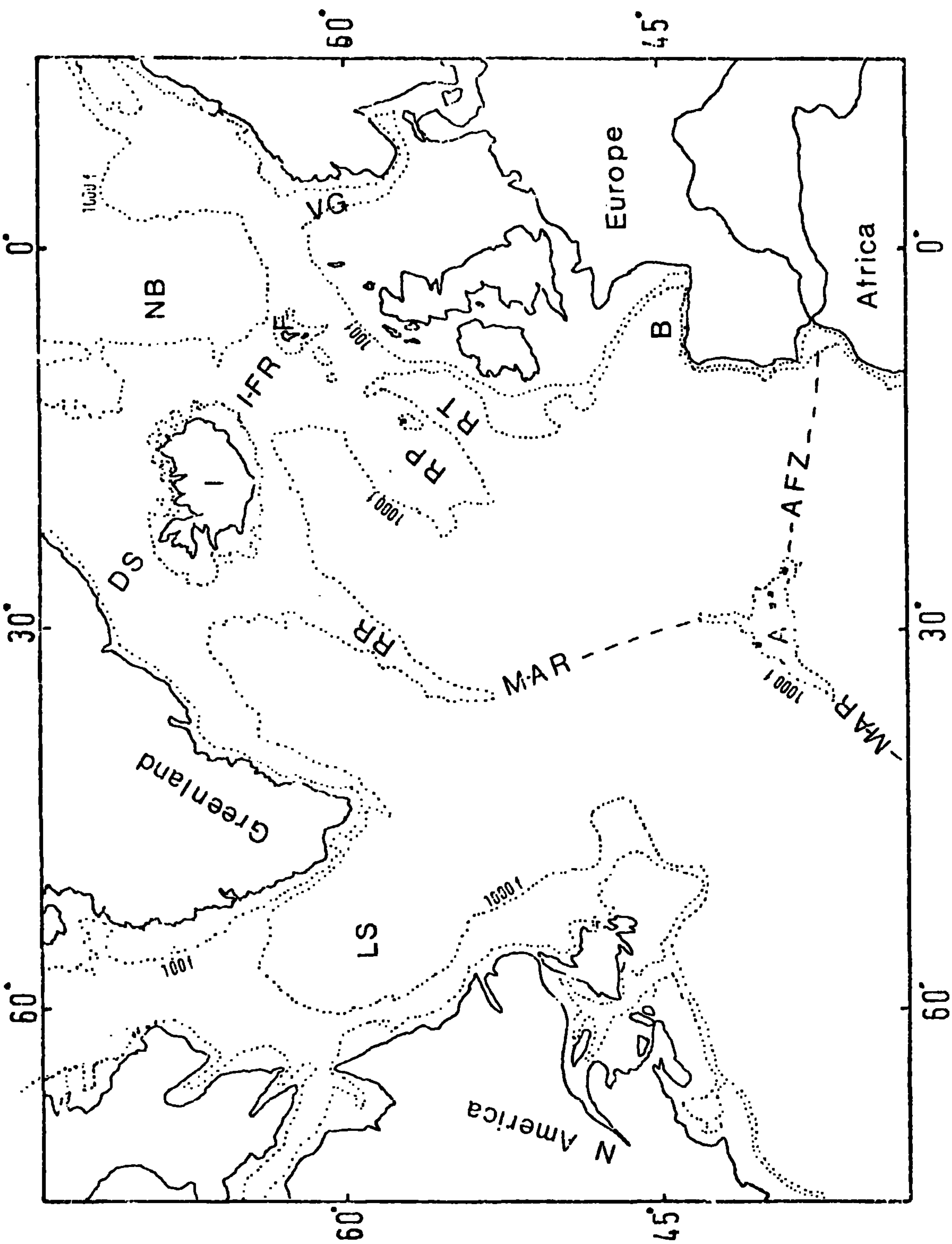

Figure 1.1 Summary map of main structural features of north Atlantic. NB - Norwegian Basin, DS - Denmark Strait, I - Iceland, I-FR - Iceland-Faeroe Ridge, F - Faeroes, VG - Viking Graben, RP - Rockall Plateau, RT - Rockall Trough, RR - Reykjanes Ridge, LS - Labrador Sea, M-AR - Mid-Atlantic Ridge, B- Biscay, A - Azores, AFZ - Azores Fracture Zone.

fairly typical continental crustal thicknesses (Scrutton and Roberts, 1971; Scrutton, 1972; Bott et al., 1974; Casten and Nielsen, 1975). Rockall Trough, and its probable northward extension, the Faeroes-Shetland Channel, are generally postulated as being formed by sea-floor spreading in late Jurassic and early Cretaceous times (Roberts, 1975a and b). Talwani and Eldholm (1972) suggested that the Faeroes-Shetland Channel is a deeply subsided continental area formed in the Tertiary.

The geology of the Scottish Mainland and the surrounding islands, including the shallow shelf areas, can be divided into two regions of separate and distinct structure. To the east of the Moine thrust belt lies a complex series of folded, metamorphosed and intruded Precambrian and Palaeozoic rocks which were caught up in the Caledonian orogeny. The Precambrian and Palaeozoic rocks to the west of the thrust formed a stable foreland region during Caledonian times and retain evidence of much earlier tectonic events. The Moine thrust can be traced across the shelf to the west of the Shetland Isles (Watts, 1971) and forms the boundary between the Caledonian mobile and foreland belts.

Since the end of the Caledonian orogeny the whole area has acted as a single tectonic unit with Mesozoic basin and graben formation in response to a broad tensional regime which was probably ultimately responsible for the opening of the Atlantic.

The refraction survey took the form of a long traverse across both the Caledonian mobile belt in the east and the stable foreland region to the west, continuing into Rockall

Trough. Shots fired in Rockall Trough were especially large to ensure that adequate energy traversed the continental margin to be recorded at the land stations. The land stations were distributed about the Scottish Mainland and Islands to extend the profile to the east and provide a strong network of observations.

1.2 The geology of the land and adjacent shelf areas

1.2.1 The Caledonian foreland

The Lewisian rocks of north-west Scotland are among the oldest rocks exposed on the north-east Atlantic seaboard. They form a much studied polycyclic gneiss complex, which is, in parts, correlateable with similar complexes in Greenland and North America. At least two major phases of high temperature and pressure metamorphism, separated by several phases of uplift erosion and dyke injection, are recognised (Sutton and Watson, 1951; Bowes, 1968; Park, 1970). The two units are known as the Scourian and Laxfordian complexes and are separated in time by about 1,000 My with the earliest metamorphism dated at about 2,600 My ago (Scourian). Rocks preserving Scourian structures outcrop in a central area of the west coast of Scotland from the Ben Stack line in the north to Gruinard Bay in the south. Laxfordian rocks outcrop to the north and south. The Scourian gneisses are often in granulite facies whereas the Laxfordian rocks are dominantly amphibolitic gneisses with some retrogressed granulites. In the Outer Hebrides, gneisses showing Laxfordian amphibolitic metamorphism are exposed but some relict Scourian rocks are present, particularly on the east coast of the Islands above the Outer Isles thrust. The Outer Isles thrust is an overthrust to the west and forms an extensive zone of intense deformation traceable along the east coasts of the Outer Hebrides. It is clearly older than the Stornoway beds (Permo-Triassic and probably Caledonian in age.

The two complexes present in the Lewisian have slightly different geophysical properties with the Scourian granulites being slightly denser and of higher velocity than the Laxfordian amphibolites (Bott et al., 1972; Smith and Bott, 1975; Hall and Al-Haddad, 1976). The relationship of the Laxfordian to the Scourian is still subject to debate but geochemical evidence suggests that the Laxfordian assemblage represents a set of supra-crustal metasediments derived from the Scourian (Holland and Lambert, 1973). Smith and Bott (1975) postulated that the two layer division of the crust observed in many continental seismic profiles is caused by a change in facies from amphibolites to granulites and that the Scourian granulites of Scotland represent lower crustal rocks.

A later metamorphic event in the Precambrian, recognised in Canada as the Grenvillian phase, is not shown in onshore Britain, although it has been recognised in rocks dredged from Rockall Plateau (Miller, Matthews and Roberts, 1973).*

Resting upon the Lewisian, with considerable landscape unconformity, are Torridonian rocks of mostly continental red bed facies. The Torridonian is now recognised to be made up of two groups of widely differing ages and palaeolatitude but of very similar facies (Irving and Runcorn, 1957; Stewart, 1966; Moorbath, 1969; Stewart and Irving, 1974). The two kilometre thick Stoer group, consisting of red

* but see later work, e.g. Brook, Brewer and Powell, 1976 Nature, 260, 515-517.

conglomerates, sandstones, shales and a few limestones, were recognised by Stewart (1966) to be an earlier formation than the main Torridonian. The Stoer group is dated as 935 My old whilst the Torridonian is 750 My old (Moorbath, 1969). A 50^{o} difference in palaeolatitude between the Stoer group and the Torridonian suggests the possibility of continental drift at the time. The Torridonian rocks are red, arkosic sandstones and conglomerates, with some shales, mostly derived from sources to the west. The environment of deposition was dominantly fluviatile with cross-beds, channel fills and overbank floodplain deposits. Some shallow lake deposits may be represented by the Diabeg shales. In places, the total thickness of the Torridonian attains about 20 km and it buries a Lewisian landscape of appreciable relief.

Resting with a planar unconformity upon the earlier formations lie Cambro-Ordovician sediments of shallow shelf-sea facies. Limestones and clean quartzitic sandstones contain fossils typical of the North American faunal province which was established at the time. Cambrian rocks of England and Wales exhibit Baltic type fauna thus indicating the existence of a faunal barrier in Cambrian times.

1.2.2 The Caledonian mobile belt

To the south-east of the Moine thrust belt lies a complex series of schists known as the Moinian and Dalradian schists, which were deformed, metamorphosed and intruded during the Caledonian orogeny(s). It is possible that the Moines were a series of sediments deposited in a seaway to the east of, and contemporaneously with, the Stoer group Torridonian rocks. In places, Lewisian rocks can be recognised beneath the Moines as small inliers and within the Moines as thrust wedges. The Caledonian orogeny was a complex period with at least two, and quite likely more, major episodes of folding and metamorphism. Rocks of Moine, Dalradian, Cambrian, Ordovician and Silurian ages were involved over an area stretching from Mid-Wales to northern Scotland during a time-span of at least 150 My. The orogeny is commonly interpreted in terms of the continental collision of the North American-Greenland and the Southern Britain-Baltic continents upon consumption of the intervening ocean. The deformation of the north Scottish region, dated as late Cambrian, predates the deformation of the Anglesey-Wales region (late Silurian) by about 100 My and has been explained in terms of subduction and deformation of the two continental masses at different times (Dewey and Bird, 1970; Phillips, Stillman and Murphy, 1976). Extensive intrusion of granitic material took place in the Caledonian mobile belt over a long period during and after the main metamorphic events. The Moine thrusts date from this period and have been variously estimated as having a lateral displacement of 40 km (A.D. Stewart, personal communication) and 100 km (Phillips, Stillman and Murphy, 1976) with overthrusting towards the west.

1.2.3 Post-Caledonian geology

At the end of the Caledonian orogeny the whole of northern Britain was the site of a large mountain chain in the centre of a very large continental mass. Devonian Old Red

Sandstones and conglomerates were deposited in large intermontane basins and attain very large thicknesses (e.g. Orcadian Basin, Moray Firth and some of the basins to the north of mainland Scotland and west of the Shetlands). The Carboniferous is well represented in southern Scotland and further south but is very scarce in northern Scotland.

The understanding of the geology of the area during Mesozoic and Cainozoic times has been greatly enhanced by the collection of marine data in recent years. Through the work of Research Institutes, Universities and Oil Companies the seas around Britain have been shown to be areas of substantial sedimentary basin development since the beginning of the Mesozoic. The Permian and Triassic rocks of northern Britain are of continental type with aolian sandstones and fluviatile rocks deposited over broad tracts or in fault bounded basins. The Permo-Triassic marks the onset of the broad subsidence of the North Sea region and deposition of evaporites, marls etc. In western Britain a series of faulted graben or half-graben basins were initiated, often along lines of pre-existing weakness (e.g. Vale of Eden, Worcestershire Graben, Minch Basins). The formation of these western basins has been linked to a tensional phase preceding the splitting of the North Atlantic between Africa and North America (Roberts, 1975b) or coinciding with a possible Permian opening of Rockall Trough (Russell, 1976).

The Jurassic of the North Sea is marked by the major subsidence of the Viking graben which continued into the Cretaceous. By Tertiary times faulting and localised graben-type subsidence had died away to be replaced by broad subsidence and deposition of up to 3.5 km of Tertiary sandstones, shales and limestones. The crust beneath the northern North Sea shows extensive thinning beneath the axial region of the Viking graben and the Tertiary downwarp (Collette, 1968; R.E. Long, personal communication).

In the west Shetland area and north of the Scottish Mainland, gravity and magnetic observations and seismic reflection and refraction data collected by Durham University have delineated a series of basement highs and fault bounded sedimentary basins (Bott and Watts, 1971; Watts, 1971; Smith and Bott, 1975). Some of these basins are of Old Red Sandstone age and others have Mesozoic sediments forming the major filling. Tertiary sediments in the area are either thin or absent except near the margin of the Faeroe-Shetland Channel where they may thicken considerably (Bott, 1975).

The Mesozoic geology of north-west Scotland has the most bearing on the present work and Figure 1.2 summarises the known geology of the area (Binns et al., 1975). Geophysical and sedimentological work has shown the presence of three Mesozoic basins: the Inner Hebrides Basin, the Sea of the Hebrides Basin (or the South Minch Basin) and the North Minch Basin.

The Inner Hebrides Basin is bounded to the west by the Camusunary fault with up to 750 m of normal movement demonstrated on Skye. The sediments dip towards the fault which passes to the east of Coll, Tiree and Rhum and outcrops on Skye. Permo-Triassic red beds, shallow marine Jurassic shales and limestones and thin Cretaceous sandstones form the basin fill and are exposed in southern Skye. The Permo-

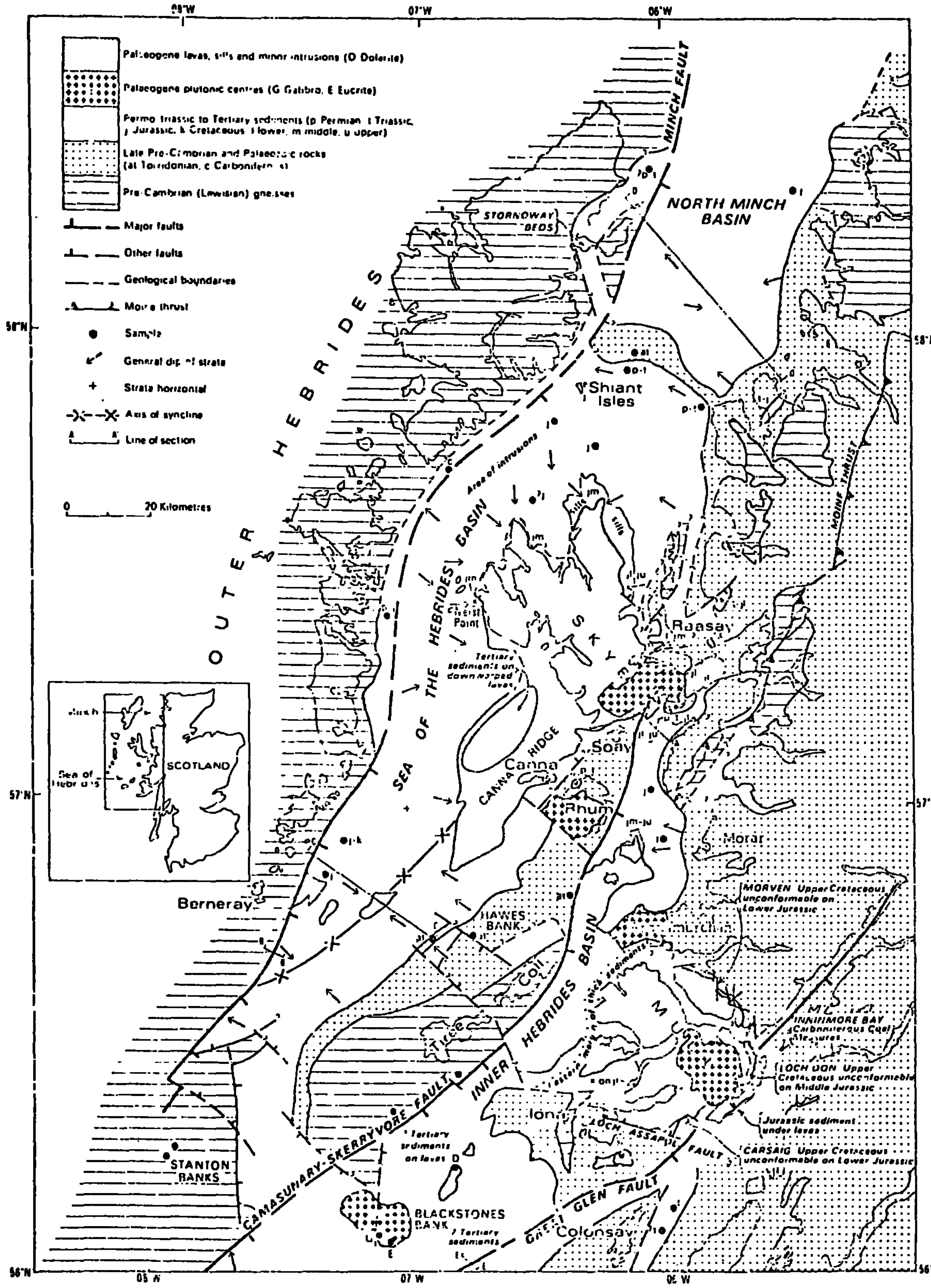

Figure 1.2 Summary map of the geology of the Inner and Outer Hebrides and the adjacent sea areas. After Binns et al., 1975.

Triassic red beds are interpreted as alluvial fan and floodplain deposits (Steel, 1974) and the Jurassic as brackish water lagoonal deposits (Hudson, 1964).

The Sea of the Hebrides Basin is bounded on the west side by the Minch fault system. The northern margin of the basin is a structural high with Torridonian rocks outcropping on the seabed whilst the south-eastern margin is the structural high to the west of the Camusunary fault. Tuson (1959) recognised a fault bounded north-eastern margin and postulated a filling of Triassic rocks. Sea bottom sampling by Chesher et al. (1972) has shown Triassic sandstones, marls and conglomerates and Jurassic shales and sandstones with interbedded sills of presumed Tertiary age. Sedimentological studies by Steel (1974) and Steel, Nicholson and Kalander (1975) have shown that the Triassic of Northern Skye represents alluvial fans and braided stream deposits derived from the north-east and deposited on a south-westerly dipping palaeoslope. Smythe et al. (1972) have suggested that the major fill of the basin is possibly 2 km of Permo-Triassic with an unknown amount of Torridonian beneath it. Tertiary lavas associated with the Tertiary igneous complex of southern Skye outcrop over large areas of both sea and land in this basin and, just north-west of Canna, are themselves covered by up to 1 km of probable Palaeocene sediments.

The North Minch Basin lies to the north of the Torridonian structural high and is bounded to the west by the Minch fault. Allerton (1968) has interpreted the observed gravity across the basin in terms of 2.2 km of material of density contrast -0.3 gm cm^{-3}. Binns et al. (1975) give an interpretation of a seismic profile which suggests that the base of the Permo-Triassic may be at a depth of 4 km or so in the centre of the basin. Sediments of Permo-Triassic and Jurassic age have been sampled on the seabed in this basin (Chesher et al., 1972). Torridonian and possibly Cambro-Ordovician rocks lie beneath the Permo-Triassic. Studies by Steel (1971) on the ~3 km thick Stornoway beds have demonstrated that they are probably of New Red Sandstone age and represent alluvial fan deposits, suggesting contemporaneous movement on the Minch fault or other local faults.

To the west of the Outer Hebrides lies a shallow Mesozoic (?) basin, shown on the IGS map of the sub-Pleistocene geology of the British Isles and the Adjacent Continental Shelf (1972), with fault bounded eastern and western margins but little is known about the depth of this basin or its age of fill.

Over much of the remainder of the shelf, to the west of the Outer Hebrides, Lewisian metamorphic or Tertiary igneous rocks outcrop with only local and very thin patches of sediments. Only very close to the margins of Rockall Trough do sedimentary thicknesses become significant.

The Tertiary of northern Britain was dominated by the volcanic centres of western Scotland, Northern Ireland and the shelf areas to the west. The volcanic province continues into Greenland and encompasses the Faeroe Isles and Rockall Islet. Volcanic centres are exposed at Arran, Ardnamurchan, Mull, Skye, Rhum, St. Kilda, Rockall Islet and in Northern Ireland. Other volcanic centres exist beneath the sea on the shelf which have been found by geophysical methods (Himsworth, 1973; McQuillin, Bacon and Binns, 1973). The volcanic activity is probably an expression of the forces at work during the split of Rockall and Greenland and is associated with fairly extensive regional uplift and erosion of suggested Palaeocene age (Stride et al., 1969).

1.3 The geology of Rockall Trough and its margins

The Rockall Trough has water depths varying from 3 km in the south to about 1 km in the north where the Wyville-Thompson Ridge separates the Trough from the Faeroe-Shetland Channel, itself thought to represent a northward extension of the Trough (Bott, 1977). On the east side of the Trough its margins are steep whilst on the west, steep sides are only shown in the south. North of 58° N Rockall Plateau gives way to a series of shallow banks and channels which are thought to form a continuation of the Plateau up towards the Faeroe Islands (Himsworth, 1973). A sediment drift, the Feni Ridge, occupies the western part of the Trough and was deposited as a contourite by cold Norwegian Sea water passing over the Wyville-Thompson Ridge (Jones et al., 1970). Deposited on the eastern side of the Trough are terrigenous sediments and fans.

Bullard, Everett and Smith (1965) made a reconstruction of the continents around the North Atlantic before the Mesozoic spreading of the Atlantic Ocean took place. They retained Rockall Plateau as a continental fragment and Rockall Trough was not closed up in this reconstruction. A later reconstruction by Bott and Watts (1971) retained both Rockall and Faeroe Plateaus as continental fragments and improved the fit of the continents particularly around northern Scotland and Greenland where the Caledonian fronts became well aligned.

Figure 1.3 is taken from Roberts (1975a) and gives the interpretation of seismic profiles across Rockall Trough, Hatton-Rockall Basin and Porcupine Seabight. Two deep boreholes were drilled on the edge of Hatton-Rockall Basin as part of the Deep Sea Drilling Project (DSDP) (Laughton and Berggren et al., 1972) and in combination with the seismic reflection data yield the following sequence:

(1) Post-R4 series - early Miocene to Recent oozes. Oligocene to early Miocene cherts.

(2) Reflector R4 - base of Oligocene unconformity.

(3) Pre-R4 series - late Cretaceous (?) to upper Eocene.

(4) Basement - Tertiary igneous and Precambrian metamorphics.

Reflector R4 is dated as 37 My and is seen to be a very widespread unconformity. Hatton-Rockall Basin has been an intermittently, rapidly subsiding basin since late Cretaceous times with the rate of subsidence sometimes exceeding the rate of sedimentation. At the bottom of DSDP hole 117 an upper Palaeocene conglomerate overlies a sub-aerial (?) basalt indicating that the area was at, or close to, the surface at that time. Further up the section deeper water sediments become dominant.

In Rockall Trough the same upper sequence is recognised, but a much thicker (~2 seconds two-way travel-time) sequence of pre-R4 sediments can be identified. Reflectors X,Y and Z

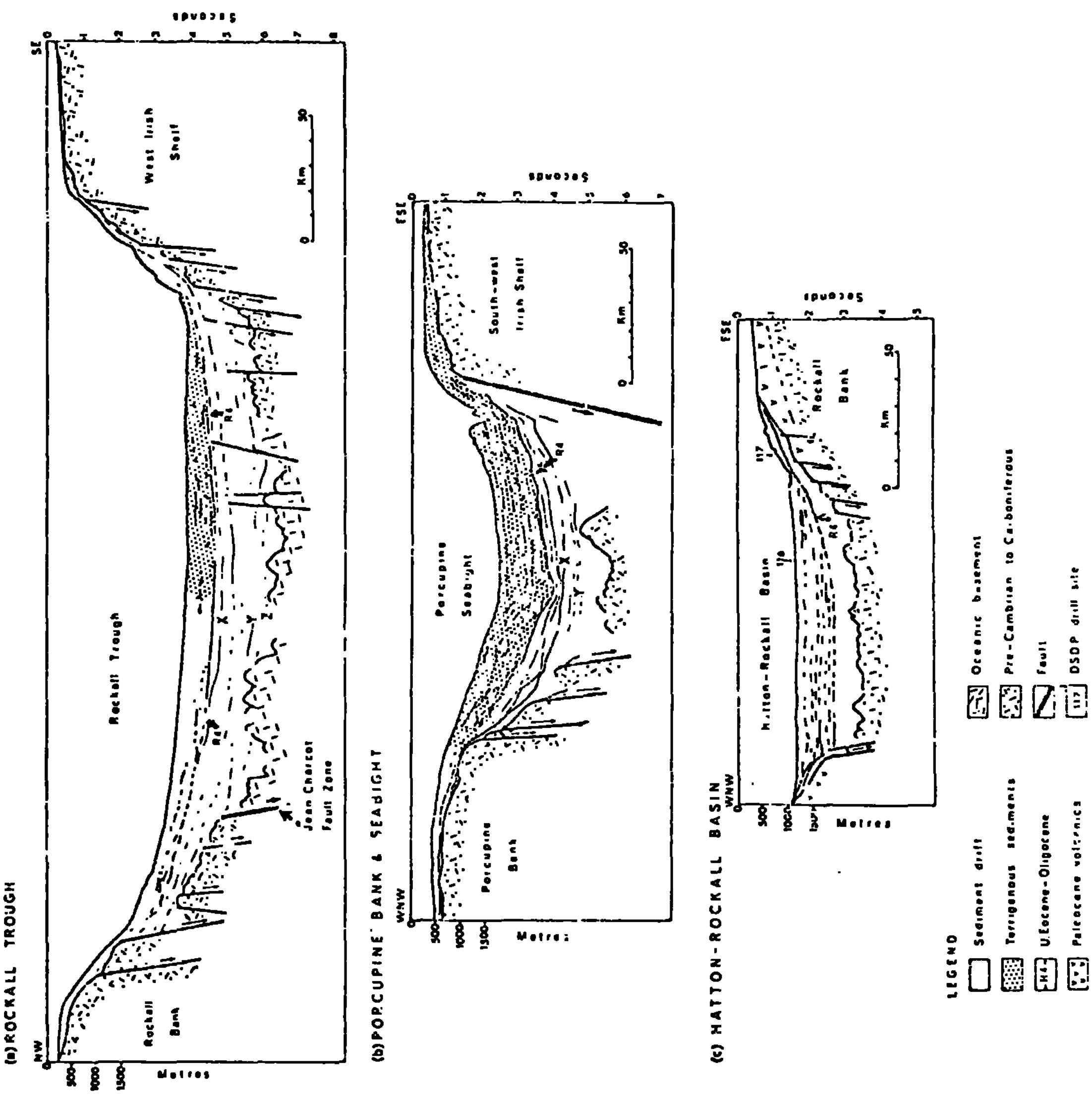

Figure 1.3 Representative seismic reflection profiles across Rockall Trough, Porcupine Seabight and Hatton-Rockall Basin. After Roberts, 1975a.

have been dated by Roberts (1975a and b) as 60, 76 and 100 My old respectively, on the basis of their pinchout on dated oceanic crust to the south and west and using typical sedimentation rates. This evidence suggests that Rockall Trough was formed a little before 100 My ago although this depends critically on the date given to reflector Z.

The continent ocean boundary used by Bullard, Everett and Smith (1965) was the 500 fathom bathymetric contour but Roberts, Ardus and Dearnley (1973) have suggested that a prominent sub-sedimentary basement scarp, called the Jean Charcot fault zone, may mark the continent ocean boundary on the west side of Rockall Trough. A similar boundary at the foot of the slope on the east side was also suggested. Closure of the Trough to these substantially congruent fault zones leads to an improved fit of Rockall Plateau and the Hebridean Shelf which does not require rotation of Porcupine Bank (Roberts, Ardus and Dearnley, 1973).

Recent DSDP drilling of the western margin of Rockall Plateau and in the Bay of Biscay has shown that presumed continental areas close to these margins have subsided by several thousand metres in response to cooling of the oceanic lithosphere since spreading began about 55 and 120 My ago respectively (Montadert <u>et al</u>., 1977). These drill holes show a thin (~0.5 km) sequence of sediments grading from Upper Palaeocene clastic shelf facies through Eocene and Miocene oozes to Recent oozes indicating that the rate of subsidence has exceeded the rate of sedimentation.

The margins of Rockall Trough, although showing more or less the classic shelf, slope and rise sequence of

Atlantic-type continental margins, are anomalous in that they show little evidence of substantial sedimentary wedges on the adjacent shelves. Acoustic basement occurs at comparatively shallow depth (0.5 km) to within a few kilometres of the shelf-break (Stride et al., 1969; Himsworth, 1973; Bailey, Grzywacz and Buckley, 1974; Riddihough and Max, 1976). There is little evidence of pre-split graben formation close to the Trough although graben development was active some 150 km to the east in Permo-Triassic times (Bott, 1977). There are small accumulations of sediments (probably Mesozoic) where the Great Glen fault is intersected by the margin (Bailey, Grzywacz and Buckley, 1974) and small thicknesses of presumed Mesozoic sediments are identified on some commercial reflection data close to the shelf edge around 58° N (F. Bouwers, personal communication). The lack of large sedimentary accumulations can be attributed to lack of subsidence or to an inadequate sediment supply. The western margin of Rockall Plateau is a sediment starved margin so that although it exhibits substantial subsidence it has only thin sediments (Montadert et al., 1977). On the other hand, the margins of Rockall Trough seem not to have suffered a similar amount of subsidence, possibly because the spreading in the Trough took place under unusually cool conditions and thermal uplift did not achieve the scale normally envisaged for continental margins (Bott, 1977). As any spreading in the Trough ceased after generating only 200 km of separation it is unlikely that it was of the vigorous type observed in modern spreading oceans.

Three prominent seamounts are situated in the Trough and are identified as such on the basis of their bathymetry, magnetic and gravity anomalies and dredge sampling (Deitrich and Ulrich, 1961; Himsworth, 1973; Jones et al., 1974). The seamounts are Rosemary Bank, Anton Dohrn seamount and the Hebrides Terrace seamount. Anton Dohrn seamount is dated as Upper Cretaceous from a nannofossil assemblage incorporated in basic lavas and tuffs (Jones et al., 1974). The flat top of Anton Dohrn suggests that it once reached the surface and has since subsided about 600 m.

1.4 Crustal structure in the region

1.4.1 Shelf areas, Rockall Plateau and the Faeroes

Figures 1.4 and 1.5 summarise the results of some previous seismic refraction experiments in the British Isles and shelf areas, the Faeroes, Rockall Trough and Rockall Plateau.

The North Atlantic Seismic Project of 1972 (NASP) was a sea to land refraction experiment using shots fired on the Scottish Shelf (north of Scotland and west of Shetland), across the Faeroes-Shetland Channel, on to the Faeroe Plateau and along the Iceland-Faeroe Ridge. Recording stations were sited on Iceland, the Faeroe Isles, the Shetland Isles and the Scottish Mainland. Two recording ships were also used. On the northern Scottish shelf area a two layer crust of velocities about 6.1 and 6.46 km sec^{-1} was observed (Smith and Bott, 1975). The mid-crustal refractor gave good first arrivals and varied in depth from 16 km to 2 km, with the shallowest part being beneath a large gravity high (High A of Bott and Watts, 1971). The depth of the refractor

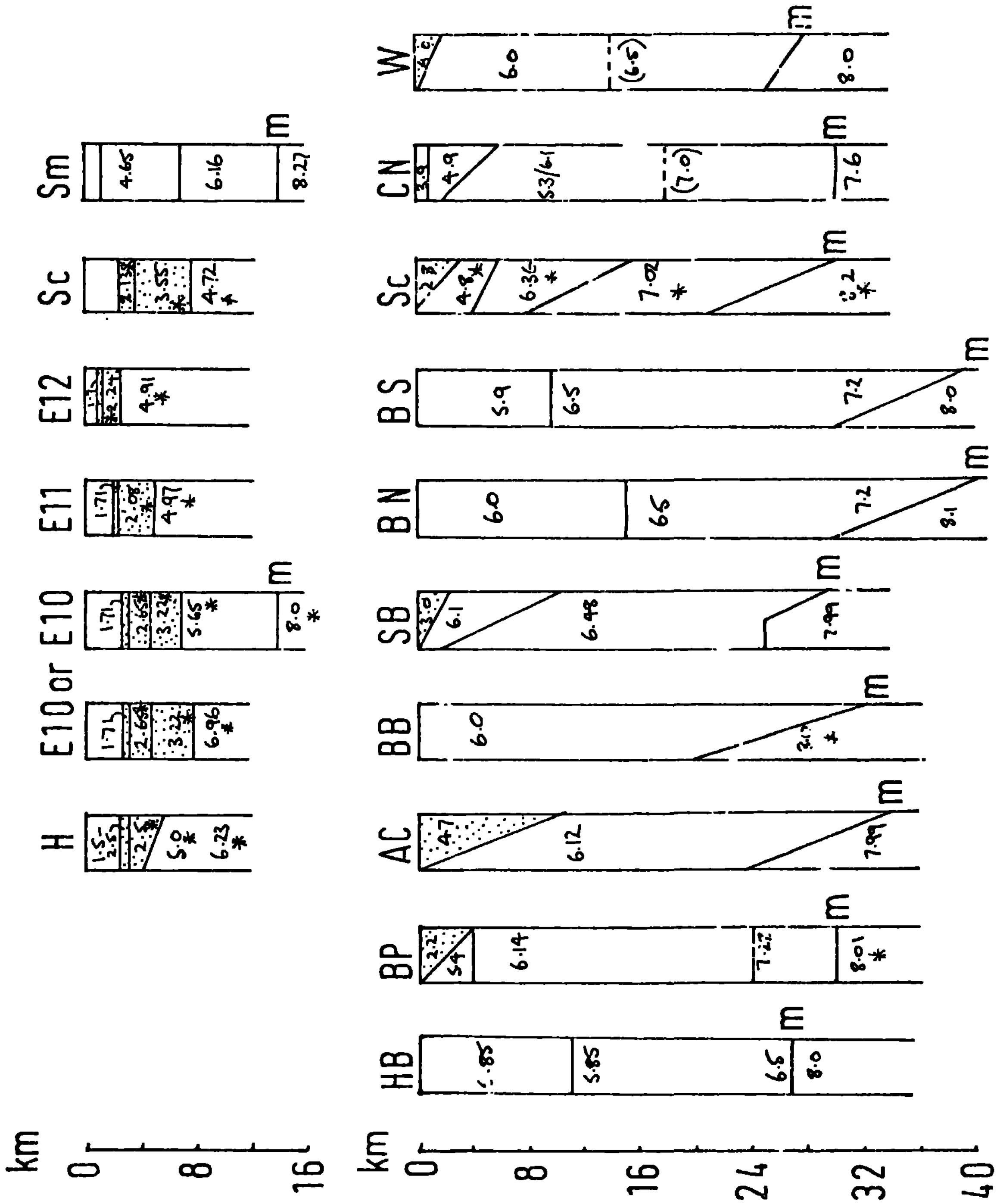

Figure 1.4 Summary of the results of previous seismic refraction work in the British Isles region. The letters refer to the authors of the studies. H - Hill, 1952; E10, E11, E12 - Ewing and Ewing, 1959; E10,- Jones et al., 1970; Sc - Scrutton, 1971; Sm - Smith, 1974; HB - Holder and Bott, 1971; BP - Blundell and Parks, 1969; AC - Agger and Carpenter, 1965; BB - Bamford and Blundell, 1971; SB - Smith and Bott, 1975; BN - Bamford et al., 1976 northern area; BS - Bamford et al., 1976 southern area; CN - Casten and Nielsen, 1975; W - Whitmarsh et al., 1974.

* unreversed observation

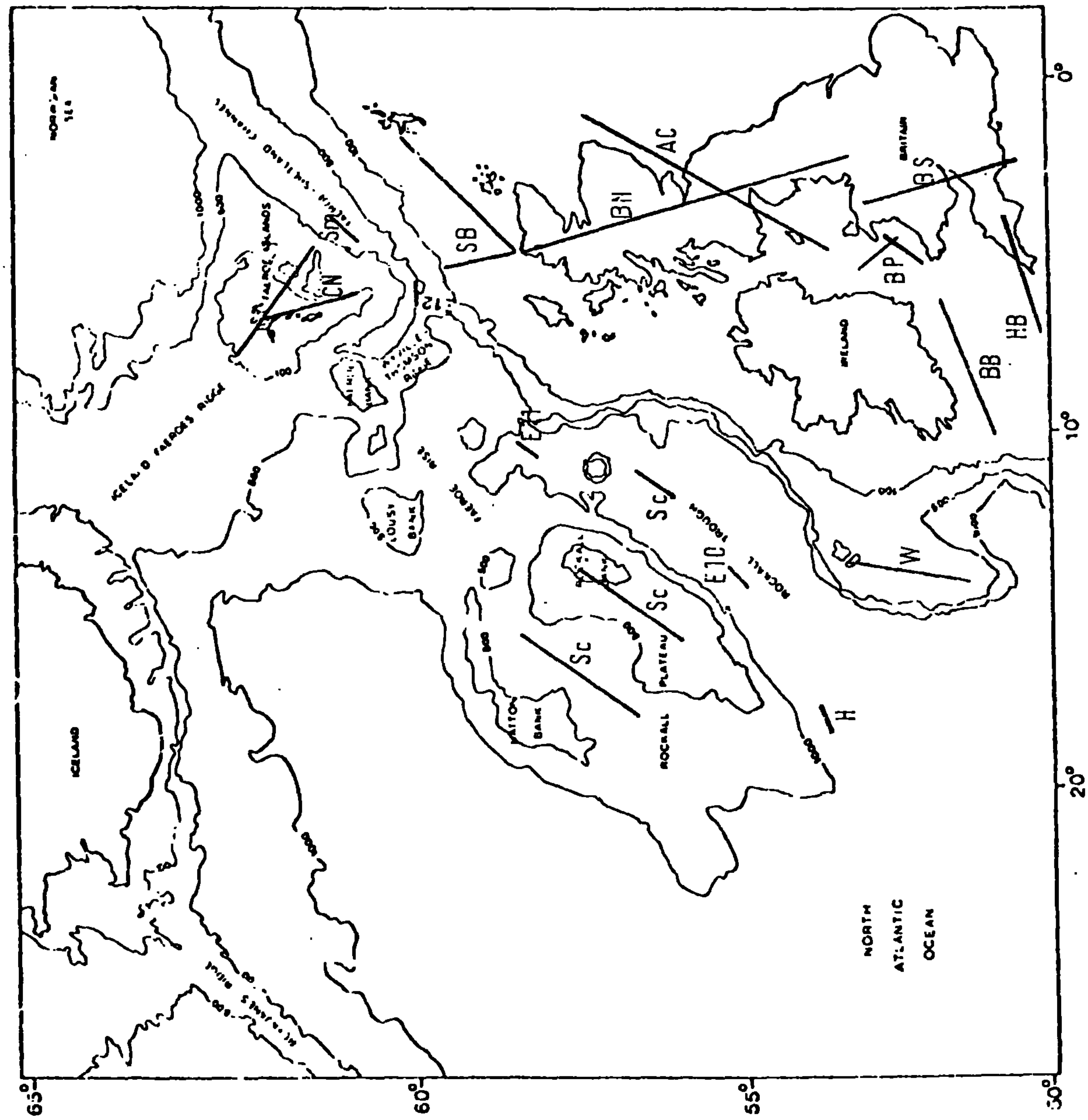

Figure 1.5 Location map of seismic refraction experiments summarised in Figure 1.4. Letters by the profiles refer to the publications listed for Figure 1.4. Bathymetric contours in fathoms.

correlates with the Bouguer anomalies and Smith and Bott (1975) suggested that the interface marks the change from an upper layer of amphibolite facies Lewisian (Laxfordian) to granulite facies Lewisian (Scourian). If this is so, the exposed granulite terrains of north-west Scotland may represent the lower crustal material. Assuming that the 6.48 km sec^{-1} layer extends to the base of the crust, the Moho depth was found to be remarkably uniform at about 26 km beneath the foreland area. Beneath the Caledonides, east of the Moine thrust, the crust is about 20 per cent thicker than beneath the foreland and the mid-crustal refractor is found at varying depth. A well determined Moho velocity of 7.99 km sec^{-1} was reported.

The Lithospheric Seismic Profile in Britain of 1974 (LISPB) was a very long range and detailed refraction profile aligned north-south, crossing the major structural trends of Britain at a high angle. Preliminary results have been presented by Bamford et al. (1976) and Kaminski et al. (1976) and more detailed results have been given by Bamford (personal communication). A three layer division of the crust has been proposed which, in the northern area, has velocities in the ranges: 6.0 - 6.2 km sec^{-1} for the top layer, 6.4 - 6.45 km sec^{-1} for the middle layer and about 6.7 km sec^{-1}, increasing to about 7.2 km sec^{-1} just above the Moho, for the bottom layer. The depths to the two mid-crustal interfaces are about 10 km and 18 km respectively, whilst the Moho is at a depth of about 28 km and overlies upper mantle material of velocity 8.00 km sec^{-1}. The identification of the top two layers is based on first arrivals and correlates well with the results of NASP further to the north. The recognition of the lowest crustal refractor is based upon the high values found from analysis of the Moho wide-angle reflections for the average crustal velocity (6.7 km sec^{-1}) and the identification of a supercritically reflected phase from the 6.7 km sec^{-1} interface. In addition to crustal arrivals, LISPB observed arrivals from reflectors deep within the lithosphere at ranges of about 350 km and above. The energy in the Moho headwave was observed to die away at about 300 km and a more energetic, and slightly faster, phase became prominent. Such lower lithospheric phases have been observed in long range profiles in France by Hirn et al. (1973) and indicate previously undetected fine structure within the lower lithosphere.

Other explosion experiments in southern Britain have shown a one or two layer crust beneath a variable layer of sediments. Bamford and Blundell (1971) have presented preliminary results from the Continental Margin Refraction Experiment (CMRE) conducted in the sea areas to the south of Ireland. Although unreversed, a Moho velocity of 8.0 km sec^{-1} at a depth varying from 25 to 32 km beneath a single crustal layer of velocity 6.0 km sec^{-1} was observed. An oceanward thinning of the crust was suggested but the magnitude of the effect was not precisely determined.

The crustal structure of Rockall Plateau has been shown to be continental in type through refraction experiments reported by Scrutton (1971) and through geochemical work by Moorbath and Welke (1969). An upper crustal layer of velocity 6.36 km sec^{-1} was observed above a lower crustal layer of 7.0 km sec^{-1} with a boundary at a depth of between 8 and 16 km

(Scrutton, 1971). Moho depths of 30 and 22 km were measured beneath Rockall Bank and Hatton-Rockall Basin respectively and an unreversed sub-Moho velocity of 8.2 km sec^{-1} found.

The crustal structure of the Faeroe Plateau was investigated during NASP and a crustal thickness of between 25 and 30 km found (Smith, 1974; Smith and Bott, 1975; Casten and Nielsen, 1975). Upper crustal velocities of 5.3 and 6.1 km sec^{-1} were observed with some slight evidence of a 7.0 km sec^{-1} refractor at depths of about 15 km. The Moho velocity was found by time-term analysis to be about 7.6 km sec^{-1} although significant dips on the Moho gave apparent velocities of from 7.1 to 8.3 km sec^{-1} (Casten and Nielsen, 1975). This low velocity was ascribed by Casten and Nielsen to the proximity of the Iceland-Faeroe Ridge structure. The evidence of continental crustal material and thicknesses beneath Rockall Plateau and the Faeroes Plateau is entirely compatible with the results of gravity interpretations in those areas (Scrutton, 1971; Bott, Browitt and Stacey, 1971).

NASP also produced evidence for fundamentally different structures between the Iceland-Faeroes Ridge and the Faeroes Plateau in the phase conversions reported by Bott, Nielsen and Sunderland (1976). Phases travelling along the ridge at velocities of about 6.7 km sec^{-1} and 7.8 km sec^{-1} were shown to change to a phase having an apparent velocity between the stations not significantly different from that of P_g within the Faeroe Block. The change takes place at the margin between the Iceland-Faeroe Ridge and the Faeroes Plateau and suggests a conversion at a fairly sharp lateral boundary.

1.4.2 Rockall Trough and the Faeroes-Shetland Channel

Seismic refraction observations in Rockall Trough are reported by Hill (1952), Ewing and Ewing (1959) and Scrutton (1971). These unreversed refraction profiles revealed velocities of assumed sedimentary rocks in the range 1.5 to 3.55 km sec^{-1} with a maximum thickness of about 5 km in the southern part of the Trough. The sediments thin northwards as the seabed rises. 'Basement' velocities of between 4.72 and 6.96 km sec^{-1} were observed, a span which encompasses possible values for oceanic layer 2 as well as consolidated sediments, crustal metamorphic and igneous rocks. No Moho arrivals were reported although a reinterpretation by Jones et al. (1970) of the line E10 of Ewing and Ewing (1959) suggested that the Moho was at a depth of 14 km with material of velocity 8.0 km sec^{-1} beneath it.

Gravity interpretations by Scrutton (1971) and Himsworth (1973) have shown that the Moho is probably at a depth of about 14 km in the south of the Trough. As the seabed rises, and the sediments thin towards the Wyville-Thompson Ridge Himsworth (1973) suggested that the crust thickens northwards.

Gravity interpretations by Watts (1970) and Himsworth (1973) in the Faeroes-Shetland Channel have suggested crustal thicknesses of about 21 and 18 km respectively. These interpretations were limited by a lack of knowledge concerning the sediment thicknesses. Seismic refraction observations by Ewing and Ewing (1959) showed a 4.91 km sec^{-1} basement refractor about 1.8 km beneath the seafloor with sediments of velocity between 1.72 and 2.24 km sec^{-1} above it. During NASP a reversed refraction profile was shot in the channel and showed refractors of 4.65, 6.16 and 8.27 km sec^{-1} at mean depths of 1.24, 6.9 and 17.1 km (Smith, 1974). This may be taken as good confirmatory evidence that the Faeroe-Shetland Channel is not floored by continental crust but by slightly anomalous oceanic crust, possibly similar to that beneath the Iceland-Faeroe Ridge.

The Greenland-Iceland—Faeroe Ridge is an aseismic ridge intersecting the Mid-Atlantic Ridge beneath Iceland. It has anomalously thick oceanic crust and is thought to have been produced by extreme differentiation of mantle material above a "hotspot" now centred beneath Iceland (Bott, Browitt and Stacey, 1971).

1.5 The plate tectonic history of the area

Most of the details of the Mesozoic spreading history are well known from work by, among many others: Heirtzler et al., 1968; Pitman and Talwani, 1972; Johnson et al., 1974; Roberts, 1975b. The dating of events in the Atlantic is mostly dependent on the age of various magnetic anomalies. An outline summary of the sequence of spreading phases is as follows:

(1)	230 - 180 My	Early rifting stage predates the split between Africa and North America.
(2)	180 My - Present	Spreading south of the Azores opens central Atlantic.
(3)	130? - 73 My	Spreading in Bay of Biscay rotates Iberian peninsula.
(4)	84 (76?) - 45 My	Spreading in Labrador Sea separates Greenland from North America.
(5)	52?My - Present	Spreading of Reykjanes Ridge separates

Rockall from Greenland. Spreading rates on Reykjanes Ridge change at about 35 My and 22 - 10 My.

The way in which the opening of Rockall Trough fits into this scheme is very difficult to assess due to the lack of oceanic magnetic anomalies. The anomalies in Rockall Trough are smooth and of small amplitude and may be interpreted as oceanic crust magnetised in one direction only. There are two long periods in this scheme of Mesozoic magnetic reversals when normal polarity periods obtained, one is from about 162 to 148 My in the middle Jurassic and the other is in mid-Cretaceous times from about 112 to 85 My (Heezen and Fornari, 1975). If Rockall Trough opened during either of the two periods, striped magnetic anomalies would not be formed. The observation that magnetic anomaly 32 cuts across the mouth of the Trough without offset or evidence for a triple junction suggests that the formation of the Trough was complete by about 73 My ago (Roberts, 1975a and b). The age of 100 My for the oldest reflector observed in the Trough (Roberts, 1975a and b) suggests that the formation of the Trough was complete by about this time. A Permian or early Jurassic age for Rockall Trough, as suggested by Russell (1976), would require rifting and spreading deep within a continental interior connected by transform faults to other plate margins and it seems most probable that Rockall Trough formed during part or all of the mid-Cretaceous quiet period between 112 and 85 My ago (Bott, 1977).

1.6 The aims of HMSP

Bearing in mind the observations made in the preceding discussion, HMSP was designed to try to answer the following questions:

(1) Does the crustal structure and thickness change significantly between the Caledonian Mobile belt and the foreland region, as was indicated in NASP and LISPB?

(2) What effect, if any, do the small sedimentary basins of the Minches and Outer Hebrides have on Moho depth and crustal structure?

(3) Do the exposed Scourian granulite terrains of the north-west Scottish area and the Outer Hebrides exhibit velocities typical of the lower crust, as suggested by Smith and Bott (1974)?

(4) Does the continental crust thin towards Rockall Trough and, if possible, what is the fine structure at the margin?

(5) Is the oceanic nature of Rockall Trough confirmed by good observations of a thin crust and does the crust in the Trough thicken northwards towards the Wyville-Thompson Ridge, as suggested by Himsworth (1973)?

(6) Are any phases converted at the margin of Rockall Trough to normal continental crustal phases, as was observed between the Faeroes and the Iceland-Faeroe Ridge by Bott, Nielsen and Sunderland (1976)?

To answer these questions the experiment was planned to use a line of stations and shots along 58° N with a second line running north-west from Skye across the Minch and outer shelf into Rockall Trough just north of Rosemary Bank (Figure 1.6).

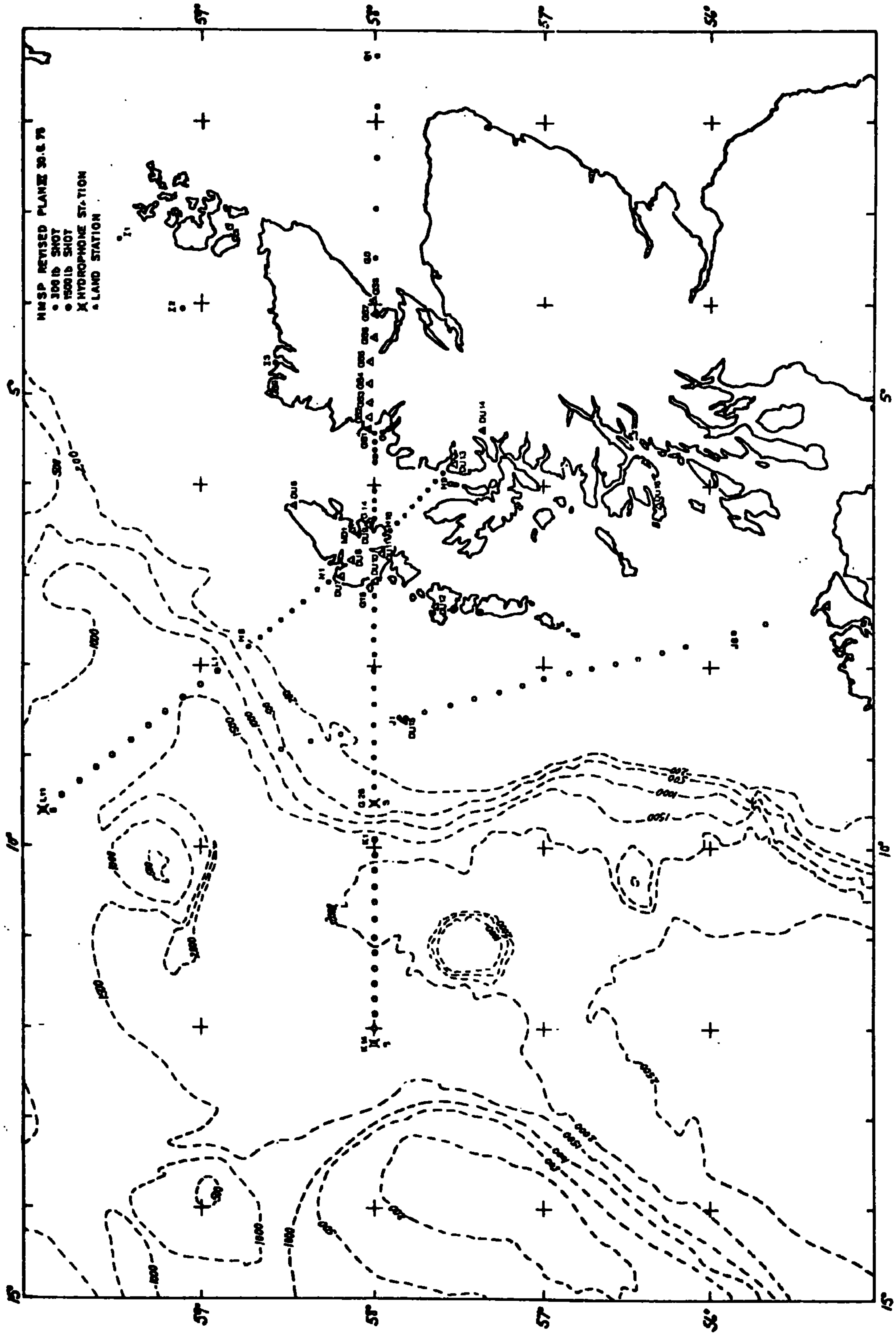

Figure 1.6 Proposed shot positions for HMSP as planned in 1975. Note the shots in Moray Firth, west of Shetlands and towards Rosemary Bank which were planned but not fired due to logistic and weather problems.

Care was taken to ensure a strong network of recordings with several reoccupations of earlier shot and station positions so that the experiment could be tied in to previous work. Shots to be fired in Moray Firth were designed to give reversal of the Moho beneath the land recording stations to the west and recording ships were to be used to reverse the outer shelf and Rockall Trough sections.

CHAPTER 2

DATA ACQUISITION AND PROCESSING

2.1 The Hebridean Margin Seismic Project (HMSP)

HMSP was a sea to land explosion experiment which took place between the 21st July and the 19th August, 1975. Shots fired by RRS Challenger were recorded at 21 temporary seismic recording stations deployed around the Outer Hebrides and the Scottish Mainland. Another temporary recording station was installed in Northern Ireland (at Lagg) by Professor T. Murphy of the Dublin Institute for Advanced Studies. In addition, recordings from the permanent array networks installed in the Midland Valley of Scotland (Lownet) and at Eskdalemuir were made available. The distribution of stations and shots achieved is shown in Figure 2.1.

The explosives used were 300 lb Minol depth charges suspended from buoys and fired electrically at "optimum depth" (see Section 2.2.2). In the shallow water of the Hebridean Shelf a single charge was used, whilst in the deeper water of Rockall Trough five separate depth charges were fired simultaneously.

During part of the project a recording ship, MV Charterer, was operated at the western ends of the shot lines but technical difficulties prevented it successfully recording the shots. A temporary recording station had been installed on Rockall Islet by the Institute of Geological Sciences (IGS) Global Seismology Unit as part of their research program but, due to the low gain employed on the recorder, no useful

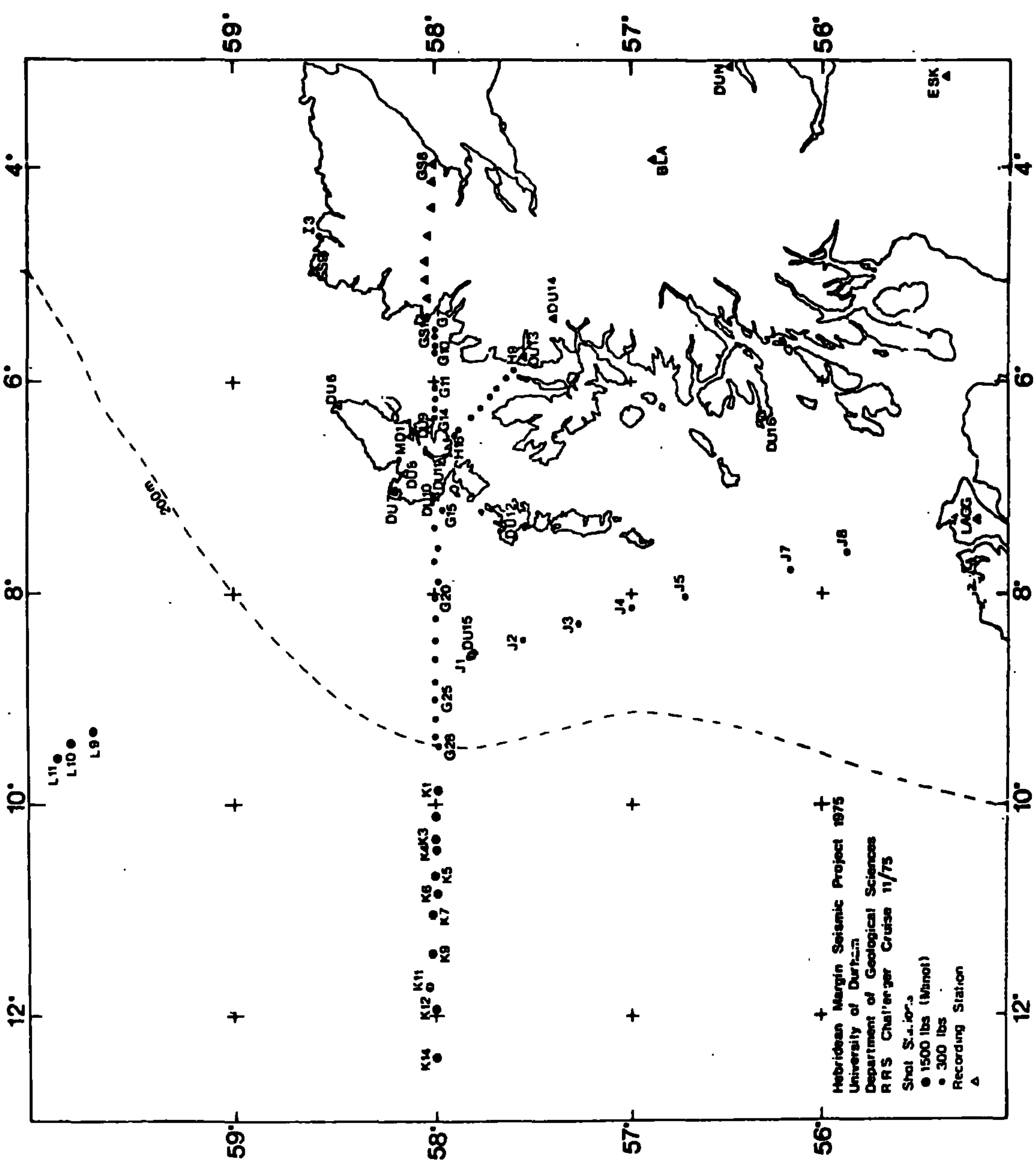

Figure 2.1 Map of shot and station positions for HMSP.

See enlarged copy in back pocket

recordings were made.

The shot distribution achieved was severely restricted by the withdrawal of the Royal Navy at a very late stage in the planning of the project. The Navy had agreed to fire some 25 depth charges west of the Shetlands, in the Moray Firth and in the North Minch, but because of mechanical difficulties with their ship, HMS Herald, they had to withdraw from the project. A reprogramming of the shots allowed the more important ones, otherwise missed, to be incorporated into the shot firing programme of RRS Challenger. The second major margin traverse (line L) was not completed however, due to adverse weather conditions and logistic difficulties.

2.2 Shot data

2.2.1 Shot lines

The major continental margin traverse was along the line of latitude 58^{o} N with an average shot spacing of 10 km on the shelf section (line G) and 15 km in Rockall Trough (line K). An extension of line G crossed the Minch where a ridge of Torridonian Sandstone separates the North Minch Basin from the South Minch Basin, whilst a second line (line H) crossed a large thickness of sediments in the South Minch Basin. A second line on the outer shelf (line J) ran south-south-east from St. Kilda towards the recording station in Northern Ireland. The shot spacing along line J was approximately 35 km. Shots I3 and J1 were specifically designed to give constraints for any time-term solutions, I3 being a reoccupation of shot N1 of LISPB and J1 being close to the two temporary recording stations sited on St. Kilda.

2.2.2 Shot timing and firing

The Senior Scientist on board RRS Challenger was Mr. G. Wylie who had responsibility for shot positions and timing. The charges were made up and fired by Commander C.C. Moore. A detailed account of the shot firing and timing procedure and general conduct of the cruise is presented in "Report on RRS Challenger Cruise 11/75 in the North East Atlantic" - Department of Geological Sciences, University of Durham, HMSP.

Investigations by Jacob (1970, 1975) have shown the advantages to be gained from firing underwater explosions as dispersed charges at "optimum depth". The method relies on constructive interference of the bubble pulse and sea-surface reflection for a particular frequency. As the range of observation increases the required charge size increases and therefore the required depth of water increases. The amplitude and predominant frequencies are consequently changed. This requirement leads to difficulties of manhandling and laying a large charge and in some cases the required depth of water is difficult to achieve, especially nearshore. By splitting the large charge into N packages of 1/N th its size, each suspended at optimum depth, Jacob (1975) has shown how the transmitted signal is simply N times the signal from a single package. For the frequencies and array dimensions considered here the directional radiation pattern has a broad maximum lobe at right angles to the array. As the take-off angles of the signals from the source are always greater than 75° to the horizontal they can be considered to be in the direction of maximum response. The major influence on the orientation of the shot array was therefore the practical desire to ensure that the ship could maintain station with the charges and buoys in a stable configuration behind her.

On the shallow continental shelf regions, if the water depth was large enough, single charges were suspended 90 m below a large buoy. At lesser depths the charge was suspended as deep as was possible whilst making sure that it was off the seabed. This avoided the danger of it snagging and hence failing through strain on the firing cable. In the deeper waters of Rockall Trough, five charges were hung 90 m beneath five separated buoys 40 m apart. Figure 2.2 shows the arrangement of charges and buoys used for the dispersed charges.

Both the suspension rope and the firing cable had disposable "blow-off ends". These could be swiftly removed on recovery of the system leaving the major portion of the firing system intact.

Firing was by dynamo-exploder connected in series to each detonator. The shot instant was found by comparing the recording made of the water wave arrival at a hull-mounted geophone with the output of a crystal clock. Clock and geophone output were recorded on to magnetic tape and displayed on an ultra-violet paper recorder. The clock was regularly calibrated against MSF Rugby radio and a knowledge of the charge configuration allowed the shot instant to be calculated to 0.02 seconds accuracy.

Close inshore positioning was by Radar, Decca, Satellite Navigator and compass bearings on landmarks. Further out to sea Decca and Satellite Navigator only were used. It is

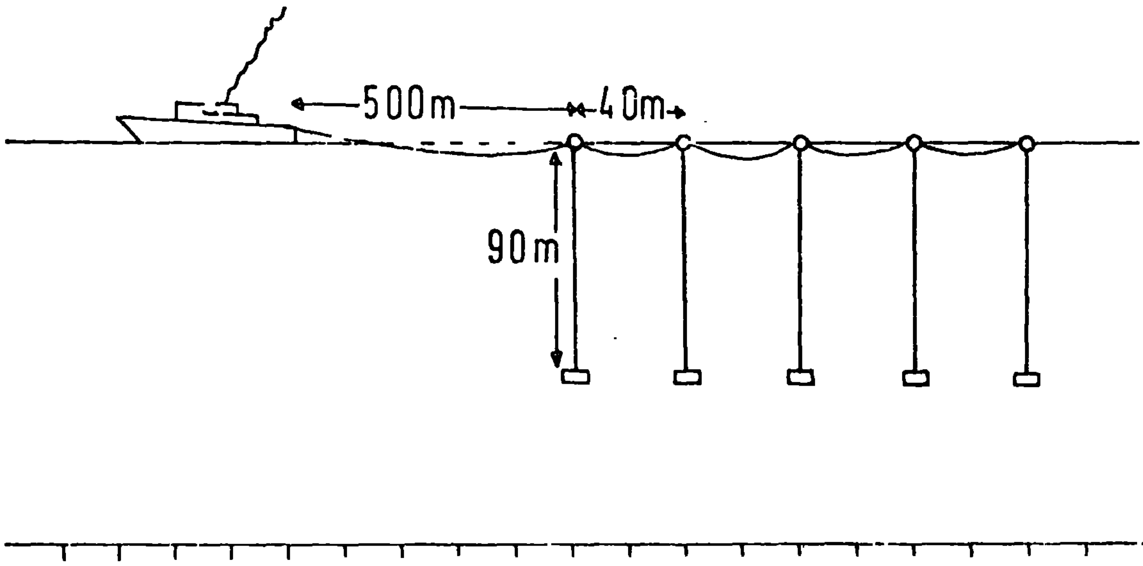

Figure 2.2 Dispersed charge layout. Each charge is 300 lb Minol.

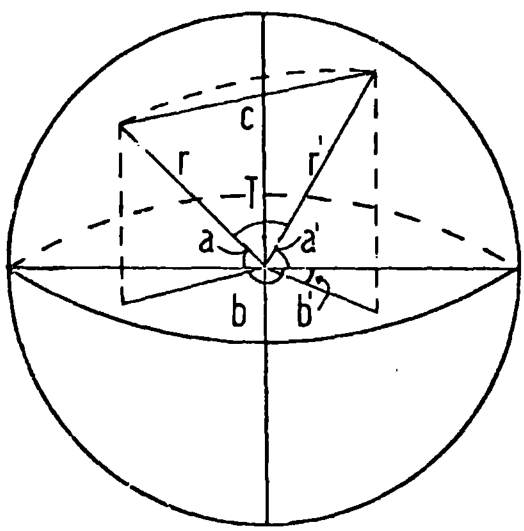

Figure 2.3 Parameters used in calculation of shot - station ranges.

thought that positioning was accurate to within 0.2 km nearshore and 0.4 km in the Rockall Trough region.

In general, radio broadcasts of expected shot times and shot completions by both RRS Challenger and MV Charterer proved ineffective due to the low quality of the receivers used by the recording station operators. However, as all the stations operated continuously it was only necessary to know the firing programme for the day in outline so that the recorder gains could be set in advance. The system finally adopted, and the one recommended for any future project, was to copy telex messages containing an updated firing programme to the major operating centres: Durham, Stornoway and Ullapool. Table 2.1 gives the shot positions and firing times.

2.2.3 Shot - station ranges

Travel distances were calculated using a computer program available at Durham which follows Rudoe's method described by Bomford (1962). Considering the earth as an ellipsoid of revolution, the radii at the shot and station position were calculated using the approximations:

$$r = e(1 - E\sin^2 a + 0.625E^2\sin^2 a)$$

where e is the equatorial radius = 6378.16 km

E is the ellipticity of the earth = 1/298.247

a is the geocentric latitude

and $a = \tan^{-1}(0.99330544 \tan \bar{a})$

where $\bar{a}$ is the geographical latitude.

Radii calculated for the shot and station are used in the

Table 2.1 Shot position, time, size and depth with water depth for all HMSP shots.

Shot	Latitude ° & 'N	Longitude ° & 'W	Date	Time (GMT) (h m sec)	Size (lb)	Shot depth (m)	Water depth (m)
G7	58 00.07	5 30.43	29-7-75	1008 59.30	300	45	45
G8	58 00.27	5 34.73	29-7-75	1148 43.52	300	91	102
G9	58 00.10	5 39.95	29-7-75	1308 21.83	300	91	100
G10	57 59.94	5 43.83	29-7-75	1436 14.36	300	91	110
G11	57 59.80	6 03.65	29-7-75	1706 19.96	300	30	48
G12	57 59.73	6 10.15	29-7-75	1821 22.46	300	45	63
G13	58 00.04	6 15.72	30-7-75	0805 46.96	300	91	118
G14	58 00.09	6 21.45	30-7-75	0942 55.52	300	91	151
G15	57 58.25	7 12.70	8-8-75	1622 05.00	300	30	40
G16	58 00.44	7 22.16	12-8-75	1021 14.04	300	91	97
G17	57 59.47	7 34.00	8-8-75	1419 25.42	300	76	94
G18	58 00.46	7 40.88	12-8-75	1233 54.78	300	90	98
G19	57 59.28	7 52.80	8-8-75	1226 10.60	300	45	70
G20	58 00.20	8 01.80	12-8-75	1441 08.02	300	91	96
G21	57 59.90	8 14.20	8-8-75	1014 53.81	300	91	143
G22	58 00.00	8 25.00	12-8-75	1705 40.99	300	91	140
G23	57 59.80	8 36.80	12-8-75	1844 19.73	300	91	153
G24	58 00.17	8 50.20	15-8-75	1345 52.43	300	91	164
G25	58 00.04	8 59.86	15-8-75	1227 36.95	300	91	172
G26	58 00.15	9 10.27	15-8-75	1028 24.04	300	91	218
G27	58 00.00	9 20.70	15-8-75	0905 31.91	300	91	275
G28	57 59.03	9 26.98	15-8-75	0731 33.42	300	91	364
H9	57 36.10	5 53.23	30-7-75	2205 45.76	300	91	124
H10	57 38.37	5 57.98	30-7-75	2039 48.51	300	55	55
H11	57 40.57	6 03.83	30-7-75	1911 32.66	300	91	149

Table 2.1 (continued)

Shot	Latitude	Longitude	Date	Time (GMT)	Size	Shot depth	Water depth
	° & ' N	° & ' W		(h m sec)	(lb)	(m)	(m)
H12	57 43.50	6 08.80	30-7-75	1740 51.81	300	91	120
H13	57 46.18	6 14.52	30-7-75	1608 45.21	300	55	74
H14	57 48.75	6 20.38	30-7-75	1446 57.53	300	60	75
H15	57 52.85	6 27.10	30-7-75	1313 45.34	300	73	73
H16	57 54.32	6 29.86	30-7-75	1206 27.09	300	91	136
I3	58 34.24	4 38.14	1-8-75	1905 35.01	300	55	55
J1	57 50.10	8 35.60	3-8-75	0739 17.77	300	45	60
J2	57 32.87	8 25.84	16-8-75	0747 44.55	300	91	174
J3	57 15.91	8 16.71	16-8-75	1033 40.40	300	91	138
J4	56 54.60	8 08.30	16-8-75	1319 38.06	300	91	134
J5	56 42.82	8 01.63	16-8-75	1606 27.28	300	91	120
J7	56 09.41	7 45.96	17-8-75	0741 49.34	300	76	90
J8	55 51.80	7 36.96	17-8-75	1030 32.38	300	91	132
K1	57 59.15	9 53.14	13-8-75	0906 15.17	1500	91	1824
K2	57 59.76	10 05.75	14-8-75	1734 54.14	1500	91	1950
K3	57 59.66	10 18.37	13-8-75	1330 39.05	1500	91	2052
K4	57 59.73	10 25.93	14-8-75	1309 54.85	1500	91	2070
K5	58 00.25	10 39.28	13-8-75	1736 41.83	1500	91	2088
K6	57 59.45	10 50.50	14-8-75	0821 28.00	1500	91	2076
K7	58 01.08	11 02.58	6-8-75	1446 39.42	1500	91	2016
K9	58 01.14	11 25.03	6-8-75	0906 42.43	1500	91	1968
K11	58 02.55	11 44.06	5-8-75	1810 54.25	1500	91	1872
K12	58 00.10	11 57.33	5-8-75	1336 21.18	1500	91	1710
K14	57 59.70	12 23.46	4-8-75	1104 56.75	1500	91	1704
L9	59 41.78	9 17.48	27-7-75	1820 08.86	1200	91	1464
L10	59 48.07	9 24.80	27-7-75	1010 24.07	1500	91	1416
L11	59 52.62	9 32.04	26-7-75	1235 30.74	1500	91	1365

cosine rule equation to give a chord length c:

$$c = (r^2 + r'^2 - 2rr'\cos T)^{\frac{1}{2}}$$

where cos T is given by:

$$\cos T = \sin a \sin a' + \cos a \cos a' \cos (b - b')$$

and where b and b' are longitudes.

Figure 2.3 is a diagram showing the parameters used in the above calculation. Table 2.2 shows the difference between the chordal distance and the arc distance method of calculating range. The chordal length, c, is given with an accuracy of one part in 10^7 (Bomford, 1962) and is used here in preference to an arc length since the chordal distance is probably a closer approximation to the actual distance of travel for ranges considered here. Any error in distances can be regarded as solely due to the inaccuracies in locations of the shots and stations and an estimate of this is included in the time-term analysis (Sections 4.4 and 4.5).

2.3 Recording stations

2.3.1 Introduction

The distribution of recording stations as shown in Figure 2.1 (and tabulated in Table 2.3) was arranged firstly, to extend the profile along 58° N and secondly, to provide stations offset from the main line in order to achieve a more suitable network of recordings for time-term analysis. A comprehensive list of shot - station ranges, travel-times, seismometer type and gain settings etc. is given in Appendix A.

Table 2.2 Comparison of arc-distance and chordal-distance method of range calculation for small distances.

Δ (deg)	Arc length (km)	Chord length (km)
1	111.352	111.350
2	222.707	222.692
3	334.056	334.017
4	445.408	445.317

Table 2.4 Laxay array pit positions and elevations in Cartesian coordinates.

Pit	East (km)	North (km)	Elevation (m)
NW4	-0.82	0.84	60
NW3	-0.62	0.63	50
NW2	-0.43	0.43	40
NW1	-0.22	0.19	41
3C	0.00	0.00	42
NE1	0.26	0.20	60
NE2	0.46	0.40	40
NE3	0.70	0.60	40

Centre pit - Latitude 58° $06.50'$ N

Longitude 06° $31.80'$ W

Table 2.3 Recording station position, elevation and geology.

Code name	Location	Latitude ° & ' N	Longitude ° & ' W	Altitude (m)	Geology
GS1	Polbain	58 02.45	5 23.70	160	Torridonian sandstone
GS2	Stac Pollaidh	58 01.95	5 12.95	75	Torridonian sandstone
GS3	Knockan	58 02.40	5 03.89	250	Cambrian quartzite
GS4	Loch Ailsh	58 02.30	4 52.70	200	Durness limestone
GS5	Glencassley	58 01.80	4 38.00	180	Moine granulite
GS6	Lairg	58 00.40	4 22.60	180	Moine granulite
GS7	Rogart	58 00.45	4 07.50	210	Moine granulite
GS8	Backies	58 00.17	3 58.75	260	Old Red Sandstone
GS9	Cape Wrath	58 37.45	4 59.77	140	Lewisian gneiss
DU6	Butt of Lewis	58 28.34	6 13.23	60	Peat on Lewisian gneiss
DU7	Uig	58 12.02	7 00.68	55	Lewisian gneiss (granitised)
DU8	Linshader	58 08.51	6 51.84	32	Lewisian gneiss
DU9	Lemreway	58 01.30	6 26.33	30	Lewisian gneiss
DU10	Husinish	57 59.31	7 04.78	0	Lewisian gneiss

Table 2.3 (continued)

Code name	Location	Latitude ° & ' N	Longitude ° & ' W	Altitude (m)	Geology
DU11	Maaruig	57 57.18	6 44.62	20	Lewisian gneiss
DU12	North Uist	57 38.80	7 21.06	20	Lewisian gneiss
DU13	Loch Torridon	57 33.60	5 46.30	130	Torridonian sandstone
DU14	Loch Carron	57 23.19	5 25.60	60	Moine schist
DU15	St. Kilda	57 48.70	8 34.65	100	Basic igneous intrusion
DU95	St. Kilda	57 48.65	8 33.75	12	Basic igneous intrusion
DU16	Mull	56 19.20	6 19.60	50	Granite
BLA	Blair Atholl	56 53.27	3 56.47	514	Caledonian granodiorite
DUN	Dundee	56 32.85	3 00.85	275	Lower Old Red Sandstone conglomerate
ESKB4	Eskdalemuir	55 19.90	3 09.58	300	Llandovery shales and grits
ESKB9	Eskdalemuir	55 22.11	3 08.00	398	Llandovery shales and grits
MD1	Laxay	58 06.50	6 31.80	44	Lewisian gneiss
LAGG	Lagg	55 18.63	7 18.67		

Twelve sets of equipment were provided by Durham University. They included six Mk II recording sets and six Mk III recording sets, basically similar to those described by Long (1974), which recorded the three components of ground motion. They were installed on Lewis, Harris, N. Uist, St. Kilda, Mull and on the Mainland at Loch Torridon and Loch Carron. They have been given the prefix DU in Figure 2.1.

Nine Geostore recorders, on loan from the Natural Environment Research Council (NERC) Seismic Equipment Pool, were installed between the west and east coast of the Scottish Mainland at 58^{o} N and at Cape Wrath and were operated by Durham University personnel. These stations are prefixed by the letters GS in Figure 2.1. All Geostore also recorded the three components of ground motion.

At Laxay, on Lewis, a temporary seismic array station, on loan from the United Kingdom Atomic Energy Authority (UKAEA) Blacknest, was installed and given the code name MD1. A Geostore recording station at Blair Atholl was supplied and manned by the IGS Global Seismology Unit. This was a site previously used during LISPB in 1974. A sketch map showing the location of these stations is given in each of the station log-books.

Nearly all the stations installed and operated by Durham University personnel were located in pits dug on to firm bedrock upon which a concrete platform had been laid to give a level surface and this meant that, in general, noise levels were quite low. Using recordings obtained during NASP, gain settings for each of the shots had been calculated and circulated to each of the operators. As the ship's programme was known in advance the system gains could be set accordingly, but see the previous note regarding the effectiveness of this procedure (Section 2.2).

In addition to these temporary seismic stations, recordings from Lownet and Eskdalemuir were used. The Lownet network consists of a radio-telemetered array of six vertical seismometers, distributed about the Midland Valley of Scotland and a three-component set of seismometers at the Edinburgh Observatory. The signals are recorded on to 1" magnetic tape at Edinburgh (Crampin et al., 1970). The Eskdalemuir array station is run by the UKAEA and has 22 vertical seismometers in an L-shaped array with an aperture of about 20 km. The seismometer outputs are relayed by cable to a 1" recording deck at a central recording site.

2.3.2 Durham Mk III recorder

The Durham Mk III recorder is a development of the recording system described by Long (1974). The tape recorder is a ¼" deck supplied by Nagra Ltd. and modified in Durham to run at 15/160 i.p.s. recording on to 8-track triple-play tape. This allows up to six days recording on each tape - a major advantage when used in isolated locations. Power is supplied by PP9 batteries which are changed at each tape change. The whole unit consists of a tape deck, three seismic amplifiers, three FM coders and a time-code generator.

The output of the three orthogonally aligned seismometers (vertical, north-south and east-west) is fed by cable directly into the recorder where it is amplified and FM modulated before being recorded on to tape. The gain of the system is electronically switched in steps of x2. This arrangement means that external FM amplifiers are avoided so cutting down on bulky equipment. In addition to the three seismic tracks, the 8-track head allows recording of a standard frequency for flutter compensation, an internally generated time-code and a radio track for either MSF Rugby or BBC GMT pips. Radio time was recorded continuously or, in some cases, intermittently allowing clock drift to be evaluated. Typically, a linear drift of about 0.01 seconds per day was found. The seismometers used were Willmore Mk II and Willmore Mk III types with natural periods set to 1 hz.

Extensive monitoring facilities are built into the recorder allowing replay, demodulation and display of any of the recorded tracks.

2.3.3 Geostore recorder

The Geostore is a 14-track, ½" tape recorder system designed and built by Racal Thermionic under the direction of a NERC committee. Amplifier modulator units installed next to the seismometers amplify and FM modulate the seismometer output before it is transmitted by cable to the recording box. Gains for each seismometer output are mechanically switched at the amplifier modulators in steps of x2 or x2.5. The recorders were operated in their 7-track auto-reverse mode, recording the output of the three orthogonal seismometers, an internally generated time-code, a radio time track and a standard frequency for flutter compensation. MSF Rugby radio was recorded at each maintainance visit in order to calibrate the internal clock. Clock drift was therefore found daily and ascertained to be quite small, typically 0.01 seconds per day. Linear drift was assumed between each radio fix. At a recording speed of 15/160 i.p.s. six days of recording were available for each 7" diameter tape-spool. A band-width of 0 - 32 hz was thus obtained. Power was provided by 12 v lead-acid car batteries which were changed about every five days.

Monitoring of the equipment performance was by means of a Field Test Box (FTB). The FTB is a comprehensive checking facility allowing:

(a) demodulation and display of amplifier modulator output

(b) monitoring of record head currents (i.e. FM signals)

(c) replay and demodulation of tape tracks (not during recording).

The seismometers used with the Geostore were Geospace HS10, Willmore Mk II and Willmore Mk III types with natural periods set to 2,1 and 1 hz respectively.

2.3.4 Laxay array

The Laxay array consisted of 7 vertical seismometers installed at about 300 m spacing in an L-shape, with a three-component set of instruments at the cross-over point. All the seismometers were of Willmore Mk II type set to a 1 hz natural period. Figure 2.4 is a map of the pit positions and Table 2.4 gives their coordinates. The pits were prepared several months in advance of the project and each was dug through about 1 m of peat or boulder clay on to Lewisian gneiss bedrock. The three-component pit consisted of a cylindrical drum about 1 m in diameter concreted on to the

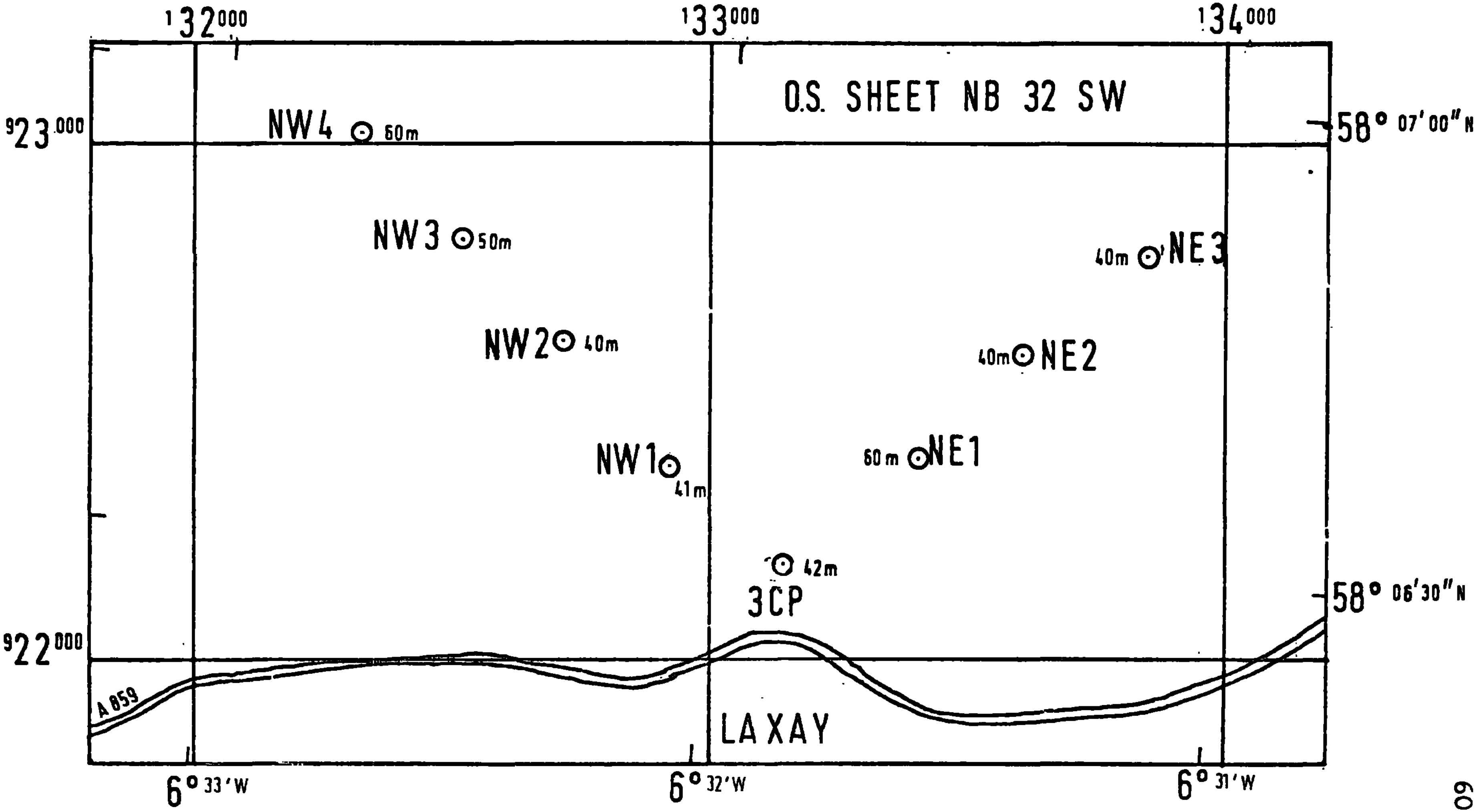

LAXAY (MD1) PIT POSITIONS

Figure 2.4 Laxay array pit positions.

bedrock and covered with planks and plastic sheeting to keep it dry. Each of the other pits contained a cylindrical tube of about 8" in diameter with a wooden lid. The seismometer and an FM amplifier unit of variable gain were placed in the pit and linked by cable to the recording caravan near the cross-over point of the array. The available cable length limited the dimensions of the array to about 1200 m on one arm and about 900 m on the other. The maximum aperture of about 1320 m was oriented in an east-west direction to give maximum velocity sensitivity for the main shot lines of the project (lines G and K).

Signals from each seismometer pit were recorded directly on to the odd or even channels of a 24-track, 1" EMI tape deck. Monitoring of the array performance was achieved by displaying demodulated signals on to a 16-channel jetpen at the same time as they were being recorded. As a check on the quality of the recording a replay head and single channel demodulator were provided.

Seismometer gains were controlled individually at each pit and required manual adjustment. Changes in gain were therefore kept to a minimum and only undertaken when a break in shot firing of at least two hours was expected.

2.4 Magnetic tape replay

2.4.1 Seismic Processing Laboratory

All the records, except those from Lownet and Lagg, were played out at Durham in the Seismic Processing Laboratory. Here ¼", ½" and 1" tapes can be demodulated and the outputs routed via a sliding-pin matrix board to any of the output devices. These are: a CTL Modular 1 computer, a 16-channel jetpen paper recorder, a 12-channel oscilloscope, an X-Y plotter, three variable frequency filters and eight fixed passband filters.

2.4.2 Durham ¼" replay

The ¼" tapes recorded on the Durham recorders were played back on an 8-track deck - the replay speed of which is fixed to be exactly 10 times that of the field recorder. This is done by means of the 100 hz reference frequency recorded on to the tape. This removes any low frequency component of flutter whilst higher frequencies are removed by subtracting the remaining signal on the reference track from each of the seismic tracks. The replay head on the playback tape recorder has adjustable skew so that the skew of the field recorder can be exactly matched.

2.4.3 Geostore replay

The ½" tapes recorded on the Geostore recorder were replayed at a speed-up factor of 10 on a playback machine loaned from the NERC Seismic Equipment Pool. Flutter compensation is achieved by subtracting the signal on the reference track from each seismic track. In general, flutter on these recording decks was found to be much less of a problem than on the Durham equipment, possibly because of their much greater inertia they were less capable of rapid speed changes. Skew on these recorders is so small that it is not identifiable.

2.4.4 Laxay and Eskdalemuir Arrays

Records obtained on the Laxay mobile array and at Eskdalemuir array station were played out at Durham through an EMI 24-track replay system. The tapes were recorded at 0.3 i.p.s. and replayed at 3 times real time. Flutter compensation was achieved by subtracting the reference track from each seismic track. The seismic tracks were found to have a high frequency noise of about 100 hz superimposed upon them, and this was removed by a set of frequency filters set to cut off frequencies above 30 hz.

2.4.5 Lownet network and the Irish station

Records from the Lownet network were replayed at the IGS in Edinburgh. Variable frequency filters were provided and a speed-up factor of 10 was used. Records from Lagg were replayed in Dublin and the records made available for use at Durham.

2.5 Reduction and processing

2.5.1 Analogue replay

Tapes from the three-component sets, both Durham equipment and Geostore were replayed directly on to the 16-channel jetpen so that the three seismic tracks and their frequency filtered versions, together with higher gain versions, were bracketed between two time-code tracks. Each event was displayed at 10 mm sec^{-1} and 50 mm sec^{-1}. The first speed provided an easily identifiable picture of the various arrivals and was used when a stacked record section was drawn by hand. The faster speed was used to enable picking of the onset times of first arrivals to an accuracy of 0.02 seconds. In order to retain a sharp onset for any event at such a fast speed it was necessary to use the unfiltered records which contain frequencies of up to about 20 hz. Filtered records were used mostly as a guide to the general shape of the train of arrivals, particularly where high frequency noise was a problem (greater than 15 hz and probably generated by wind at the recorders).

2.5.2 Digitisation

In order to facilitate further processing, approximately 50 per cent of the records were digitised on to magnetic tape using the Modular 1 computer. The three-component records were digitised at 50 samples sec^{-1} on to 8-track magnetic tape as three seismic tracks, three filtered seismic tracks (filtered between 1 - 15 hz) and a time-code. The Laxay array tapes were digitised at 83 samples sec^{-1} on to 16-track tape as eight seismic tracks (filtered between 0.1 - 30 hz) and a time-code.

2.5.3 Computer stacking

A major tool in the interpretation of most crustal refraction projects is the stacked record section, or "$T - \Delta/6$" plot. Here, all shots recorded at one station are displayed side-by-side at a reduced time and with a spacing which depends on their range (Δ). A program was written in FORTRAN IV for use on the Northumbrian Universities Multiple Access Computer (NUMAC) IBM 370/168 which takes digital magnetic tapes recorded on the Modular 1 computer and produces a stacked record section on a Calcomp 11" or 30" X-Y plotter. An example of such a stacked record section is given in Figure 2.5.

For each event there is a particular time which occurs at zero on a $T - \Delta/6$ plot which can easily be found from the origin time and range of the event. As each event is recorded on a tape-file as a string of digits, the number of the sample which contains that time can be found and used to correctly position the event on the plot.

The program allows the amplitude of each seismic trace to be adjusted to take account of any recorder gain changes made in the field and also, by multiplying each trace by the inverse of the range, to take account of some of the dependence of amplitude on distance. Any of the tracks on tape can be plotted and a plot of time-codes was found particularly useful in positioning the traces. A Tektronix 4013 storage oscilloscope was found useful for previewing the plot before sending it to the X-Y plotter. A listing of the program, together with a sample sequence of run commands, is given in Appendix C.

2.6 Cambridge University North Sea shots

As explained in Section 2.1, the withdrawal of the Royal Navy prevented the firing of shots planned for Moray Firth in 1975. As part of a crustal refraction project in the North Sea, Cambridge University Department of Geodesy and Geophysics fired a series of large shots in the North Sea and Moray Firth in June and July, 1977. As such shots

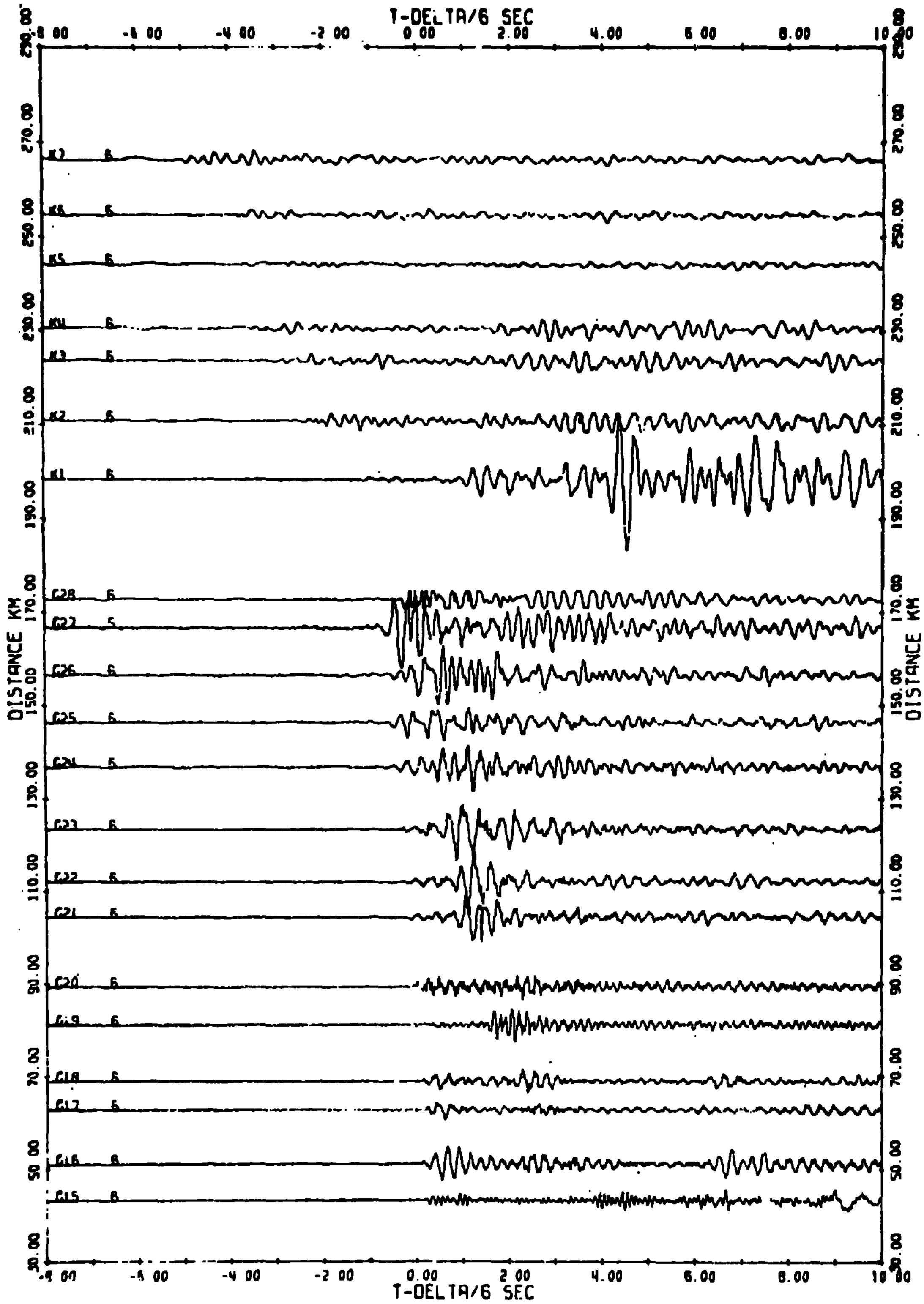

Figure 2.5 Example of computer drawn stacked record section for G and K shots recorded at Laxay. Filtered vertical seismometer.

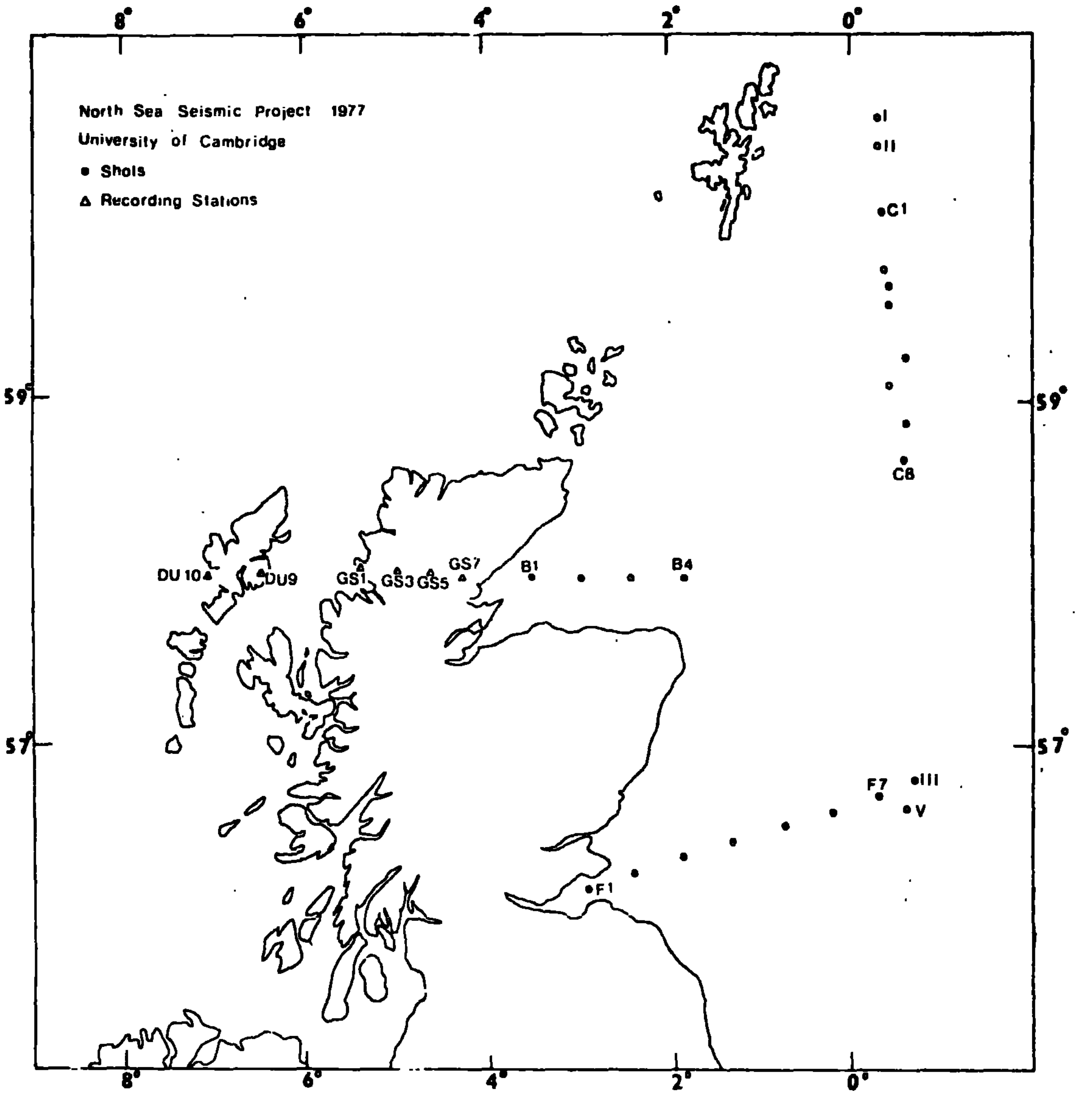

Figure 2.6 Map of shot positions for Cambridge University North Sea project 1977 with HMSP stations reoccupied by Durham University.

would effectively give reversal over the land section of HMSP, six of the stations on the Mainland and Outer Hebrides were re-occupied by Durham University personnel using four <u>Geostore</u> recorders borrowed from NERC and two <u>Durham Mk II</u> recorders. The stations reoccupied were GS1, GS3, GS5, GS7, DU9 and DU10. The shots fired by Cambridge University are shown in Figure 2.6. The records were replayed in Durham and the arrivals have been included in the analysis in Section 4.5.

CHAPTER 3

INTERPRETATION METHODS

3.1 Introduction

The first method of interpretation used in any refraction project is the construction of first arrival travel-time graphs. This enables an estimate to be made of the number of refractors and their apparent P-wave velocities. Reversed coverage of a line enables dipping refractors to be identified from apparent velocity measurements in opposite directions. In instances where it is difficult to decide whether the refractor has a constant velocity, and reversed coverage is available, the plus-minus method of Hagedoorn (1959) is useful.

Once the refractors have been identified and the arrivals from them selected, a time-term analysis can be performed following the approach of Willmore and Bancroft (1960). This method is particularly useful where the shots and stations do not form straight lines but are distributed in a network with stations and shots offset from the major lines. An estimate can then be made of the change in refractor depth at each station or shot - and a crustal structure produced.

After the analysis of first arrivals has revealed the basic crustal structure, later arrivals can be used to supplement the data. In particular, low velocity zones or thin layers are impossible or difficult to observe using refraction alone and their identification often relies on an interpretation of the wide-angle reflections which always occur as late arrivals. The identification of phases such as P_mP or P_mS (reflections from the Moho) and P*P or P*S (reflections from the Conrad) is greatly eased by the construction of stacked record sections. The P_mP phase, in particular, has previously been used in a study of south-west England (Holder and Bott, 1971) to determine estimates of mean crustal velocity and mean crustal thickness. Information from such later arrivals can then be used to modify the original interpretations.

3.2 Travel-time calculations

The onset times for first arrivals were picked for each record from an unfiltered seismometer channel. This was usually the vertical or the in-line horizontal instrument. The quality of the pick was assigned a value which reflected the quality of the record and this was used as a weighting factor in the time-term calculations.

Onset times were corrected for the following errors:

(a) Clock errors - due to drift of the clock. These were found by using the recording of a radio time track and were assigned a negative value, if slow relative to standard time, and a positive value if found fast, relative to standard time.

(b) Static error - due to misalignment of some of the jetpens.

Corrections due to shot depths, water depths and station elevation were not applied at this early stage because these depended upon the type of wave recorded and upon assumptions concerning the velocity structure at the shot.

3.3 Travel-time graphs

In the case where there are n layers above a half-space, the travel-time graph has n+1 segments governed by the travel-time equation. In the simple case of plane parallel layers, the travel-time equation for the headwave in the nth layer is: (Dobrin, 1960)

$$TT = x/v_n + 2\sum_{i=1}^{n-1} z_i(v_n^2 - v_i^2)^{\frac{1}{2}}/v_n v_i$$

where x is the range of observation

v_i is the velocity in the ith layer below the surface

v_n is the velocity of the refractor

and z_i is the thickness of the ith layer below the surface.

Figure 3.1(a) shows the shape of the travel-time curves for the above situation. The gradient of any segment of the curve gives the velocity in the refractor, whilst the intercept on the time axis gives the delay time which is governed by the thickness of the layers and their velocities. The thickness, z_{n-1}, of any of the layers can be found by observing the velocities of the n layers and the intercept time Ti_{n-1}:

$$z_{n-1} = Ti_{n-1}v_n v_{n-1}/2(v_n^2 - v_{n-1}^2)^{\frac{1}{2}} - 2\sum_{i=1}^{n-1} z_i(v_n^2 - v_i^2)^{\frac{1}{2}}/v_n v_i$$

An extension of the method allows the calculation of depths and velocities when the layers are uniformly dipping at some angle, a, and observations 'updip' and 'downdip' are available (Figure 3.1(b)). The gradients of the refractor travel-time segments here depend on the dip angle as well as the velocity, v_2. The gradients can be used to find the true velocity, v_2, and the dip angle, a.

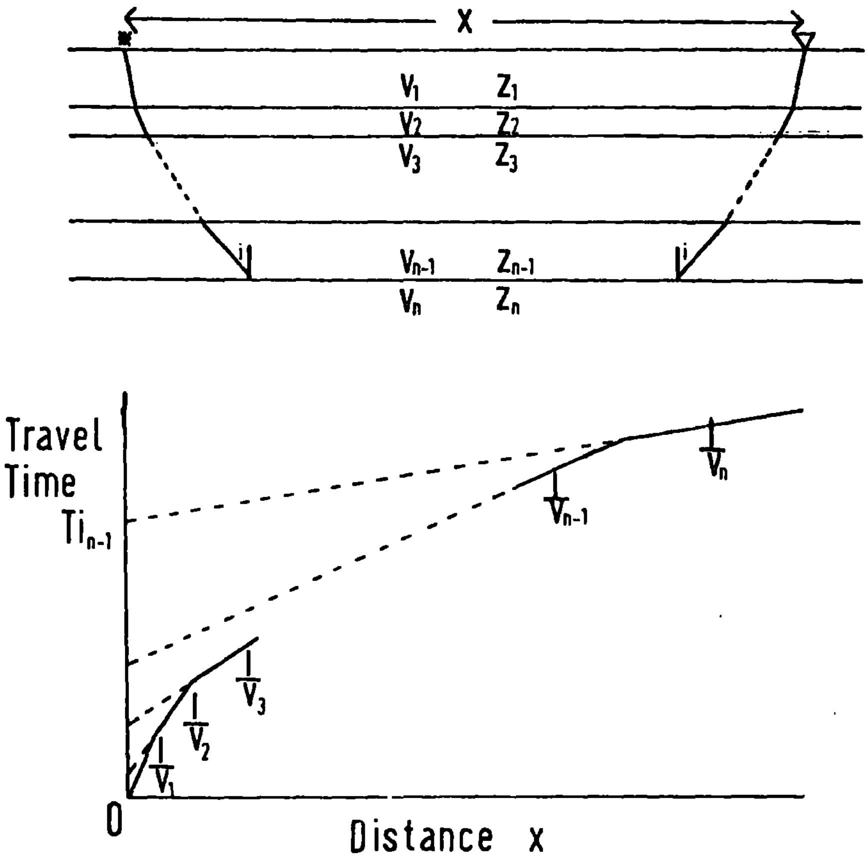

Figure 3.1(a) Travel-time graph for simple plane parallel layered model.

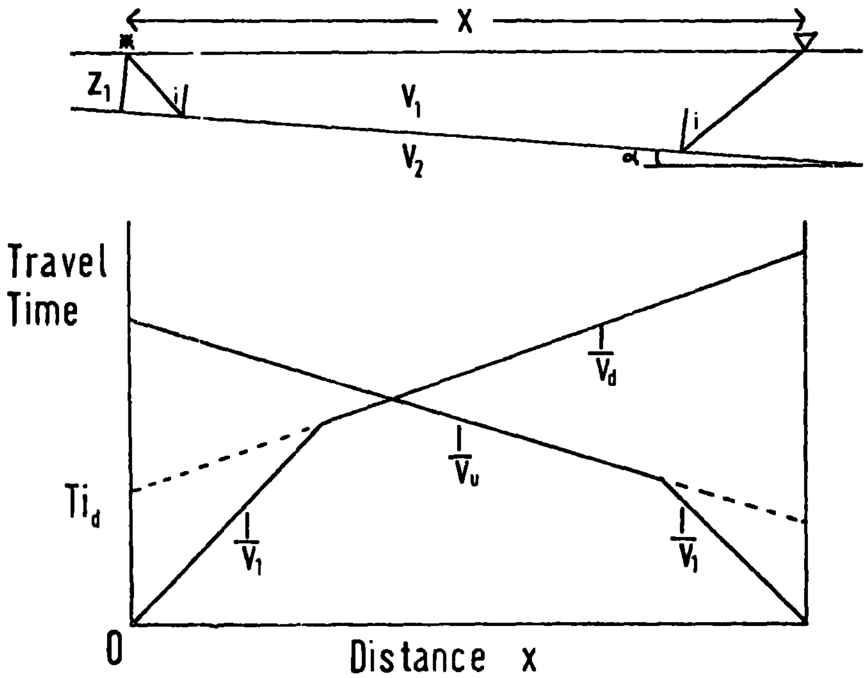

Figure 3.1(b) Travel-time graph for dipping layer model.

This diagram is incorrect. For correct version see Dobrin, 1960 p82.

$$a = \tfrac{1}{2}(\sin^{-1} v_1/v_d \; - \; \sin^{-1} v_1/v_u)$$

$$2(\cos a)/v_2 = 1/v_d \; + \; 1/v_u$$

where v_d is the apparent velocity when shooting 'downdip'
and v_u is the apparent velocity when shooting 'updip'.
Once the dip and velocity have been found the depth to the refractor, z_1, can be found using the intercept time, Ti_d.

$$Ti_d = 2z_1(v_2^2 - v_1^2)^{\frac{1}{2}}/v_1 v_2$$

where Ti_d is the intercept time when shooting 'downdip'.

Further developments of the method can be made to calculate the parameters of more complicated models including layers of increasing velocity with depth.

In practice, the observations are fitted to straight-line segments by the method of least-squares which is programmed for use on the NUMAC IBM 370/168.

The travel-time graph method assumes plane parallel layers with generally step-like changes in the velocity - depth function and gives accurate depths and identification of the number of layers only if the velocity always increases with depth and refractions from each layer give first arrivals. In the case of a crustal refraction project assumptions such as these may not be valid, particularly with regard to low velocity zones and "hidden" layers. A low velocity zone does not produce headwaves but "delays" waves travelling through it to and from the next refractor. A "hidden" layer is a high velocity layer which does not produce first arrival headwaves. Such a situation occurs if the layer is so thin that refractions from it arrive at a recording station after the refractions from a layer beneath it. A missed low velocity zone results in over estimates of depths to lower refractors, while "hidden" high velocity layers result in underestimates of such depths.

3.4 Plus-minus method

The plus-minus method of Hagedoorn (1959) is a method of establishing velocity structure laterally within a non-planar refractor. It is used in reversed refraction profiles where the shots are in a line between two stations or, conversely, the stations are in a line between two shots (Figure 3.2).

$$TT_{AN} = AN/v_2 + D_A + D_N$$

$$TT_{BN} = BN/v_2 + D_B + D_N$$

$$TT_{AB} = AB/v_2 + D_A + D_B$$

where D_A, D_B and D_N are delay-times at A, B and N,

and TT_{AB} is the travel-time between A and B, and so on.

$$\text{Minus-time} = M = TT_{AN} - TT_{BN} = (AN - BN)/v_2 + D_A - D_B \quad (1)$$

$$\begin{aligned}\text{Plus-time} &= TT_{AN} + TT_{BN} - TT_{AB} = (AN + BN - AB)/v_2 + \\ &\qquad D_A + D_B + 2D_N - D_A - D_B \\ &= 2D_N\end{aligned}$$

In order to determine the plus-times it is necessary to have a shot and station coincident so that the end-to-end time, TT_{AB}, can be found. The plus-time can then be interpreted in terms of depth to the refractor, z, by means of the

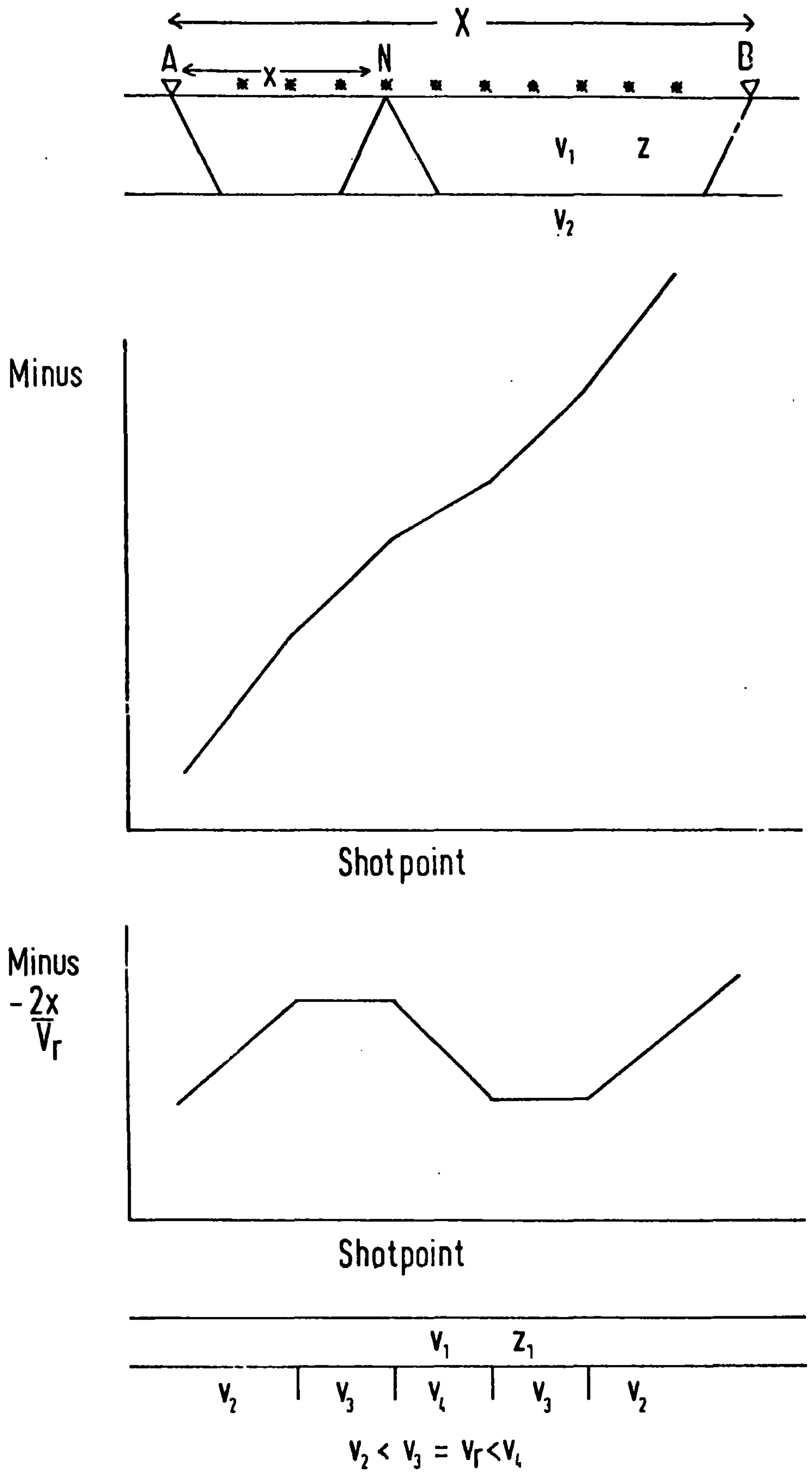

Figure 3.2 Minus-time graph and reduced minus-time graph for refractor with laterally varying velocity.

relationship:

$$\text{Plus-time} = 2z(v_2^2 - v_1^2)^{\frac{1}{2}}/v_1 v_2$$

In this respect the plus-time is a method of evaluating a time-term using a pair of observations in opposite directions. In the method of time-term analysis, considered later (Section 3.5), all observations for a particular shot are used to calculate the time-term.

If the velocity of the refractor is not v_2 but varies laterally, this will be revealed by a plot of minus-time versus position of the shot, N. Re-expressing equation (1):

$$\text{Minus-time} = M = (X - 2x)/v_2 + \text{constant}$$

The minus-time can be seen to be independent of the delay-time at the shot but to be dependent on the velocity of the refractor at the shot. A plot of minus-time against shot position N, shows, by changes in gradient, where any velocity changes occur in the refractor. In order to amplify such changes in gradient, a reduced minus-time is plotted in a similar manner to that adopted on stacked record sections. In this case the reduction velocity, v_r, is selected to be near to the velocities to be expected in the refractor.

$$M - 2x/v_r = (X - 2x)/v_2 - 2x/v_r + c$$

The gradient of a plot of $M - 2x/v_r$ against position of shot N, x, is given by:

$$G = (X - 2)/v_1 - 2/v_r$$

so that

$$v_1 = (X - 2)v_r/(Gv_r + 2)$$

Figure 3.2 shows the minus-time graph and reduced minus-time graph for a refractor with several different velocities.

Once the velocity structure has been established and the depth to the refractor found at each shot, a new estimate of the travel distance, x, can be obtained and an iterative procedure adopted to 'home in' on the detailed structure.

In the case where station and shots are not in a line, that is, one of the stations is offset from the line, the reduced minus-time graph can still be used to identify velocity changes within the refractor. If a single velocity refractor gives rise to refractions observed at stations S1 and S2 the reduced minus-time graph does not have a single gradient, but is curved. A set of curves constructed for a single velocity refractor with a varying recording network geometry is shown in Figures 3.3 and 3.4. Such theoretical curves can be compared with the observed curves to determine the difference from a constant velocity refractor. A computer program was written for use on the NUMAC IBM 370/168 which allows a comparison of the theoretical and observed curves for the actual geometry of the recording arrangement (Appendix C). This approach was found very useful in interpreting the results from HMSP since the stations could not be sited exactly in line with a series of shots.

3.5 Time-term analysis

The travel-time equation of a refracted headwave between

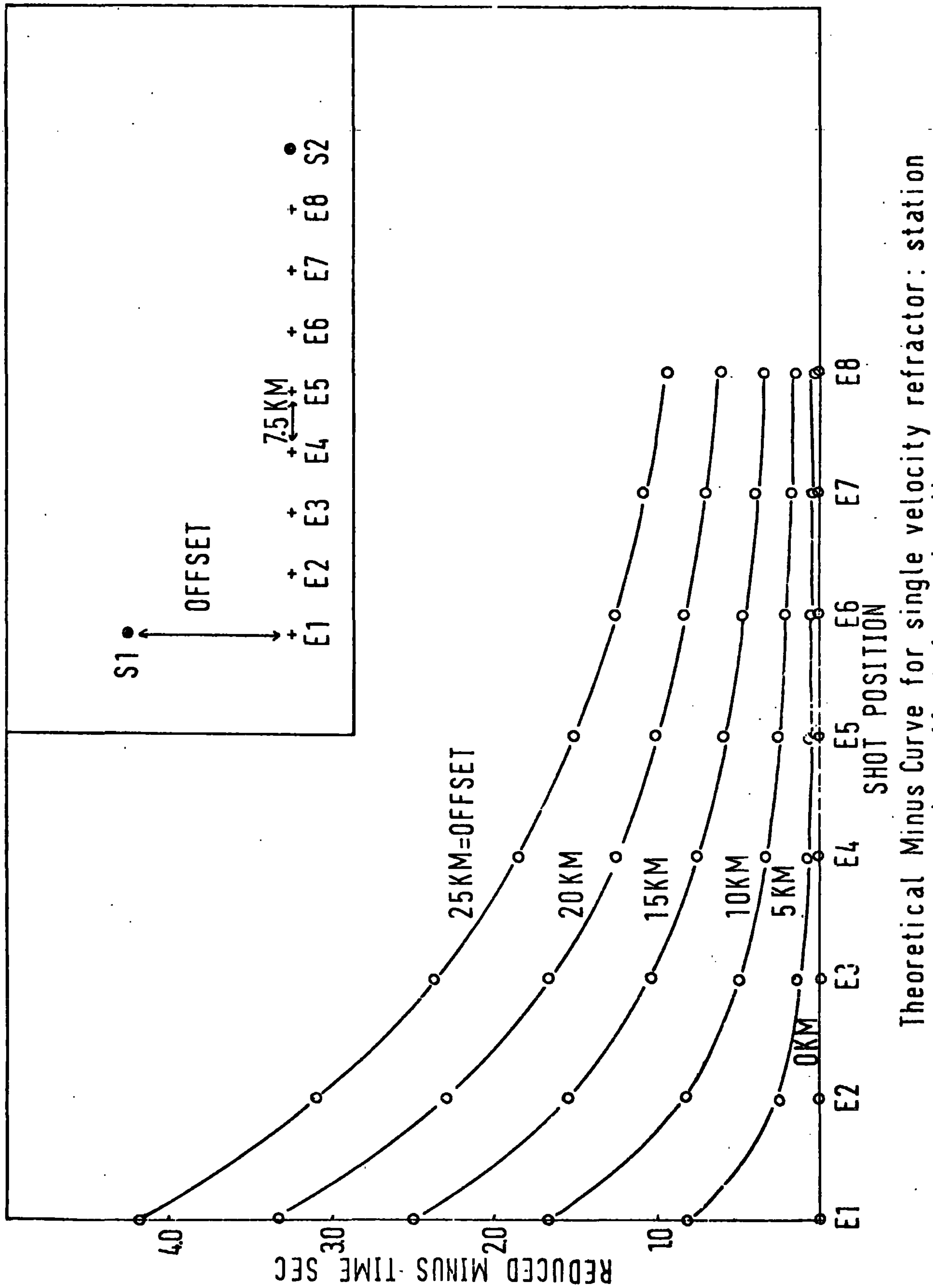

Figure 3.3 Reduced minus-time graph for uniform velocity refractor observed with one station offset from the shot line.

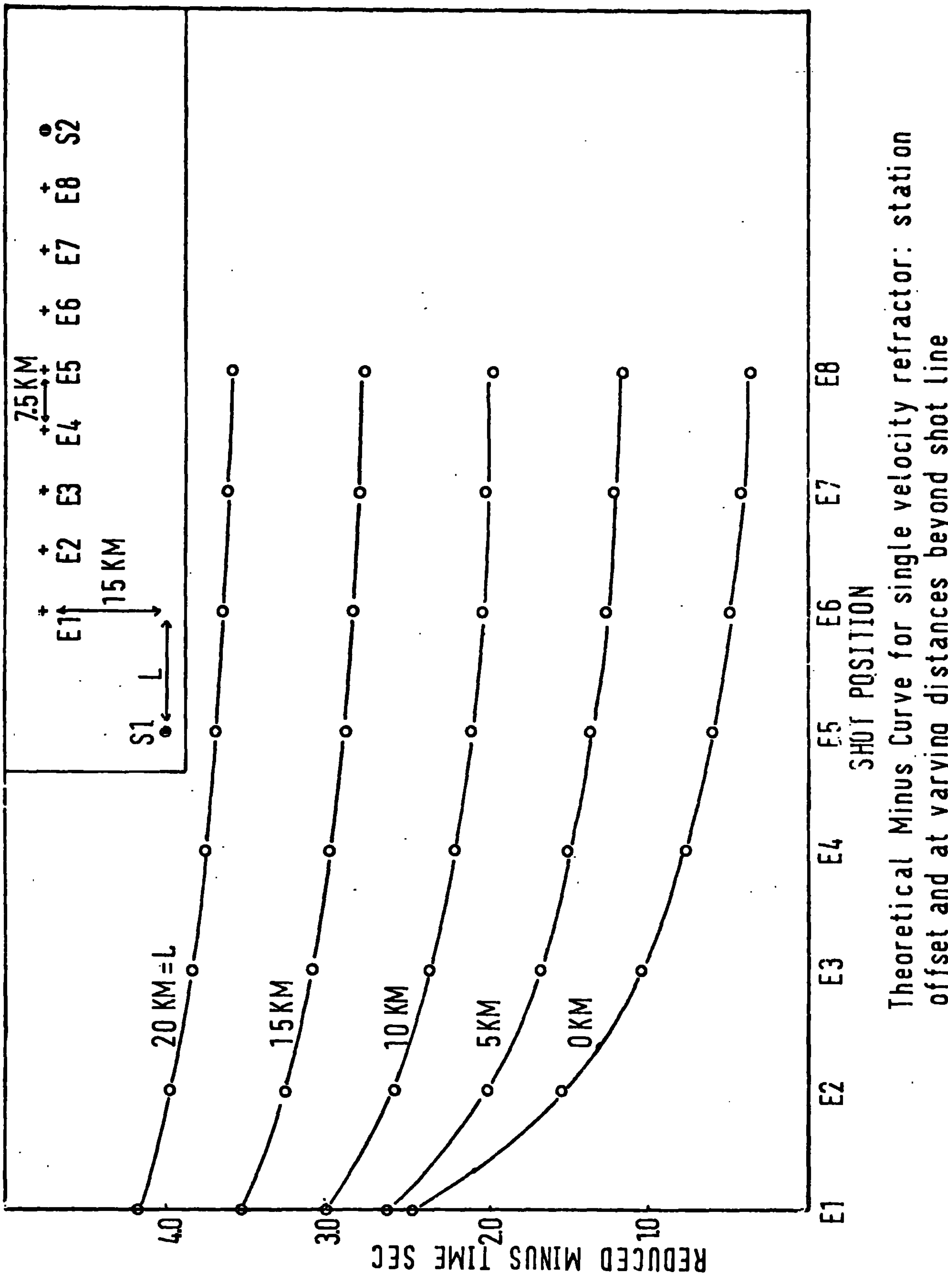

Figure 3.4 Reduced minus-time graph for uniform velocity refractor observed with one station offset from, and beyond the end of, the shot line.

two stations can be expressed as:

$$T_{ij} = x_{ij}/v + a_i + a_j + \delta_{ij} \qquad (2)$$

where T_{ij} is the travel-time between station i and shot j

x_{ij} is the distance between station i and shot j measured along normals to the refractor

a_i is a time-term at station i) together equal to the intercept time on a travel-time graph

a_j is a time-term at shot j)

δ_{ij} is an observational error

and v is the velocity in the refractor.

In the case of a refraction project such as HMSP, the total number of observations of T_{ij} exceeds the number of unknowns - a_i, a_j and v. The set of equations is thus over-determined and the unknowns can be found by regression analysis.

The method of time-term analysis requires that:

(1) the refractor has small dip so that the time-terms calculated from differing azimuths apply to points of similar depth on the refractor

(2) the curvature of the refractor is small, i.e. headwave follows the top of the refractor

(3) the velocity of the refractor is constant

(4) the velocity structure of the overburden is dependent only on the perpendicular distance to the refractor

(5) the value of the time-term can be constrained in some way.

Allowances can be made if any of these criteria are not satisfied.

The computational technique of Berry and West (1966) has been adapted by Swinburn (1975) for use on the NUMAC

IBM 370/168 and is followed here. Linear regression is performed to minimize the sum of the squares of the residuals between observed and calculated travel-times.

The m equations (m observations) like equation (2) can be written in matrix form

$$[A][a] = [T] - \frac{1}{v}[x]$$

where $[A]$ is a m x n coefficient matrix (n = i + j)

$[a]$ is a n x 1 column matrix of unknown delay-times

$[T]$ is a m x 1 column matrix of travel-times

and $[x]$ is a m x 1 column matrix of distances.

For the sum of the squared residuals, $\sum R^2$, to be a minimum, the time-term matrix, $[a]$, is given by:

$$[a] = [A^T A]^{-1}[A^T][T] - \frac{1}{v}[A^T A]^{-1}[A^T][x]$$

or $$[a] = [e] - \frac{1}{v}[f]$$

where $[e] = [A^T A]^{-1}[A^T][T]$

and $[f] = [A^T A]^{-1}[A^T][x]$

For each travel-time equation quantities are assigned:

$$C_{ij} = T_{ij} - e_i - e_j$$

$$D_{ij} = x_{ij} - f_i - f_j$$

The residual now becomes:

$$\delta_{ij} = C_{ij} - D_{ij}/v$$

Differentiating the sum of the squares of the residuals with respect to the velocity, v, gives the least-squares velocity, v.

$$v = \sum_i \sum_j D_{ij}^2 / \sum_i \sum_j C_{ij} D_{ij}$$

An estimate of the variance of the solution for the least-squares velocity is:

$$\sigma^2 = \sum_i \sum_j \delta_{ij}^2 / (m - n - 1)$$

and the standard error of the velocity is given by:

$$Se(v) = v^2 Se(1/v)$$

where $Se(1/v) = \sigma^2 / \sum_i \sum_j D_{ij}^2$

The standard error of the k th time-term is given by Berry and West (1966) as:

$$Se(a_k)^2 = \sum_{i=1}^{L} \delta_{ij}^2 / L(L-1)$$

where L is the number of observations of time-term a_k.

The confidence limit for each time-term is estimated by multiplying this standard error by the appropriate value in the student's t-distribution table (two-ended) for L-1 degrees of freedom.

In order to fully determine the absolute values of all the time-terms it is necessary to constrain the solution in some way. If there is no constraint, an arbitrary constant k, say, could be added to all the station time-terms and subtracted from all the shot time-terms without affecting the travel-times. In practice, if a shot and station are coincident they will each have a time-term calculated, from which the value k can be found. Alternatively, if the value of a time-term is known, either from a good knowledge of the geological structure or from previous work, the solution can be constrained.

In HMSP little difficulty was experienced in constraining the Moho refraction, P_n, because several of the stations had known time-terms. However, for the basement refractor, P_g, constraints were difficult to determine in some instances as shots close to stations were normally sited on very different geological structures. For example, the station at Lemreway (DU9) was on Lewisian gneiss whereas the adjacent shot (G14), only 5.3 km away, was on a substantial thickness of sediments.

The strength of a time-term analysis lies in its ability to accurately and confidently determine the refractor velocity and shape when no true reversal exists. Consider the worst possible layout of a refraction experiment - a line of shots recorded at a line of stations sited all to one side. This is the classic case of an unreversed refraction project. Without strong constraints on the value of two or more of the time-terms a least-squares solution would be impossible to obtain, as a significant change in velocity could be accommodated by systematic changes in the time-terms (dip) without affecting the fit of the solution. If, however, the network has been arranged so that links between shots and stations are measured over a variety of azimuths, the true velocity and refractor shape can be found. Consider a recording station well offset at right angles from the main line so that it only differs in range from each shot by a small amount. Nearly all the variation in travel-times observed for the shots will be due to the variation of time-terms at the shots and will have no significant dependence on the refractor velocity used in the solution. Such an arrangement thus defines the relative values of the time-terms which the remainder of the network uses as a constraint on the solution. In Chapter 4 an example will be given of the improvement made to a solution, obtained by adding to the data set a station offset from the shot line.

The extent to which a time-term solution fulfills some of the required criteria of effectiveness can be assessed from the systematic variation of the observed minus calculated residuals. If the velocity of the refractor increases with depth (or distance) the residuals should be systematically positive at small distances and negative at large distances. Anisotropy of the refractor with direction should also be revealed by a residual versus azimuth plot (Bamford, 1973).

Using a program by Swinburn, the time-term analysis can be extended to allow for a linearly increasing velocity with distance which could be interpreted as an increasing velocity with depth within the refractor. A velocity function $v(x)$ is proposed:

$$v(x) = v_o - kx$$

where v_o is the initial velocity

x is the distance from source

and k is a constant.

The distance dependent term in the travel-time equation for a headwave is:

$$t_{ij} = \int_i^j (v_o + kx)dx = \frac{1}{k} \ln(1 + kx_{ij}/v_o)$$

$$= x_{ij}/v_o + kx_{ij}^2/2v_o^2 + k^2x_{ij}^3/3v_o^3 + \ldots \text{ terms in } k^3 \text{ and above.}$$

If k is small (i.e. 10^{-1}) terms in k^2 and above are below the measured time accuracy and the travel-time equation becomes:

$$t_{ij} = x_{ij}/v_o - kx_{ij}^2/2v_o^2 + a_i + a_j + \delta_{ij}$$

which can be solved for v_o, k and the time-terms a_i and a_j by linear regression.

3.6 Wide-angle reflections

In addition to the refracted arrivals observed in a crustal refraction experiment there are usually supercritical reflections from the Moho and sometimes from other interfaces. Indeed, the evidence for the existence of crustal low velocity zones relies mainly on observations of wide-angle reflections from the top and bottom of such zones (e.g. Braile and Smith, 1974).

The travel-times of reflections can be interpreted by the classical reflection technique (called "T^2/X^2" method) to give an average crustal thickness and average crustal velocity. Figure 3.5 shows the arrangement of the wave paths and the travel-time curves. The equation for the travel-time is:

$$T^2 = X^2/V_1^2 + Z^2/4V_1^2$$

So a plot of T^2 against X^2 is a straight line with gradient $1/V_1^2$ and intercept time $Z^2/4V_1^2$.

In addition to the travel-time information, the wide-angle reflections show interesting amplitude information. Theoretical calculations by Berry and West (1966), based

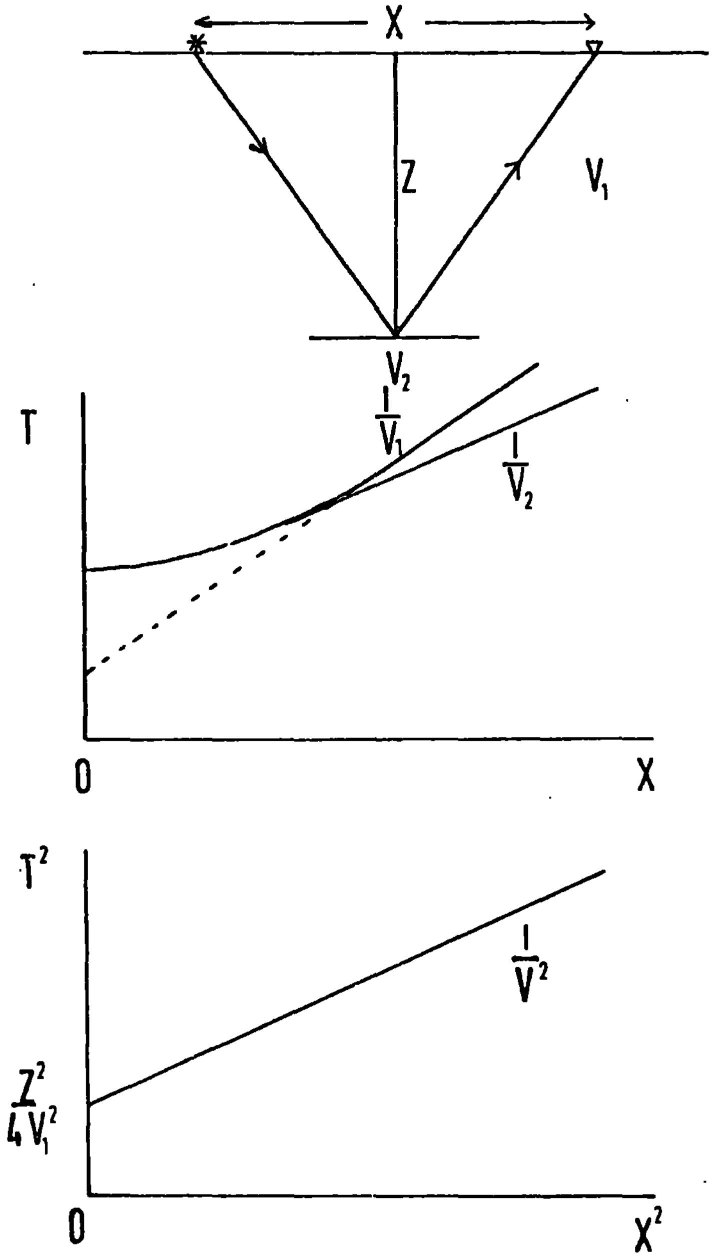

Figure 3.5 Travel-time graph and T^2/X^2 graph for wide-angle reflections.

on geometrical wave theory, show a substantial maximum in amplitude close to the critical distance. Červený (1966) has shown that, in the region of the critical distance, geometrical ray theory is not an adequate approximation and that the maximum amplitude of the reflection occurs at some distance beyond the critical distance. The size of this excess value is dependent upon the frequency of the wavelet. For a signal of 3 hz, the distance beyond the critical distance at which the maximum in amplitude occurs is about 15 km.

Holder and Bott (1971) showed how the thickness, T, and average crustal velocity, $\overline{V}$, could be found when the crustal velocity increases with depth by observing the critical distance and intercept time. They gave the approximate relations:

$$T = \tfrac{1}{2}(x_c t_i V_n)^{\frac{1}{2}} \qquad \text{and} \qquad \overline{V} = V_n/(V_n t_i/x_c + 1)^{\frac{1}{2}}$$

where t_i is the intercept time

V_n is the velocity of the Moho headwave

and x_c is the critical distance.

To use this method good observations in the region of the critical distance must be made so that the critical distance and intercept time can be found accurately. Also, the amplitude response of the shot - station pair must be accurately known so that the maximum in amplitude can be identified confidently.

3.7 Velocity filtering

Up to this point the processing techniques described have concentrated upon a single phase of arrivals and have not been generally applicable to all the arrivals in the record. Velocity filtering is a method developed from statistical communication theory which can identify the apparent surface velocity (ASV) and azimuth of any correlatable signal arriving at a number of seismometers distributed in an array. Birthill and Whiteway (1965) showed how the method could be used for the identification and processing of teleseismic data where uncorrelated noise may obscure the signal and where, in general, the phases are widely spaced in time.

Consider an L-shaped array recording a plane wavefront signal with ASV, v, and azimuth, α (Figure 3.6(a)).

The arrival time at each seismometer relative to the origin at O is:

$$t_i = l_i\cos(\beta_i - \alpha)/v = l_i\cos\beta_i\cos\alpha/v + l_i\sin\beta_i\sin\alpha/v$$

$$= y_i\cos\beta_i/v + x_i\sin\beta_i/v$$

So, for any arrival of a given velocity and azimuth, a delay-time can be found for each seismometer, i, which, when applied to the signal, will bring it into phase with all the other traces. All the signals can then be added together which will, in general, improve the signal-to-noise ratio by $n^{\frac{1}{2}}$, where n is the number of traces added. Uncorrelated noise will tend to cancel out on addition.

The difference in travel-time produced by considering a curved wavefront as a plane can easily be found (Figure 3.6(b)).

$$\delta x = x - (x^2 - a^2)^{\frac{1}{2}} \qquad \delta t = (x - (x^2 - a^2)^{\frac{1}{2}})/v$$

Figure 3.6(a) Diagram to show parameters used in calculating the delay-time for any pit located at x_i, y_i for an arrival of apparent surface velocity, $\bar{v}$, and azimuth, α.

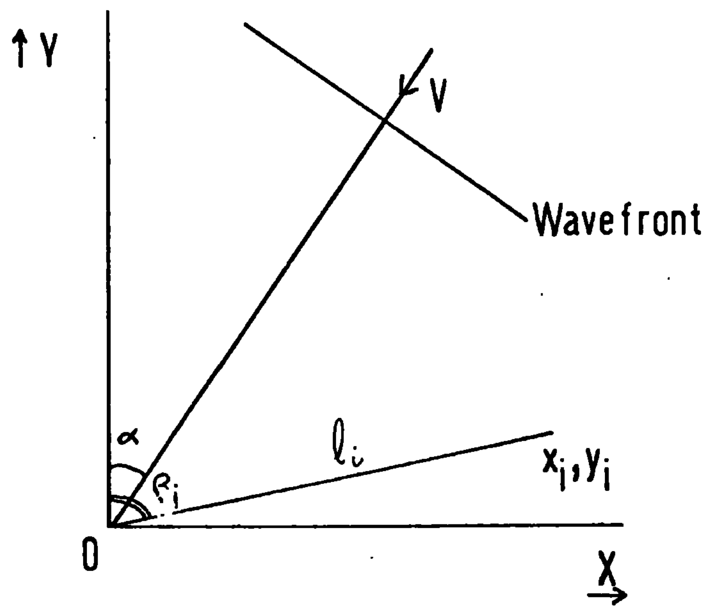

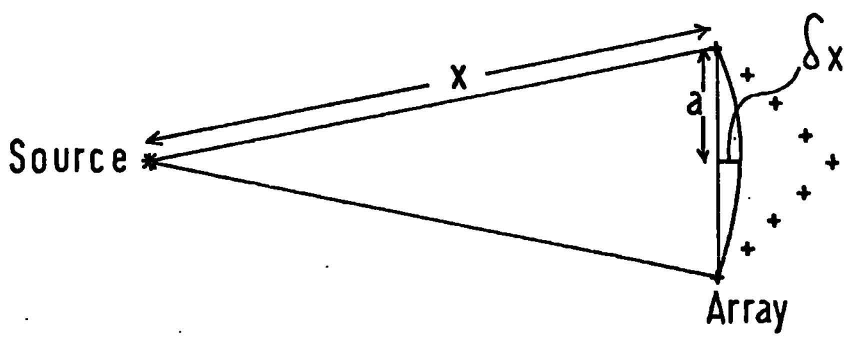

Figure 3.6(b) Diagram to show the parameters used in the evaluation of plane wavefront approximation for an arrival from a distance, x, recorded at an array of half-aperture, a.

where a is the half-aperture of the array

x is the range of the event

and v is the apparent surface velocity.

For the Laxay array (MD1, aperture less than 2 km) with an event of range 40 km and ASV 6 km sec^{-1}, δt is of the order of 0.002 seconds. This is well within the required accuracy.

Events recorded at the Laxay array were transferred on to digital magnetic tape at 83 samples sec^{-1} using the Modular 1 computer at Durham. A search was then made for the maximum amplitude of any particular phase by allowing the ASV and azimuth to vary.

Birthill and Whiteway (1965) showed how the most sensitive measurement technique was to form two partial sums of the data for any particular ASV and azimuth and cross-multiply them point by point. The correlator function thus obtained was smoothed over a time-window of a length comparable to the period of one cycle of the signal. A program for the Modular 1 computer was written in a special language called SERAC (Seismic Record Analysis Compiler) by P.A. Forth and is here adapted to perform a search over a range of velocities and azimuths. An anotated listing of the program is given in Appendix C. Usually an azimuth was selected and the correlelograms for up to 10 velocities were displayed side-by-side on a Hewlett - Packard X-Y plotter. An example of the computer output is given in Figure 3.7. At the far left of the diagram the signal to be processed, as recorded at one seismometer, is displayed. A playout of the time-code is displayed alongside. There follows a series of correlelograms for a particular azimuth and a variety of apparent

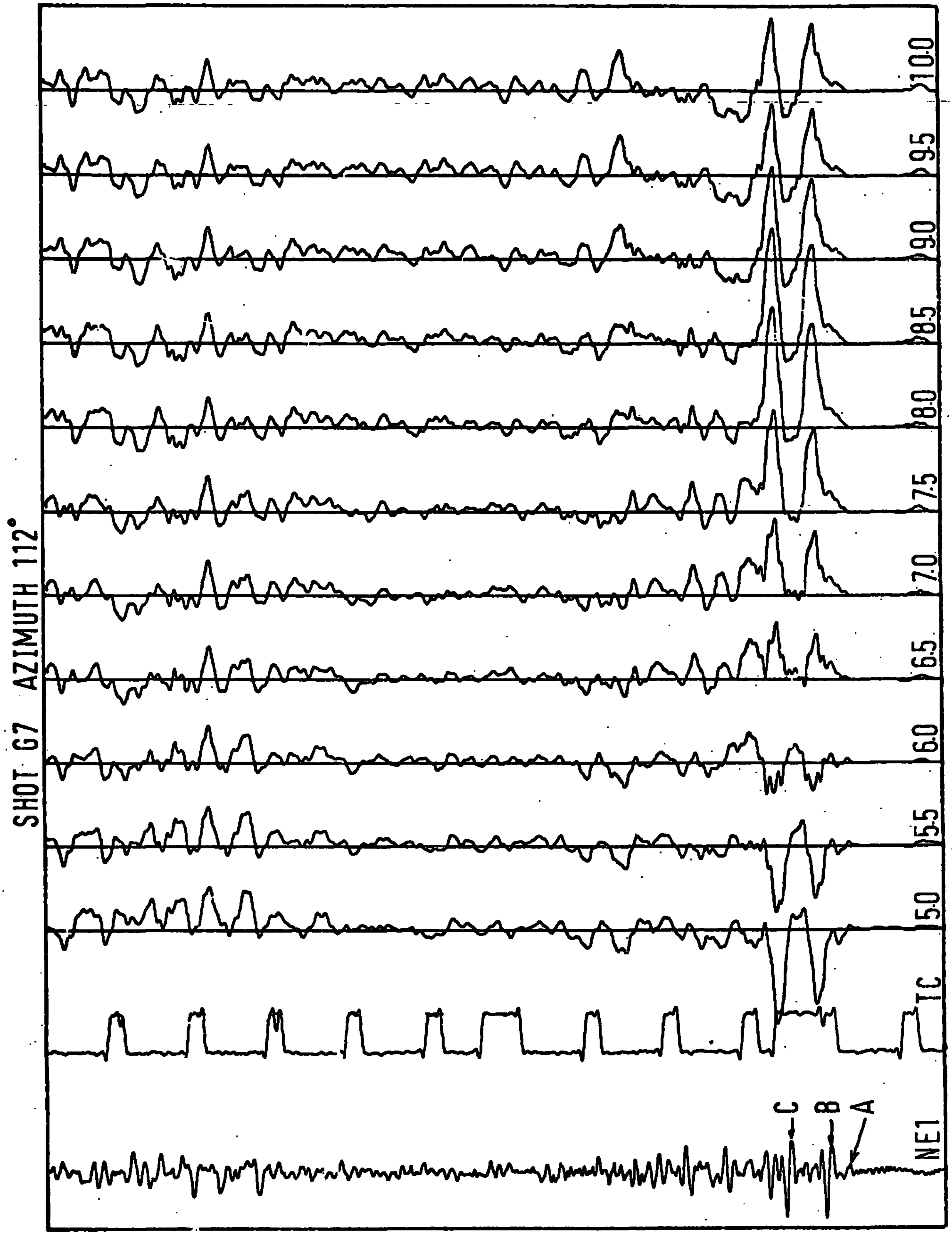

Figure 3.7 Example of computer drawn velocity filter for an explosion recorded at the Laxay array. Smoothed correlelograms for a single azimuth and a series of apparent surface velocities are displayed alongside a time-code and a single seismometer recording of the explosion.

surface velocities. Each maximum peak in the correlelogram corresponds to an arrival in the seismogram and defines its apparent surface velocity.

The resolution of velocity and azimuth is fundamentally controlled by the dimensions of the array relative to the apparent surface wavelength of the signal being considered. If the wavelength of the signal is greater than the array aperture the width of the maximum sensitivity peak is large "... for sharp velocity filtering with high attenuation of signals from the same azimuth it is clear that the dimensions of the array should be at least equal to several signal wavelengths" (Whiteway, 1965). However, too large an array can suffer from lack of coherence of the signal across the array caused by changes in the geologic structure.

It can be seen that the Laxay array falls short of the ideal. (Signals from explosions at the ranges considered have wavelengths of the order of 1 km, i.e. the order of the array aperture). However, velocity determinations of about 0.2 km sec^{-1} accuracy and azimuth resolution of about 10^{o} have been obtained. Typical plots of the azimuth and velocity resolution obtained are shown in Figures 3.8(a), 3.8(b) and 3.8(c).

No real difficulties were encountered due to the limitations in storage capacity of the Modular 1, although this can be the case when dealing with larger arrays. Because delays have to be inserted into each seismic channel a certain amount of data must be present in the memory of the computer at one time. The number of digits so stored obviously depends on the sampling rate, the number of seismic

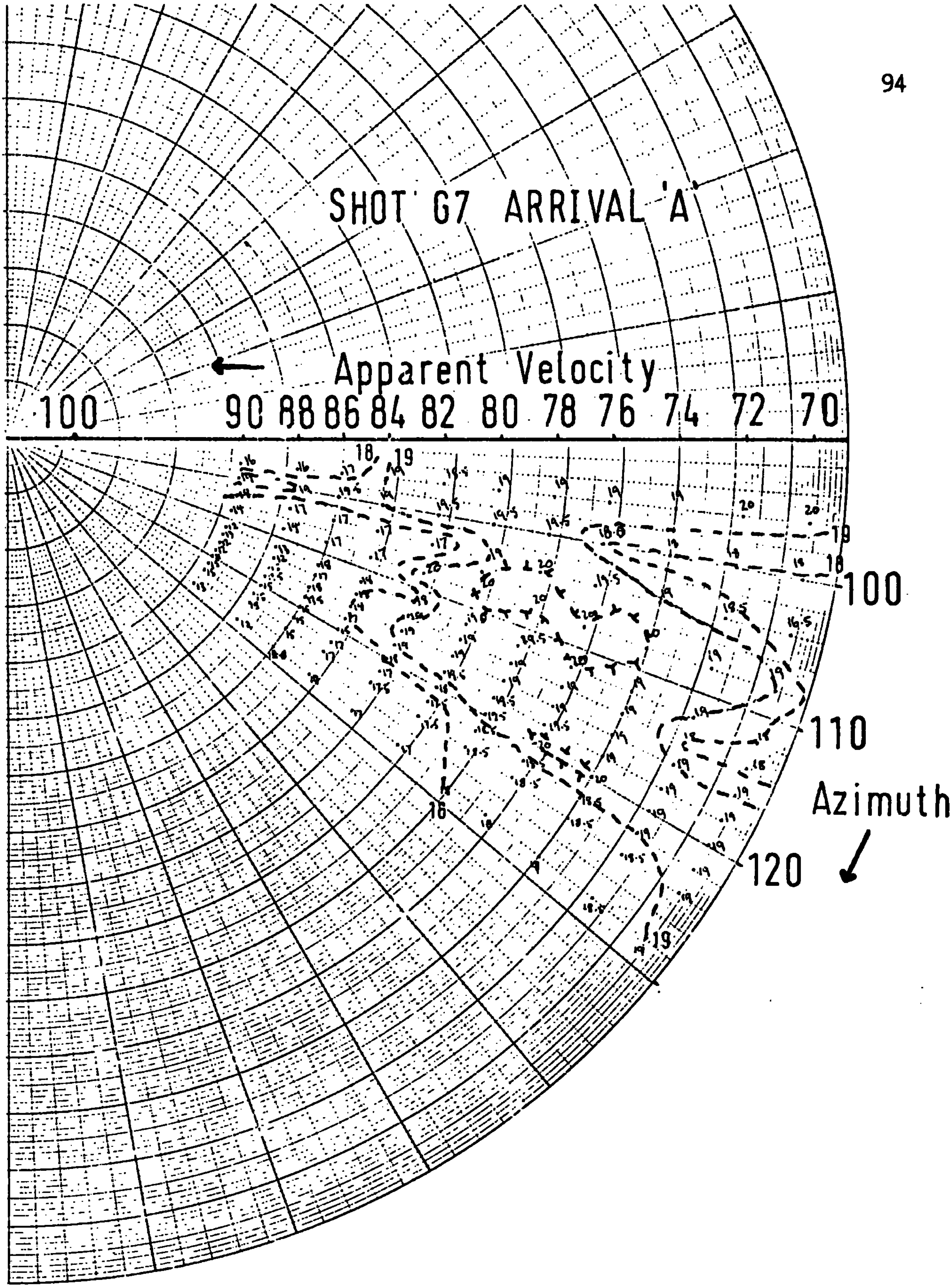

Figure 3.8(a) Contoured velocity/azimuth response plot of the arrival marked A in Figure 3.7. Numbers are the amplitude of the correlation function in mm. The arrival has azimuth about 107° and apparent velocity about 7.7 km sec^{-1}.

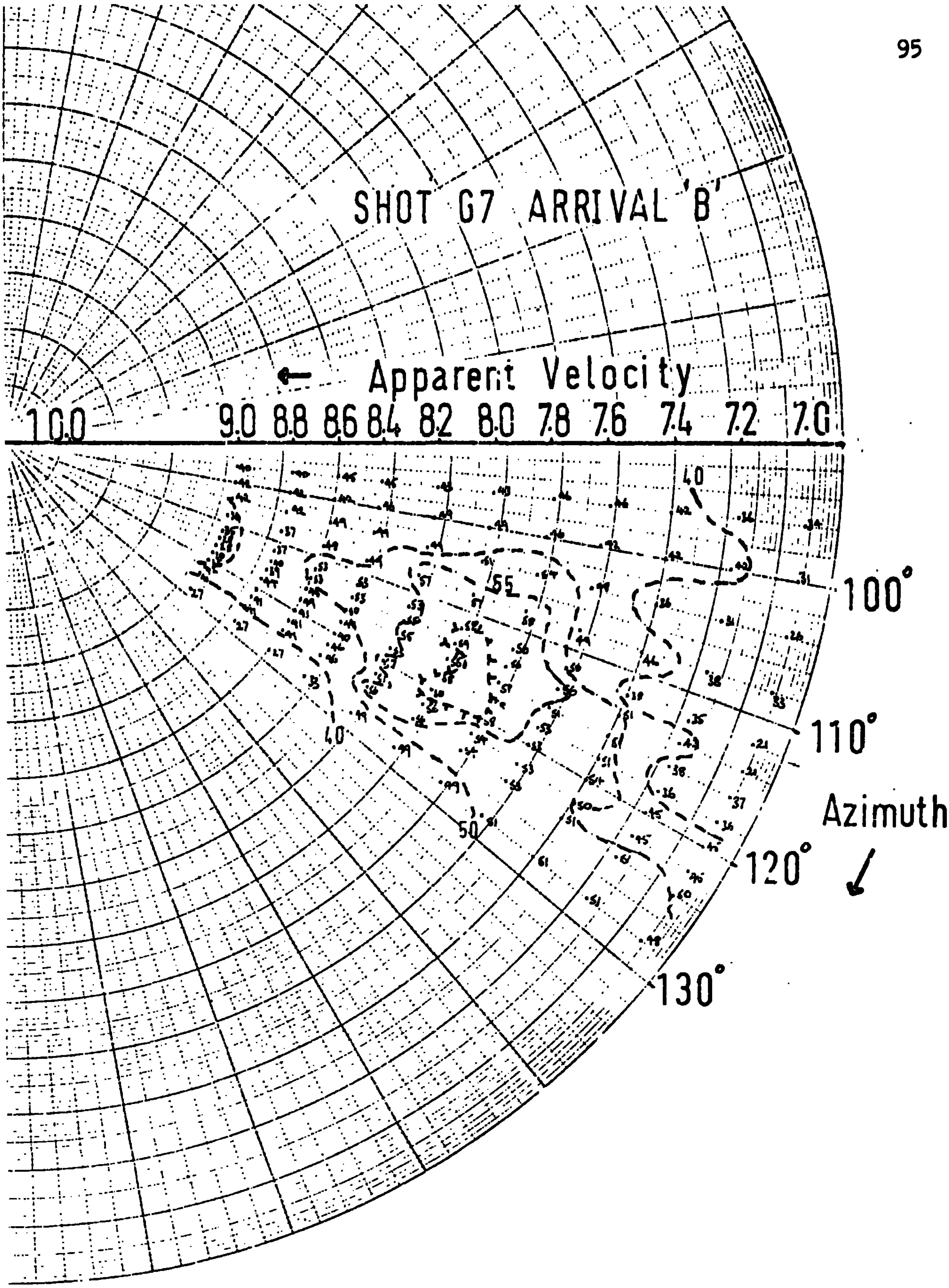

Figure 3.8(b) Contoured velocity/azimuth plot of the arrival marked B in Figure 3.7. The arrival has azimuth about 120° and apparent velocity about 8.0 km sec^{-1}.

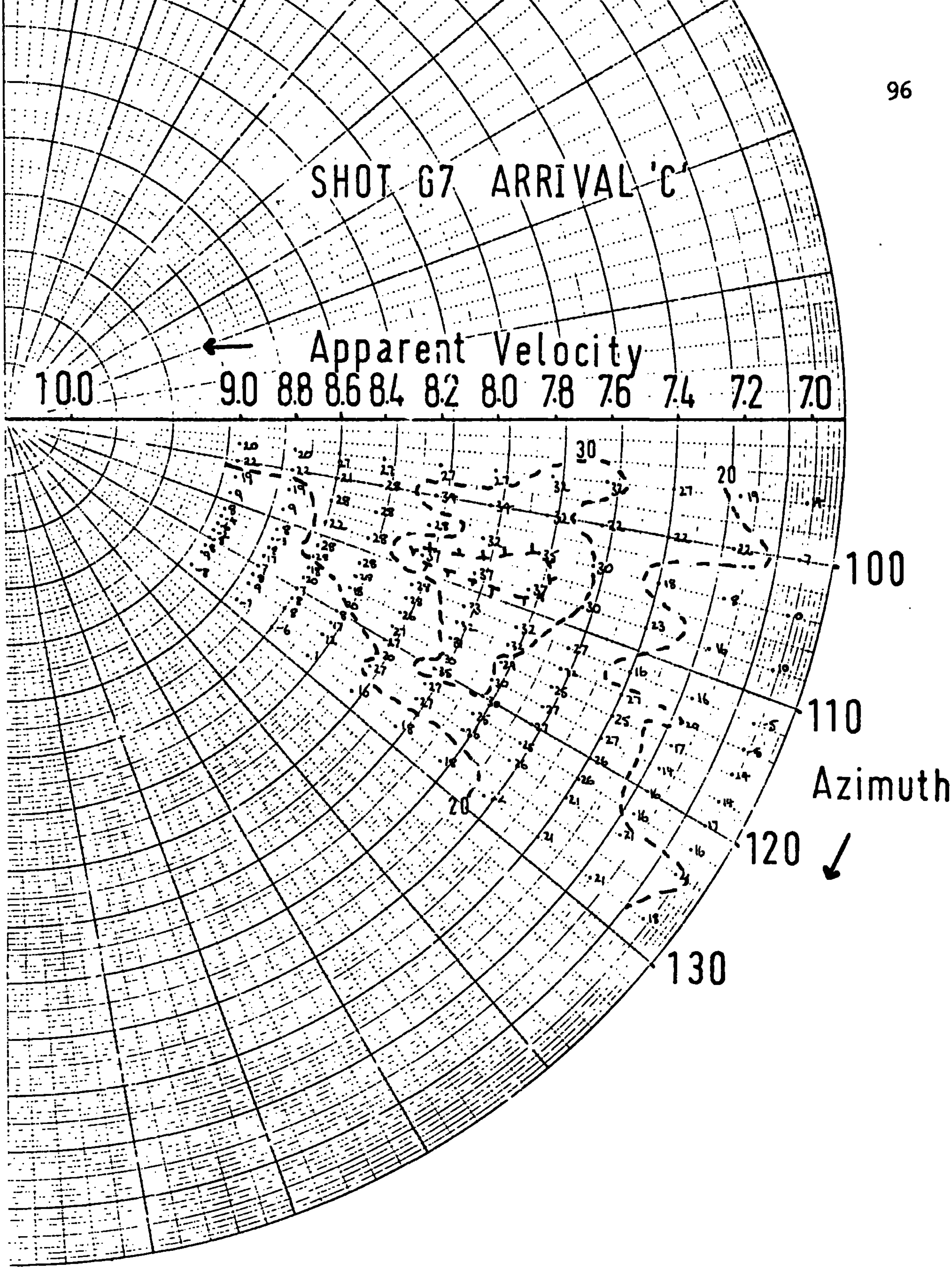

Figure 3.8(c) Contoured velocity/azimuth plot of the arrival marked C in Figure 3.7. The arrival has azimuth about 108° and apparent velocity about 8.0 km sec^{-1}.

channels and the size of the time-delays involved. This last value is determined by the ASV and azimuth of the signal and the dimensions of the array. Manipulation of 16 time-series channels at 83 samples sec^{-1} was easily achieved for signals with velocities as low as 4 km sec^{-1} across this array with its aperture of 1.32 km.

Velocity filtering and its development have been primarily concerned with the processing of teleseismic signals. Attempts to extend the treatment to local earthquakes or local explosions have generally met with less success due to the multiplicity of correlated signals within the records. Maguire (1974) has shown that considering P to S conversions and signals within three orders of magnitude, up to 60 arrivals can be expected within the first 10 seconds of the record from an earthquake at a range of 55 km. Obviously, interference of arrivals is expected to occur. The advantage of knowing the exact range to each shot and hence being able to produce a stacked record section for an array station just as for any other station is now apparent. The results of velocity filtering can be used in conjunction with a $T - \Delta/6$ plot; the major arrivals can be picked out and, by tracing them from shot to shot, interference phenomena may be identified. McCamy and Meyer (1964) used velocity filtering techniques to analyse results from a crustal refraction project and found a wealth of correlated second arrivals, many of which were difficult to explain in terms of simple reflections and refractions.

3.8 Particle motion processing

It was felt useful to process some of the data from HMSP using the method of Shimshoni and Smith (1964) which attempts to separate signals recorded by a three-component station on their particle motions. Once again the construction of a T - Δ/6 plot provided the possibility of checking correlations from shot to shot against the results of this method.

In principle, the method separates rectilinear particle motions, those in phase and those 180° out of phase, from elliptically polarised motions. For arrivals at a pair of seismometers, one vertical and one radial (that is, a horizontal instrument aligned along the direction of the propagating wave), Figure 3.9 shows, diagrammatically, how the responses vary with the type of incident wave. It can be seen from the relative motions how a P-wave has in-phase vertical and radial components which, when multiplied together, give a positive correlation. S-waves are 180° out of phase and hence give a negative correlation on multiplication. Elliptically polarised motions give both positive and negative correlations which have a higher frequency than the original signal.

The practical method used is to form the radial component from the two horizontal components by a simple rotation of axes. The vertical and radial are then multiplied point by point and the resultant correlation smoothed by averaging within a time window, the length of which is adjusted to be the same as one period of the signal. This has the effect of averaging the elliptical motion correlations towards zero,

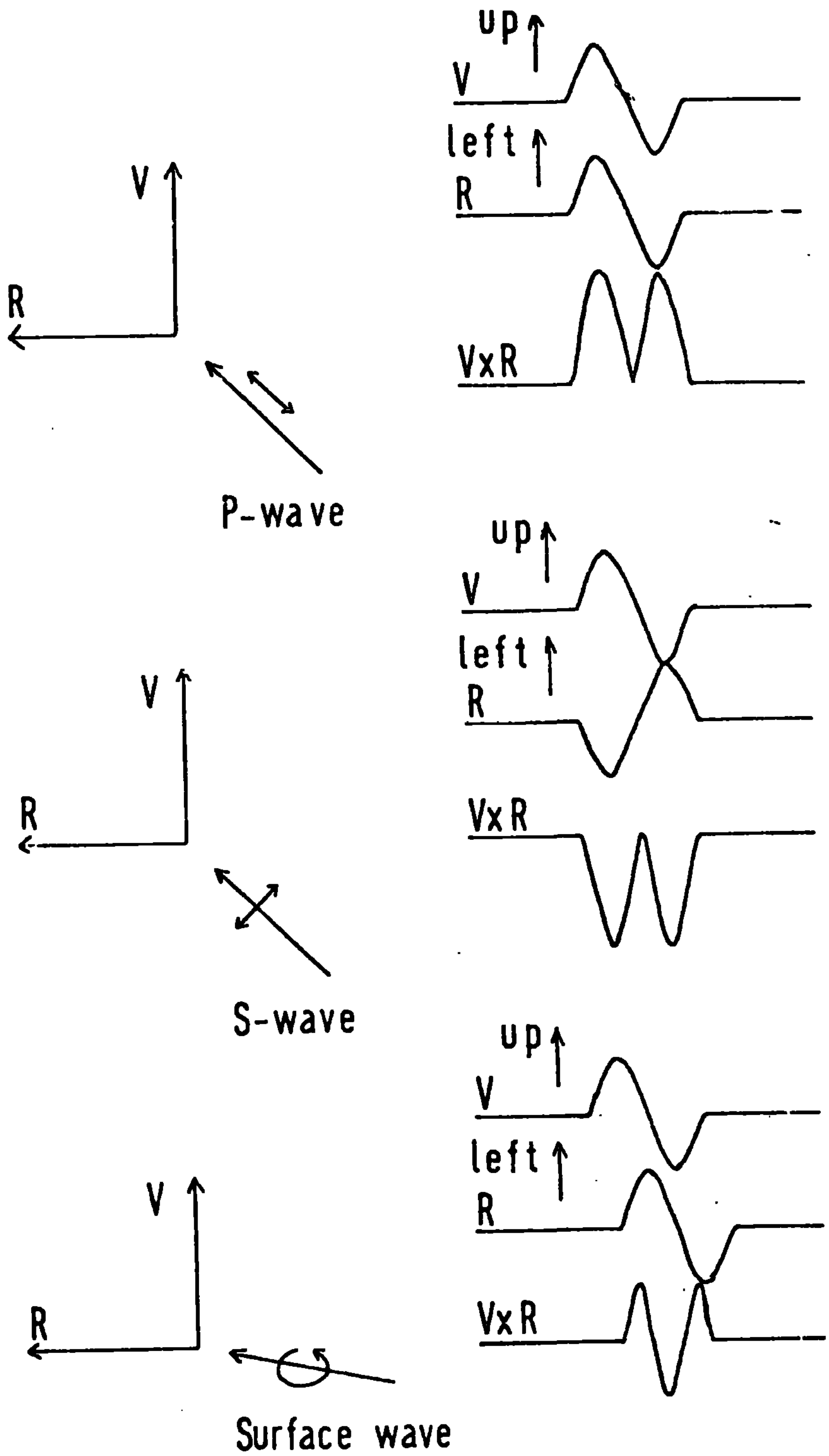

Figure 3.9 Diagrammatic representation of the origin of the form of the V x R correlator function.

and extending the positive P correlations and negative S correlations. When performed on the Modular 1 it is also useful to use this correlator function to operate on the seismic trace so as to enhance rectilinear motions of either P or S type. An example of the computer output is given in Figure 3.10. Signal-generated noise produced near the recording site is usually elliptically polarised and is thus discriminated against. Wind noise, usually short period Rayleigh waves, is also attenuated by this method of processing.

In practice, however, observations made at the earth's surface contain motions due to the reflected waves as well as the incident wave. Substitution of the boundary conditions into the solution of the wave-equation for an incident P-wave shows how the resultant motions from it, and the reflections caused by it, are in phase, and hence rectilinear, for all angles of incidence. For the case of an incident S_v-wave there are only a limited range of angles of incidence for which 180^o out of phase motion is preserved. For angles greater than a critical angle, i_c, the interference of incident and reflected waves creates elliptical motions (Nuttli, 1961; White, 1964). This critical angle is given by $\sin^{-1}(\beta/\alpha)$ where α is the P-wave velocity and β is the S-wave velocity. For Poisson's ratio of 0.25 (the value generally quoted for crustal rocks) this angle is 35^o.

Figure 3.11 shows the travel paths and travel-time graph for various phases which could be expected in a crustal refraction project. Table 3.1 shows the various angles of approach. The crust here is 30 km thick with a velocity close to the surface of 6.1 km sec^{-1} and a sub-Moho velocity of

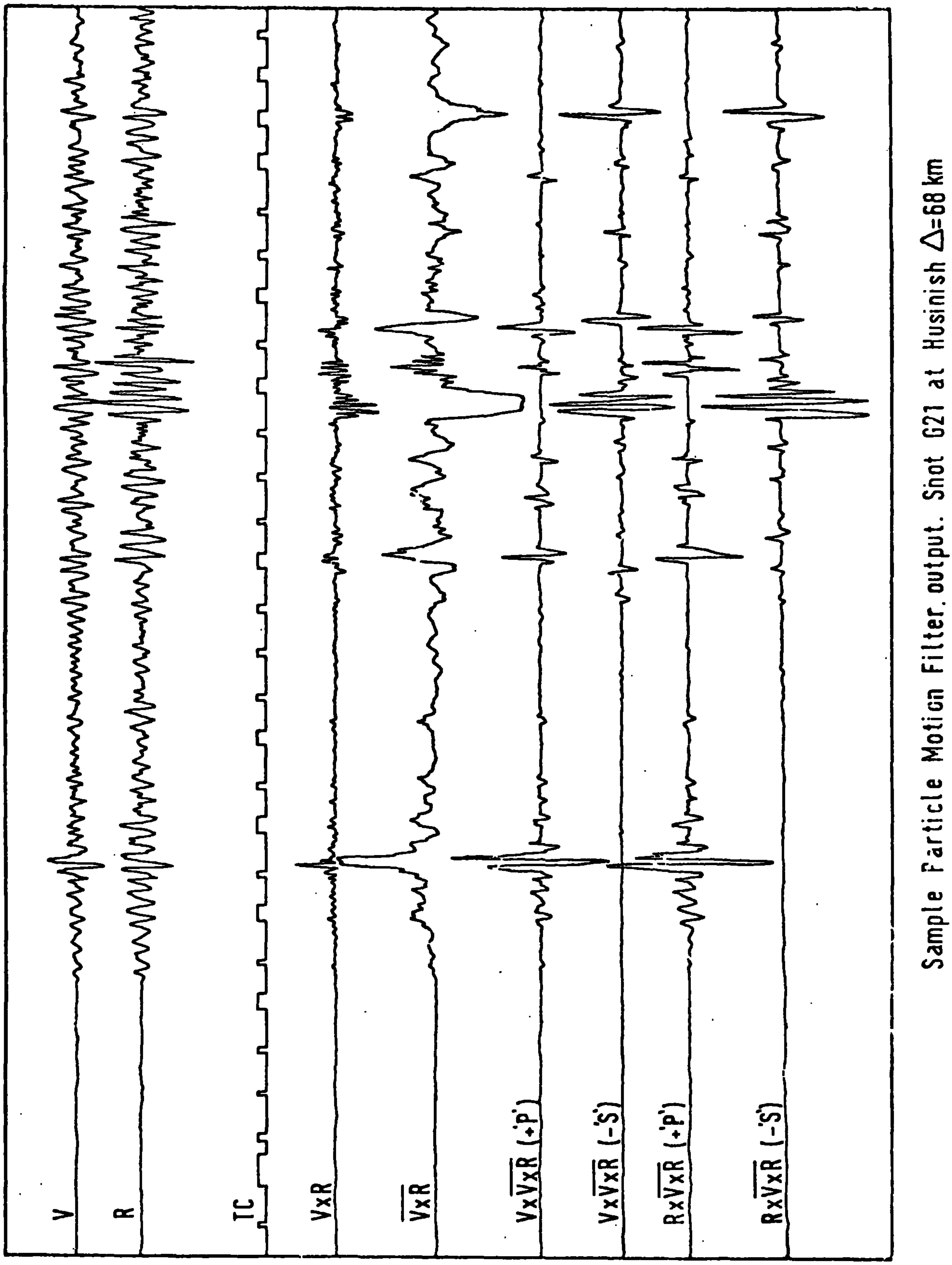

Figure 3.10 Example of computer output for an explosion 68 km from a 3-component station (Husinish, DU10). Traces are, from top to bottom: vertical seis., radial seis., time-code, V x R correlator, smoothed V x R correlator, vertical seis. x +ve parts of smoothed V x R correlator (enhanced P motion), vertical seis. x -ve parts of smoothed correlator (enhanced S motion), and same for radial seis.

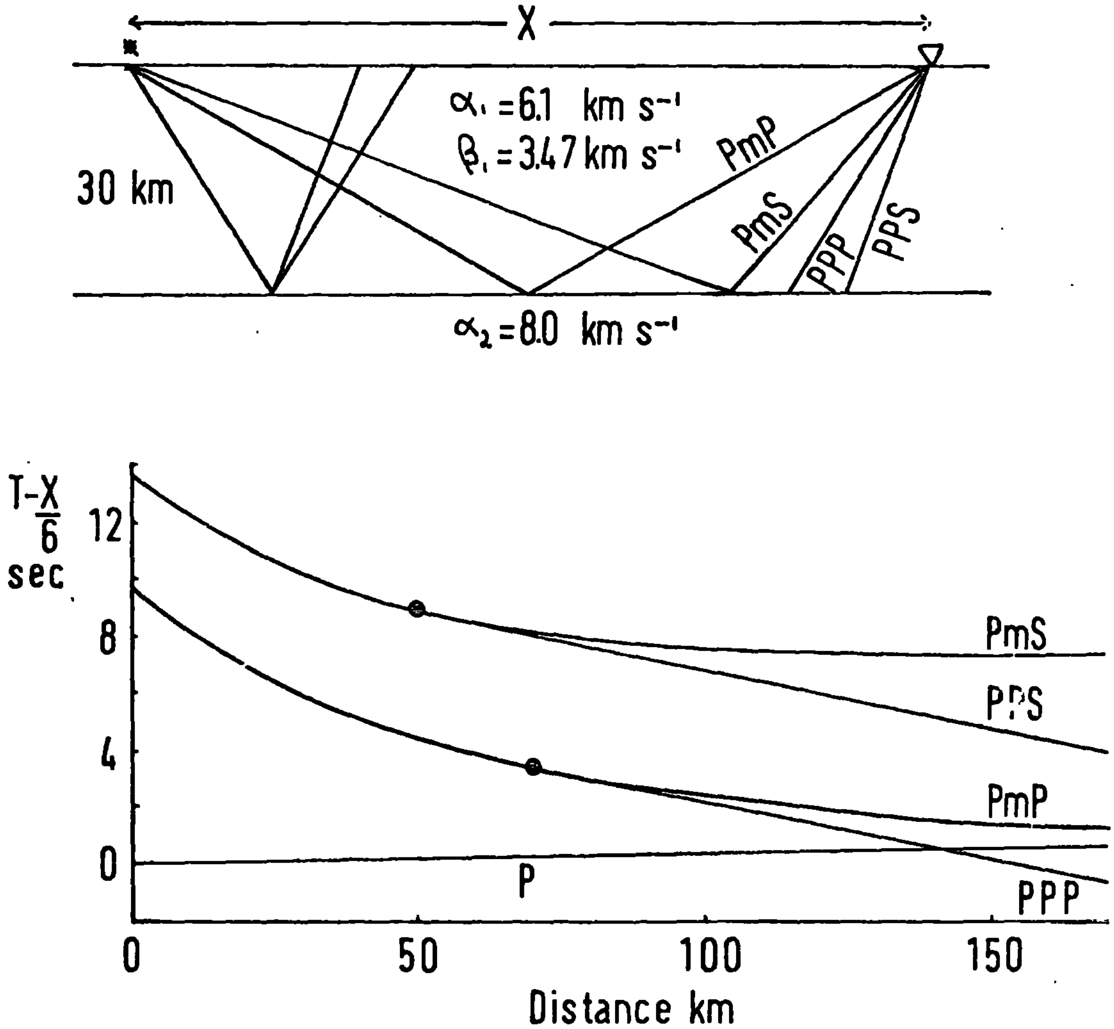

Figure 3.11 Reduced travel-time plot and travel paths for some possible phases in a crustal refraction project.

Table 3.1 Angles of approach for various crustal phases in Figure 3.11.

Phase	Distance (km)	Angle of Approach (degrees)
PPS	> 49	25.71
P_mS	50	32.31
	100	35.83
PPP (SSS)	> 70	49.69
P_mP	50	39.81
	100	59.04
S_g	All distances	~ 80.00

8.0 km sec^{-1}. It can be seen that the wave travelling as P_mS has angles of incidence sufficiently steep to preserve rectilinear motion. Rectilinear motion should also be observed for the wave travelling as a Moho headwave (P) and converted at the Moho to travel up through the crust as an S_v-wave (PPS). (This wave has the same apparent velocity as the Moho headwave (PPP) and should follow it with a constant time-lag).

In most crustal refraction experiments P_mS reflections are not usually observed and possible reasons have been given by Fuchs (1975). He has shown, by theoretical calculations and the use of synthetic seismograms, how a transition zone at the Moho (1 km wide) would reduce the supercritical P_mS reflection to 1/10th of the amplitude observed for the reflection from a first order discontinuity. The amplitude of the P_mS reflections is also substantially reduced if Poisson's ratio is increased in the mantle. This can occur if there is a degree of partial melting, which serves to reduce the S velocity, leaving the P velocity unchanged. However, this effect remains small until a large degree of melting has occured.

An explosion experiment in the Minch in NW Scotland, performed by the IGS Global Seismology Unit, was specifically designed to detect the presence of P_mS. Very closely spaced shots were fired along the axis of the North Minch Basin, where the geological structure was expected to remain constant. Recordings were made at a three-component station at Cape Wrath (Jacob and Booth, 1977). Using the method of particle motion processing a convincing identification of P_mS was made.

CHAPTER 4

RESULTS FROM SCOTTISH SHELF AREA

4.1 The general pattern of arrivals from stacked records

This chapter will deal with the results obtained from shots fired in the shallow water of the Hebridean Shelf. Stacked record sections, constructed by the program FPLOT (Appendix C), or drawn by hand, reveal the basic pattern of arrivals over the area and show up details which vary from zone to zone.

Figures 2.5 and 4.1 to 4.7 show a first arrival with an apparent velocity of 6.1 to 6.2 km sec^{-1} out to ranges of between 120 and 160 km. Here, an arrival of apparent velocity 7.7 to 8.1 km sec^{-1} takes over as first arrival. These two arrivals are identified as P_g and P_n respectively. At ranges greater than about 250 km the P_n headwave diminishes in amplitude and is very difficult to select from the noise, even on the analogue records where the scales are much greater than those in the diagrams presented here. A well correlated late arrival is shown at a number of stations and is interpreted as the P-wave reflected from the Moho (P_mP) because of its travel-time and amplitude characteristics. (Figures 2.5, 4.3 and 4.4). The P-wave reflected at the Moho and converted to an S-wave (P_mS) is not seen, although a more thorough search was conducted by particle motion processing (Sections 3.8 and 4.7). A first arrival with an apparent velocity of 6.4 to 6.8 km sec^{-1}, corresponding to a mid-crustal refractor of the type observed in NASP and several

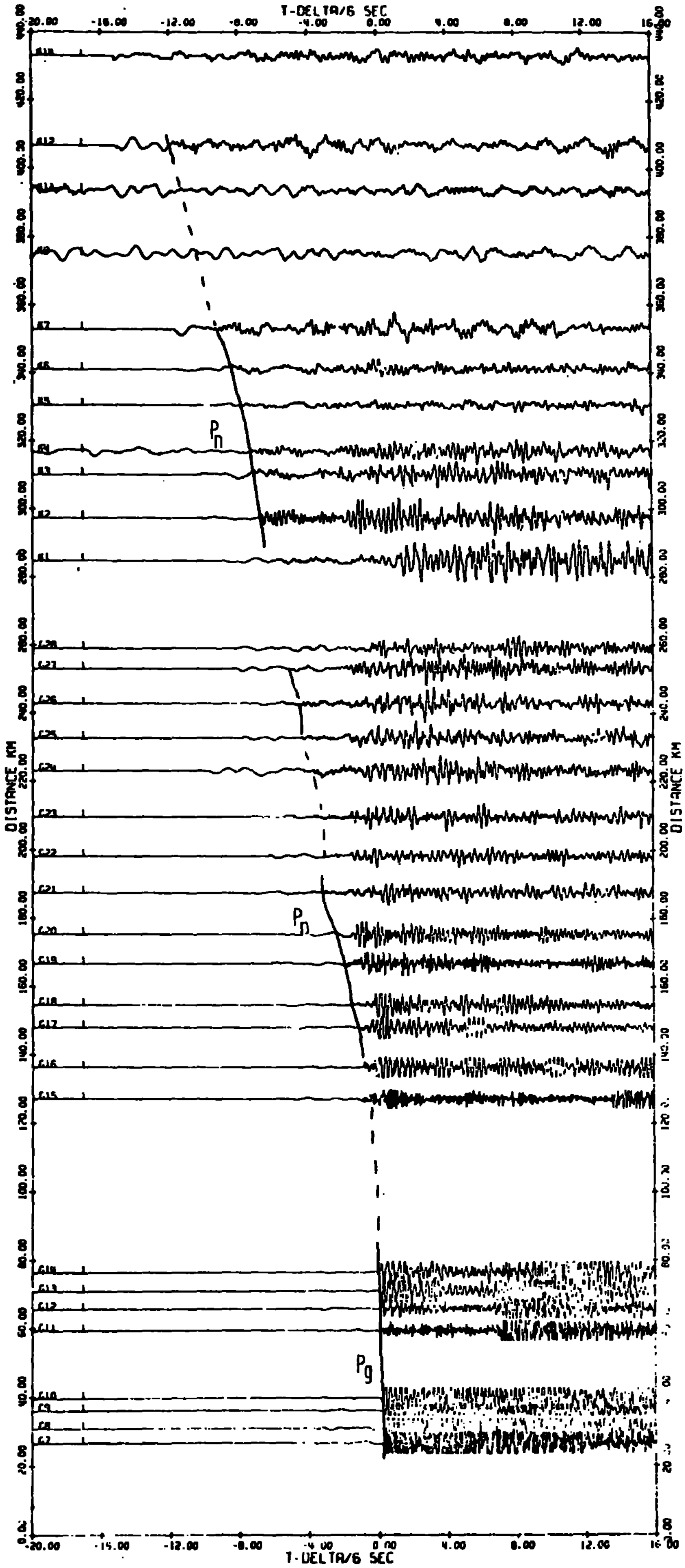

Figure 4.1 Computer drawn stacked record section of G and K shots recorded at Knockan (GS3). Unfiltered E-W seismometer.

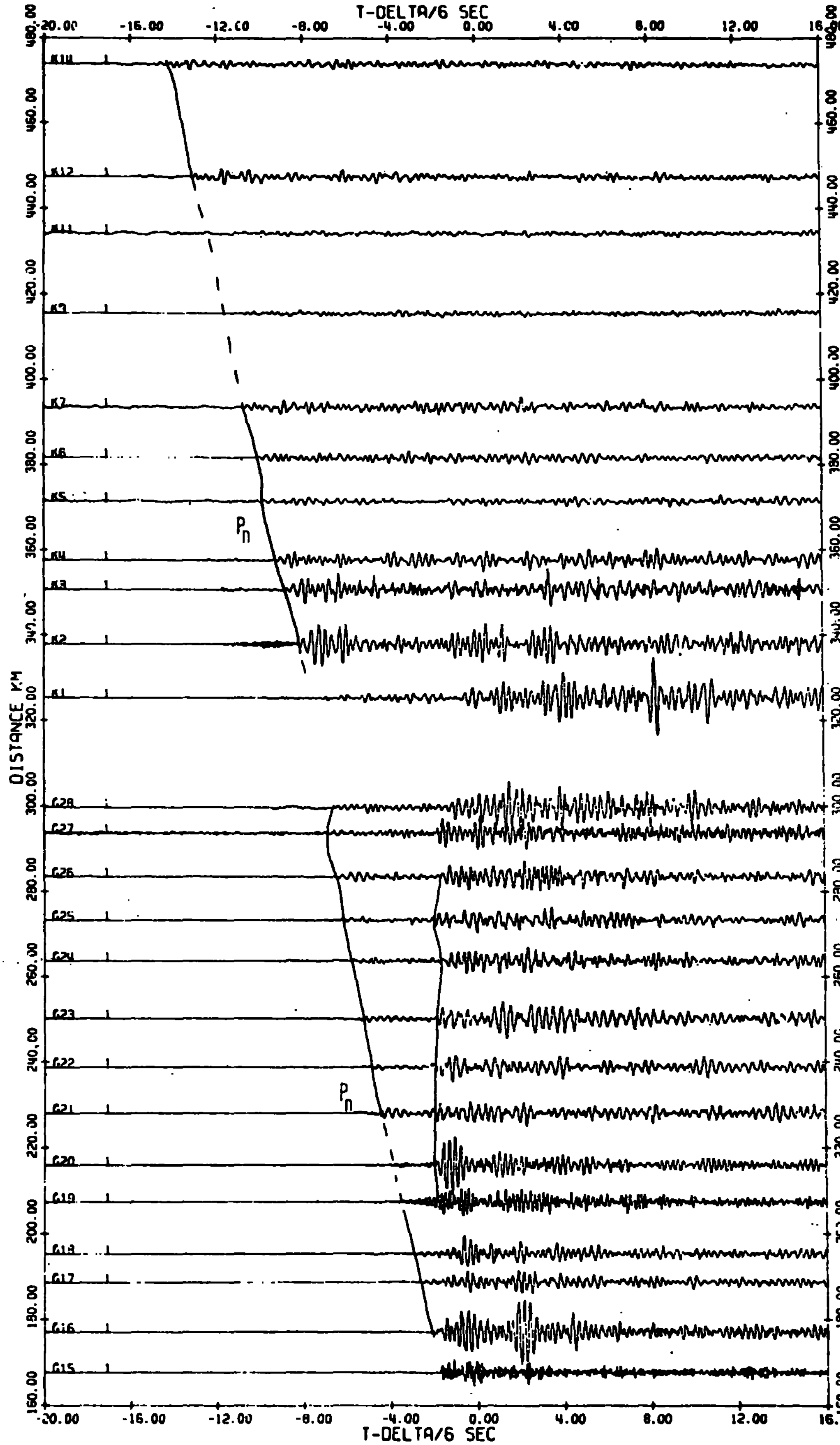

Figure 4.2 Computer drawn stacked record section of G and K shots at Lairg (GS6). Unfiltered E-W seismometer.

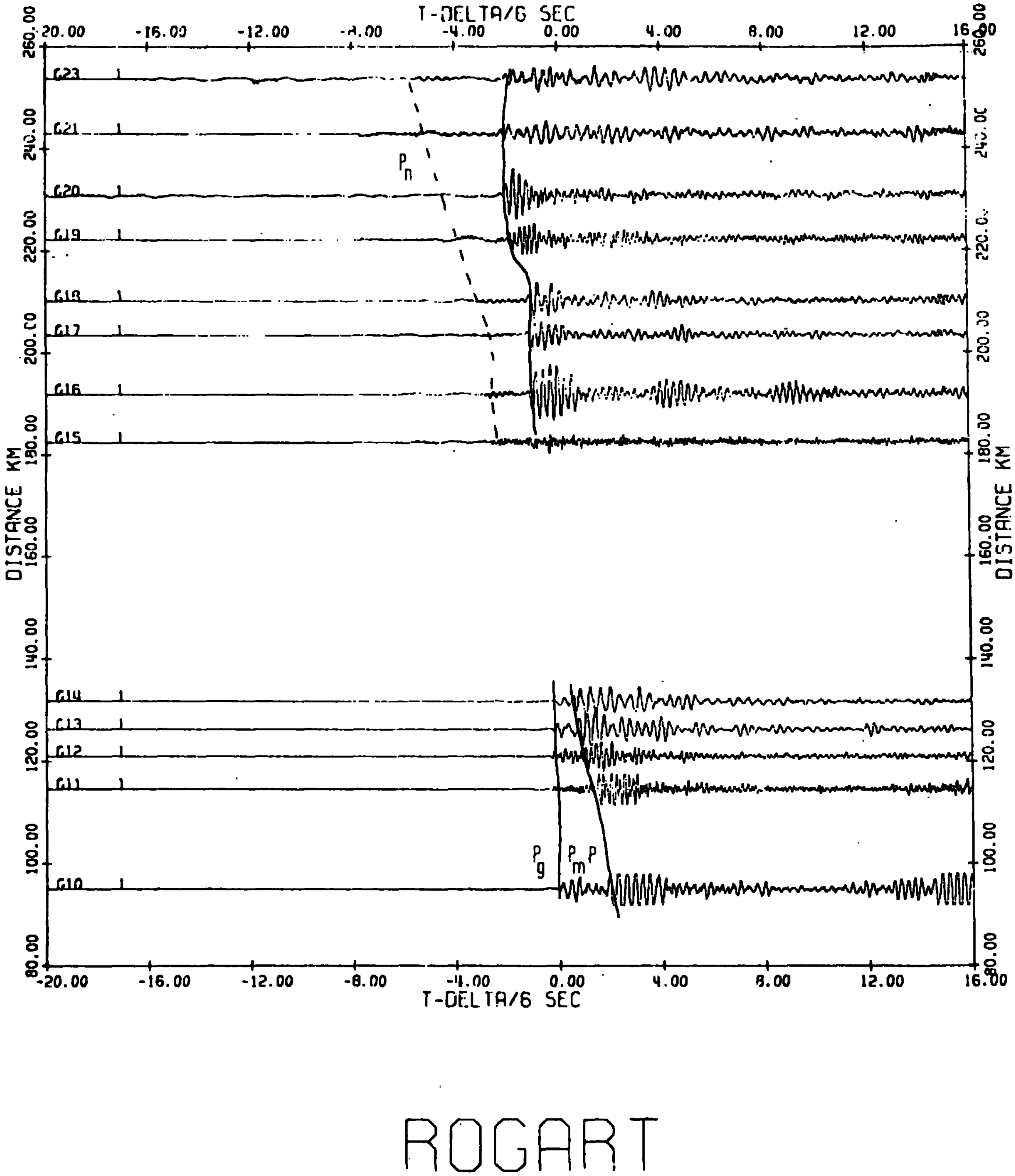

Figure 4.3 Computer drawn stacked record section of G shots at Rogart (GS7). Unfiltered E-W seismometer.

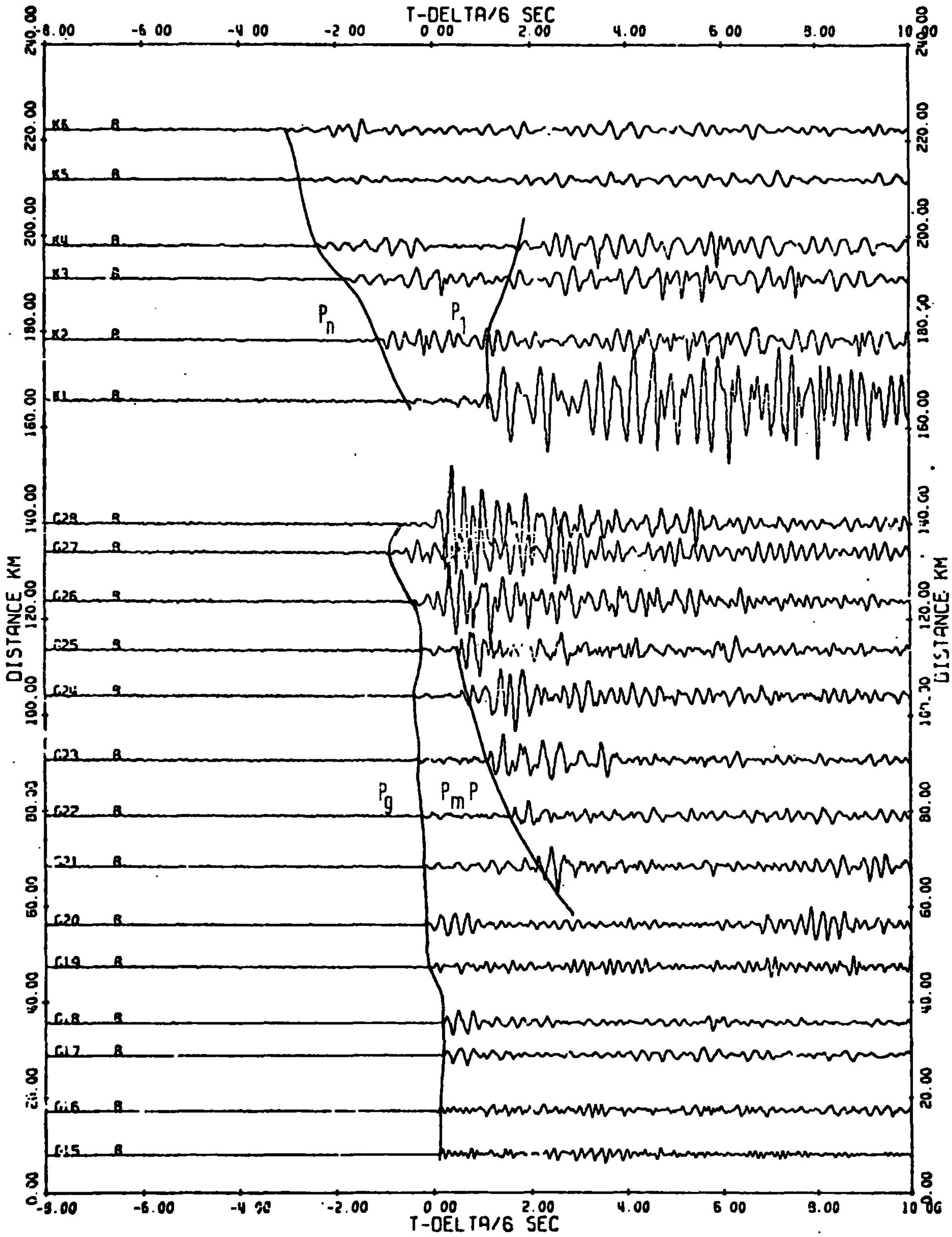

HUSINISH

Figure 4.4 Computer drawn stacked record section of G and K shots at Husinish (DU10). Filtered vertical seismometer.

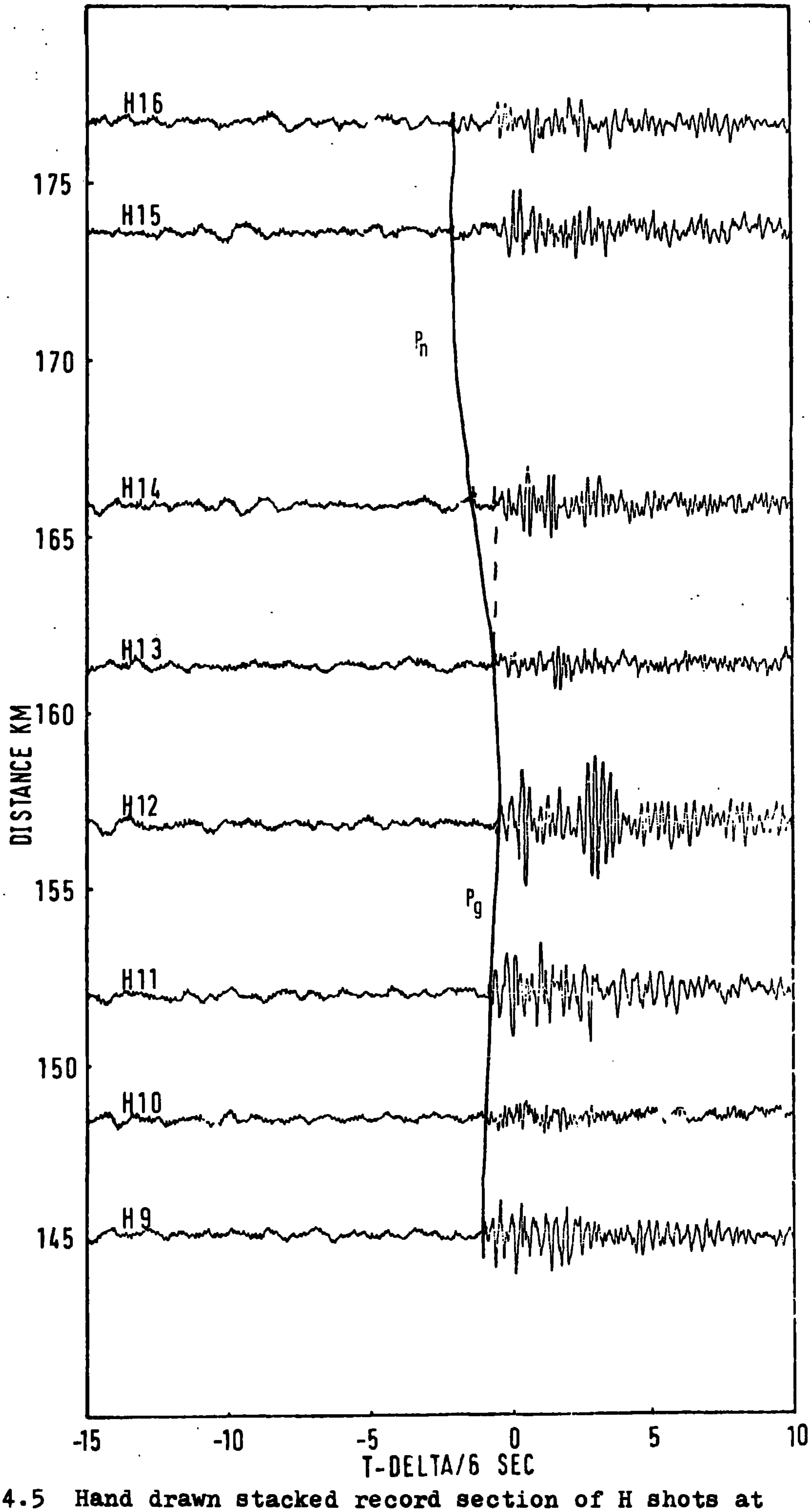

Figure 4.5 Hand drawn stacked record section of H shots at Mull (DU16). Unfiltered vertical seismometer.

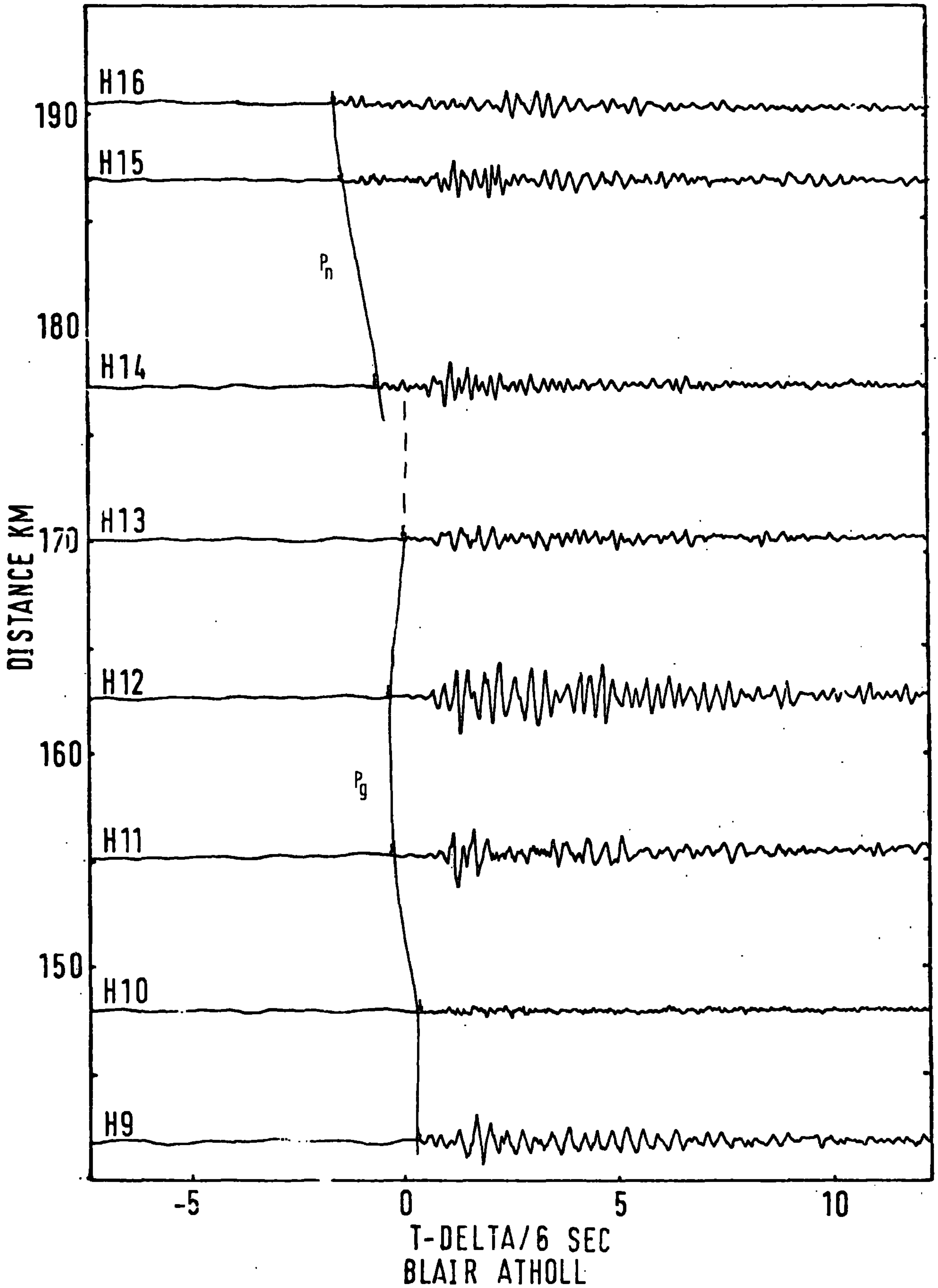

Figure 4.6 Hand drawn stacked record section of H shots at Blair Atholl (BLA). Filtered vertical seismometer.

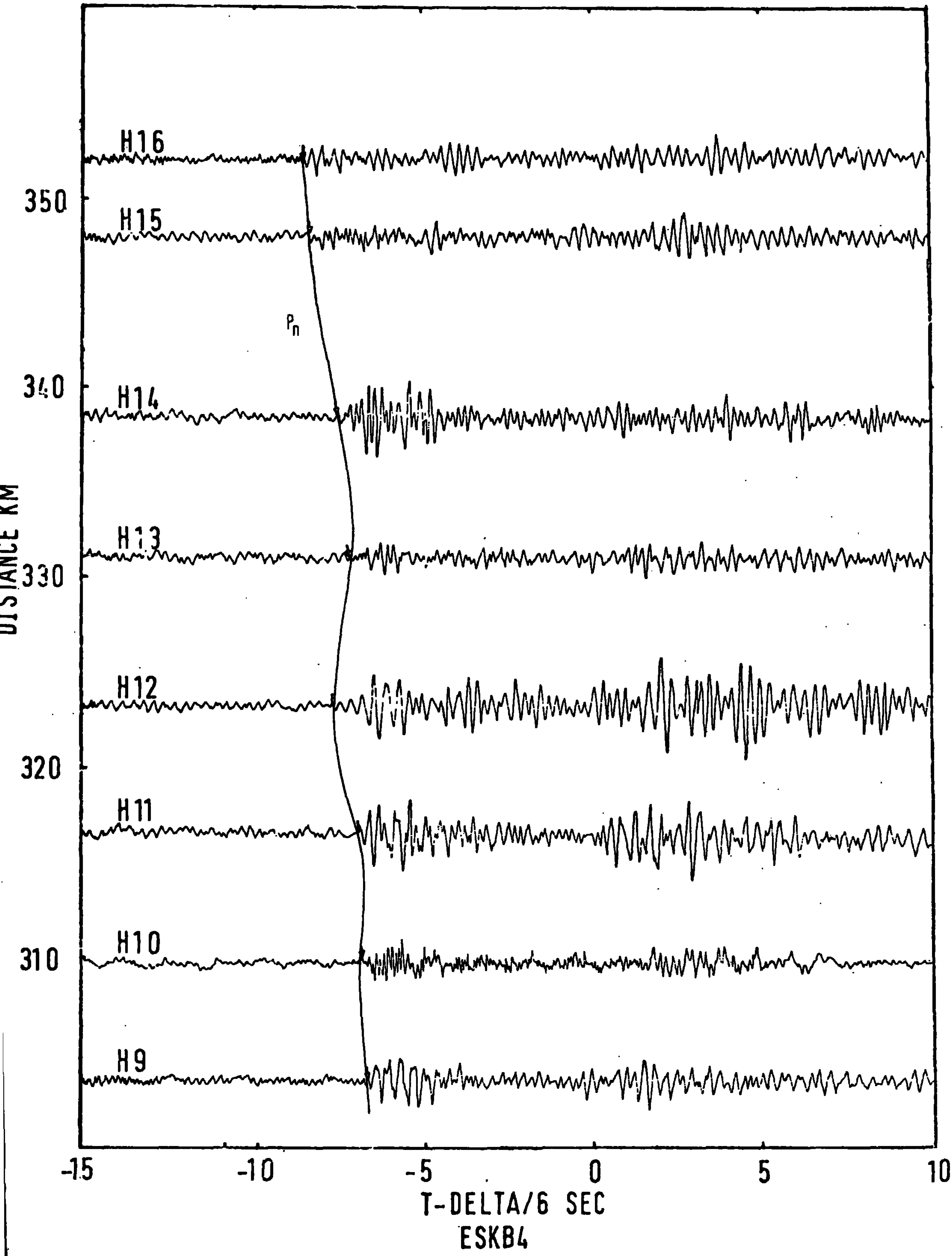

Figure 4.7 Hand drawn stacked record section of H shots at pit B4 of Eskdalemuir (ESK). Unfiltered vertical seismometer.

other explosion experiments, is not seen. However, if such a refractor has a depth greater than 10 to 12 km, refractions will not occur as first arrivals but will follow some time behind the P_g and P_n arrivals. Under such circumstances it would be difficult to identify these refractions which have very small amplitudes. Reflections from such a layer, which would be of higher amplitude and therefore possibly more easy to identify, are not clearly seen.

The effect of sedimentary cover is well shown at some shots where a rapidly changing thickness of sediments distorts sets of arrival times from the straight lines and smooth curves normally expected. Figures 4.1 to 4.4 show particularly well the presence of a sedimentary basin between shots G16 and G18 with the refractor coming close to the surface again at shot G19.

The frequency content of certain shots shows large departures from the average. Figures 4.1 to 4.7 show that signals from shots G7, G15, G19 and H10, recorded at widely separated stations, have a significantly wider frequency content than the other shots. It can also be seen that they have a lower overall power output, that is, at large ranges they are recorded at lower amplitudes. The amplitude frequency spectra of several shots have been obtained by means of a Fast Fourier Transform program adapted by Mr. A. Nunns from a program in Claerbout (1976) for use on the NUMAC IBM 370/168. The wide frequency range and higher dominant frequency for shot G19 is evident in Figure 4.8 and is due to it being fired in shallow water at less than the optimum depth (Section 2.2.2) so that the sea-surface reflection and

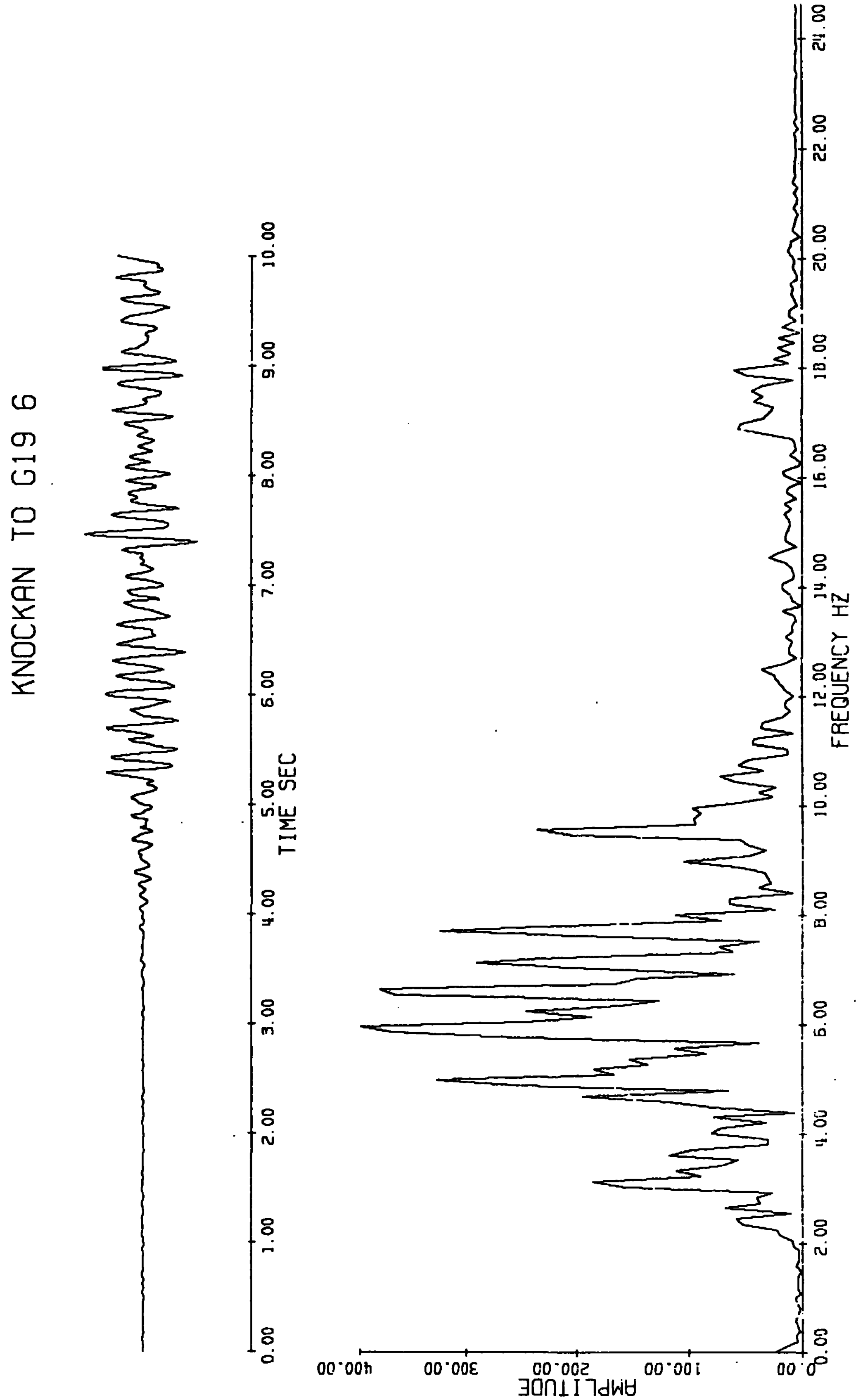

Figure 4.8 Computer drawn amplitude/frequency plot for shot G19 recorded at Knockan (GS3) filtered between 2 and 15 hz. Amplitude scale is in arbitrary units.

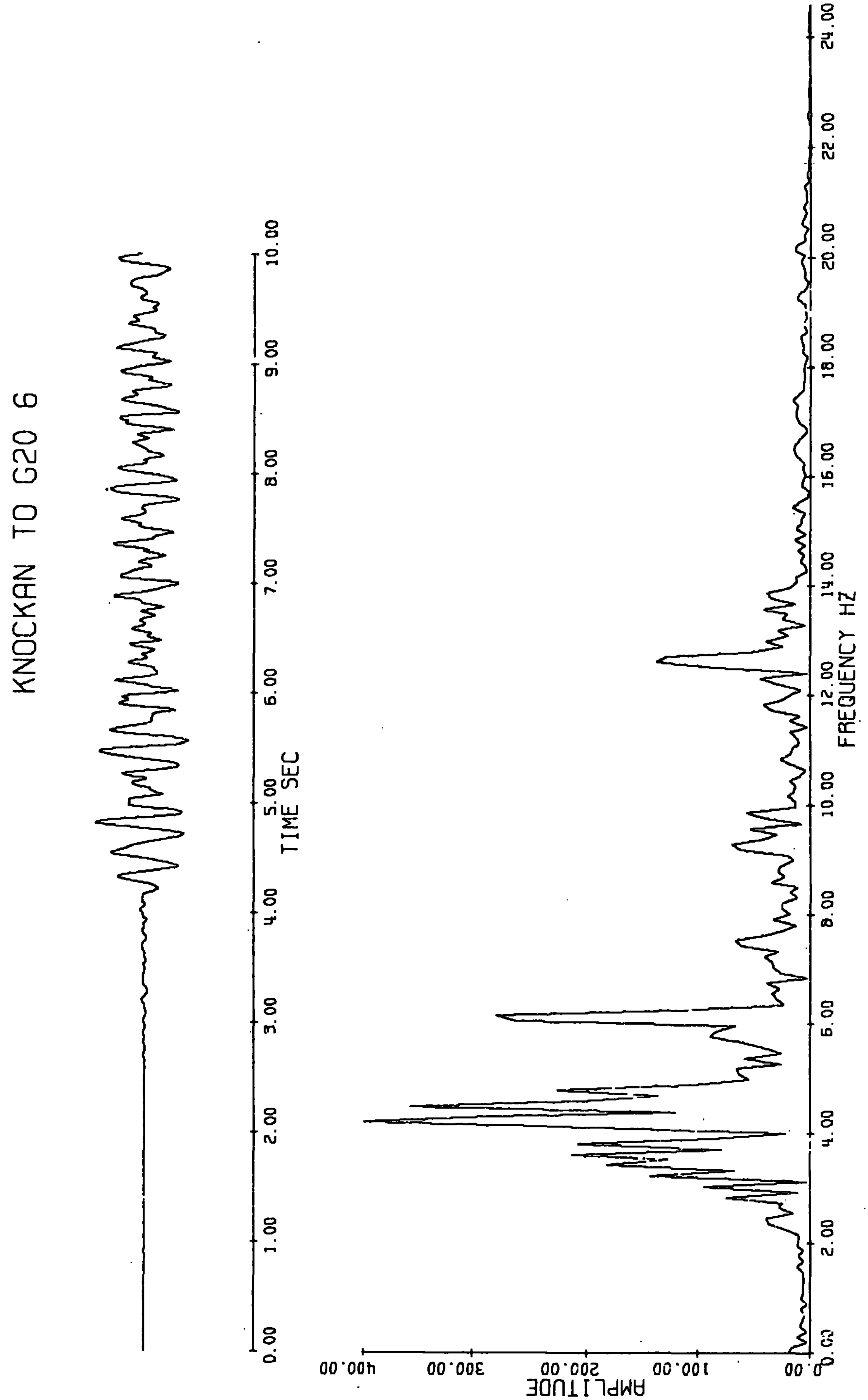

Figure 4.9 Computer drawn amplitude/frequency plot for shot G20 recorded at Knockan (GS3) filtered between 2 and 15 hz. Amplitude scale is in arbitrary units.

the bubble pulse did not constructively interfere. Shot G20, on the other hand, was fired at the correct depth and the lower dominant frequency and narrower frequency range is shown in Figure 4.9. The reason that a signal like G19, with broad band characteristics, is not desirable for a long range refraction project lies in the fact that transmission losses are greater for higher frequencies. Shots such as G19 give very good characteristics when recorded at short ranges, with pulse-like arrivals, but their power is considerably reduced at larger ranges.

4.2 Travel-time graphs

Figures 4.10, 4.11 and 4.12 show reduced travel-time graphs for five stations which are typical of those constructed for all the stations. Further graphs are given in Appendix B. Figures 4.13 and 4.14 and Table 4.1 summarise the information contained in all the graphs. For interpretation purposes the survey area was split into zones and the least-squares velocity for each zone at each station was calculated. The contribution to the travel-time made by the time-term is included in the plots at this stage. The least-squares apparent velocities so obtained were plotted against the average distances from the station to the shots. Arrows are used to represent the direction in which the sequence of shots was recorded and point towards the station. For example, station GS2, to the east of shots G7 to G14, is at an average distance of 44 km and gave a least-squares velocity of 6.19±0.11 km sec^{-1}. Station MD1, however, recorded the same shots in the opposite direction at the same average distance and gave a least-

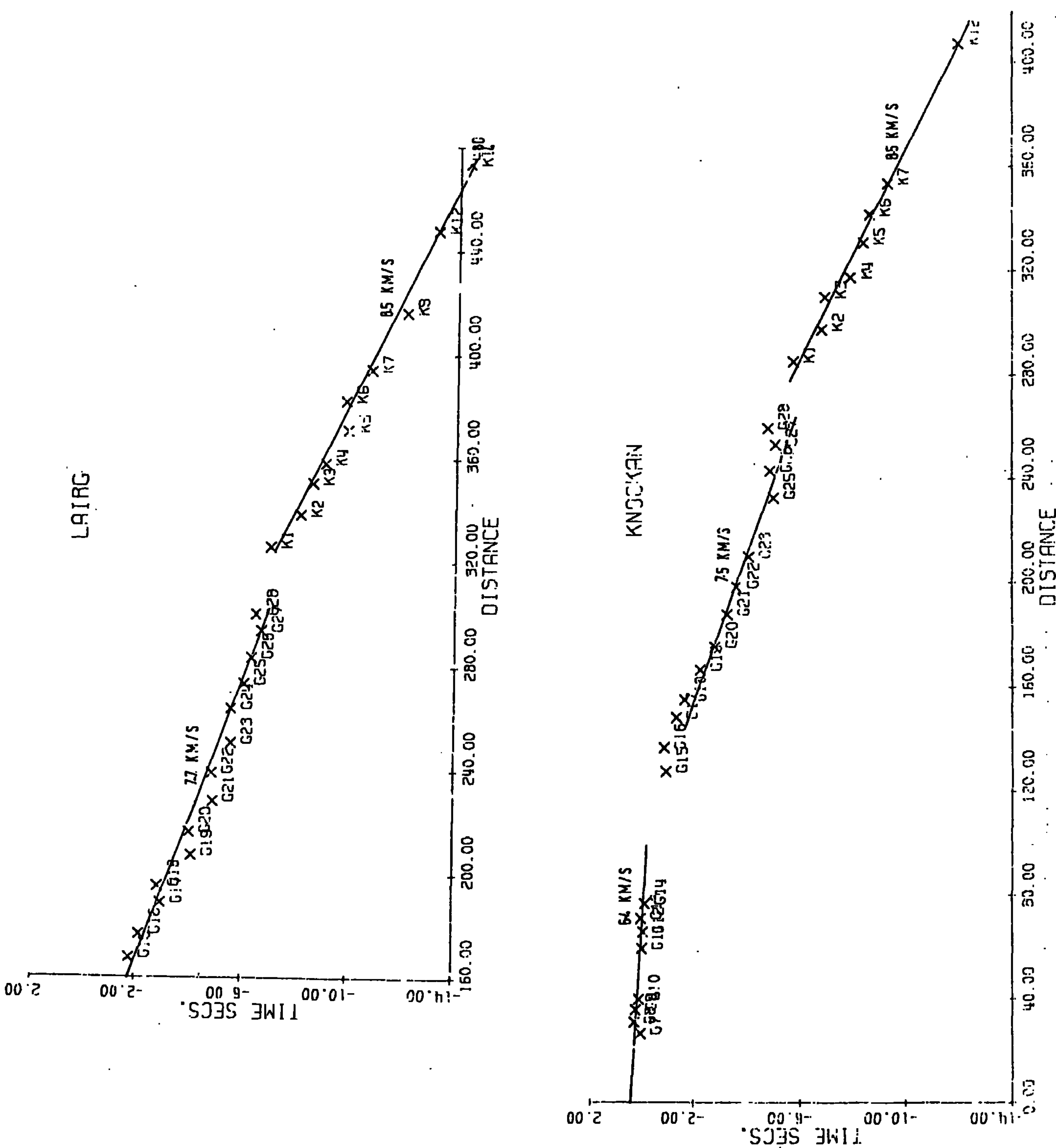

Figure 4.10 Reduced travel-time graphs of first arrivals at Knockan and Lairg (GS3 and GS6). Reduction velocity is 6.0 km sec^{-1}.

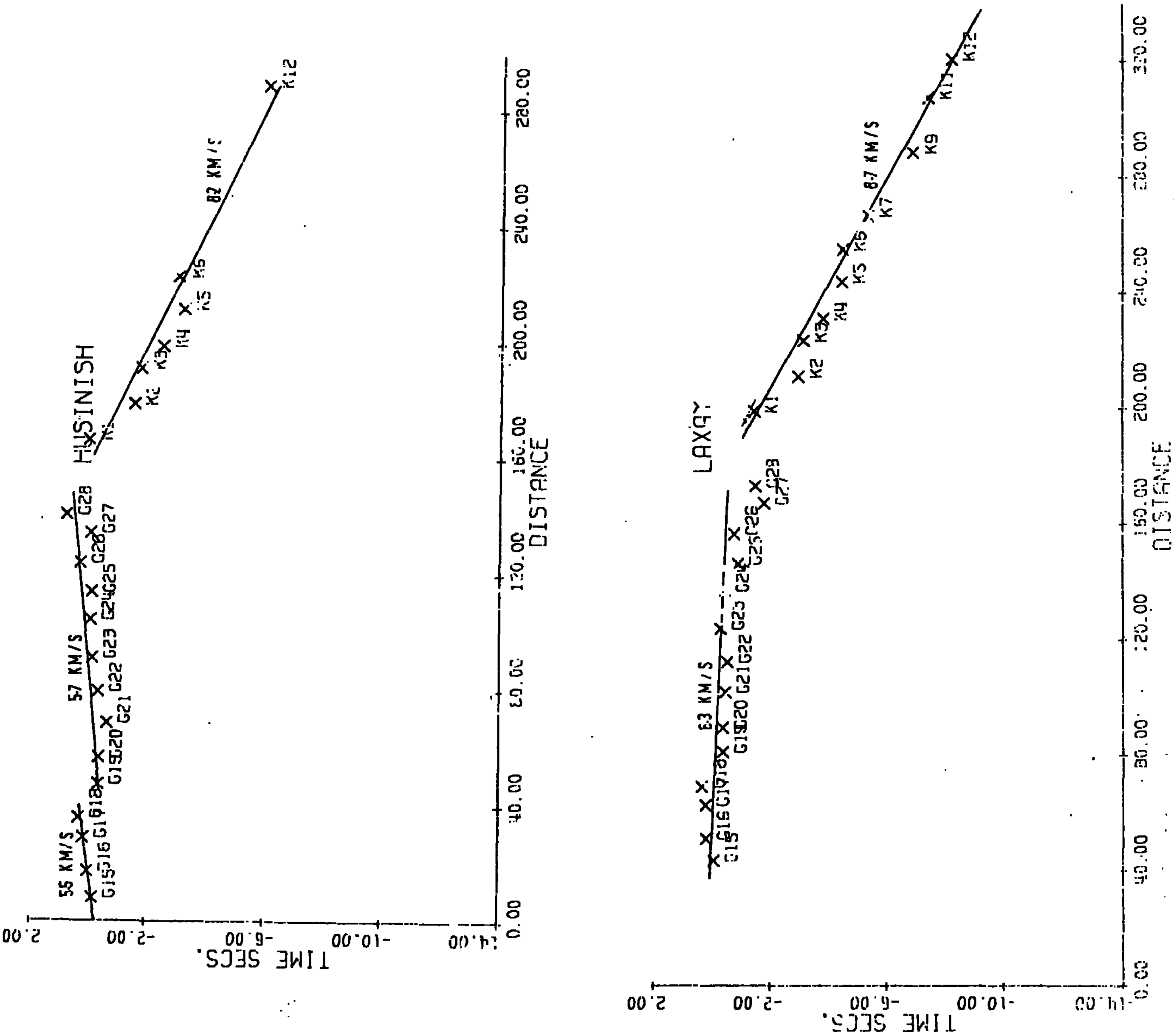

Figure 4.11 Reduced travel-time graphs of first arrivals at Laxay and Husinish (MD1 and DU10). Reduction velocity is 6.0 km sec^{-1}.

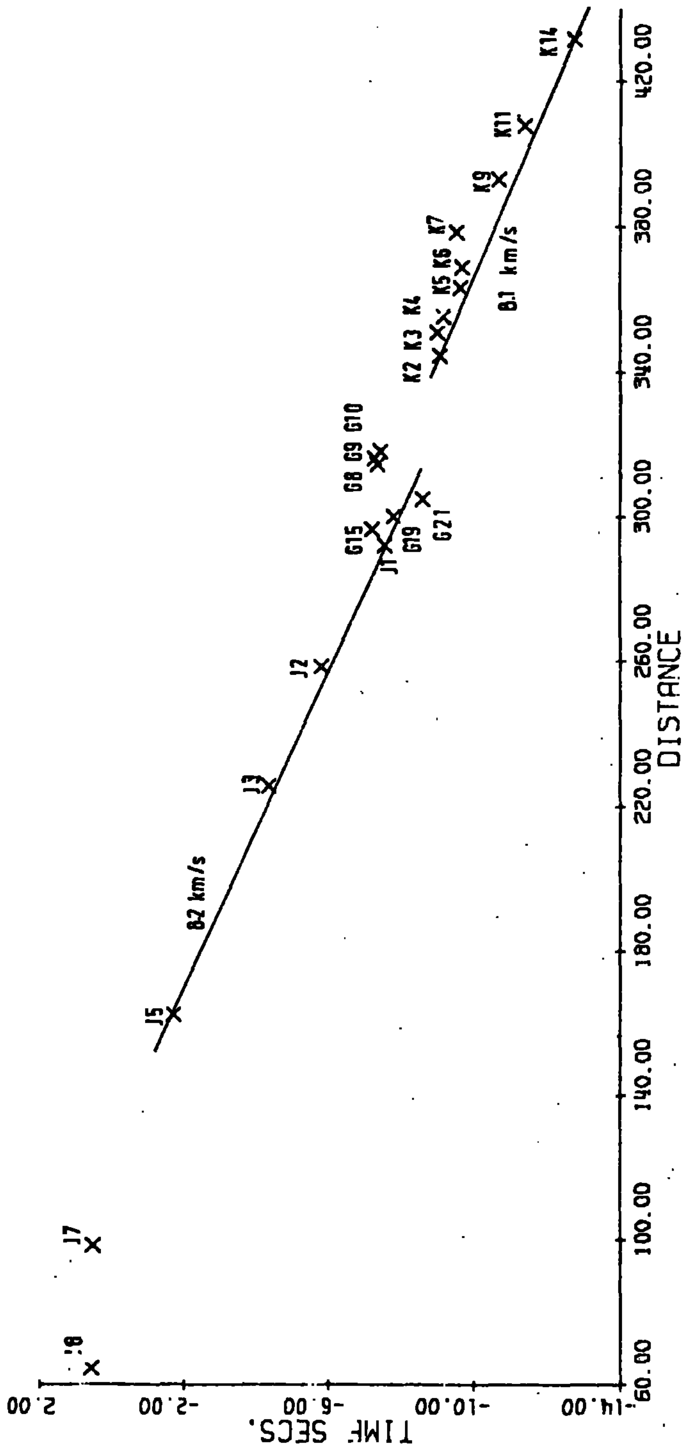

Figure 4.12 Reduced travel-time graph of first arrivals at Irish station Lagg. Reduction velocity is 6.0 km sec^{-1}.

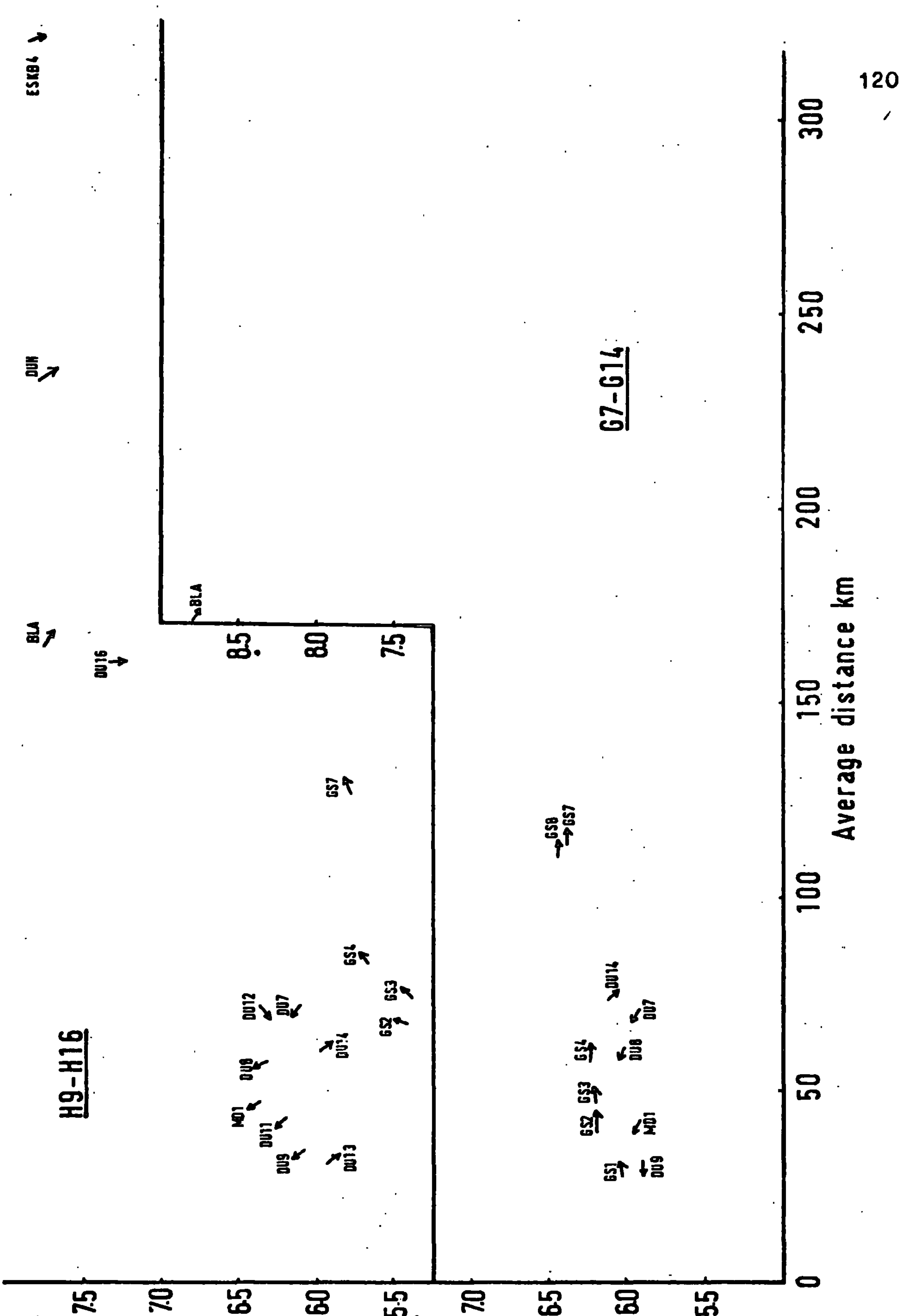

Figure 4.13 Compilation of results of least-squares fitting for G and H shots (Minch). The least-squares velocity is plotted against average of the distances between shots and the station for each station. Arrows represent the direction to the station. North is at the top.

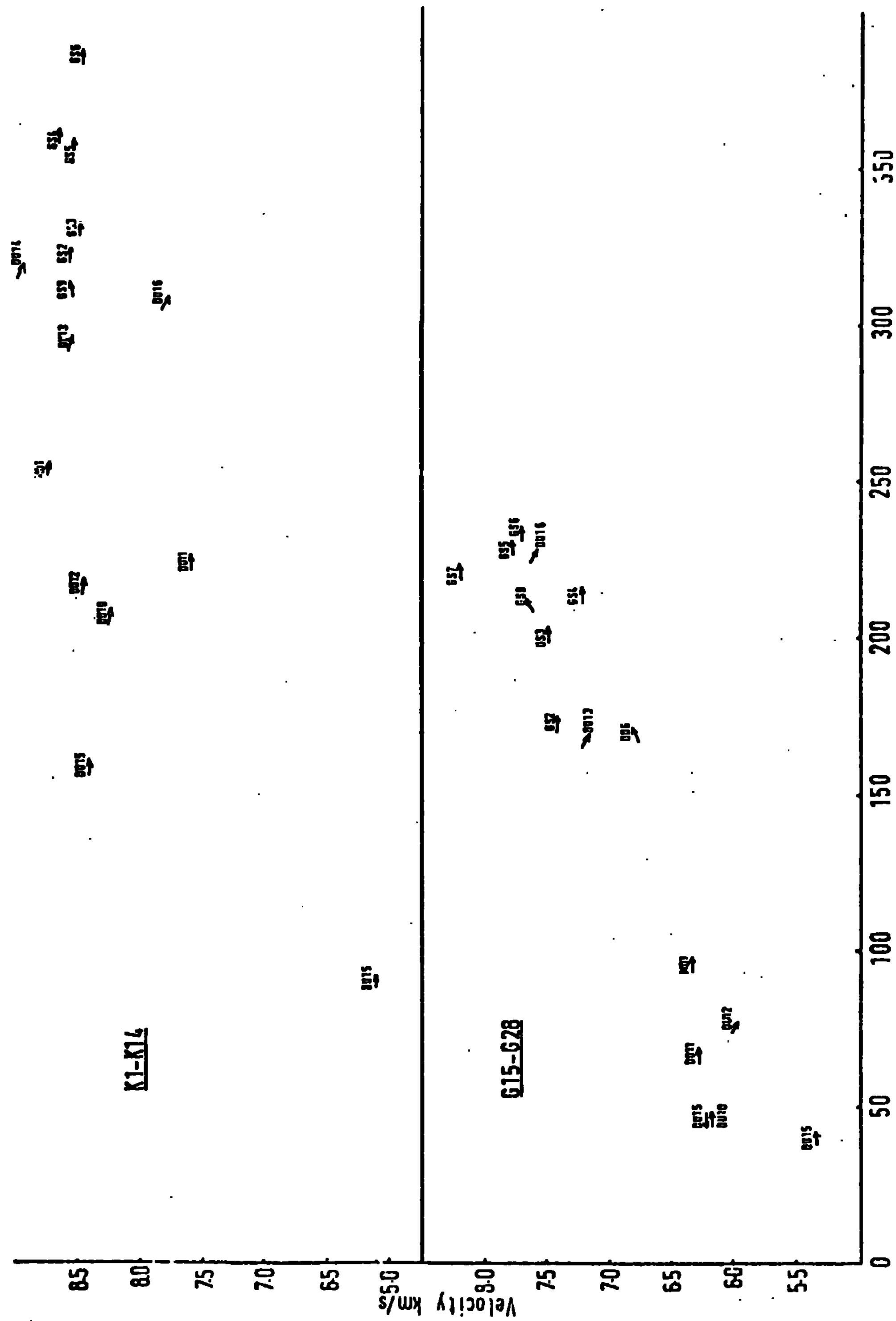

Figure 4.14 Compilation of the results of least-squares fitting to the first arrival segments for the G shots on the outer shelf and the K shots in Rockall Trough. Conventions as in Figure 4.13.

Table 4.1 Summary of the results of fitting least-squares velocities to first arrival segments recorded at each station.

Station code name	North Minch G7 to G14			Outer shelf G15 to G28			South Minch H9 to H16			Outer shelf J1 to J8		
	A	B	C	A	B	C	A	B	C	A	B	C
GS1	31	E	6.04				60	NE	4.53			
GS2	44	E	6.19	174	E	7.41	68	NE	5.49			
GS3	50	E	6.20	202	E	7.49	76	NE	5.44			
GS4	61	E	6.23	215	E	7.20	85	NE	5.71			
GS5				230	E	7.77						
GS6				234	E	7.68				259	E	8.01
GS7	117	E	6.37	222	E	8.17	130	E	5.81			
GS8	114	E	6.43									
GS9				211	NE	7.66						
DU6				170	E	6.80						
DU7	68	W	5.96	123	NE	5.43	65	NW	6.15			
DU8	58	W	6.04				56	NW	6.40			
DU9	27	W	5.89				31	NW	6.16			

A = average distance (km); B = approximate direction; C = least-squares velocity (km sec^{-1}).

Table 4.1 (continued)

Station code name	North Minch G7 to G14			Outer shelf G15 to G28			South Minch H9 to H16			Outer shelf J1 to J8		
	A	B	C	A	B	C	A	B	C	A	B	C
DU10				47	E	6.18						
DU11				68	E	6.27	40	NW	6.27			
DU12				76	SE	5.94	69	W	6.30	83	E	6.65
DU13	53	SE	6.76	168	E	7.17	33	SE	5.85	162	E	8.30
DU14	76	SE	6.08	207	E	7.35	61	SE	5.90			
DU15				48	W	6.32						
DU95				47 41	W E	6.21 (P_g) 5.33 (P_g)				80	N	6.26
DU16				227	SE	7.57	172 152	S S	14.00 (P_n) 5.40 (P_g)			
MD1	39	W	5.95	97	E	6.33	45	NW	6.44	147	E	7.14
BLA	172 159	SE SE	8.77 (P_n) 6.55 (P_g)				166	SE	7.76			
DUN	238	S	10.5				234	S	7.71			
LAGG										234	S	8.18
ESK	342	S	11.4				327	S	7.71			

squares velocity of 5.95 ± 0.08 km sec^{-1}. Such observations indicate a dip of the refractor beneath G7 to G14 of about 2^{o} to the east.

Figure 4.13 also shows the increase in least-squares velocity with increasing average distance for shots G7 to G14. Observations at GS1 give a velocity of 6.04 ± 0.22 km sec^{-1} rising steadily to 6.43 ± 0.12 km sec^{-1} at GS8 where the average distance is 114 km. This indicates that the refractor velocity may be increasing with depth, a phenomenon which usually gives rise to a curved travel-time graph. However, a small curvature of the size suggested here could be masked by the variability of the time-terms at each shot. The time-term analysis discussed later (Section 4.4) gives an estimate of the magnitude of the velocity change.

At larger ranges these shots (G7 to G14) were recorded showing a very small P_n headwave as first arrival (Figures 4.15 to 4.17). The four stations which recorded these shots at large ranges were Blair Atholl (BLA), the Dundee station of Lownet (DUN), the Eskdalemuir array (ESK) and the Irish station Lagg. They all lie to the south of the shots. The distance from these stations to each of the shots changes only a little and a fairly small change in P_n time-term from shot to shot may therefore serve to obscure the real velocity. The cross-over distance is seen to be of the order of 175 km (Figure 4.15) and the apparent velocities observed are as high as, and as poorly defined as, 11.4 ± 4.13 km sec^{-1}.

One point worthy of note in Figure 4.12 is the delay of shots G8, G9 and G10 recorded at Lagg. The distant J shots, J1 to J5, and the outer shelf shots, G15, G19 and G21,

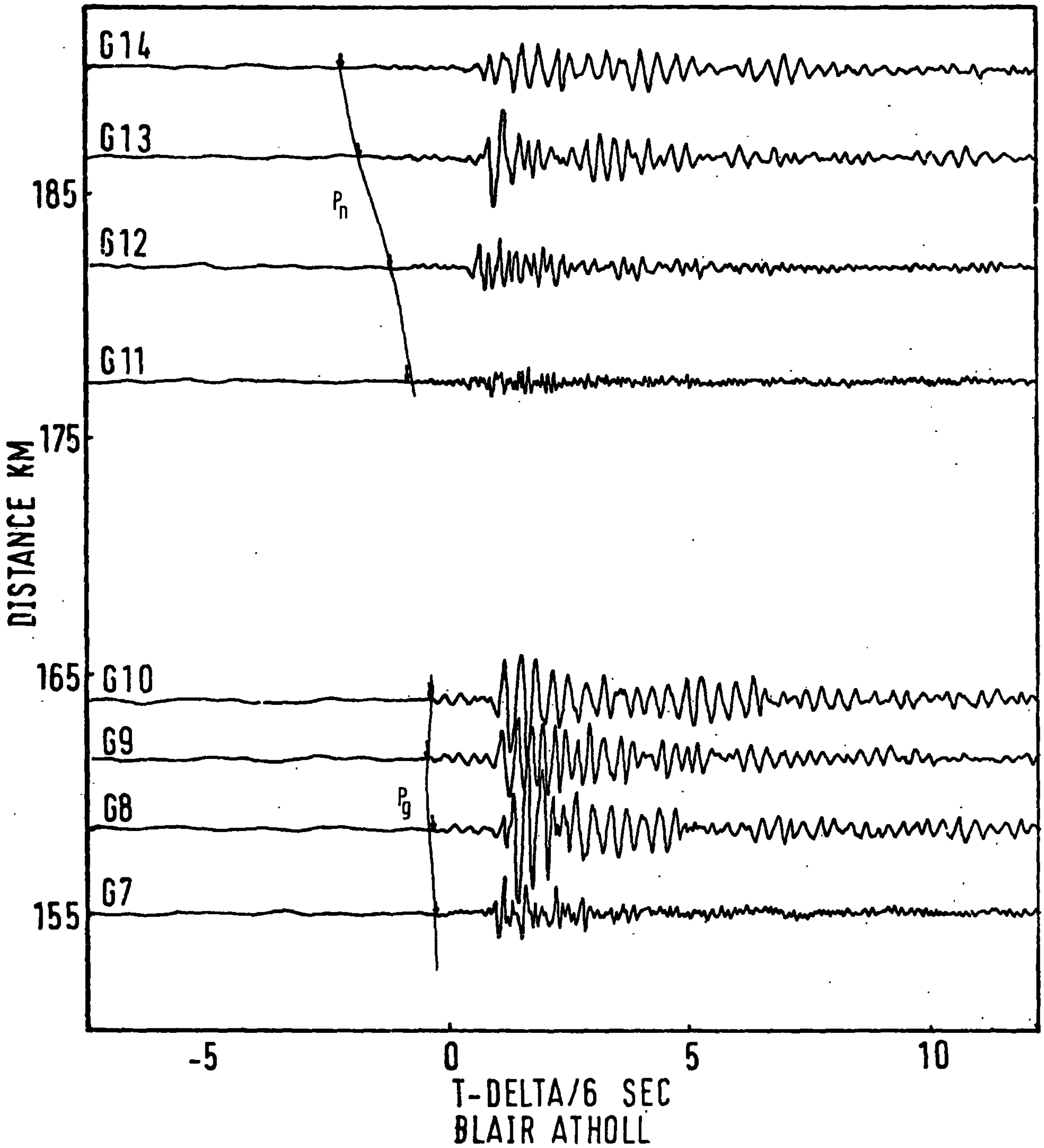

Figure 4.15 Hand drawn stacked record section of G shots in the Minch at Blair Atholl (BLA). Unfiltered vertical seismometer.

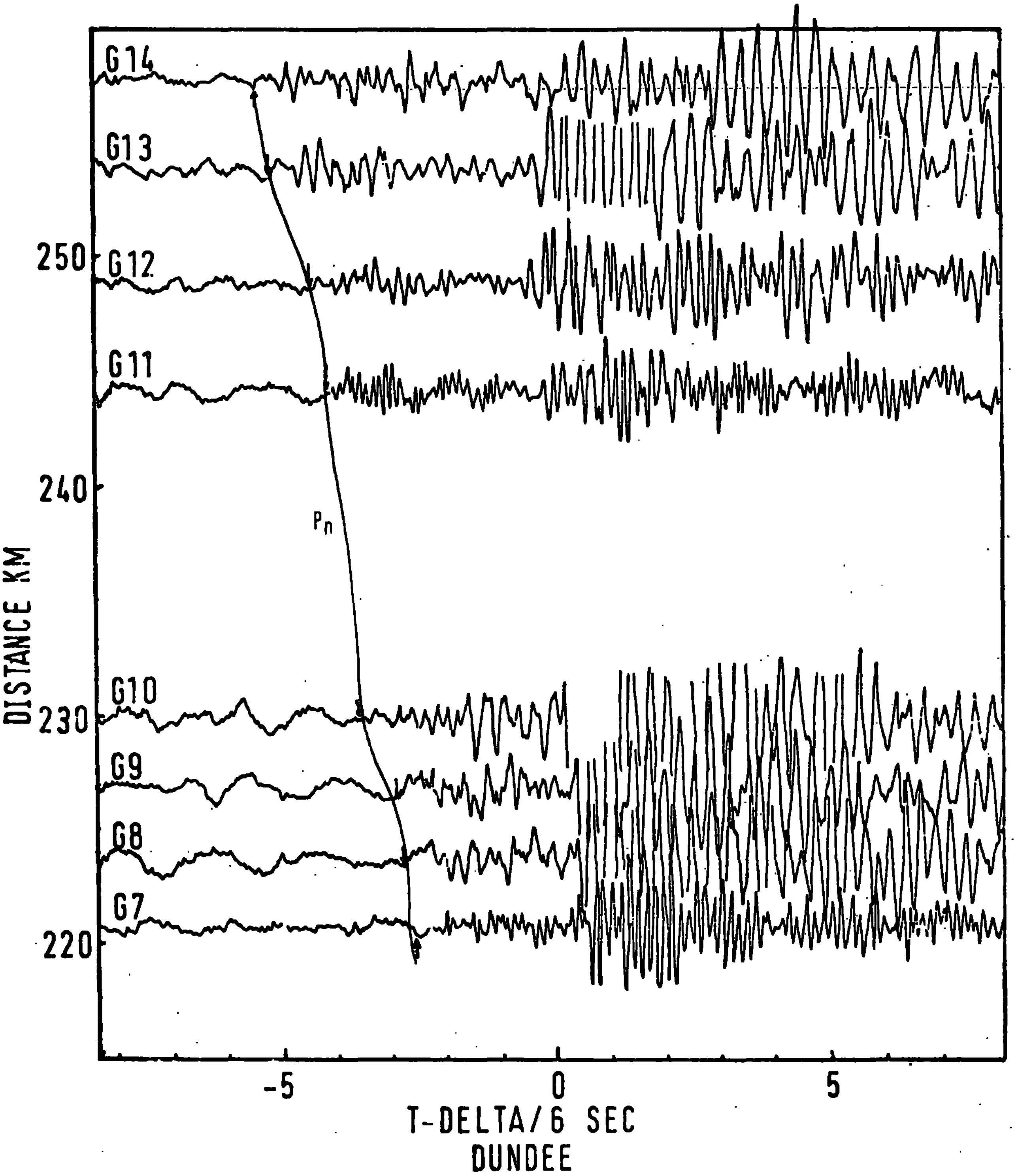

Figure 4.16 Hand drawn stacked record section of the G shots in the Minch recorded at the Lownet station, Dundee (DUN). Unfiltered vertical seismometer.

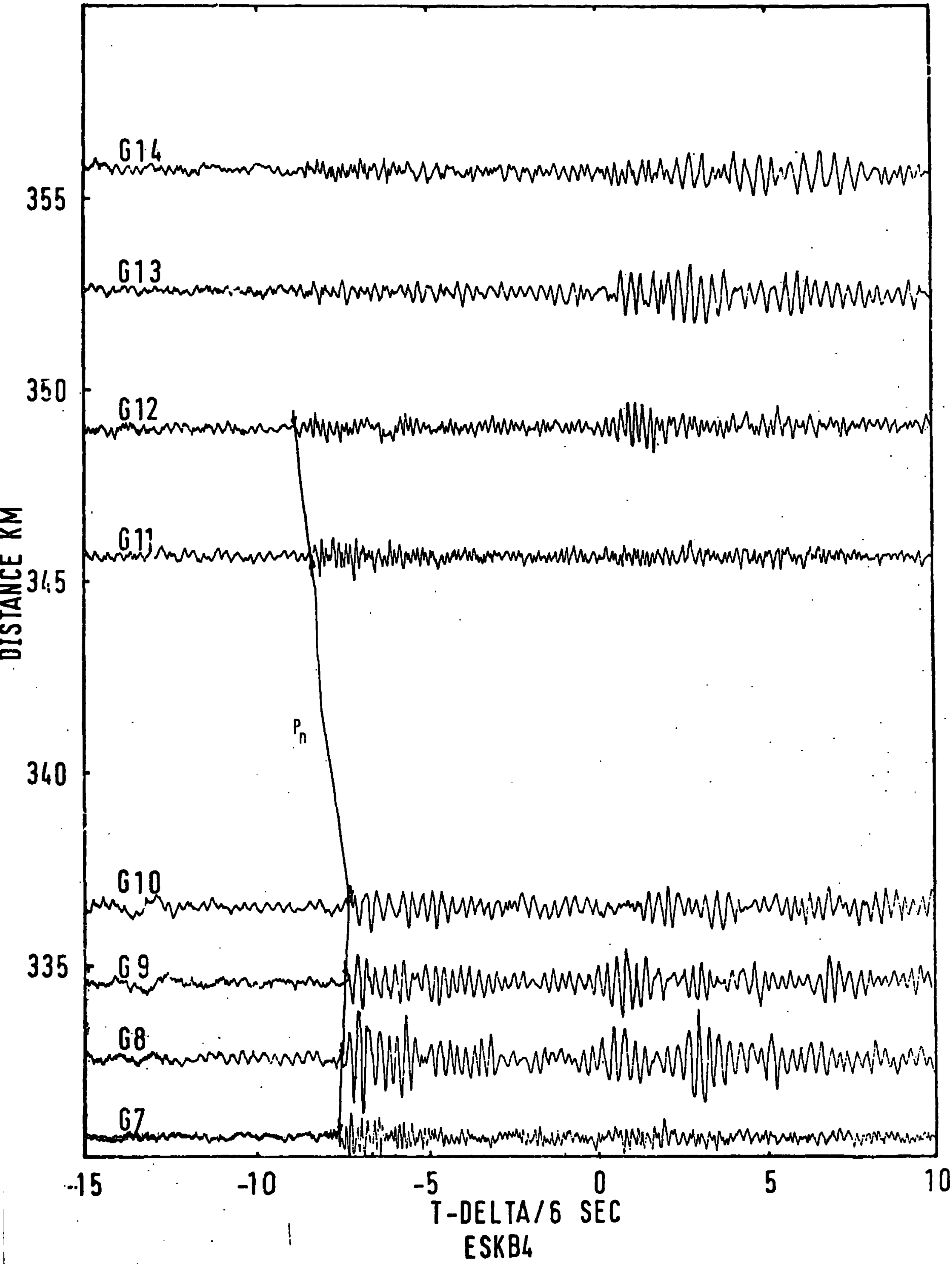

Figure 4.17 Hand drawn stacked record section of G shots in the Minch at pit B4 of Eskdalemuir (ESK). Unfiltered vertical seismometer.

line up as a P_n segment of velocity 8.2$\pm$0.4 km sec^{-1}. Shots G8, G9 and G10 are at almost the same range as the outer shelf shots but are delayed by about 1 second relative to them. This indicates substantially large delay-times for these shots, a point which is expanded upon in the discussion of the P_n time-term solution in Section 4.5.

Shots across the South Minch Basin (H9 to H16), recorded at low ranges, also show different velocities in different directions although the magnitude of any dip is not so easy to determine. A glance at the stacked record sections in Figures 4.18 and 4.19 show that the first arrivals form a curve. This could be mistaken as evidence for an increasing velocity with depth. However, when comparison is made of the same shots recorded at a wide variety of ranges, that is. as P_g <u>and</u> P_n, it is evident that the curvature is due to increasing time-terms towards the centre of the basin.

At larger ranges the first arrival for shots H9 to H16 becomes P_n and the cross-over distance can be seen in Figures 4.5 and 4.6 to be about 165 km. Apparent velocities of about 7.8$\pm$1.00 km sec^{-1} are observed at Eskdalemuir. The recordings of these shots made at Mull (Figure 4.5) demonstrate the difficulty in calculating the correct velocity for the P_n headwave when there are large changes in time-terms at the shots and the range variation is small. The shots H9 to H13 fit a straight line of velocity 5.4$\pm$0.9 km sec^{-1}, whilst the shots H14 to H16 give a velocity of 14.0$\pm$6.0 km sec^{-1} (Table 4.1). However, when allowances are made for the substantial thickness of sediments in the middle of the Minch, the observed velocities are changed significantly to

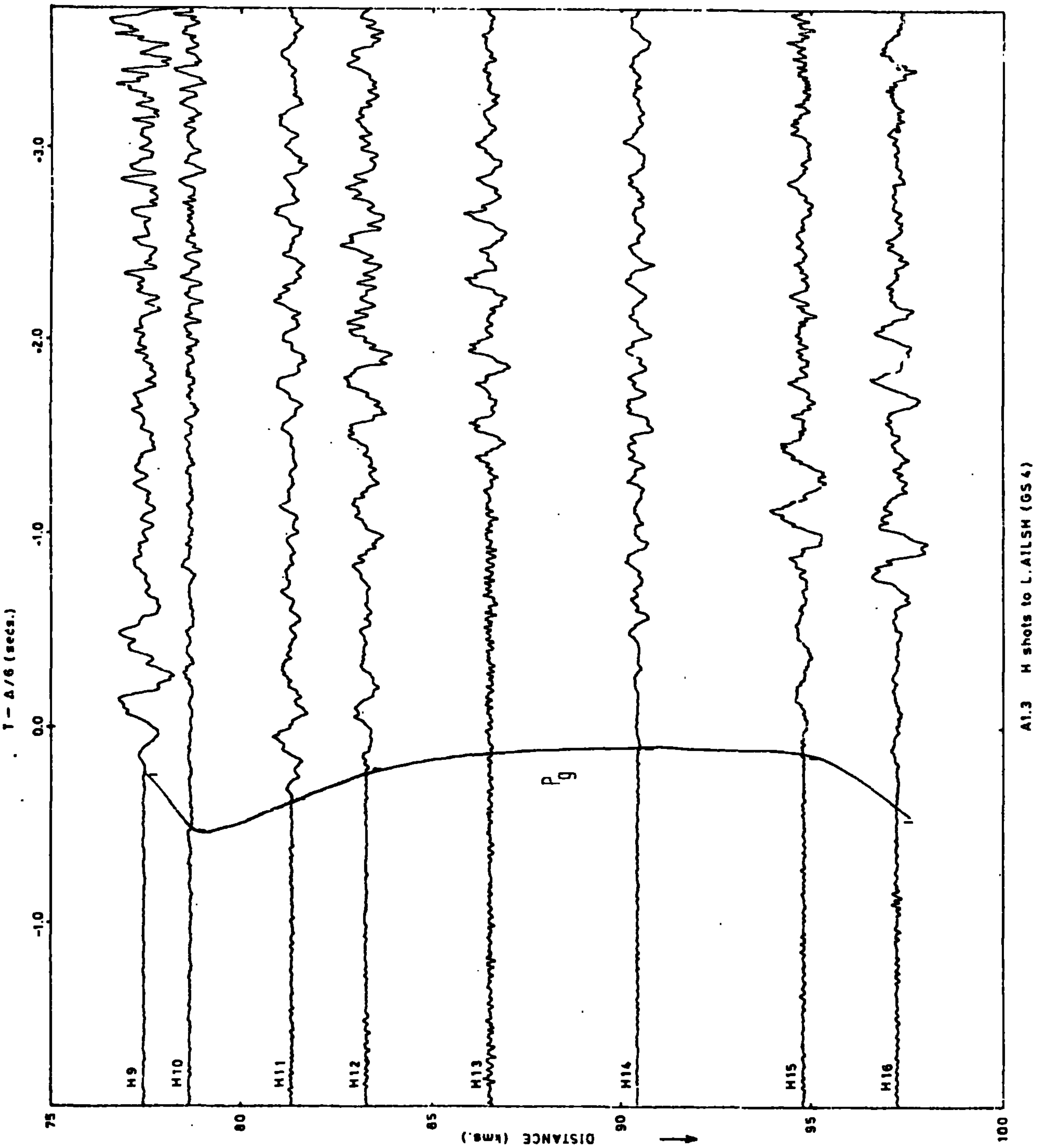

Figure 4.18 Hand drawn stacked record section of H shots in the Minch at Loch Ailsh (GS4). Unfiltered vertical seismometer, after Scott, 1976.

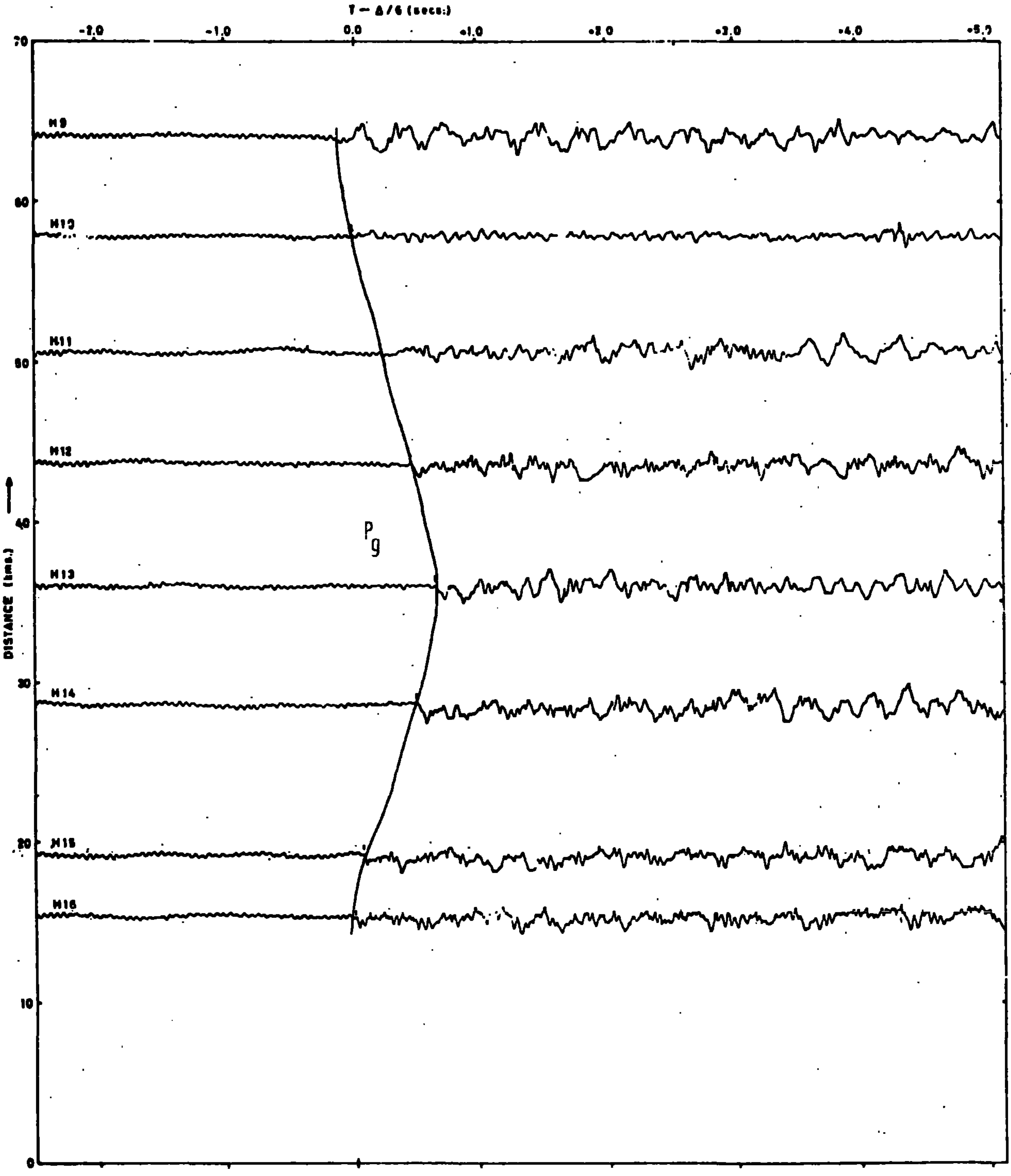

Fig. 4.2 H shots to MAARUIG (DU 11)

Figure 4.19 Hand drawn stacked record section of H shots in the Minch recorded at Maaruig (DU11). Unfiltered vertical seismometer. After Scott, 1976.

6.3 ± 0.9 km sec^{-1} and 10.9 ± 6.0 km sec^{-1} respectively. The P_n velocity is still quite different from the value normally expected and can possibly be attributed, by the same reasoning as above, to changing P_n time-terms.

The shelf shots to the west of Lewis (G15 to G28) show least-squares velocities of about 6.2 ± 0.3 km sec^{-1} when recorded to the east at an average distance of less than 100 km. The same shots recorded at St. Kilda (at an average distance of 47 km) also show a velocity of about 6.2 ± 0.2 km sec^{-1}. This indicates no regional dip beneath G15 to G23, where the coverage is reversed. A substantial change in P_g time-term <u>is</u> suggested, however, as mentioned earlier, and is shown in Figures 4.1 to 4.4. Rapidly changing time-terms, that is, a substantial dip on the basement, may be responsible for the low apparent velocity observed for shots G24 to G28 recorded at St. Kilda (Figures 5.1 and 5.6). This region of shots is not reversed and therefore suffers from the usual problem of distinguishing a dip from an anomalously low velocity refractor. However, because of the large and regular offsets from a smooth travel-time curve, evident in Figures 4.4 and 5.1, it seems likely that the observation of low velocity is caused by increasing depth to basement towards the shelf edge.

Shots G15 to G28 gave P_n as first arrival at stations at large ranges to the east and south-east. Least-squares velocities of about 7.7 ± 0.3 km sec^{-1} were observed (Figure 4.10) and are lower than the normally observed sub-Moho velocity of about 8.0 km sec^{-1} and possibly indicate the presence of dipping boundaries beneath this area.

4.3 Plus-minus method on P_g

Shots G7 to G14 in the North Minch were ideally suited to treatment by the plus-minus method, as described in Section 3.4 making due allowance for any offset. Stations on the Outer Hebrides and Scottish Mainland effectively gave reversed coverage over a range of distances, with the average distances from shots to stations ranging from 35 to 91 km. The small amounts of offset of the Outer Hebrides' stations could be allowed for by calculating theoretical curves for a single velocity refractor. Figure 4.20 shows the results of allowing the reduction velocity (v_r in Section 3.4) and the velocity of the refractor to vary. The fit between observed and calculated curves is given as the velocity is varied. For the station pair Polbain - Laxay, the best-fitting velocity is about 6.05 ± 0.05 km sec^{-1} and is quite well defined. Figure 4.21 shows the results of such an analysis for four different station pairs of steadily increasing separation. The fact that the best-fit velocity increases from 6.05 km sec^{-1} to 6.25 km sec^{-1} as the average recording distance increases from 35 to 91 km indicates a possible increasing velocity with depth, in accordance with the results of fitting straight lines to the data.

In contrast to the single segment reduced minus-time graphs for G7 to G14, graphs drawn for shots H9 to H16 and G15 to G22 show a more complex situation. Figure 4.22 shows an analysis of the H shots in the Minch recorded at four different station pairs. Velocities of 6.0 and 6.1 km sec^{-1} were used for the construction of the curves but,

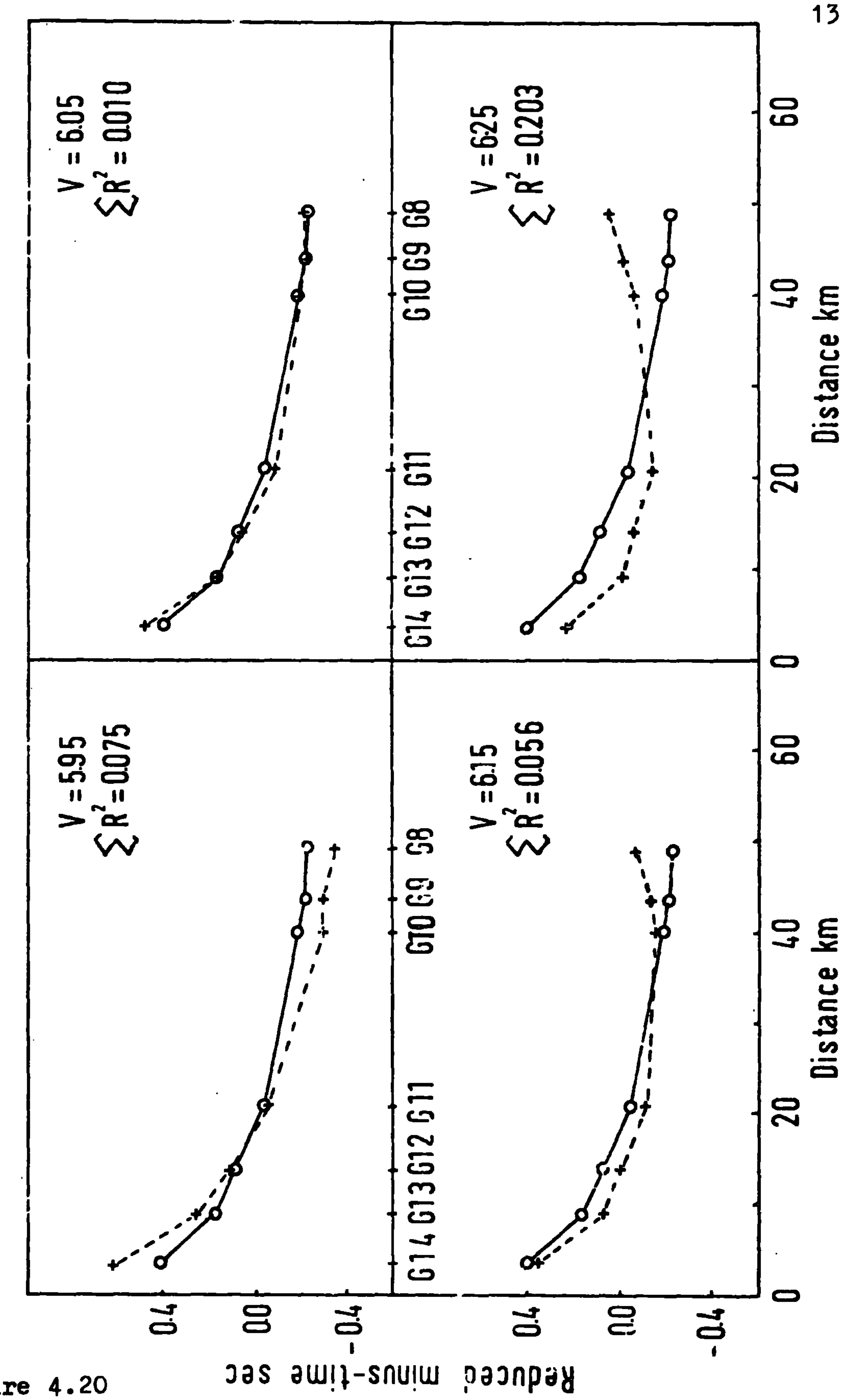

Figure 4.20

4 reduced minus-time graphs for G shots in the Minch recorded at the station-pair Polbain and Laxay (GS1 and MD1). o - calculated reduced minus-time for recording network geometry and single velocity refractor; + - observed reduced minus-time. Refractor and reduction velocity and sum of residuals squared are given in the top right hand corner.

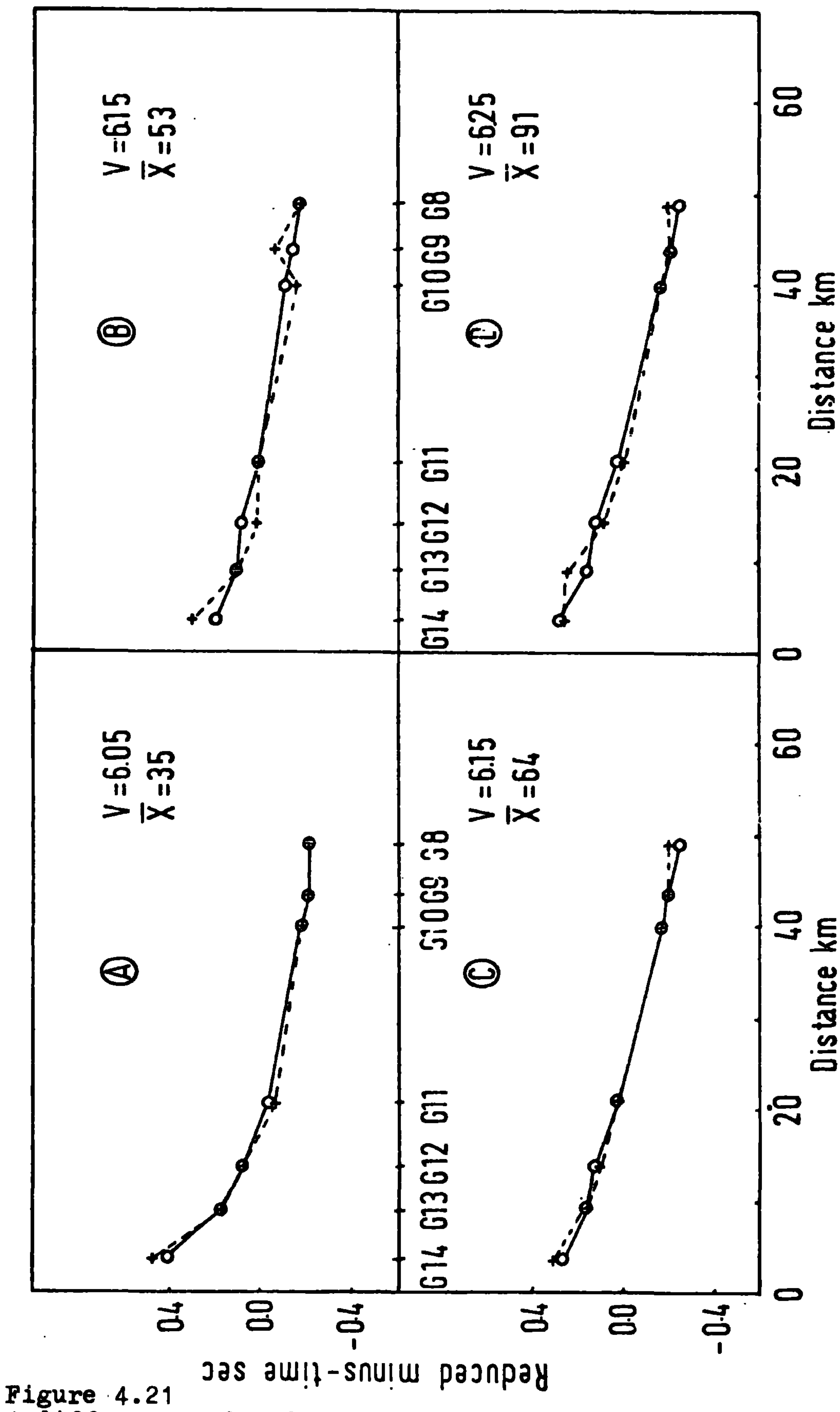

Figure 4.21
4 different reduced minus-time graphs for G shots in the Minch. O - calculated; + - observed. A is GS1 to MD1, B is GS3 to DU8, C is GS4 to DU7 and D is GS8 to DU7. The best-fitting velocity and the average of the travel distances from the shots to each station pair is given.

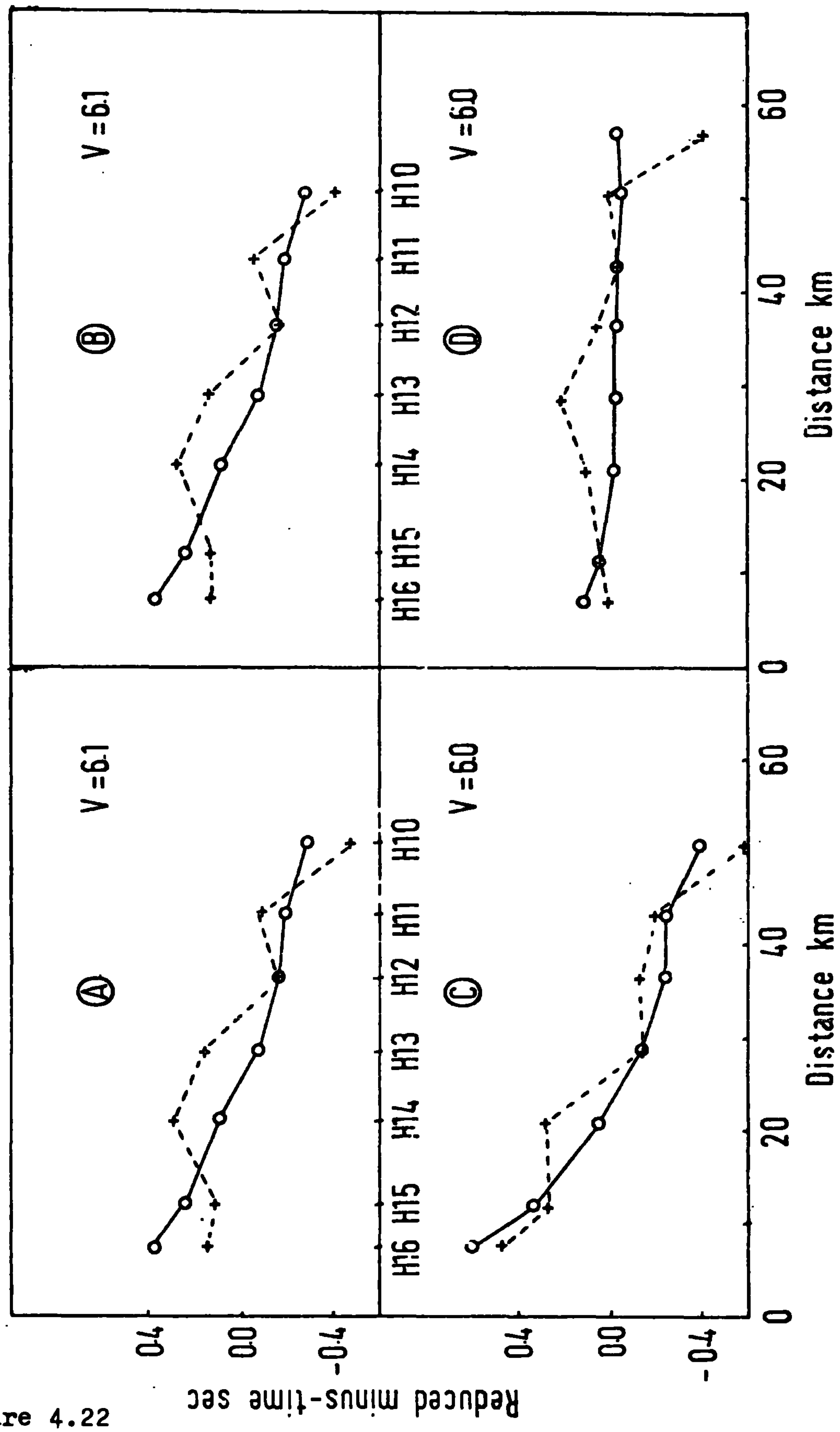

Figure 4.22
4 reduced minus-time graphs for H shots in the Minch.
O - calculated; + - observed. A is DU14 to MD1, B is DU13 to MD1, C is DU13 to DU9 and D is DU13 to DU11. The best-fitting velocity is given for each pair.

clearly, the refractor has not got a single velocity. The actual velocities in the refractor and the points at which they change cannot be determined, owing to the large spacing of the shots. Scott (1976) has independently produced a model for the structure beneath the H shots in which he has combined an interpretation of the P_g time-terms with the gravity and magnetic evidence. Figure 4.23 is taken from Scott (1976) and shows that a dense body beneath the south-eastern part of the Minch is required to fit the gravity data. The shape of the sedimentary basin in the Minch is derived from his interpretation of the time-terms for the H shots. The presence of the postulated dense body at shallow depth within the basement may be expected to give rise to changes in velocity of the type found by plus-minus analysis.

Figure 4.24 shows the best-fitting velocity for the shots G15 to G22. The very large rise in the theoretical curve towards shot G22 can be accounted for by the large offset of St. Kilda from the shot line. However, a plot of observed minus calculated residuals shows a clearer picture. The velocity of the refractor beneath G15 to G18 and G20 to G22 is in the region of 6.0 km sec^{-1}. Beneath G18 to G20 refractor velocities as high as about 7.0 km sec^{-1} are indicated. Figure 4.25 shows the correlation between the changes in refractor velocity, the plus-times and the magnetic and Bouguer gravity anomaly over the area. The plus-times have been calculated by constraining H10 and G19 to be exactly zero. Quite clearly, the high velocity material forms a rise in the basement and has a large positive

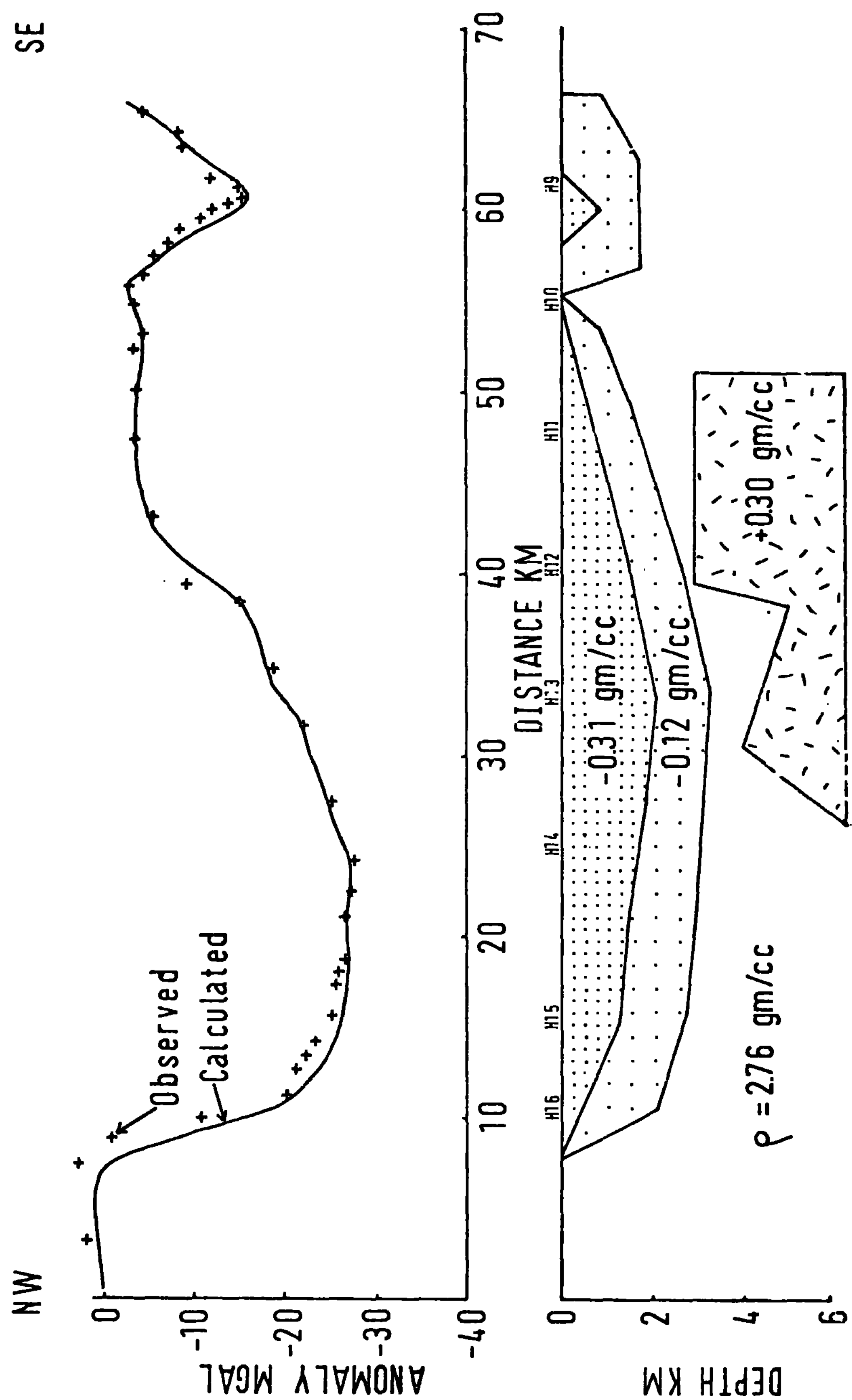

Figure 4.23 Comparison of observed and calculated gravity anomalies across the South Minch Basin. Model of sediments is based on an interpretation of P_g time-terms and dense body is required to fit gravity data. Redrawn from Scott, 1976.

See figure 2.1

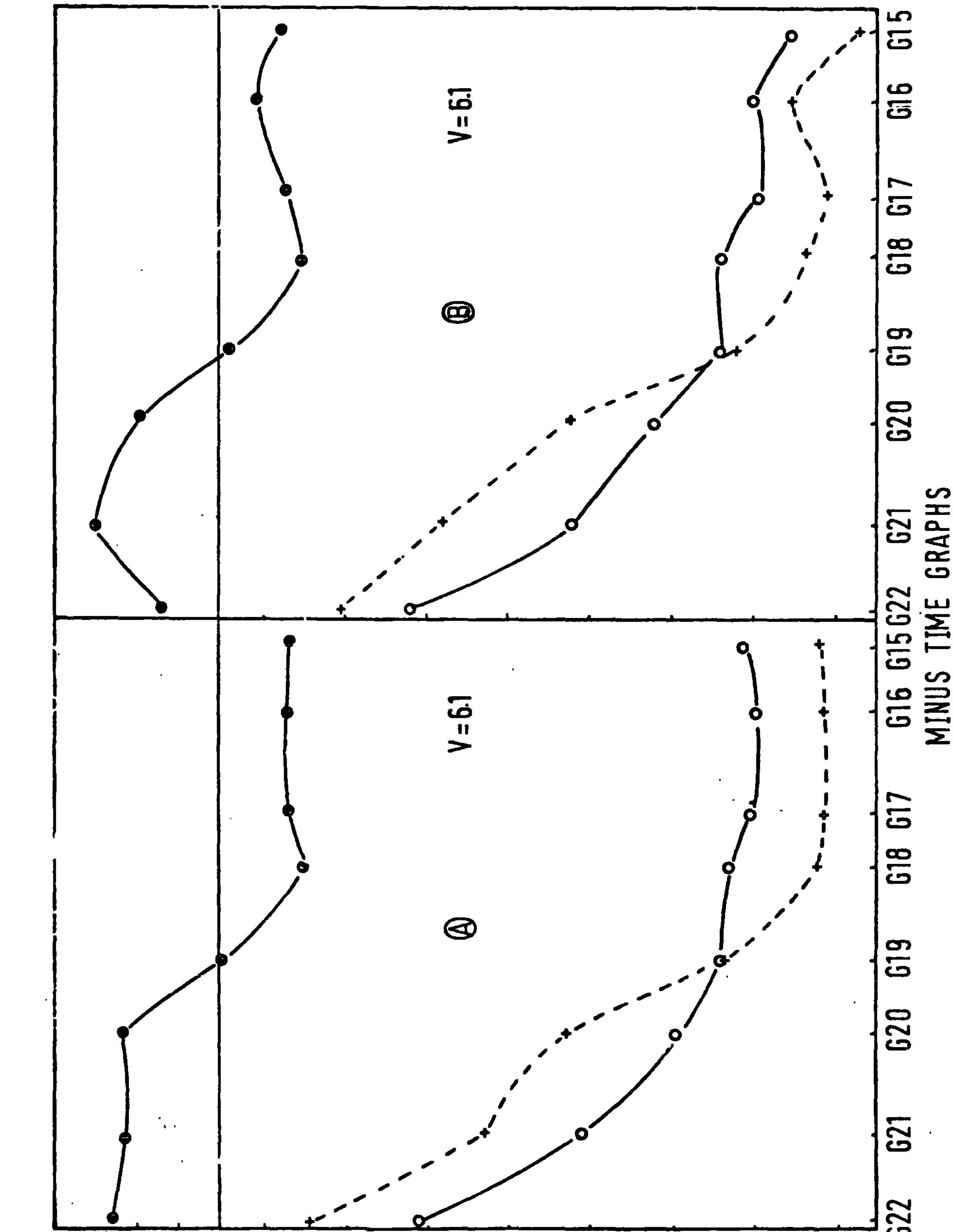

Figure 4.24
2 reduced minus-time graphs for shots on outer shelf. o - calculated; + - observed. A is DU15 to MD1, B is DU15 to DU10. Best-fitting velocity is given for each pair. Observed minus calculated residuals are given and show changes of refractor velocity in vicinity of G20 and G18.

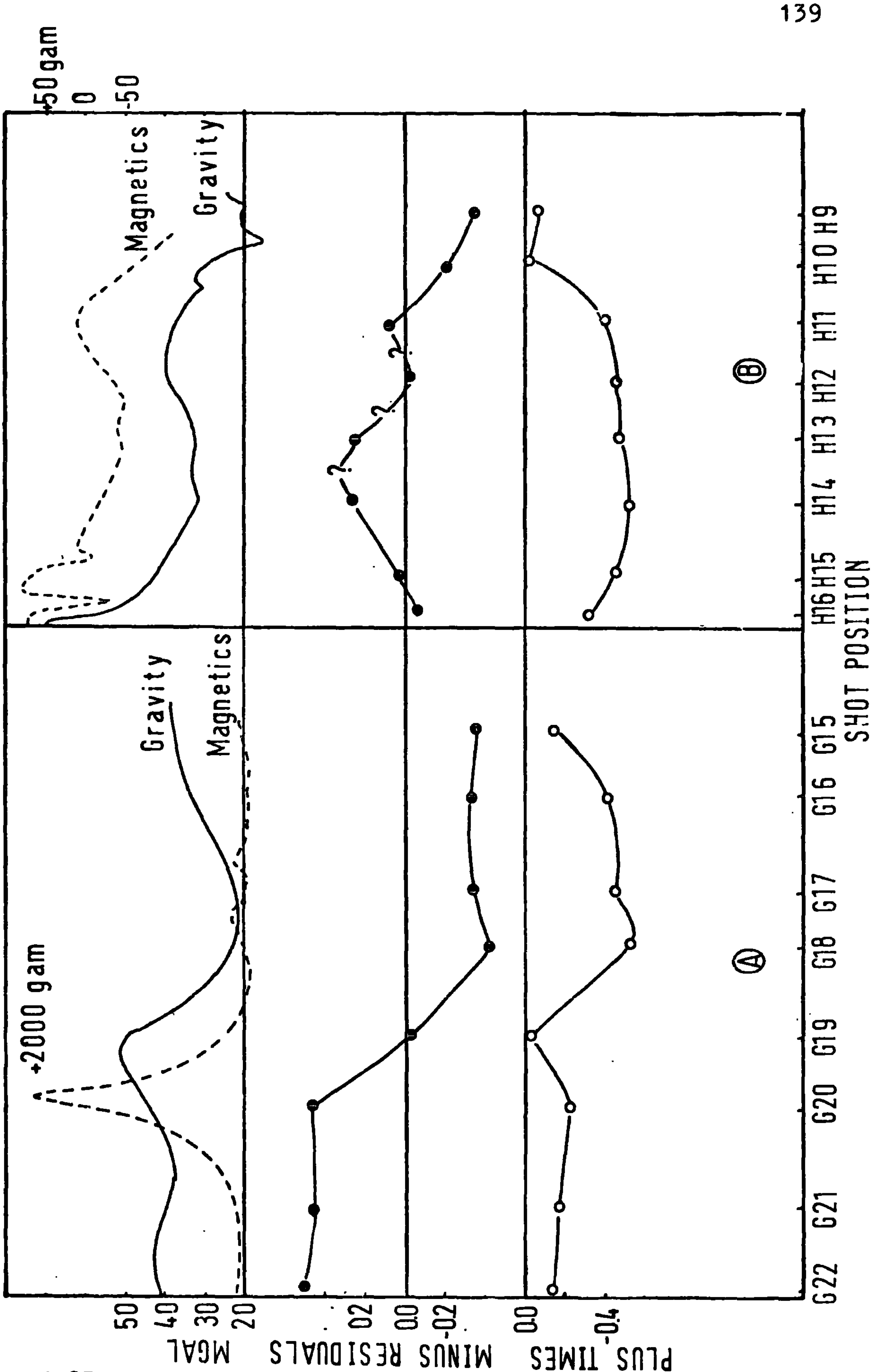

Figure 4.25
Bouguer anomaly, magnetic anomaly, reduced minus-time residuals and plus-times for profiles across outer shelf (DU15 to MD1) and the South Minch Basin (DU13 to MD1).

magnetic anomaly and a large positive gravity anomaly. In fact, the profile crosses the positive gravity anomaly to the south of the peak value of 72 mgal which occurs about 10 km to the north of shot G19 (Hydrographic Department, Free-air gravity map, 1973). Very large positive magnetic anomalies are associated with the gravity anomaly and continue to the north of the line for about 15 km (Aeromognetic map of Great Britain and Northern Ireland, Sheet 12). The gravity low in the region of shots G17 and G18 extends in a north-north-easterly direction passing to the east of the Flannan Isles and terminating at about 58° 30' N. The Flannan Isles are composed of hornblende gneiss and pegmatite sheets of Lewisian age (Stewart, 1933) and are sited on a northward extension of a region of positive gravity anomalies stretching from St. Kilda, passing to the north of G19, and on towards a large positive anomaly at about 58° 47'N, 6° 33'W. The difference between the structure beneath shots G16 to G18 and G19 to G21, shown by the magnetic, gravity and seismic refraction evidence, is also demonstrated by the character of the seafloor. Profile 24/71 of Himsworth (1973) shows very clearly that the seabed in the region of the gravity high near shot G19 is very rough and comparatively shallow (60 m) whilst to the east of this region near shots G16 to G18, a smoother seafloor is observed. Evidence from seismic reflection profiles (F. Bouwers, personal communication) also shows the change between shots G18 and G19. From G18 eastwards there is some indication of correlated reflectors down to depths of about 1 second two-way travel-time, corresponding with the gravity low. The region around G19 to G21 has no correlated energy returning from the subsurface and is separated from the area to the east by a zone of diffractions dipping steeply to the east. A fault, downthrowing to the west with an indeterminate amount of throw, is also shown between shots G16 and G17 on the reflection profiles.

Himsworth (1973) has interpreted the gravity anomalies over St. Kilda and at 58° $48'$N, 6° $33'$W as being caused by Tertiary igneous centres similar to those of Ardnamurchan, Mull and Skye. In contrast to the magnetic signature of St. Kilda, and the other Tertiary igneous centres of Scotland, which have both positive and negative parts, the magnetic anomalies in the vicinity of shots G19 to G20 are almost entirely positive. In this respect they are more similar to the type of anomaly found over the metagabbros of the South Harris igneous complex and their probable seaward extension (Westbrook, 1974). It therefore seems likely that the magnetic and gravity anomalies are due to dense and strongly magnetised Lewisian basement rocks outcropping at the seafloor beneath shots G19 to G21.

4.4 Time-term analysis of P_g

A total of about 300 recordings of P_g were made by the shot - station network. Because of the variability in structure indicated by the preceding analysis, the data was split into three sets. Recordings of shots G7 to G14 in the North Minch made up the first set, whilst the second set consisted of recordings of H9 to H16. Recordings of the shots to the west of Lewis, that is, G15 to G28 and the J shots made up the third set.

Each data set was put through a standard procedure of analysis. Firstly, a time-term solution was found for each set, assuming a uniform velocity refractor. The observed minus calculated residuals were scrutinised for obvious errors in the data which could be checked and either corrected or rejected from the data set. Using this refined data set the time-term analysis was repeated. Solutions for increasing velocity of the refractor with distance and increasing velocity with depth were then found.

The solution involving increasing velocity with depth was found by means of a non-linear optimisation program written by Dr. G.K. Westbrook using the library program Minuit (James and Roos, 1969). A numerical iterative method is used to minimise the sum of the squared residuals with respect to the variable parameters: velocity, velocity gradient and time-terms. Each time-term was assumed to be constant for arrivals recorded over the whole distance range, an approximation which may lead to small errors, particularly where the distance range and velocity gradient are both large.

In an attempt to determine whether the data fitted a two layer travel-time curve, the data set was split into two by separating it into recordings above and below a designated distance. Both of these sets were solved using the single velocity refractor model. The variances for each solution were then compared to find the best solution. The residuals were checked to see if they had any obvious dependence on distance or azimuth.

4.4.1 P_g analysis of shots G7 to G14

Figures 4.26(a) and (b) summarise the results of performing this analysis on the shots G7 to G14. 110 recordings at ranges less than 140 km were used to determine the 25 time-terms. A graph of the sum of squared residuals against the constrained velocity of the refractor shows that the least-squares velocity of 6.13 ± 0.02 km sec^{-1} is well determined. The minimum sum of squared residuals is 0.88 sec^2 and should be compared with values of 0.71 sec^2 when the velocity of the refractor is allowed to vary with distance and 0.56 sec^2 when the velocity of the refractor is allowed to vary with depth.

Figure 4.26(b) is an attempt to determine whether the data fits a two segment first arrival curve better than it fits the single segment curve. The distance at which the data is split into two groups is plotted along the bottom axis. The sum of squared residuals is plotted for each group together with the composite sum of squared residuals for both groups together. A summary of the results is given in Table 4.2.

It can be seen, firstly from the sum of squared residuals, but more rigorously from the variance ratio, that the two layer model is a significant improvement over the single layer model and similarly that the model allowing an increase in the refractor velocity with depth also gives a significant improvement. For the number of degrees of freedom of the F statistic available here, a variance ratio above about 1.2 is highly significant. The difference between the two layer model and the increasing velocity with

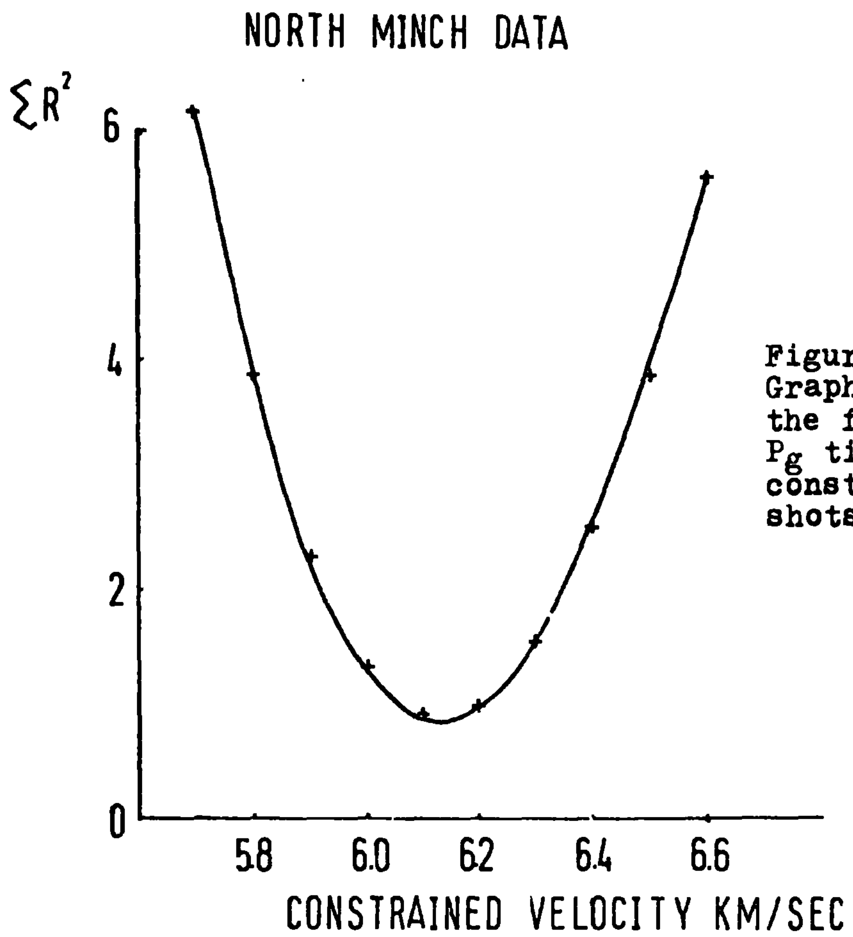

Figure 4.26(a)
Graph of the variation of the fit of single velocity P_g time-term solution with constrained velocity. G shots in Minch.

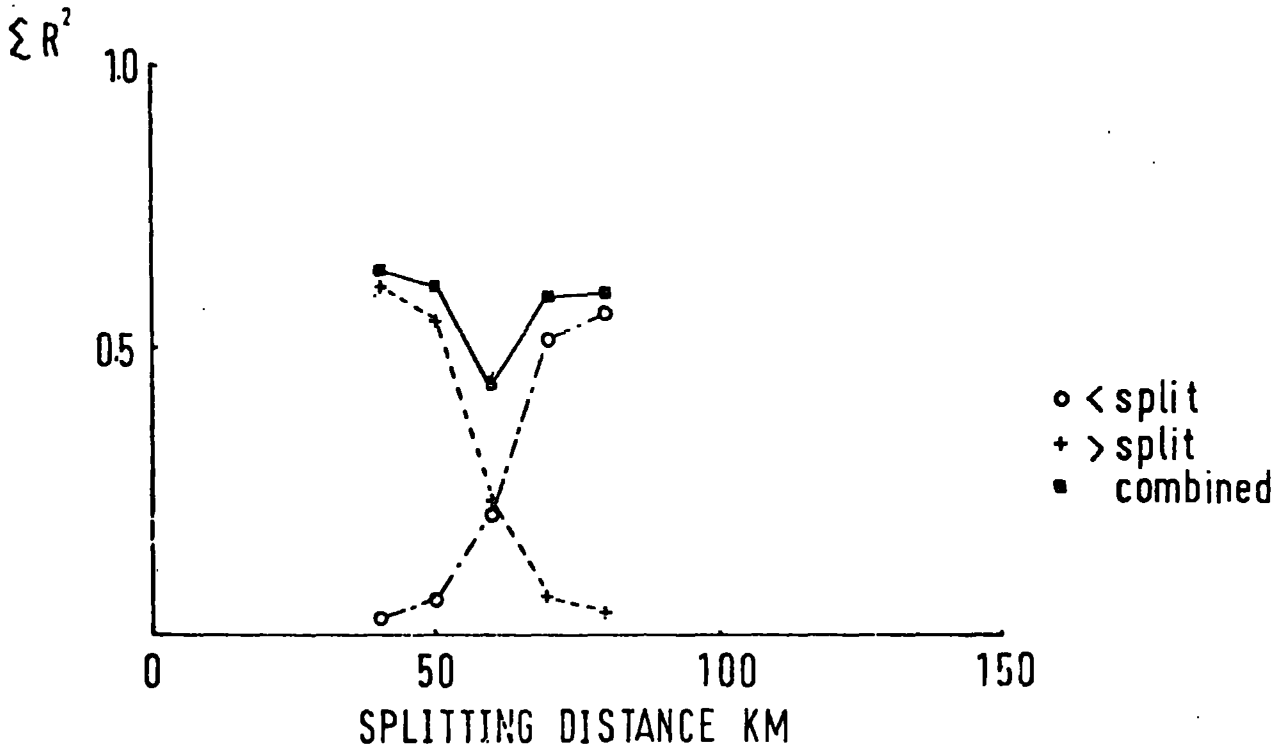

Figure 4.26(b) Graph of variation of the fit of the two layer time-term solution with point at which data set has been split into two. G shots in Minch.

Table 4.2 Summary of P_g time-term analysis of G7 to G14.

Type of Solution	Least-squares velocity (km sec^{-1})	R^2 (sec^2)	Degrees of freedom	Variance (sec^2)	Variance ratio[b]
Single velocity	6.13	0.88	85	0.0103	1.00
$V=V_0+0.0013x$	$V_0=5.93$	0.71	84	0.0084	1.22
$V=V_0+0.03z$	$V_0=6.02$	0.56	84	0.0066	1.56
All data<40 km	7.11[a]	0.03	7	0.0092[c]	1.12
All data>40 km	6.17	0.61	62		
All data<50 km	5.94	0.06	16	0.0091[c]	1.13
All data>50 km	6.17	0.55	51		
All data<60 km	6.06	0.21	35	0.0065[c]	1.58
All data>60 km	6.22	0.23	32		
All data<70 km	6.05	0.52	51	0.0088[c]	1.17
All data>70 km	6.21	0.07	16		
All data<80 km	6.07	0.56	59	0.0089[c]	1.16
All data>80 km	6.15[a]	0.04	6		

a These values are calculated for very few degrees of freedom (that is, the data set is only just determined). Hence, reliance cannot be placed on the least-squares velocities.

b Variance ratio is the F statistic used for finding the significance of differences in variances. Values above about 1.2 are significant for these large degrees of freedom.

c The composite variance of the split solution is found from:

$$\sigma^2 = \frac{R_1^2 + R_2^2}{df_1 + df_2}$$

where σ^2 is the composite variance

R_1^2 is the sum of squared residuals for the first data set

R_2^2 is the sum of squared residuals for the second data set

df_1 is the degrees of freedom of the first data set

df_2 is the degrees of freedom of the second data set.

depth model is probably quite insignificant. Comparison of the velocity - depth functions implied by the various solutions and the results of experimental work by Christensen and Fountain (1975) on the relationship between pressure (depth) and velocity in granulites of varying density is given in Figure 4.27. The indicated structure is quite compatible with a velocity increase with depth due only to an increase in pressure and does not require any significant compositional changes with depth. The least-squares velocity of 6.22 ± 0.03 km sec^{-1} determined for the lower layer does not approach the velocity expected for the mid-crustal refractor observed in NASP.

Many of the recording stations were situated on, or close to, Lewisian gneiss basement and would be expected to have a zero time-term (Table 4.5). The fact that several stations have negative time-terms indicates that, locally, the Lewisian has a higher velocity than the one found as an average over the whole area. To interpret the time-terms and produce a depth to basement the velocity of the sediment filling the Minch must be found. Shallow seismic reflection, refraction and bottom sampling by the IGS Continental Shelf Unit and Glasgow University (Chesher *et al.*, 1972; Smythe *et al.*, 1972; Binns *et al.*, 1975) have revealed the extent and some age details of the basins in the Minch. The line G7 to G14 just crosses the southern edge of the North Minch Basin, with Mesozoic sediments (probably Jurassic and New Red Sandstone) being restricted to a thin sheet between shots G8 and G11 and the Torridonian outcropping at the seabed along the remainder of the line.

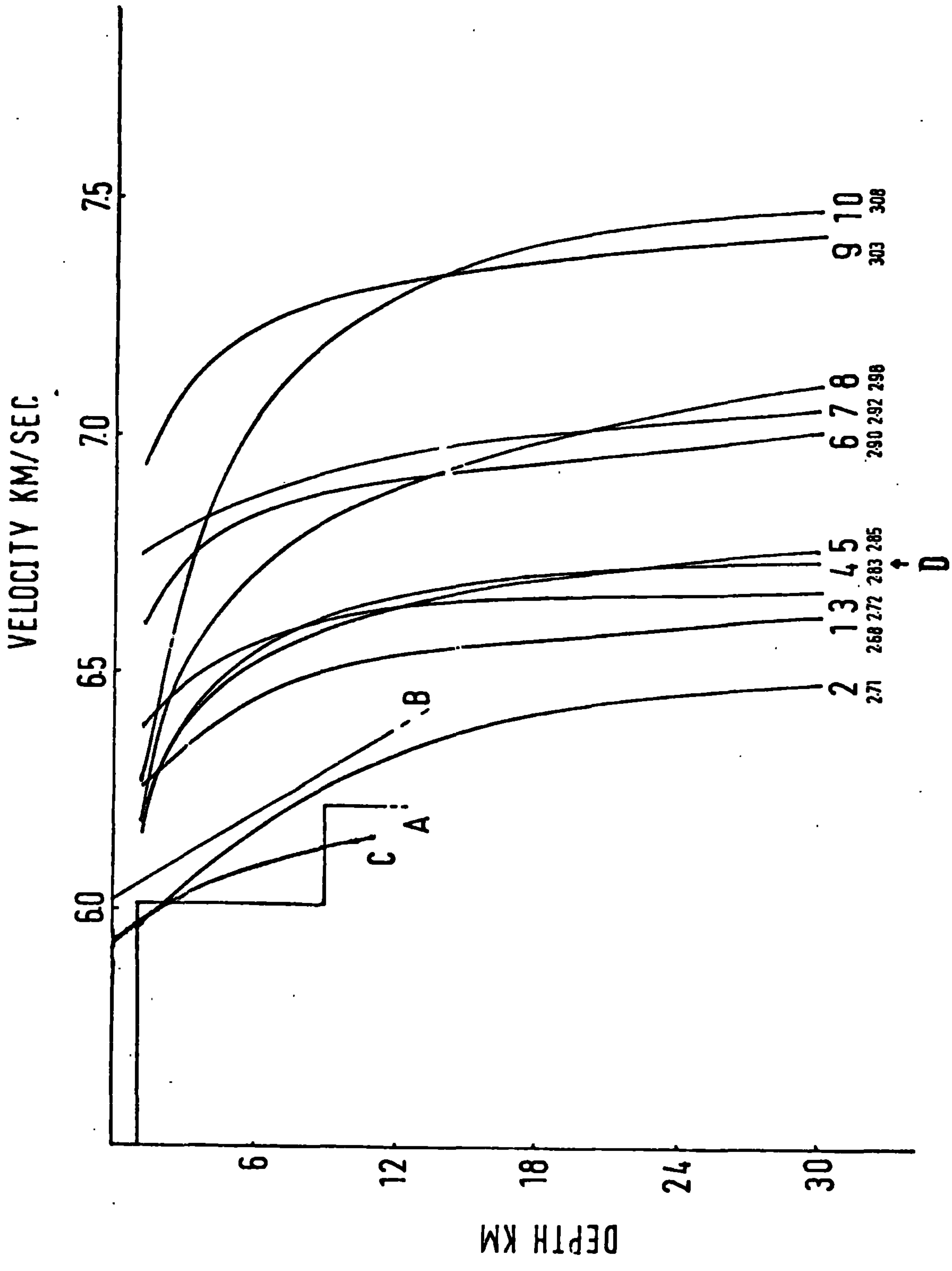

Figure 4.27 Comparison of velocity/depth models derived from time-term analysis of the G shots and some experimental work on velocity/pressure relationships in granulites (Christensen and Fountain, 1975). 1 to 10 - their samples with densities in gm cm^{-3}. A is two layer time-term solution, B is solution with increasing velocity with depth, C is the solution with increasing velocity with distance. D is density of a north-west Scottish granulite in Bott et al., 1972.

Before the time-terms can be interpreted in terms of depth to the refractor they must be corrected for the delaying effect of the water and for the speeding up effect of being fired below sea level. The observed time-term for a refractor, r, is given by an expression of the form:

$$(wd - sd)(V_r^2 - V_w^2)^{\frac{1}{2}}/V_rV_w \quad + \quad \sum_{i=1}^{n-1} z_i(V_r^2 - V_i^2)^{\frac{1}{2}}/V_rV_i$$

where wd is the water depth

sd is the shot depth

z_i is the thickness of each layer above the refractor

V_w is the velocity of the water

V_i is the velocity of each layer above the refractor

and V_r is the velocity of the refractor.

To allow for the water depth and shot depth effects a correction is made to replace the water layer with the material directly beneath it and to move the shot to the surface. The time-term would then be of the form:

$$(z_1 + wd)(V_r^2 - V_1^2)^{\frac{1}{2}}/V_rV_1 \quad + \quad \sum_{i=2}^{n-1} z_i(V_r^2 - V_i^2)^{\frac{1}{2}}/V_rV_i$$

The difference between these two expressions is:

$$(wd - sd)(V_r^2 - V_w^2)^{\frac{1}{2}}/V_rV_w \quad - \quad wd(V_r^2 - V_1^2)^{\frac{1}{2}}/V_rV_1$$

For a P_g refractor of velocity 6.2 km sec^{-1} with sediments of 3.0 km sec^{-1} above it, the correction to be subtracted from the time-term is:

wd(0.36) - sd(0.65)

For the shots fired on the shallow continental shelf this correction varies between -0.02 and +0.06 seconds. Varying the velocity of sediments by a small amount does not make any significant difference.

For a P_n refractor of velocity 8.0 km sec^{-1} and with rocks of sedimentary velocity 3.0 km sec^{-1} above it, the correction is:

$$wd(0.34) - sd(0.65)$$

For the shelf shots considered here this correction was between -0.03 and +0.06 seconds. It is only when the water depth becomes quite large that this correction becomes really significant.

The corrected time-term can now be converted to a depth to the refractor by means of the formula:

$$\text{time-term} = \sum_{i=1}^{n-1} z_i(V_r^2 - V_i^2)^{\frac{1}{2}}/V_rV_i$$

where there are n layers above the refractor.

No direct observation of velocities within the Torridonian were made during HMSP, but refraction observations by Glasgow University and the IGS (Smythe <u>et al</u>., 1972) indicate that a velocity of about 4.8 km sec^{-1} is likely. Using this velocity for the Torridonian and a velocity of 3.0 km sec^{-1} as an estimate of the Mesozoic velocity, the depth to the basement can be found from the time-terms. Figure 4.28 gives the shape of the basement so determined, together with the interpreted geological structure and Bouguer anomaly profile.

The Minch fault is   a normal fault downthrowing to the east and preserving Mesozoic sediments in the Minch Basins (Allerton, 1968; McQuillin and Binns,

Figure 4.28 Time-terms for G shots in Minch and the adjacent land areas together with the interpreted geological structure and observed Bouguer anomaly profile. Error bars are 95% confidence limits. See figure 2.1

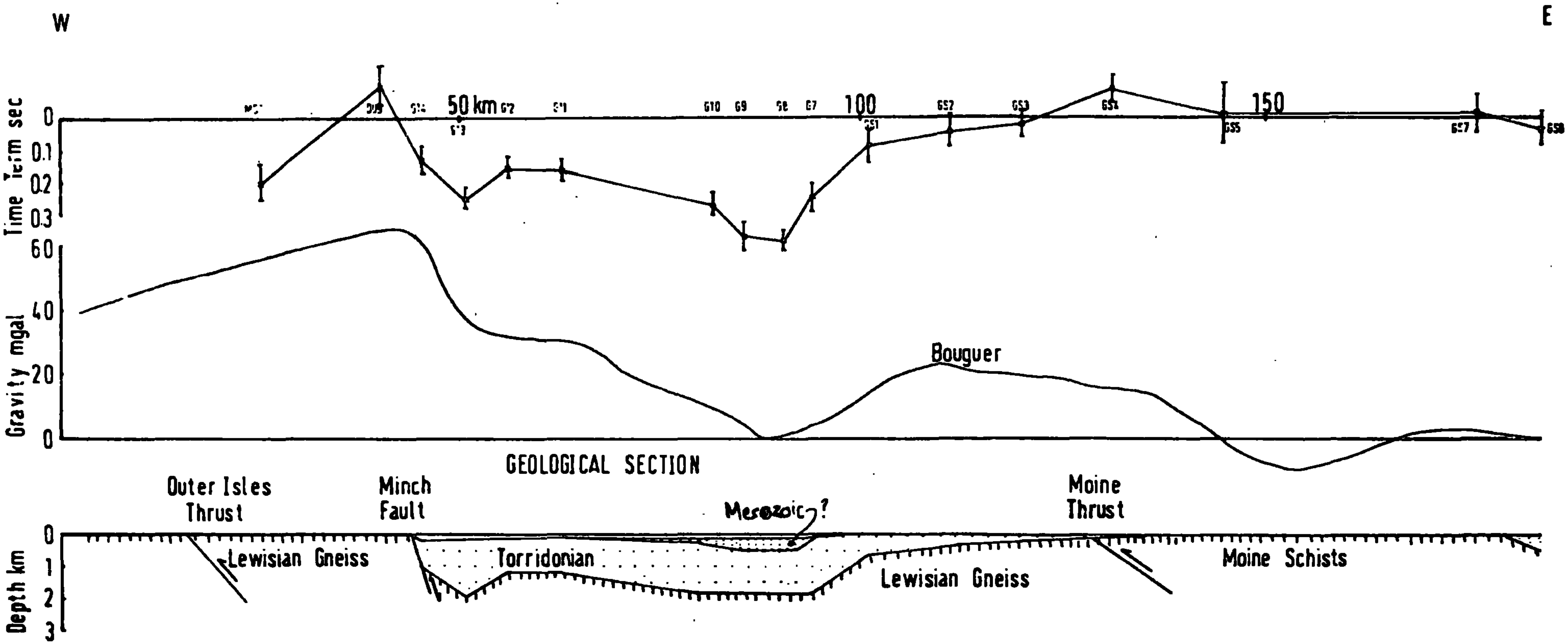

†

1973). The 124 km sinistral transcurrent movement postulated by Dearnley (1962) on the basis of the correlation of metamorphic provinces on the Scottish Mainland and Outer Hebrides is considered unlikely because the fault trace is now known not to be a small circle but to bend around parallel to the east coast of the Outer Hebrides (Figure 1.2). The evidence of Torridonian preserved to the east of the fault suggests the possibility that the fault is as old as the Torridonian although it may be more likely that the movement was post-Torridonian.

The Bouguer anomaly profile in Figure 4.28 is taken from an unpublished gravity map compiled from Hydrographic Department and various American data for the sea areas and from McQuillin and Watson (1973) and IGS data for the land areas. The small scale anomalies in the Minch seem to correlate well with the sediment structure determined. For a model with -0.12 gm cm^{-3} and -0.28 gm cm^{-3} as the density contrast of the Torridonian and Mesozoic with the Lewisian basement (Tuson, 1959), the anomaly caused by the sediments in the Minch is always less than 15 mgals. So, when the known sediment structure is allowed for there are still substantial large scale anomalies, the explanation of which must lie in deeper structures. McQuillin and Watson (1973) have pointed out that the uniform drop in the Bouguer anomaly across Lewis coincides with the increasing migmatisation of the gneisses which causes a decrease in density of the surface layers. On the east coast of the Outer Hebrides, to the east of the Outer Isles thrust, rocks of granulite facies, or retrogressed granulite facies, tend to

† This sentence is unnecessary since Dearnley's postulated fault occupies a central position in the Minch and would not be the same fault as the normal Minch fault.

occur, whilst on the west coast veins and pods of granite can make up 50 per cent of the gneisses which are typically in amphibolite facies (Coward et al., 1970).

4.4.2 P_g analysis of shots H9 to H16

Figures 4.29(a) and (b) and Table 4.3 detail the results of the time-term analysis for P_g recordings of these shots in the South Minch Basin. 107 recordings at ranges less than 140 km were used to find the 25 time-terms. The least-squares velocity of 6.0 ± 0.03 km sec^{-1} is quite well determined and a two layer solution improves the variance of the solution significantly, from 0.0112 to 0.0059 sec^2. An increasing velocity with depth solution does not make a similar improvement.

Figure 4.30 shows the time-terms found from the single velocity model. Mesozoic sediments outcrop over the whole line except near H10 where a Lewisian basement ridge strikes north-north-east from Raasay and Rona. Two shallow core holes drilled by the IGS in 1971 (Chesher et al., 1972) show sediments of Jurassic age close to the present profile. Permo-Triassic sediments were also found outcropping on the seabed slightly to the north-east of the profile, close to where the Torridonian outcrops on the seabed. Three kilometres of New Red Sandstone are preserved in the fault bounded Stornoway basin (Steel, 1971) and up to 800 m of New Red Sandstone may be present under northern Skye (Tuson, 1959; Steel, Nicholson and Kalander, 1975; Smythe et al., 1972).

It is also likely that Torridonian, and possibly Cambrian, sediments lie beneath the Mesozoic in this basin

SOUTH MINCH DATA

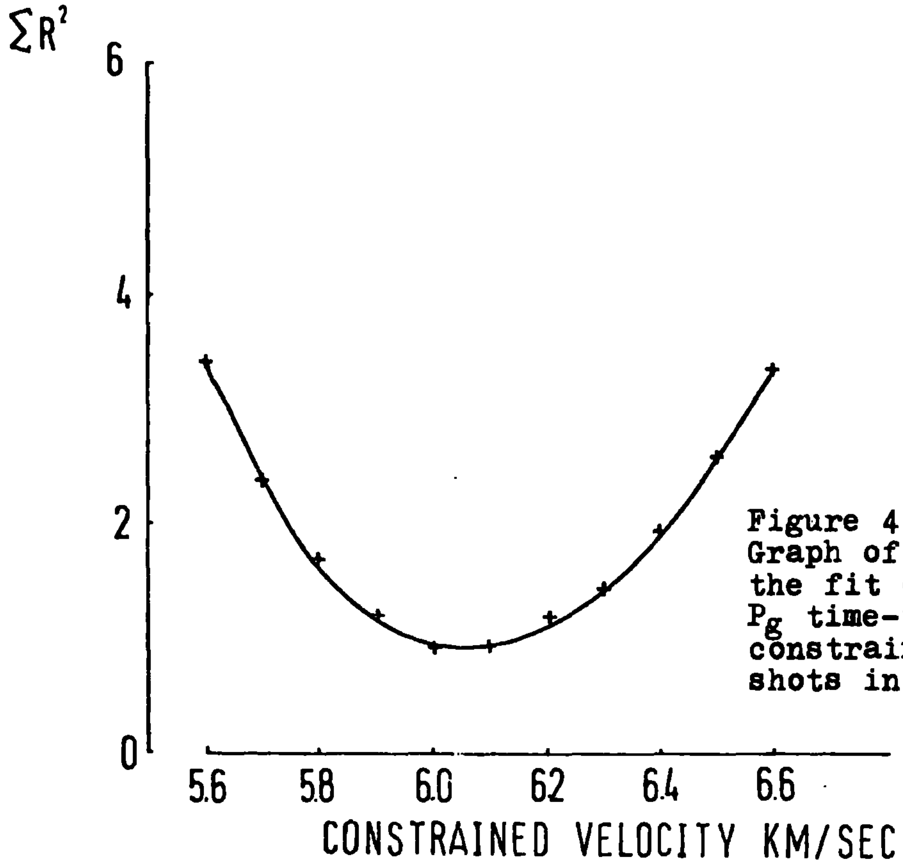

Figure 4.29(a)
Graph of the variation of the fit of single velocity P_g time-term solution with constrained velocity. H shots in Minch.

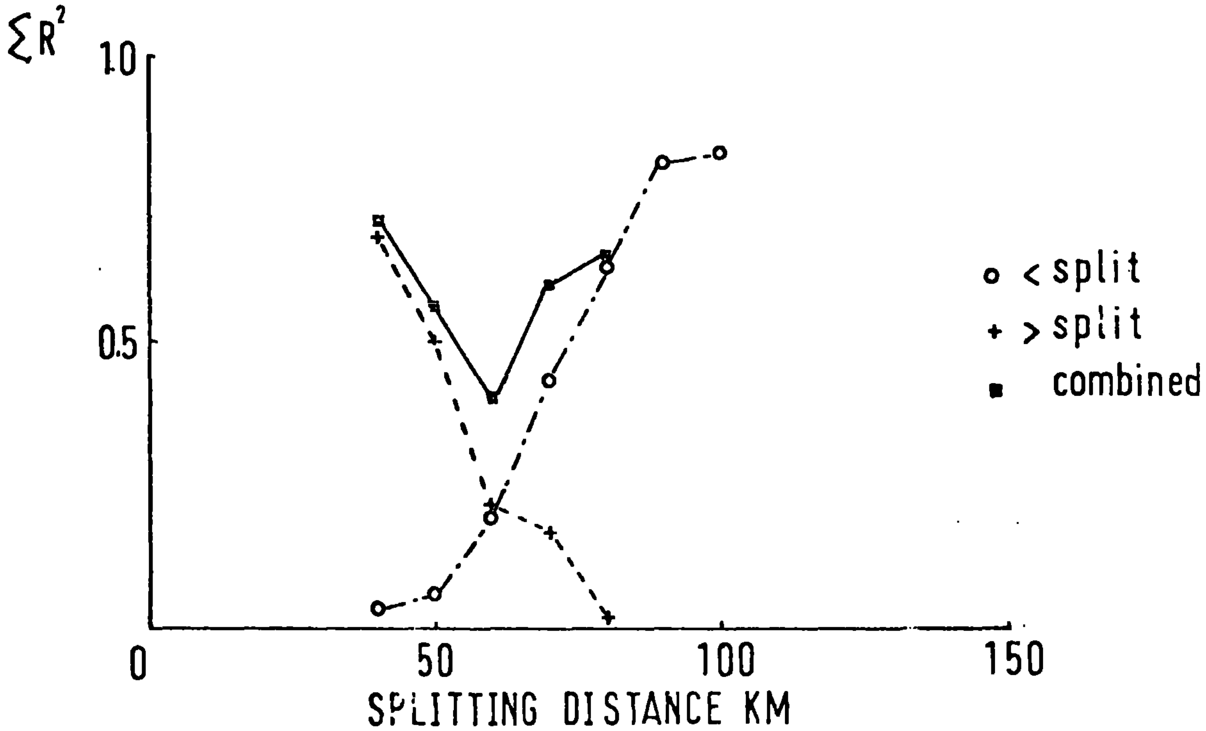

Figure 4.29(b) Graph of variation of the fit of the two layer time-term solution with point at which data set has been split into two. H shots in Minch.

Table 4.3 Summary of P_g time-term analysis of H9 to H16.

Type of Solution	Least-squares velocity (km sec^{-1})	R^2 (sec^2)	Degrees of freedom	Variance (sec^2)	Variance ratio[b]
Single velocity	6.06	0.91	81	0.0112	1.00
$V=V_o+0.0018x$	$V_o=5.86$	0.84	80	0.0105	1.06
$V=V_o+0.03z$	$V_o=5.98$	0.85	80	0.0106	1.05
All data<40 km	5.86[a]	0.03	5	0.0107[c]	1.04
All data>40 km	6.17	0.68	61		
All data<50 km	6.10	0.06	14	0.0084[c]	1.33
All data>50 km	6.20	0.50	52		
All data<60 km	6.01	0.19	27	0.0059[c]	1.89
All data>60 km	6.36	0.21	40		
All data<70 km	6.00	0.43	41	0.0092[c]	1.21
All data>70 km	6.40	0.17	24		
All data<80 km	6.03	0.63	61	0.0097[c]	1.15
All data>80 km	6.80[a]	0.02	6		

for the Torridonian is shown outcropping at the seabed just to the west of the Raasay-Rona Ridge in Chesher et al. (1972). An interpretation of the time-terms must use two distinct velocity units. Figure 4.30 gives the basement shape determined from the time-terms assuming, as a best estimate, an equal delay-time contribution of Torridonian and Mesozoic. The structure proposed is not, therefore, definitive, nor are any detailed age relations implied for the movement on the Minch fault. It is intended solely as a guide to the probable thickness and extent of the basin.

The observed gravity fits the north-west side of the basin but discrepancies arise on the south-east side and these have been interpreted by Scott (1976) as being caused by a dense body within the basement (Section 4.3, Figure 4.23).

4.4.3 P_g analysis of shots G15 to G28 and J1 to J8

Ninety-five recordings of shots fired on the outer shelf were used to find the 32 time-terms. A least-squares velocity of 6.22 ± 0.03 km sec^{-1} is well determined and a two layer solution gives a significant improvement (Figures 4.31(a) and (b)). The solutions using increasing velocity with depth and distance failed to make any significant improvement. Negative time-terms for shots G19, G20 and G21 (Table 4.4) are caused by the high velocity material beneath these shots, as was indicated by minus-time analysis in Section 4.3. Figure 4.32 gives the time-term profile and shows a small basin beneath shots G16, G17 and G18 with time-terms in the region of 0.3 seconds. This could be interpreted as 2.3 km of Torridonian, with a velocity of

Figure 4.30 Time-terms for H shots in Minch and the adjacent land areas together with interpreted geological structure and observed Bouguer gravity anomaly profile. Error bars are 95% confidence limits. See figure 2.1

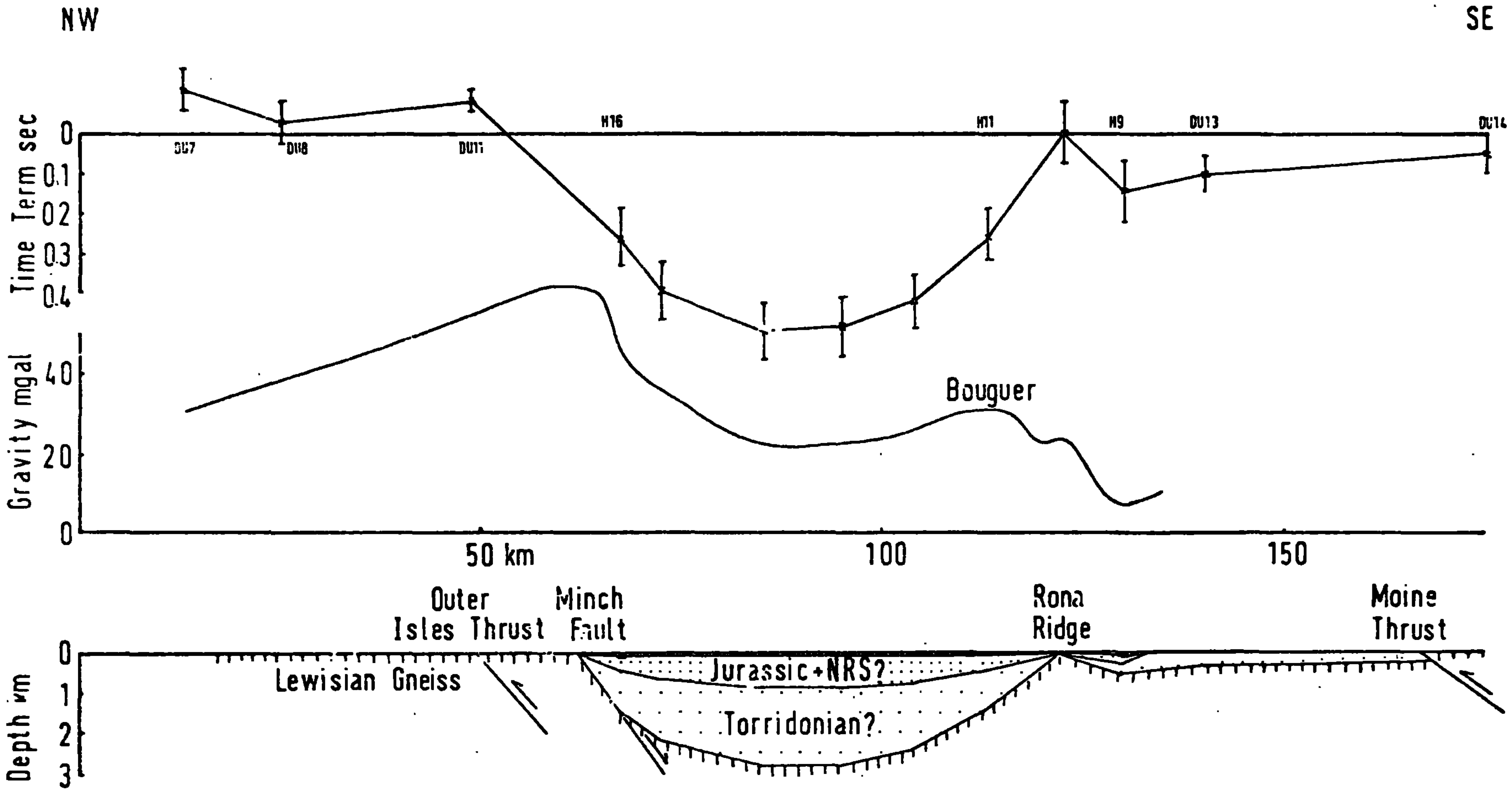

OUTER SHELF DATA

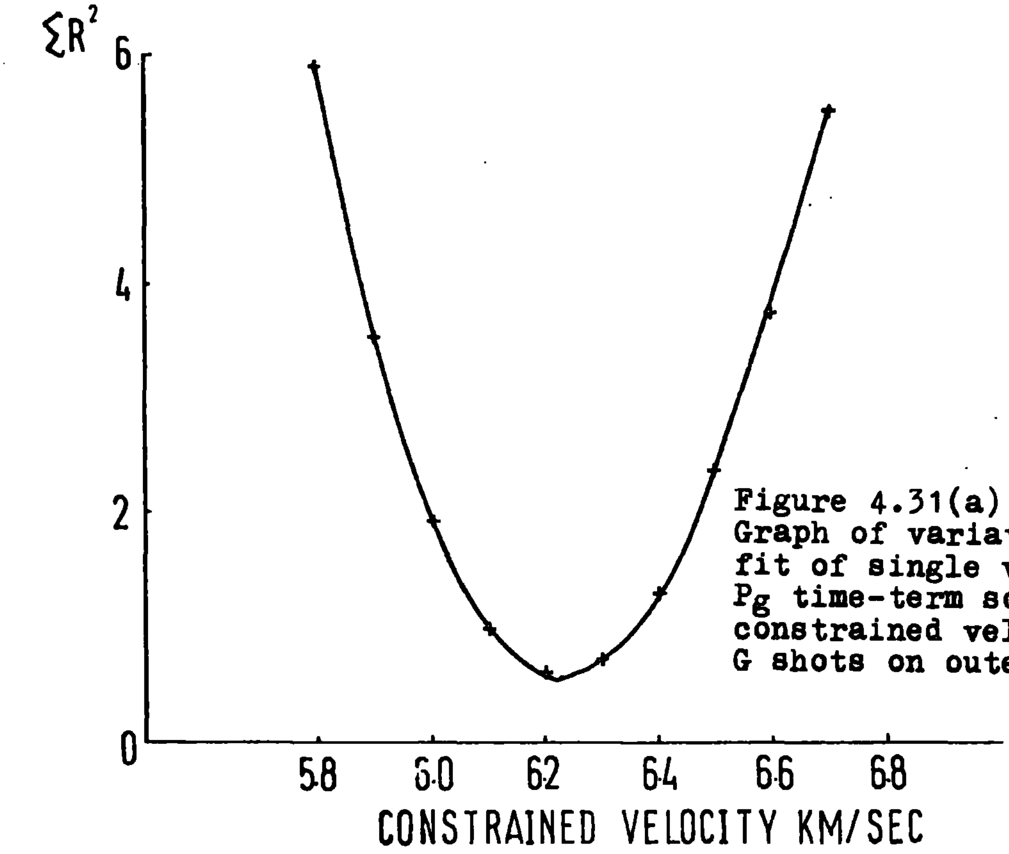

Figure 4.31(a)
Graph of variation of the fit of single velocity P_g time-term solution with constrained velocity.
G shots on outer shelf.

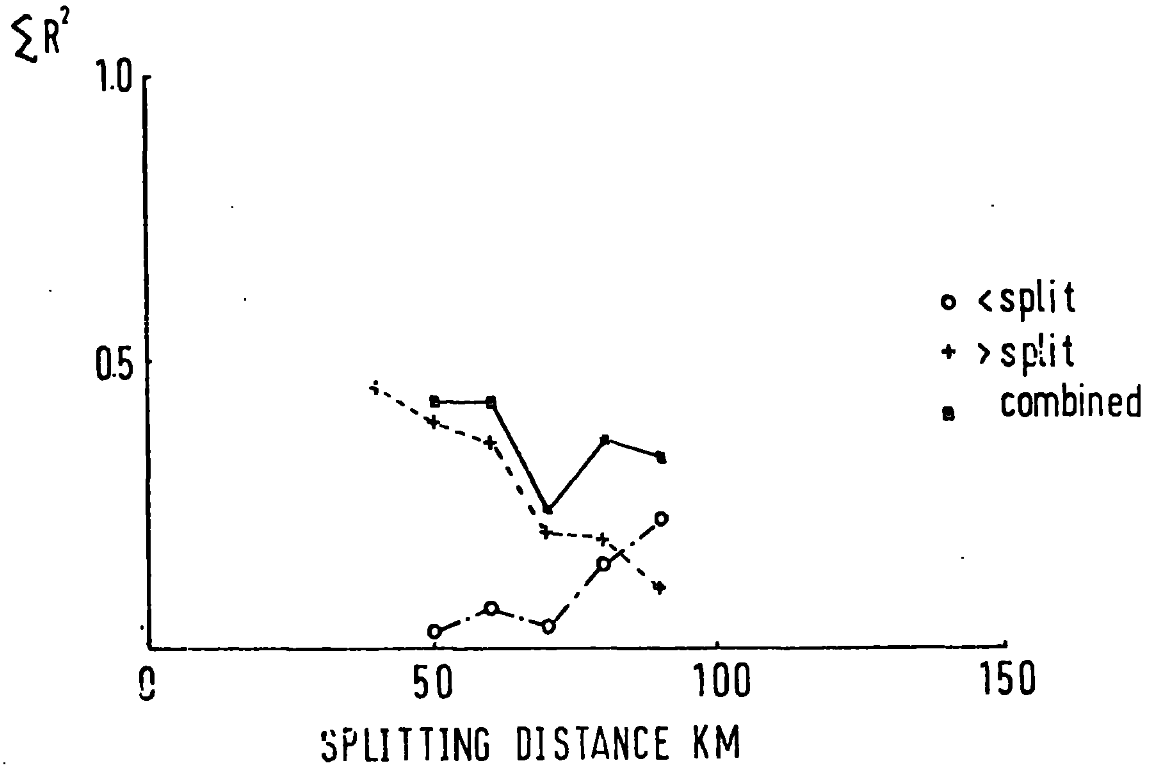

Figure 4.31(b) Graph of the variation of fit of the two layer time-term solution with point at which data set has been split into two. G shots on outer shelf.

Table 4.4 Summary of P_g time-term analysis of G15 to G28 and J1 to J8.

Type of Solution	Least-squares velocity (km sec^{-1})	R^2 (sec^2)	Degrees of freedom	Variance (sec^2)	Variance ratio[b]
Single velocity	6.22	0.58	62	0.0093	1.00
$V=V_o+0.0007x$	$V_o=6.13$	0.56	61	0.0091	1.02
$V=V_o+0.019z$	$V_o=6.17$	0.55	61	0.0091	1.02
All data<40 km	n.a.	n.a.	n.a.	n.a.	n.a.
All data>40 km	6.24	0.46	51		
All data<50 km	6.19[a]	0.03	5	0.0091[c]	1.02
All data>50 km	6.26	0.40	42		
All data<60 km	6.07	0.07	8	0.0097[c]	0.95
All data>60 km	6.29	0.36	36		
All data<70 km	6.29	0.04	12	0.0058[c]	1.60
All data>70 km	6.36	0.20	29		
All data<80 km	6.21	0.17	20	0.0086[c]	1.08
All data>80 km	6.35	0.19	22		
All data<90 km	6.21	0.22	26	0.0080[c]	1.16
All data>90 km	6.40	0.11	15		
All data<100km	6.20	0.23	30	0.0082[c]	1.13
All data>100km	6.25[a]	0.08	9		

4.8 km sec^{-1}, or as 1 km of Mesozoic sediments, with a velocity of 3.0 km sec^{-1}. This basin is referred to by both Kent (1975) and Whitbread (1975) and is shown as having a fault bounded eastern margin. The evidence here suggests a fault bounded western margin bringing the sediments into contact with the high velocity material beneath shots G19 to G21. Time-terms beyond G23 increase towards the continental margin although the velocity used in the solution is determined by the reversed section of the line (G15 to G23) and may not be accurate for the shots to the west of G23.

From reflection profiles on the margin in the region of G23 to G25, Himsworth (1973) was able to recognise reflections down to an unconformity which he interpreted as the base of the Tertiary strata. The thickness of these sediments decreased from about 700 m on profile 14/71 to about 300 m on profile 24/71, that is, from the shelf edge to the north of the Butt of Lewis to the shelf edge just north of St. Kilda. No reflections beneath this unconformity were observed.

Stride et al. (1969) however, were able to recognise reflectors beneath this unconformity on their Arcer profile across the Hebridean Shelf. A set of ill-defined reflectors dipping to the west were just visible below the unconformity and were considered to be "of Palaeozoic aspect". Further to the west and closer to the shelf edge their bedding is slightly better defined and their age was thereby considered more likely Mesozoic.

More recent commercial data show fairly clearly that these westward dipping reflectors extend to at least 1.5 seconds two-way travel-time beneath the base Tertiary

Figure 4.32 Time-terms for G shots on the outer shelf and adjacent land areas together with interpreted geological structure and observed Bouguer anomaly. Error bars are 95% confidence limits. See figure 2.1

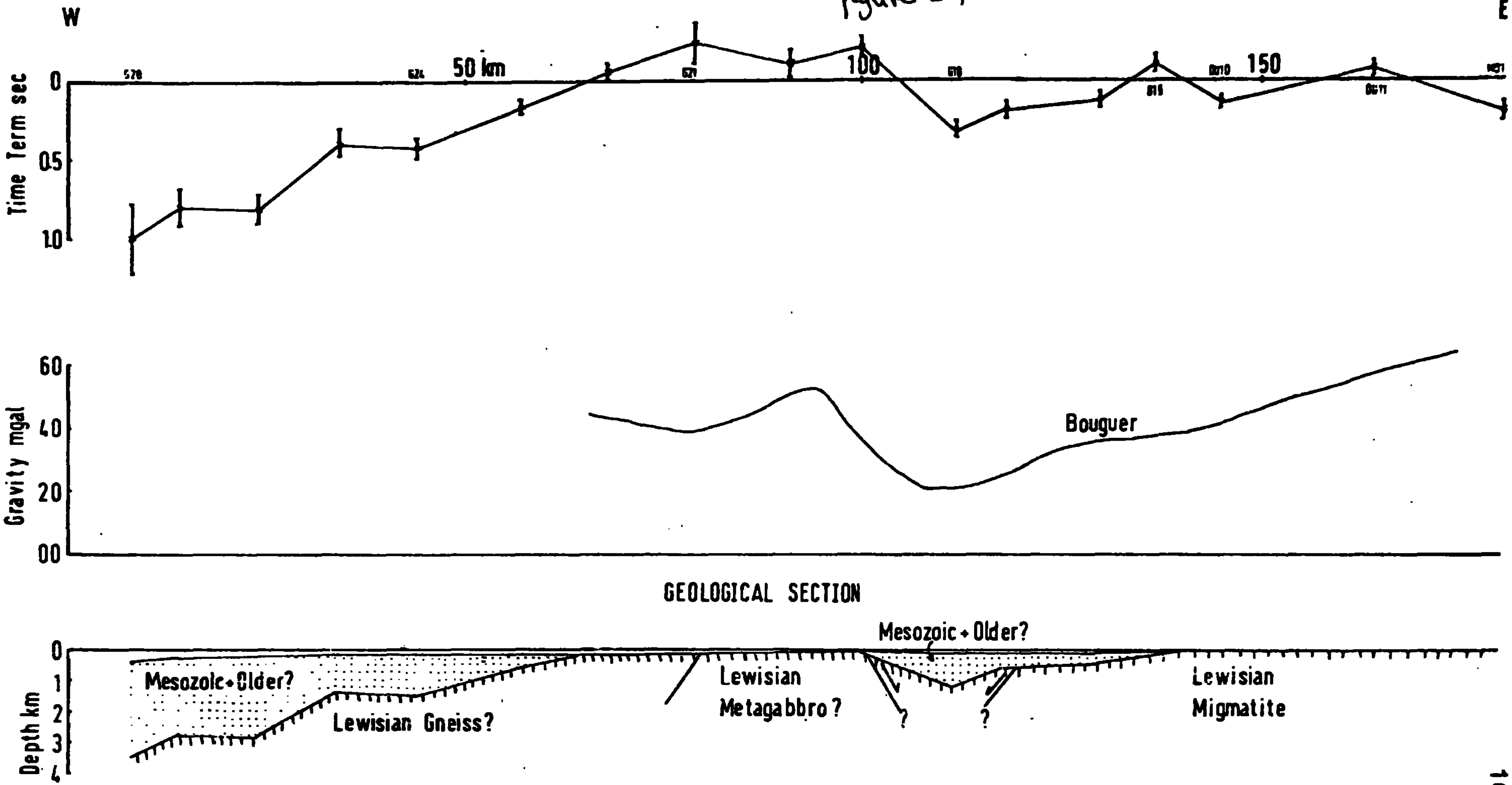

unconformity (F. Bouwers, personal communication). There is therefore a strong likelihood of at least 2 km of Palaeozoic or Mesozoic sediments on the shelf close to the margin.

4.5 Time-term analysis of P_n

Shots fired in the shallow water of the Hebridean Shelf and recorded at large ranges were included in the P_n data set. When using only the shots fired during HMSP in 1975 it was essential to include the recordings made at the Irish station, Lagg, offset to the south of the 58^o N line, to enable a well defined least-squares velocity to be found. However, the shots fired in June 1977 in the Moray Firth and the North Sea, and recorded at some of the HMSP recording sites, gave true reversal of the observations. Inclusion of both the Lagg recordings and the shots in Moray Firth and the North Sea gave a well defined least-squares velocity of 8.01 ± 0.04 km sec^{-1}. Figure 4.33 shows how the sum of squared residuals varies for three different data sets.

The solution was constrained simply by fixing the time-terms of two stations which were known from previous work using the P_n time-term at Eskdalemuir of 2.87 seconds (Agger and Carpenter, 1965) and at Cape Wrath of 2.45 seconds (Smith, 1974). The similar values of time-terms at adjacent stations and shots gives confirmation that the solution is correctly constrained (e.g. GS1 = G7; DU9 = G14; DU13 = H9). The poor comparison of DU10 and shot G15 may arise because only two arrivals define the P_n time-term at DU10 and hence the errors may be large.

Correction can be made to the P_n time-term for the

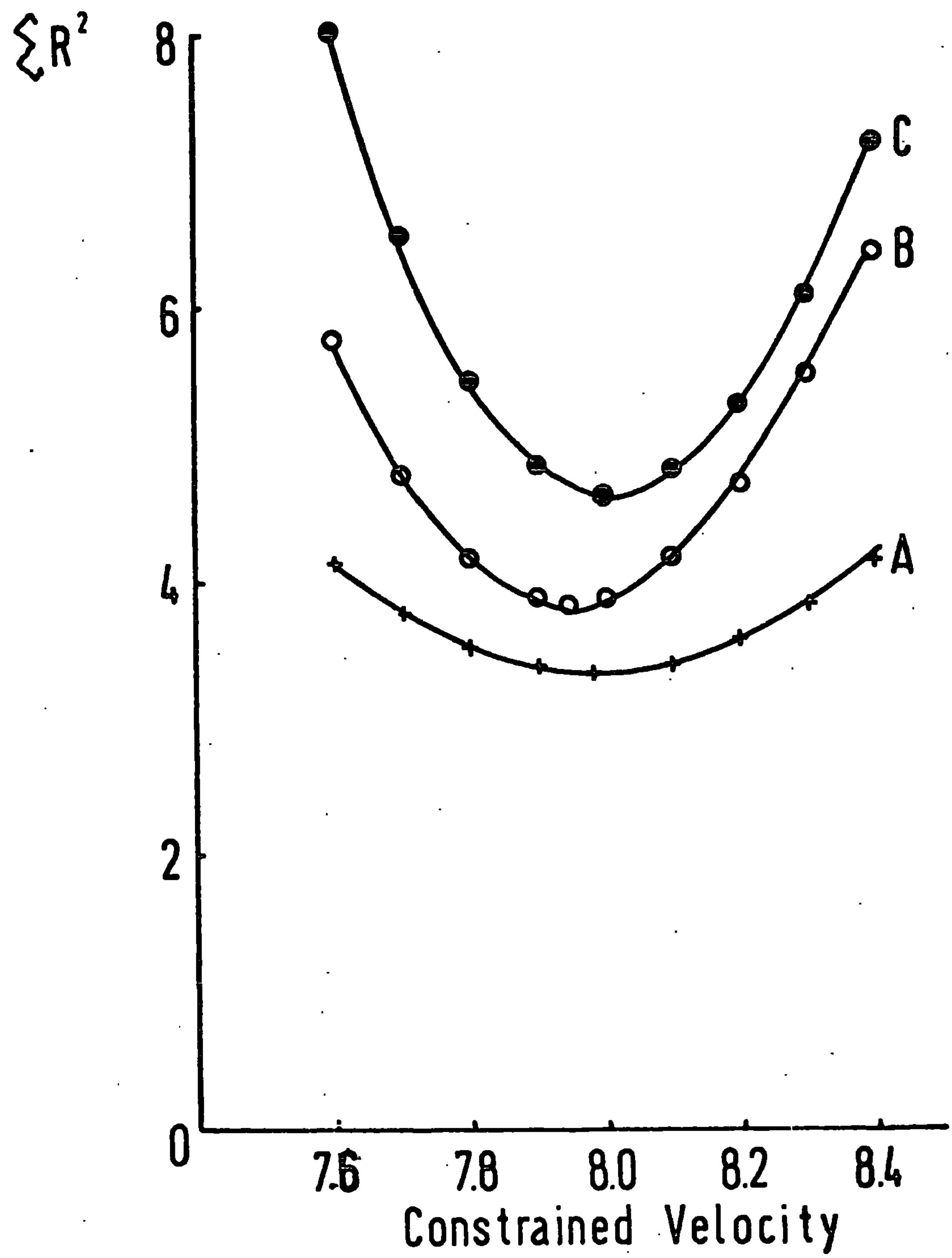

Figure 4.33 Graph of variation of fit of single velocity P_n time-term solution for shots fired on shelf. A is all data except North Sea shots and recordings from Lagg, B is all data except North Sea shots, C is all data.

delay caused by the sediments using the formula:

$$P_n' = P_n - P_g\left[(V_r^2 - V_s^2)^{\frac{1}{2}}V_b - (V_r^2 - V_b^2)^{\frac{1}{2}}V_s\right]/(V_b^2 - V_s^2)^{\frac{1}{2}}V_r$$

where P_n is the P_n time-term

P_g is the P_g time-term

V_s is the velocity of the sediments

V_b is the velocity of the P_g phase

V_r is the velocity of the P_n phase

and P_n' is the corrected P_n time-term which can then be interpreted directly in terms of a single layer of average crustal velocity, V, above the Moho.

For a sedimentary velocity of 3.0 km sec^{-1} (Mesozoic) the correction is 0.67 P_g and for a velocity of 4.8 km sec^{-1} (Torridonian) the factor is 0.39 P_g. Where Mesozoic and Torridonian sediments are equally present the average velocity would be about 4.0 km sec^{-1} and the correction would be 0.53 P_g. Figures 4.34 and 4.35 and Table 4.5 show the P_g, P_n and P_n' time-terms assuming an average sedimentary velocity of 4.0 km sec^{-1}. The region can be divided into areas where the value of the time-terms is approximately the same (Table 4.6).

It is apparent that significant differences in crustal thickness between the Caledonian mobile and foreland belts at 58° N only arise if different average crustal velocities are used for each region. Discounting the anomalous area of the Minch for the moment, the time-terms for the Mainland stations, the Outer Hebrides stations and the shots on the outer shelf are very similar. Section 4.8 presents the analysis of Moho wide-angle reflections which confidently

Figure 4.34 The P_g, P_n and corrected P_n time-terms for the line of stations and shots along 58° N. Error bars are 95% confidence limits, o - corrected P_n time-terms.
See figure 2.1

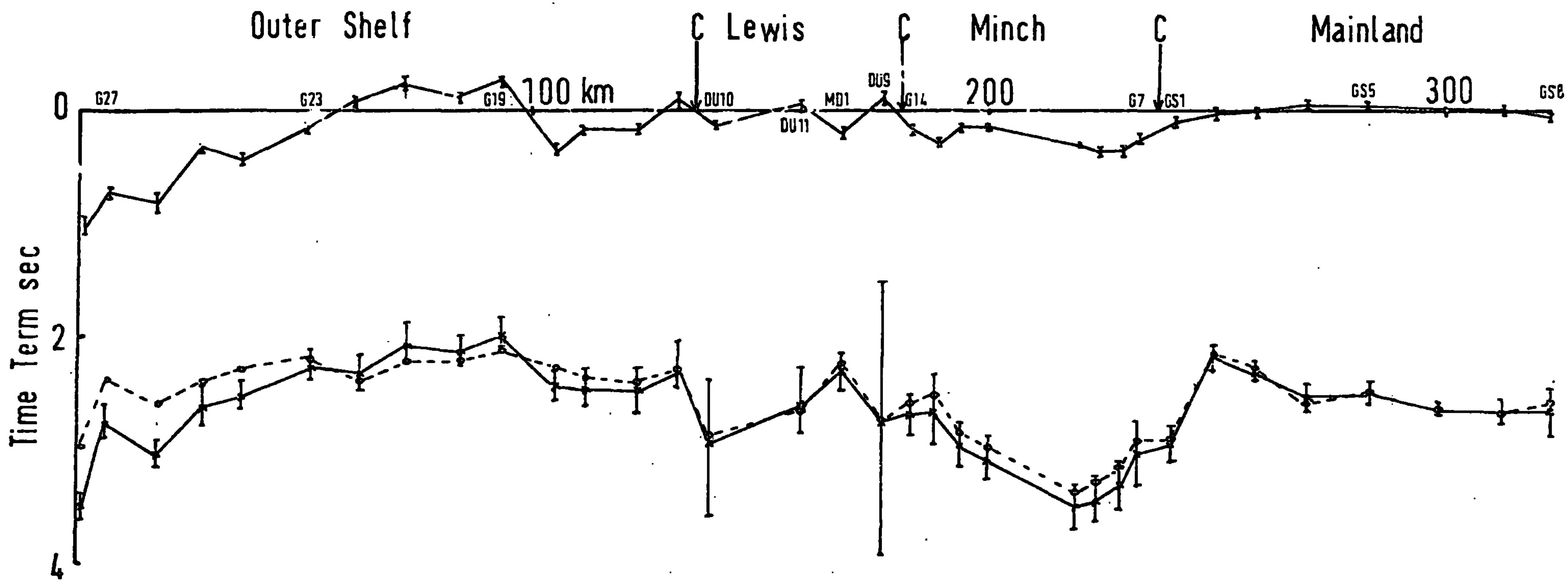

Figure 4.35 The Pg, Pn and corrected P_n time-terms for the H line in the Minch and the adjacent land areas. Error bars are 95% confidence limits, o - corrected P_n time-terms. See figure 2.1

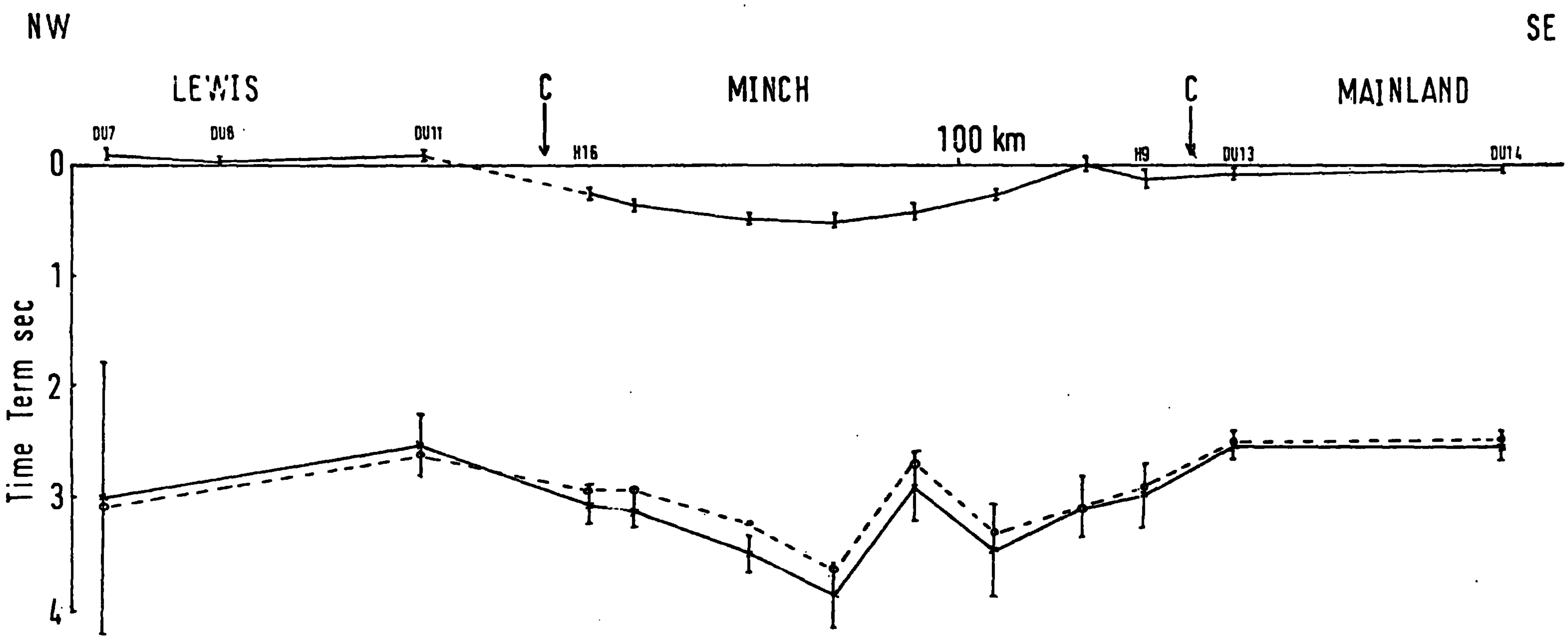

Table 4.5 P_g, P_n and P_n' time-terms for all data on the shelf area.

Station		P_g T.T.	95% conf.	N	P_n T.T.	95% conf.	N	P_n'
Polbain	GS1	0.08	0.05	8	2.78	0.10	11	2.74
Stac Pollaidh	GS2	0.04	0.05	8	2.09	0.12	8	2.07
Knockan	GS3	0.02	0.04	9	2.21	0.08	16	2.20
Loch Ailsh	GS4	-0.09	0.04	9	2.48	0.11	10	2.51
Glencassley	GS5	-0.02	0.10	4	2.48	0.08	14	2.49
Lairg	GS6				2.54	0.07	17	2.58
Rogart	GS7	-0.02	0.06	6	2.59	0.08	16	2.60
Backies	GS8	0.04	0.05	8	2.51	0.23	4	2.49
Cape Wrath	GS9				2.42	0.10	9	2.42
Butt of Lewis	DU6	0.23	0.05	8	2.64	0.32	3	2.52
Uig	DU7	-0.11	0.05	8	2.94	2.97	1	3.00
Linshader	DU8	-0.03	0.05	8				
Lemreway	DU9	-0.10	0.06	7	2.59	2.98	1	2.65
Husinish	DU10	0.15	0.02	14	2.94	0.60	2	2.86
Maaruig	DU11	-0.08	0.02	13	2.52	0.24	4	2.56
North Uist	DU12	0.00	0.02	16	2.53	0.80	2	2.53
Loch Torridon	DU13	0.10	0.04	9	2.53	0.12	8	2.49
Loch Carron	DU14	0.05	0.05	8	2.52	0.14	7	2.50
St. Kilda	DU15	0.07	0.01	22	2.23	0.12	8	2.19
Mull	DU16	-0.83	0.14	5	2.35	0.09	12	2.79
Laxay	MD1	0.20	0.05	8	2.27	0.16	6	2.16
Blair Atholl	BLA				3.15	0.09	12	3.15
Dundee	DUN				2.78	0.09	13	2.78
Eskdalemuir	ESK				2.87	0.08	16	2.87
Lagg	LAGG				2.34	0.10	10	2.34

N is the number of observations used to calculate the time-term.

Table 4.5 (continued)

Shot	P_g T.T. (sec)	95% conf.	N	P_n T.T. (sec)	95% conf.	N	P_n' (sec)
G7	0.24	0.04	12	3.16	0.31	3	3.03
G8	0.38	0.03	12	3.46	0.18	5	3.26
G9	0.37	0.04	12	3.58	0.15	6	3.38
G10	0.27	0.03	13	3.60	0.18	5	3.46
G11	0.16	0.03	13	3.20	0.23	4	3.12
G12	0.15	0.03	14	3.08	0.23	4	3.00
G13	0.25	0.03	13	2.77	0.31	3	2.63
G14	0.13	0.04	12	2.79	0.18	5	2.72
G15	-0.12	0.03	9	2.46	0.18	5	2.48
G16	0.14	0.03	11	2.60	0.23	4	2.51
G17	0.17	0.04	7	2.58	0.18	5	2.49
G18	0.35	0.04	8	2.59	0.14	7	2.30
G19	-0.22	0.05	6	2.14	0.12	8	2.26
G20	-0.12	0.08	4	2.29	0.15	6	2.35
G21	-0.24	0.12	3	2.14	0.16	6	2.27
G22	-0.06	0.04	7	2.51	0.18	5	2.54
G23	0.17	0.04	7	2.41	0.12	8	2.32
G24	0.43	0.06	5	2.69	0.12	8	2.46
G25	0.39	0.08	4	2.75	0.16	6	2.54
G26	0.81	0.08	4	3.19	0.10	10	2.76
G27	0.79	0.11	3	2.96	0.14	7	2.49
G28	1.00	0.22	2	3.68	0.11	10	3.17

Table 4.5 (continued)

Shot	P_g T.T. (sec)	95% conf.	N	P_n T.T. (sec)	95% conf.	N	P_n' (sec)
H9	0.14	0.07	12	3.08	0.31	3	3.01
H10	0.00	0.07	10	3.23	0.31	3	3.23
H11	0.26	0.06	15	3.56	0.56	2	3.42
H12	0.42	0.06	16	3.05	0.31	3	2.77
H13	0.48	0.07	14	4.02	0.31	3	3.73
H14	0.49	0.07	13	3.62	0.18	5	3.36
H15	0.39	0.07	14	3.25	0.15	6	3.06
H16	0.26	0.07	13	3.22	0.13	7	3.08
J1	0.07	0.01	22	2.23	0.12	8	2.20
J2	0.29	0.06	5	2.52	0.14	7	2.37
J3	-0.22	0.22	2	2.89	0.14	7	3.13
J4	-1.17	0.23	2	2.09	0.59	2	2.73
J5	0.24	0.22	2	2.93	0.24	4	2.80
J7				2.52	0.36	3	2.52
J8				3.08	2.92	1	3.08
B2				2.55	2.97	1	2.55
B3				3.31	0.32	3	3.31
B4				3.29	0.32	3	3.29
F1				3.62	0.23	4	3.62
F2				3.38	0.23	4	3.38
F3				3.37	0.23	4	3.37
F4				3.75	2.92	1	3.75
F5				3.65	2.92	1	3.65
F6				3.06	2.92	1	3.06

Table 4.6 P_n time-terms and crustal thicknesses for five areas of broadly uniform structure. Two values of average crustal velocity are used.

Area	Stations and Shots	Average time-term (corrected) (sec)	Crustal thickness (km)	
			V = 6.2	V = 6.6
Outer shelf	G15 to G28; DU15.	2.47	24.7	28.7
Outer Hebrides	DU6 to DU12; MD1.	2.61	26.1	30.4
Minches	G7 to G14; H9 to H16.	3.14	31.4	36.6
Mainland - west of Moine thrust	GS1 to GS4; GS9; DU13; DU14.	2.46	24.6	28.7
Mainland - east of Moine thrust	GS5 to GS8; BLA.	2.66	26.6	31.0

suggests an average crustal velocity in the region of 6.2 km sec^{-1} for the outer shelf area. Wide-angle reflections beneath the Caledonian mobile belt are very poorly observed in HMSP but good results were obtained from LISPB (Bamford et al., 1976) which suggests that average crustal velocities of 6.5 to 6.7 km sec^{-1} should be used in this area.

The P_n time-terms beneath the outer shelf area show correlations with the P_g time-term data which are substantially removed by correcting for the sedimentary structure (Figure 4.34). No large changes are indicated between G15 and G25 where, using an estimate of 6.2 km sec^{-1} for the average crustal velocity, there is a uniform crustal thickness of about 25 km. G26 to G28 are close to the shelf edge and show a slight increase in time-term towards Rockall Trough. This increase also shows a strong correlation with the P_g time-terms and it is possible that the correction for sedimentary delay has been underestimated in this region.

The average P_n time-term of 2.54 seconds for the four stations at 58° N to the east of the Moine thrust could be interpreted as crust about 30 km in thickness using a higher average crustal velocity of 6.6 km sec^{-1}. Similarly, the time-term at Blair Atholl would give an estimate of 35 km for the crustal thickness.

Both time-term profiles across the Minch show an increase towards the centre with values at each side closely comparable with the stations closest to them (Figures 4.34 and 4.35). Corrections for the sedimentary delay effect remove only a small part of this increase. If the change in time-term is taken at face value and interpreted in terms of a thickening of a uniform velocity crustal layer then the crust is about 8 km thicker beneath the Minch than on either side.

A large part of the observed increase towards the Minch (Figure 4.34) takes place between stations GS2 and GS1. In a linearly designed refraction project the station (or shot) P_n time-terms apply to points on the refractor offset towards the shot (or station) by about 30 km. The aim of a wide azimuthal coverage, or reversal, is to average a whole set of offset points around the observation point. Exclusion of the Cambridge North Sea shots (Figure 2.6) from the P_n data set led to a time-term solution which showed that one of the largest single changes in time-term between two observation points was between GS2 and GS1. A time-term solution using only the North Sea shots independently confirms the relative values of the time-terms at GS1, GS3, GS5 and GS7 and hence supports the existence of a big difference between the time-terms of GS1 and GS2 (GS3). When viewed in the light of the large changes in time-term between adjacent stations and shots, the observation that the GS1 time-term has the same value in opposite directions suggests that it cannot truly represent crustal thickness since the points where the refractions leave the Moho are about 60 km apart. It is more likely that the value of the time-term and the changes between closely spaced observation points are linked to velocity variations in the upper parts of the crust, close to the station, so that the arrivals from opposite directions sample the same variations.

Figure 4.35 shows that the time-term at H12 is much smaller than the ones at H11 and H13. These shots were observed at P_n range at three stations to the south and the advance of H12 arrivals relative to the other shots can clearly be seen on the stacked record sections (Figure 4.7 and Appendix B). Figure 4.23 shows, from an interpretation of the minus-times and gravity observations, that H12 is possibly located over a mass of dense and high velocity rocks which might reduce the size of the delay-time. This raises the question as to how much of the observed changes in time-terms near the Minch can be attributed to lateral velocity variations within the crust.

These increases in time-term could be attributed to the presence of abnormally low velocity crust beneath the Minch but no evidence of this is shown by the preceding analyses. An analysis of wide-angle reflections in Section 4.8 possibly indicates a slightly higher average crustal velocity beneath the Minch than beneath the outer shelf region. However, reflections from shots in the Minch probably do not give an accurate estimate of average crustal velocities since most of the travel paths lie beneath the Scottish Mainland.

If we take the average crustal velocity to be 6.2 km sec^{-1} over the whole area, then the crust beneath the centre of the Minch must be between 10 and 14 km thicker than the crust on either side. If, as the T^2/X^2 results indicate, the average crustal velocity in the Minch area is 6.6 km sec^{-1}, compared to 6.2 km sec^{-1} in the surrounding region, then a crustal thickening of about 15 km is implied. On the other hand, a reduction in average crustal velocity beneath the Minch of about 6 per cent could explain the results without the need for crustal thickening.

The presence of thick, or abnormally low velocity, crust beneath the Minch should show up as a gravity low. As mentioned in Section 4.4.1, after correcting for the sediment structure derived from P_g time-term analysis, there is still a substantial residual anomaly over the Minch of about -40 mgal. The shape of the Moho derived from a simple interpretation of the P_n time-terms cannot explain the shape of this gravity anomaly without the introduction of anomalous bodies within the crust beneath the Minch. The fall in Bouguer gravity anomaly on Lewis from +65 to +35 mgal was interpreted by McQuillin and Watson (1973) as being caused by increasing migmatisation and granitisation towards the west. On the P_n time-term profiles we can see abnormally high values of 2.86 and 3.00 seconds for DU10 and DU7, the western most stations on Lewis, which are possibly caused by such changes in the state of the Lewisian basement. These changes in facies of the near-surface rocks are not strikingly evident in the P_g analysis of shorter range observations and it is possible that the gravity anomaly and P_n time-term profile in the Minch are caused by variations in upper crustal structure not shown by the analysis of P_g arrivals.

4.6 Results of velocity filtering

As mentioned in Section 3.7, determinations of apparent surface velocity at the Laxay array were possible with an accuracy of about 0.2 km sec^{-1}. No azimuth anomalies of greater than 10^o (the probable accuracy) were observed. Figures 3.7, 4.36 and 5.10 show outputs from the Modular 1

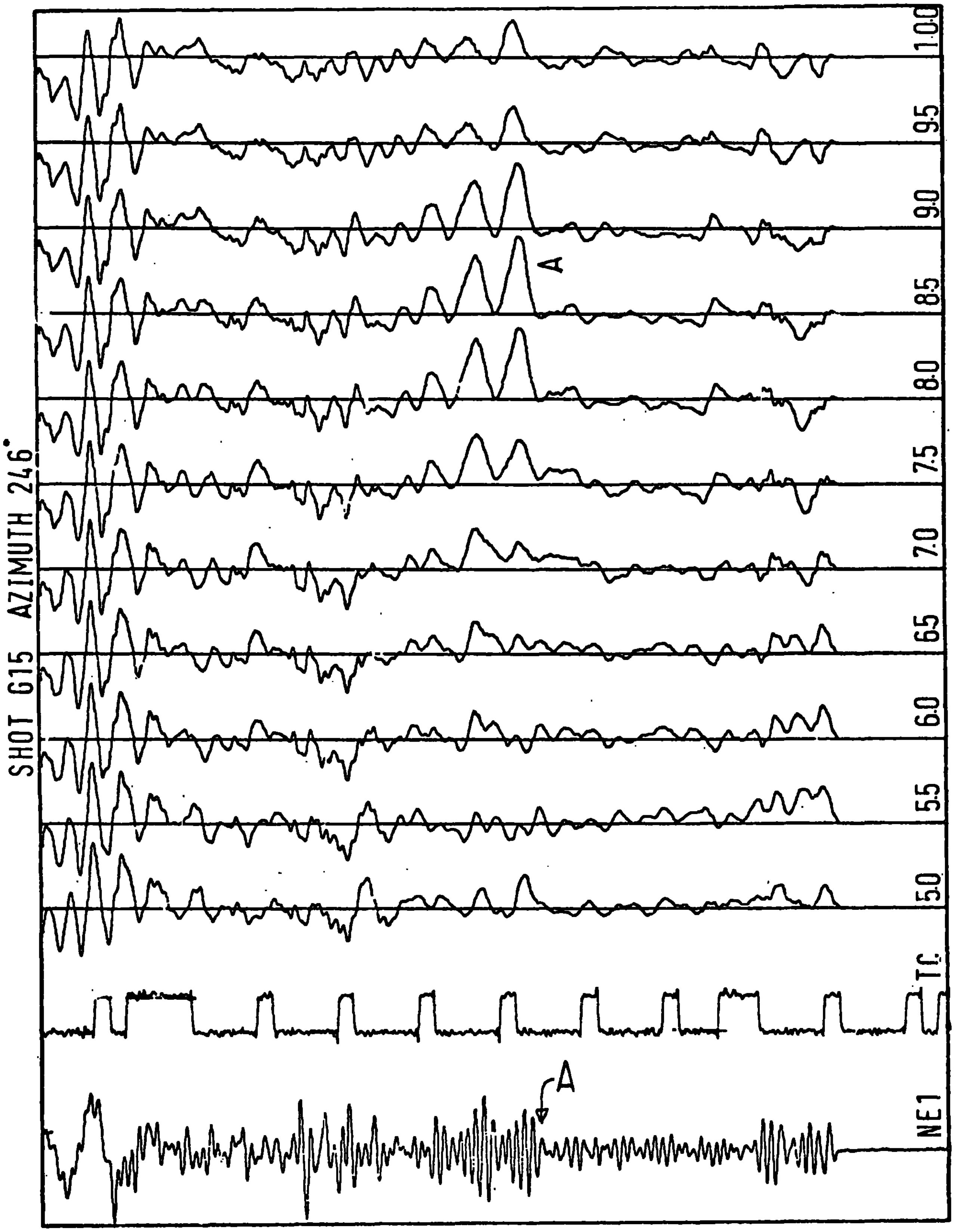

Figure 4.36 Computer drawn output from velocity filter program for shot G15. Signal marked A is the wide-angle reflection from the Moho.

velocity filtering program typical of those observed for all the shots. It can be seen that each record has about 10 distinct arrivals in the first 10 seconds of the recording. Particularly well shown in Figure 4.36 is the Moho wide-angle reflection, marked A, with a very high apparent surface velocity of about 8.5 km sec^{-1}. The results of a detailed velocity filter analysis on each of the G and K shots is given in Figures 4.37 to 4.40. The apparent surface velocity, arrival time and relative amplitude of each arrival have been plotted using the same scale as the related stacked record section.

Figures 4.37 and 4.38, showing the analysis of shots G7 to G14, indicate that although the first arrivals have an apparent velocity between the shots of about 6.0 km sec^{-1}, they have an apparent surface velocity at the array of about 8.0 km sec^{-1}. Figure 4.39 shows that the difference between the velocity at the shots and at the array is smaller for shots to the west - 6.3 km sec^{-1} at the shots and between 5.7 and 6.3 km sec^{-1} at the array.

A possible explanation for these observations lies in the proximity of the array to the Outer Isles thrust fault. The major thrust plane outcrops some 5 km to the west of the array and dips to the east at about 23^{o} (Janet Watson, personal communication). A wide zone above and below the main thrust plane shows large scale shearing and thrusting. The presence of an easterly dipping interface close to the array would tend to increase the angle of approach of waves coming from the east. We would expect that an arrival from

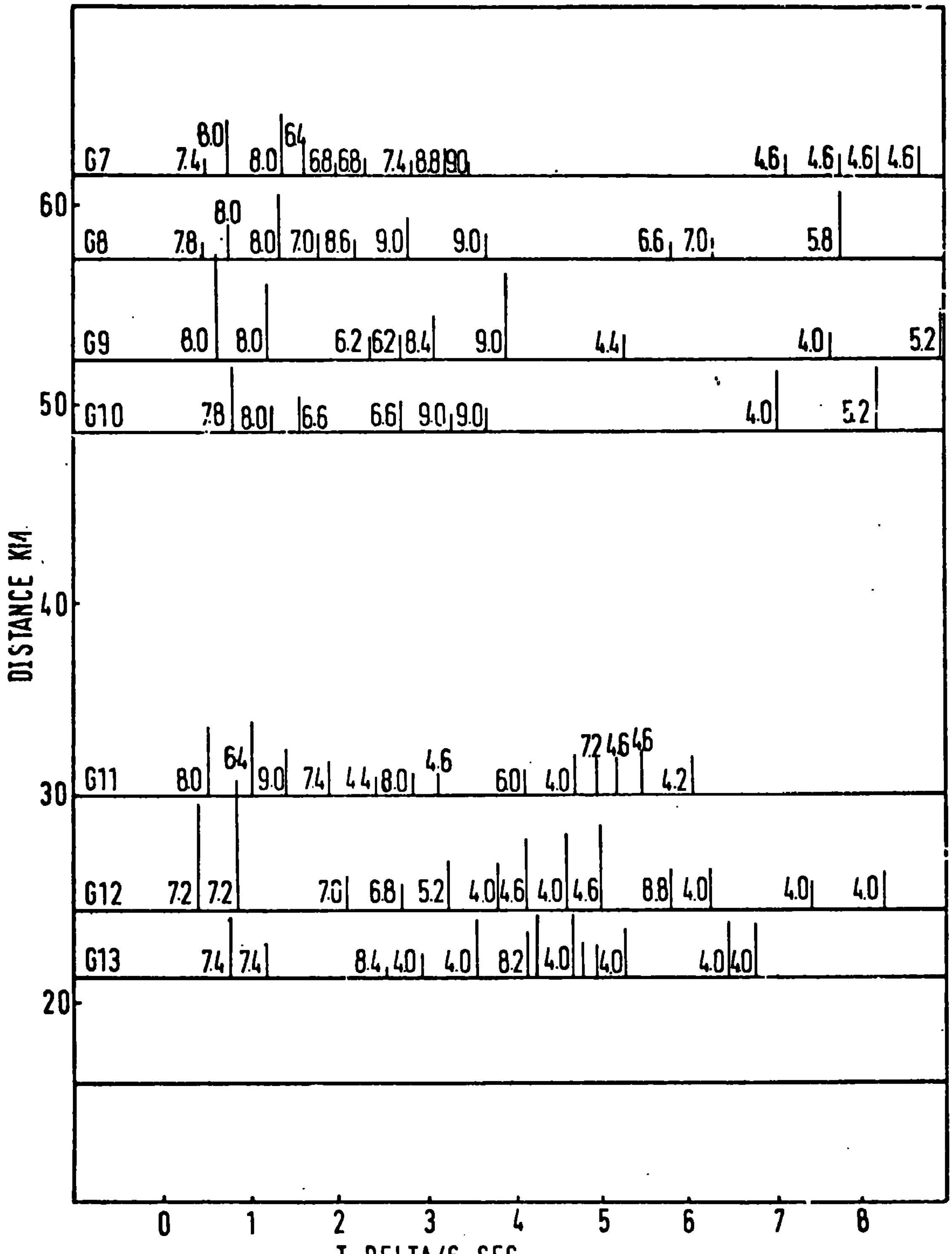

VELOCITY FILTER RESULTS FROM LAXAY

Figure 4.37 Compiled results of velocity filtering for the shots G7 to G14 recorded at Laxay. The bars represent arrivals and their velocities are given in km sec^{-1}. The height of the bar is proportional to arrival amplitude.

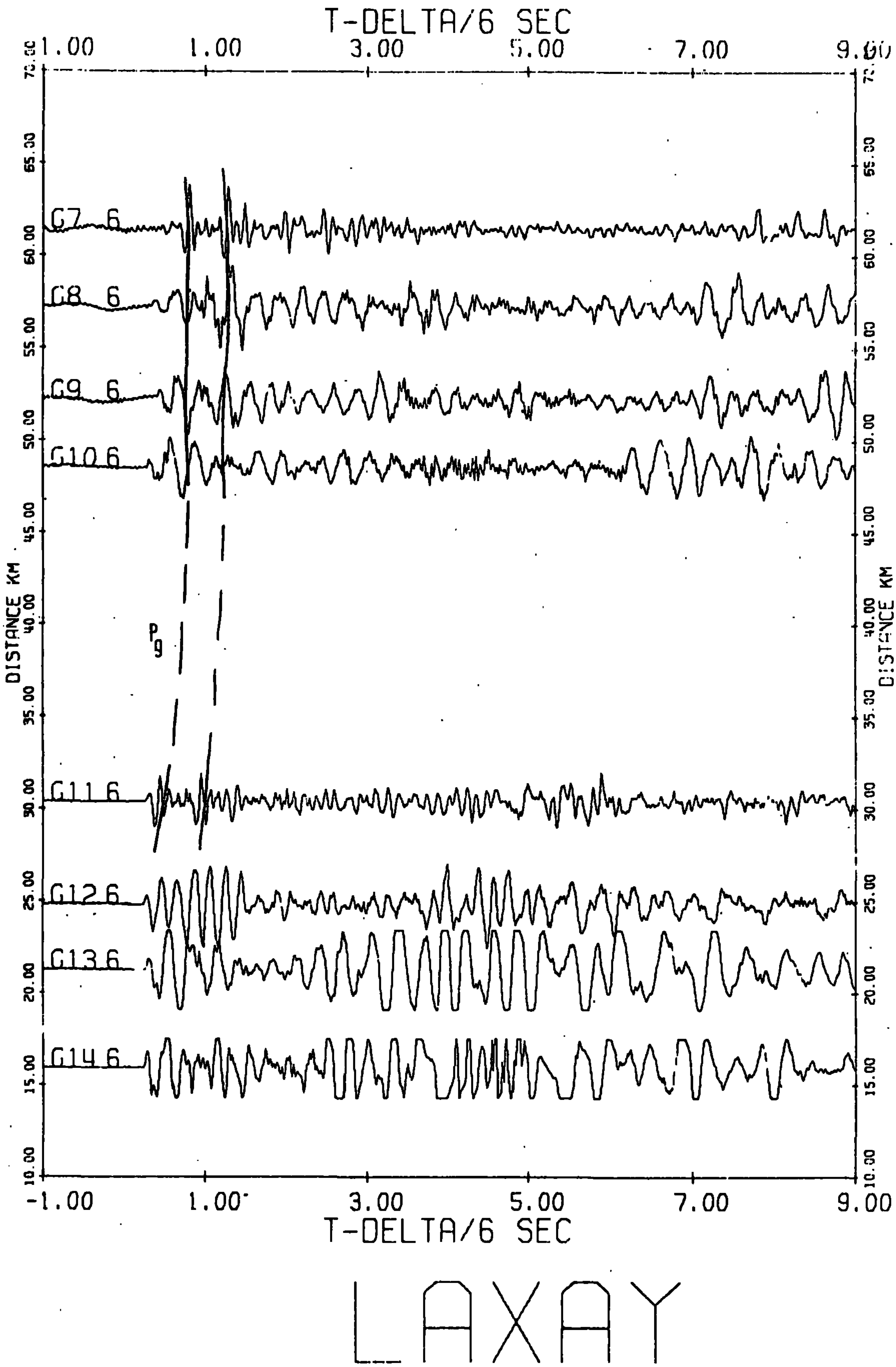

Figure 4.38 Computer drawn stacked record section for G shots in Minch at Laxay. Filtered vertical seismometer. Note double pulses for G7 and G11.

the west would be refracted to give a shallower angle of approach and hence a lower apparent surface velocity. A dip of 26^{o} to the east on an interface between rocks of 6.0 and 6.2 km sec^{-1} would be needed to explain the observed increase in apparent surface velocity for shots from the east and would also give an apparent surface velocity of 6.0 km sec^{-1} for shots from the west.

The proximity of the array to the Minch fault could also explain the observations. The Minch fault is a large normal fault of about 2 to 4 km total displacement downthrowing to the east. A headwave travelling within the basement beneath the Minch at 6.2 km sec^{-1} might be expected to have its angle of approach increased by diffraction about the fault. To reproduce the observed apparent velocity of 8.0 km sec^{-1}, the Minch fault, 13 km to the east of Laxay, would need a throw of about 10 km. The P_g time-term of 0.25 seconds at G14 indicates a thickness of sediments of about 2.3 km. Allerton (1968) has interpreted the gravity anomalies along 58^{o} N in the Minch as 3.8 km of sediments using a density contrast of -0.20 gm cm^{-3}. Clearly, the likely thickness of Torridonian sediments in the Minch does not approach the value required to explain the observed increase in apparent surface velocity. The most plausible explanation is therefore considered to be the refraction of arrivals at a dipping interface close to the Outer Isles thrust plane.

Correlated later arrivals are difficult to observe although the S-wave group shows up as a set of low velocity arrivals. The variability of frequency content is well shown in these records. Shots G7 and G11 contain a broader band of frequencies than do the other shots and are hence much more pulse-like in their character. They show two distinct arrivals with very similar waveforms 0.5 seconds apart (arrivals B and C of Figure 3.8). Close inspection of several of the other records reveals two similar arrivals at comparable separation. The two arrivals have the same apparent surface velocity at the shots and substantially the same apparent surface velocity at the array. A possible origin is some kind of multiple at the shot. A multiple between seabed and sea surface should be phase inverted and separated in time by only about 0.05 seconds and the reflection points are therefore more likely to be the top and bottom of the sediments. For Torridonian sediments of 4.8 km sec^{-1} velocity, the thickness indicated is about 1.4 km, which is of the same order as the thickness already suggested by time-term analysis. However, the second arrival does not show a significant decrease in amplitude as might be expected if it was a multiple of the first arrival.

Figures 4.39 and 4.40 show the compiled results of velocity filtering for shots to the west of Lewis. Included in the diagram are the large shots in the Rockall Trough which are discussed in Chapter 5. From the mass of correlated arrivals within each record, only a few can be confidently traced from one shot to the next. These are the first arrivals, P_g and P_n, and the wide-angle reflection P_mP.

The apparent surface velocity found for P_g varies between 5.7 and 6.3 km sec^{-1}, whilst that for P_n varies

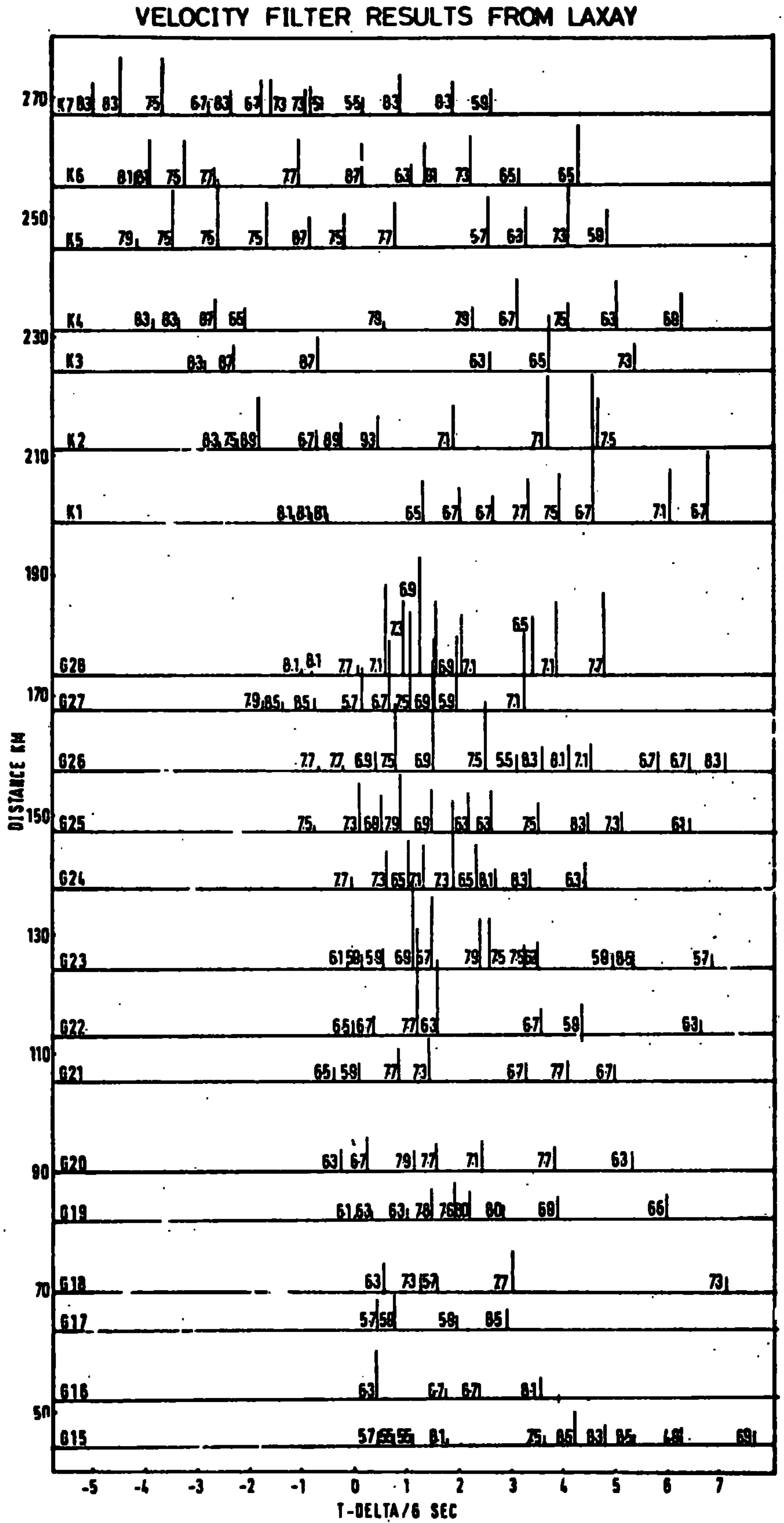

Figure 4.39 Compiled results of velocity filtering for G and K shots at Laxay. Conventions as in Figure 4.37.

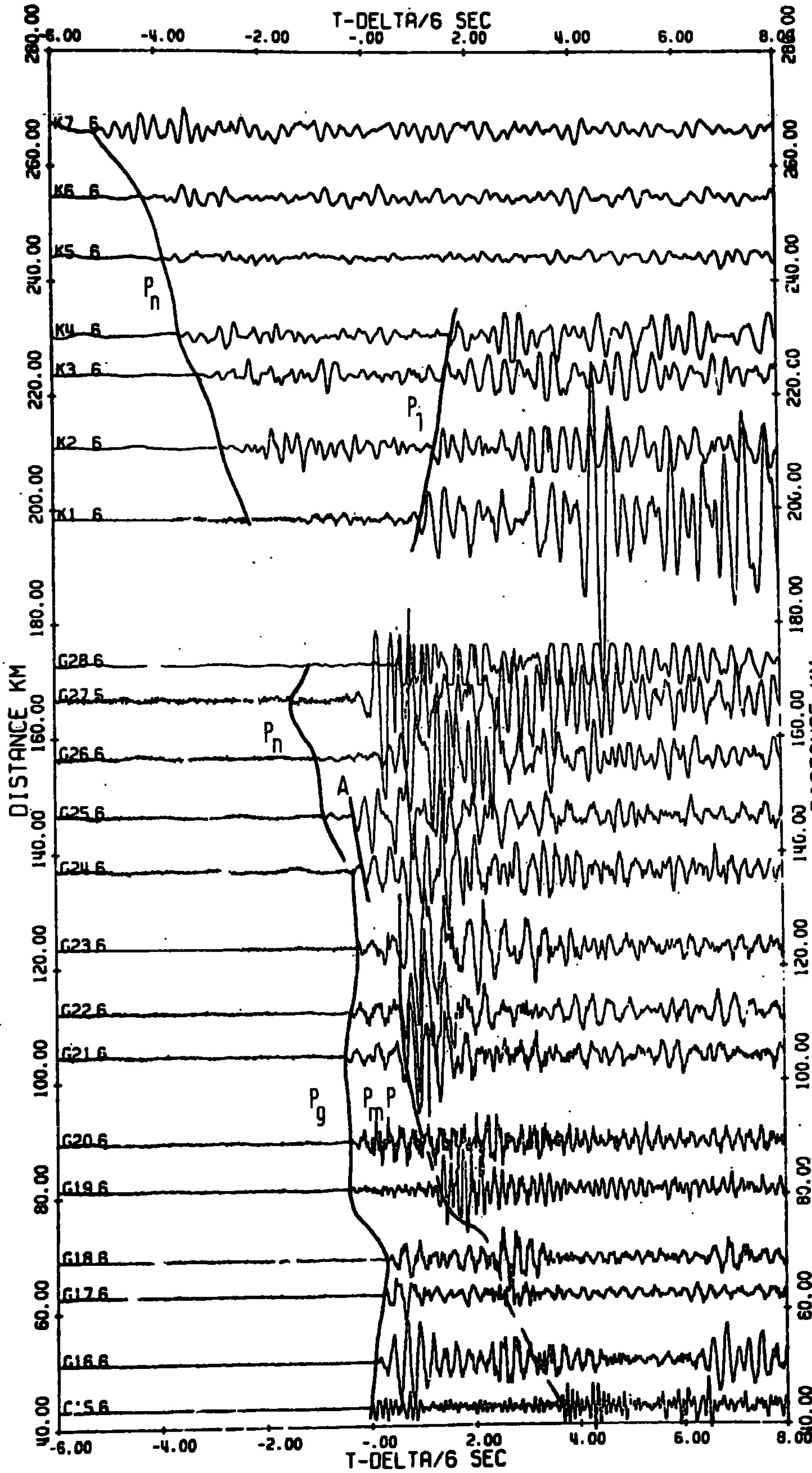

LAXAY

Figure 4.40 Computer drawn stacked record section for G and K shots at Laxay. Unfiltered vertical seismometer. Arrivals, A, may be reflection from mid-crustal layer. Note P_1 phase and large amplitudes behind P_n in Rockall Trough.

from 7.7 to 8.1 km sec^{-1}. The wide-angle reflection is quite clearly shown with a high apparent surface velocity of 8.5 km sec^{-1} at low ranges (large angles of incidence) decreasing to about 6.8 km sec^{-1} as the range increases to 130 km.

One other tentatively correlated arrival could arise from a mid-crustal refractor. Shots G24 and G25 show a second arrival (marked A in Figure 4.40) which does not belong to the P_n or P_mP branch of the travel-time curves and has a larger amplitude than, and different character from, P_g. The apparent surface velocity at the array is determined as 7.3 km sec^{-1} and at the shots as 6.5 km sec^{-1}. This last estimate is uncorrected for any change in sedimentary delay-time effect but this has been shown in Section 4.4.3 to be small for these shots. The arrivals could possibly be refractions from a mid-crustal refractor although its amplitude may be considered to be too large. A very wide-angle reflection from the top of a mid-crustal interface is a possible explanation and such arrivals have been observed in LISPB (Bamford, personal communication). Unfortunately, the phase is not traceable into records at larger ranges as complicating effects of sedimentary delay-time occur close to the margin with Rockall Trough. If this phase is a reflection the very sharp rise in amplitude near G24 and G25 suggests that the critical distance is about 140 km. Application of the observation of Červený (1966) that the maximum in amplitude occurs some small distance beyond the critical distance would reduce this estimate to about 125 km. An interface between rocks of 6.2 and 6.4 km sec^{-1} would need to be at a depth of 16 km to produce the observed position of the maximum in amplitude. For a stronger velocity contrast of 6.2 to 6.6 km sec^{-1} the depth should be about 23 km. As it has been shown that the Moho depth in this region is about 25 km (Section 4.5) it is unlikely that a 6.2 to 6.6 km sec^{-1} interface exists at such a depth. More likely is an interface of smaller velocity contrast at slightly shallower depth.

Arrivals corresponding to this phase can be seen in Figure 4.44 which shows the recordings of these shots made at Husinish (DU10). Shot G27 shows an arrival, marked A, behind the first arrival segment but before the probable continuation of the P_mP phase; again the identification is tentative because of the large delays imposed by the changing sediment thicknesses.

4.7 Results of particle motion processing

As described in Section 3.8, certain records were found suitable for particle motion processing. Figure 4.41 shows the smoothed correlator function, which is the product of the radial and vertical component, of the North Minch shots recorded at Loch Carron. Figure 4.42 is a stacked record section of the same shots. The Moho wide-angle reflections which follow about 2 seconds behind a very small first arrival (P_g) are well shown by the large positive correlations. Shot G11 clearly shows the double pulse-like character discussed in the preceding section (Figure 4.42). The direct S-waves, with negative correlations, are shown later in the records of G11 to G14 and can be correlated from shot to shot. However, the onsets of S-waves for shots

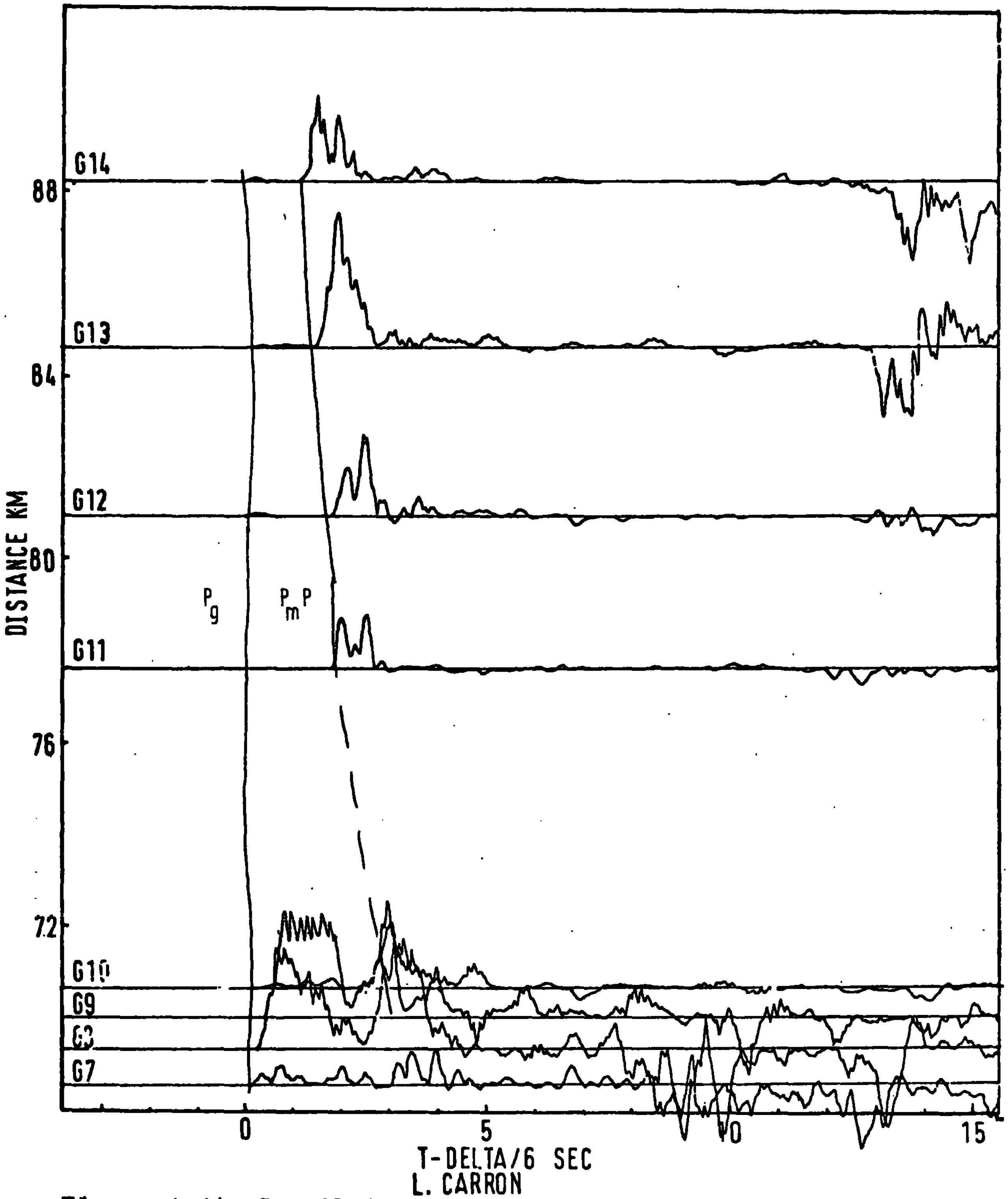

Figure 4.41 Compiled results of particle motion processing for shots G7 to G14 recorded at Loch Carron (DU14). Positive correlations are P-waves, negative are S-waves.

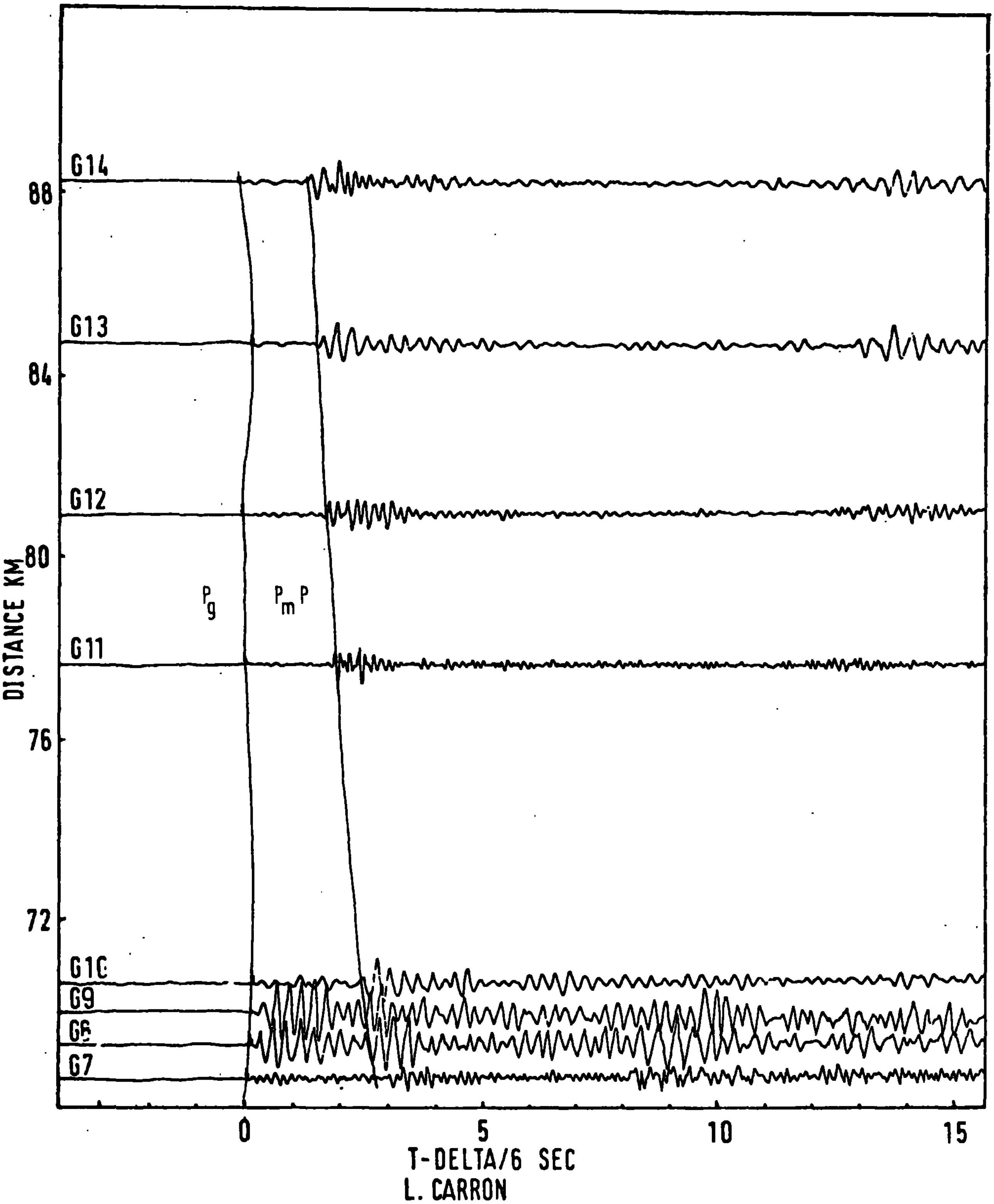

Figure 4.42 Hand drawn stacked record section of G shots at Loch Carron. Unfiltered vertical seismometer. Note double pulses of G11 P_mP reflection.

G7 to G10 are difficult to determine. Correlations corresponding to P_mS (negative correlations at about 5 to 6 seconds behind the first arrival) are definitely not present.

Figure 4.43 shows the same smoothed correlator function for shots G15 to G28 and K1 to K6 recorded at Husinish (DU10) and Figure 4.44 is a stacked record section of these shots. The P_mP reflection starts at about shot G19 and can be traced confidently to shot G26 as strong positive correlations. A poorly developed second wide-angle reflection, marked B, follows some seconds behind the P_mP phase. The S-wave arrivals cannot be seen as a distinct pattern of arrivals but rather as a group of arrivals for which correlations can be negative or positive due to conversions close to the recorder. No arrivals or correlations corresponding to the converted P_mS reflection, seen at Cape Wrath by Jacob and Booth (1977), can be identified.

4.8 Analysis of wide-angle reflections

The arrival times of the prominent Moho wide-angle reflections (P_mP) shown at Husinish, Laxay, Rogart, Maaruig and other stations (Figures 3.7, 4.3 and 4.4) were picked from the analogue records. The wide-angle reflections from the Moho are well developed out to ranges of about 120 km and their arrival times can be picked and used in a T^2/X^2 analysis to estimate the average crustal velocities and thicknesses. Figures 4.45 and 4.46 show T^2/X^2 graphs for the outer shelf shots recorded at four of the stations on the Outer Hebrides. Table 4.7 lists the best-fitting straight lines for this data from which estimates of the average crustal velocity and thickness have been derived.

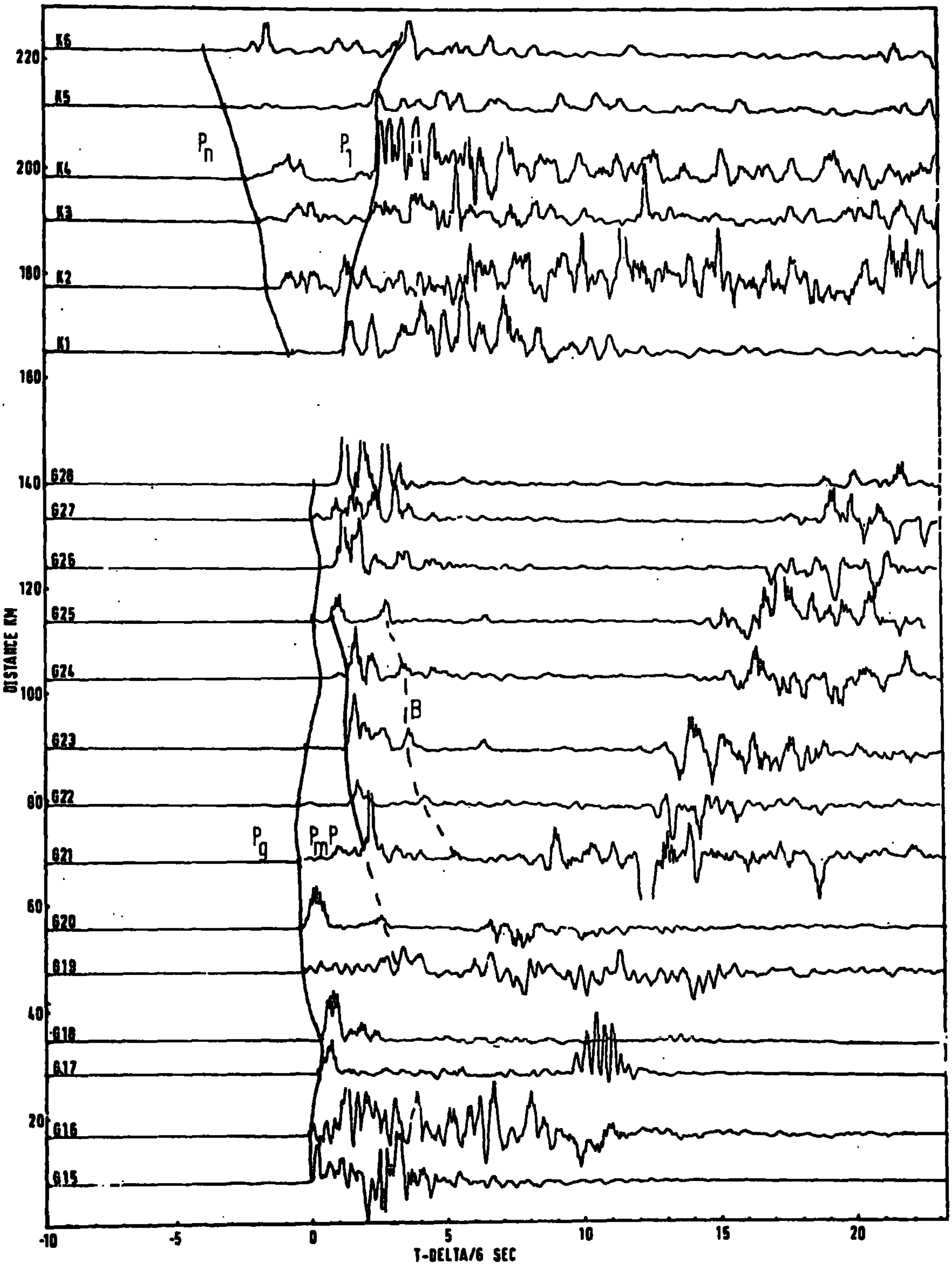

PARTICLE MOTION RESULTS FROM HUSINISH

Figure 4.43 Compiled results of particle motion processing for G and K shots at Husinish (DU10). Note P_1 phase in Rockall Trough.

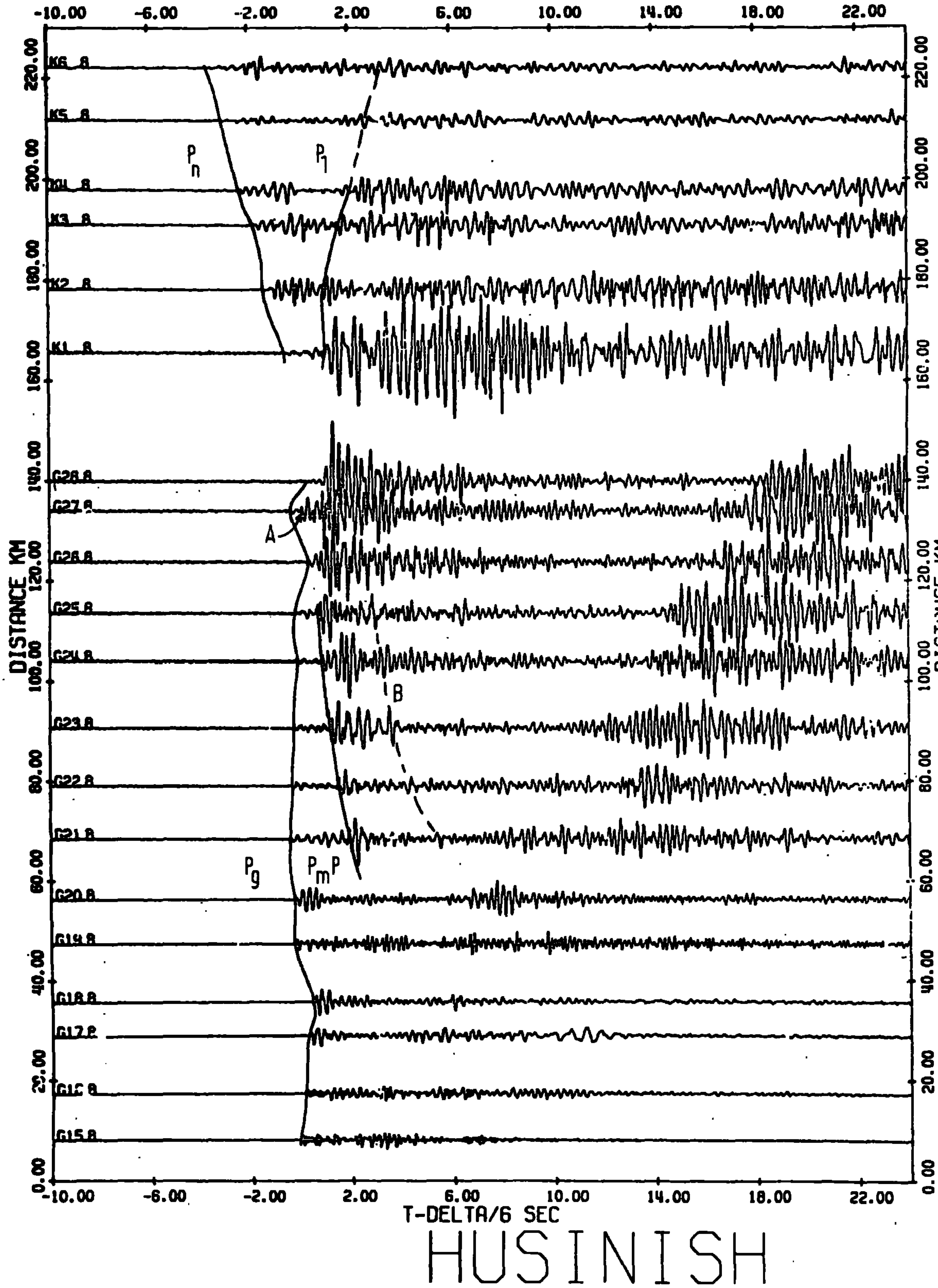

Figure 4.44 Computer drawn stacked record section of G and K shots at Husinish. Filtered vertical seismometer. A is possible wide-angle reflection from mid-crustal layer, B is complex wide-angle reflection discussed in text.

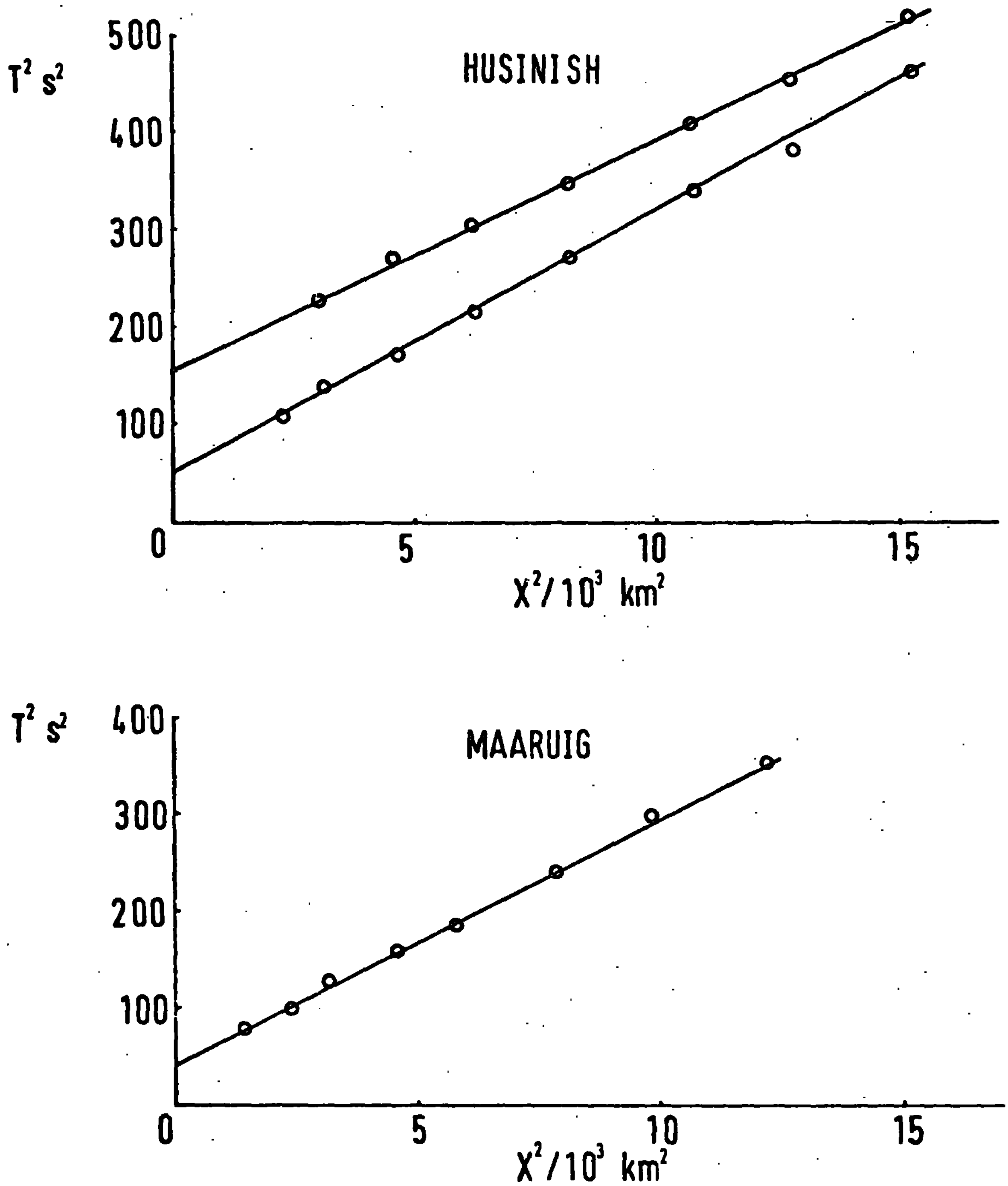

Figure 4.45 T^2/X^2 plots of Moho wide-angle reflections recorded at Husinish and Maaruig (DU11). Second line on Husinish plot is reflection marked B on Figure 4.44.

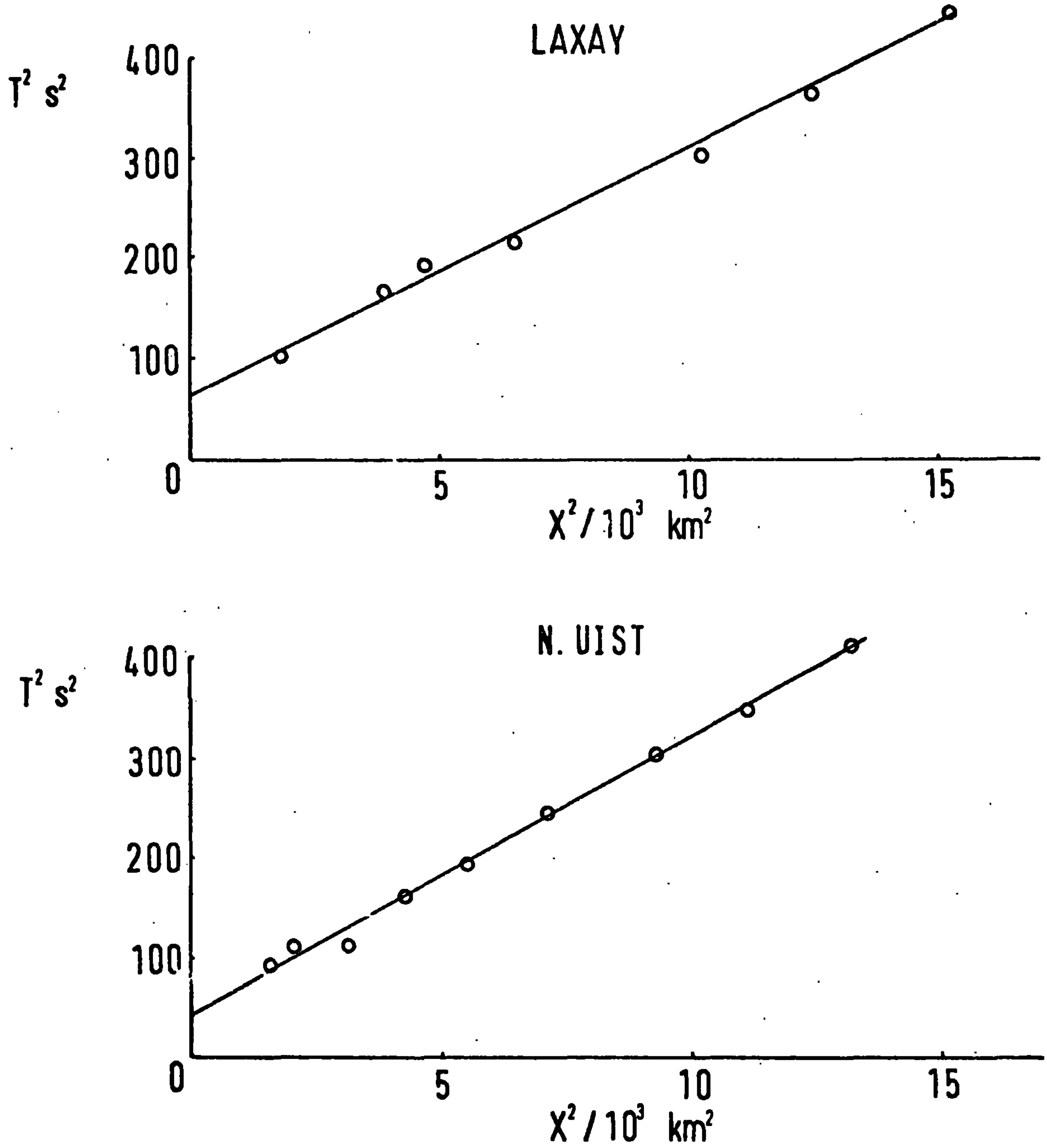

Figure 4.46 T^2/X^2 plots of Moho wide-angle reflections recorded at Laxay and North Uist (DU12).

Table 4.7 Summary of the results of T^2/X^2 analysis of the P_mP wide-angle reflection.

Station		Shots	Range of Distances (km)	Correlation Coefficient	Average Velocity (km sec^{-1})	Intercept (sec^2)	Thickness (km)
Stac Pollaidh	GS2	H11 - H16	67 - 77	0.9911	7.09±1.20	78	31.4
Rogart	GS7	G10 - G14	94 - 131	0.9991	6.59±0.50	104	33.7
Rogart	GS7	H11 - H16	120 - 140	0.9932	6.19±0.90	72.8	26.4
Average		Minch	67 - 140		6.62		30.5
Husinish	DU10	G19 - G26	47 - 123	0.9992	6.13±0.24	50.3	21.7
Maaruig	DU11	G17 - G23	37 - 110	0.9988	6.26±0.30	42.9	20.5
North Uist	DU12	G17 - G26	40 - 115	0.9960	6.00±0.44	43	19.8
Laxay	MD1	G15 - G23	43 - 123	0.9971	6.43±0.55	66	26.1
Average		Outer shelf	37 - 123		6.20		22.0

The mean estimate yielded values of 6.2 km sec^{-1} for the velocity and 22 km for the thickness. Shots in the Minch were recorded at several stations on the Mainland, all at a smaller range of distances and they therefore give slightly poorer estimates. The mean velocity of 6.62 km sec^{-1} and thickness of 30.5 km are, however, significantly higher than the estimates for the outer shelf. This is in agreement with the estimates made from Moho wide-angle reflections from some shots fired in the Minch and recorded at Cape Wrath (Jacob and Booth, 1977). They give an estimated average velocity of 6.64 ± 0.03 km sec^{-1} and a thickness of 28.9 ± 0.3 km.

At ranges above about 120 km the curvature of the wide-angle reflection becomes less pronounced and the records take on a much more complex appearance (Figures 4.40 and 4.44). At greater ranges a strong late phase of apparent velocity about 6.0 km sec^{-1} and reduced time about 0 seconds is developed and continues out to ranges of about 300 km (Figure 4.2). This is too low an apparent velocity for the phase to be a simple very wide-angle Moho reflection. It is probably a continuously refracted wave trapped in the upper parts of the crust by a velocity increase with depth. Unfortunately, the change from a true P_mP to this phase occurs at a range of distances where the observation scheme of HMSP is weakest. For shots on the outer shelf the complicating effects of large P_g delay-time changes obscures the change over. For stations on the Mainland no shots were fired in the distance range of interest because of the Outer Hebrides themselves.

Another phase which can be correlated from shot to shot can be seen in Figures 4.43 and 4.44 showing the recordings of the shots on the outer shelf recorded at Husinish. The arrival, marked B, follows between about 4 and 1.5 seconds after P_mP, being closer at longer ranges. It is a P-wave and the curved correlations in Figures 4.43 and 4.44 suggest that it is some sort of wide-angle reflection. Figure 4.45 shows the T^2/X^2 graph for this phase recorded at Husinish, which indicates an average velocity of 6.4 ± 0.3 km sec^{-1} and intercept time of 150 sec^2. It is not, therefore, a crustal-wide multiple of the Moho reflection as it follows too closely behind it and has a significantly higher average velocity. An origin as some sort of complex lower crustal multiple reflection seems likely.

The method of Holder and Bott (1971) was difficult to apply in this survey because it relies on finding the peak in amplitude of the wide-angle reflection in order to identify the critical distance. Only shots on the outer shelf gave a sufficient range of observation for an estimate of the critical distance to be made. Shots in the Minch, whilst quite clearly showing the wide-angle reflection, were, in general, recorded over a range of distances of about 40 km and it was not possible to determine the critical distance. Figure 4.47 shows the amplitude plots at Husinish and Laxay for the outer shelf shots. They have been corrected for any changes in the gain of the recording system but still show substantial variability which may be due in great part to the variability in input frequencies and power at each shot, as mentioned in Section 4.1. Estimates of

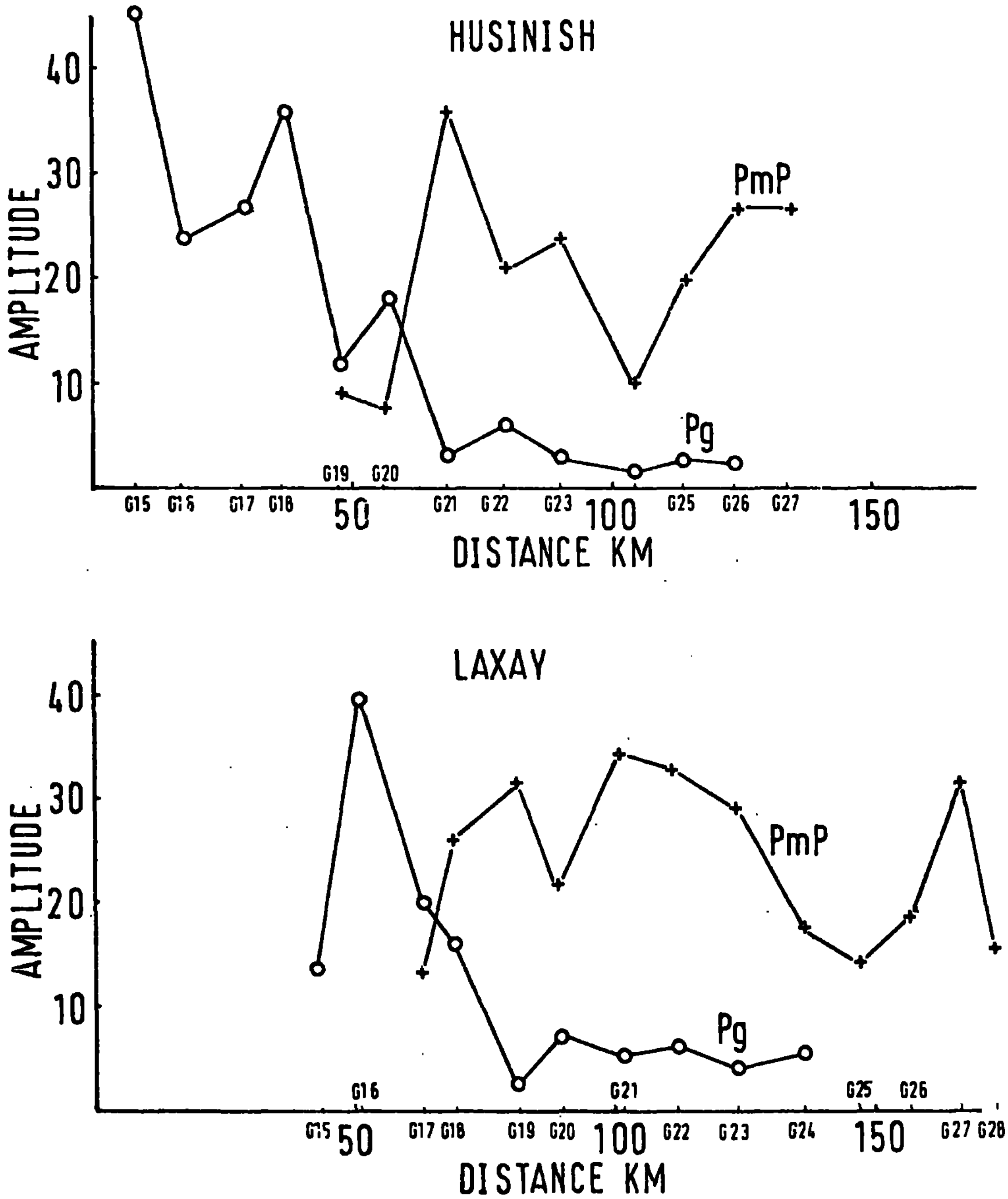

Figure 4.47 Amplitude plots of Moho wide-angle reflections and P_g recorded at Husinish and Laxay.

22.5 km and 27 km are obtained for the crustal thickness and of 6.1 km sec^{-1} and 6.5 km sec^{-1} for the average crustal velocity.

An alternative explanation for the absence of a smooth amplitude curve may lie in a true variability of the Moho structure at the reflection points. Results of Russian deep seismic sounding experiments have shown that the correlation of the P_mP phase is often irregular, the arrival times and amplitudes changing drastically over distances of 10 km or so (Davydova, 1972). This sort of variability can only be defined well by observations spaced very close together and may be due to changes in Moho structure from a first order discontinuity to a transition zone or a zone of interfingering velocity reversals.

The results of the two analysis methods used are broadly in agreement although in the present work most confidence is attached to the results of the T^2/X^2 method applied to the outer shelf shots.

4.9 Summary

Analysis of arrivals observed on the shelf and surrounding land areas indicate the following structures:

(1) A first arrival from a basement refractor with a velocity of between 6.1 and 6.2 km sec^{-1} occurs over the whole region.

(2) No first arrivals from a mid-crustal refractor were confidently observed. A few shots in the Minch recorded at large ranges to the south show apparent velocities in the range 6.4 to 6.7 km sec^{-1}. It is

possible that these arrivals represent refractions from a mid-crustal layer. The depth to such a refractor would be fairly large because it is only observed at these very large ranges where the P_n arrivals are not first arrivals.* Alternatively, it is possible that these arrivals represent P_g arrivals with a small systematic change of delay-time. The small distance range over which observations were made make a conclusive choice between these alternatives impossible.

(3) Beyond ranges of between 130 and 170 km a P_n first arrival with a least-squares velocity of 8.01 ± 0.04 km sec^{-1} occurs. The lower cross-over distances are observed for shots on the outer shelf whilst much larger distances are observed for shots in the Minch, suggesting larger delay-times for the Minch shots. The amplitude of P_n drops off at large ranges so that at ranges of about 350 km it is very difficult to observe.

(4) Sedimentary thicknesses vary from 0 to 3 km and small sedimentary basins correlate with gravity and magnetic anomalies.

(5) Some lateral variations in basement velocity are present and these correlate with gravity and magnetic anomalies, e.g. the structure beneath the shots G19, G20 and G21. Figure 4.25

(6) Some evidence of a small scale increase of velocity with depth in the upper parts of the crust is shown but this need not imply compositional changes.

* The change of delay-time required for this argument is opposite to the observed effect.

(7) Wide-angle reflections from the Moho clearly show a low average velocity of 6.2 km sec^{-1} and a thickness of 22 km for the crust of the outer shelf region. Results from this experiment show higher average crustal velocities of about 6.6 km sec^{-1} and thicknesses of about 30 km for the area between the Minch and mainland stations. The Caledonian mobile belt has been shown in NASP (Smith and Bott, 1975) and in LISPB (Bamford et al., 1976) to have average velocities of about 6.6 km sec^{-1}.

(8) Changes of P_n time-terms must be studied carefully before converting to an estimate of crustal thickness. For the outer shelf area and Outer Hebrides a thickness of about 25 km is estimated whereas on the Mainland, using the higher average crustal velocities, an estimate of about 30 km is made. Over the Minch, very large increases in P_n time-term probably do not simply represent thickened crust but rather velocity anomalies in the upper parts of the crust which cannot be completely defined. *

(9) No evidence of the converted wide-angle reflection, P_mS, can be found although good observations have previously been made just to the north of the present area (Jacob and Booth, 1977). The Moho is thus implied not to be a very sharp compositional boundary but to be a zone of gradational change possibly spreading over 2 or 3 km (Fuchs, 1975). Most crustal refraction experiments similarly do not identify P_mS reflections.

* There remains an unresolved contradiction with this velocity anomaly. Time-term analysis suggests low velocities whereas wide-angle reflection and plus-minus analysis suggests the possibility of higher velocity material.

(10) A clear identification of a wide-angle reflection from a mid-crustal interface cannot be made. However, slight evidence is presented which would suggest a very large depth for such an interface in the outer shelf area. This is in keeping with the low average crustal velocities found in this area. If such a deep interface exists it offers a possible explanation for a late reflection observed at Husinish (Figures 4.43 and 4.44) as a multiple between this interface and the Moho.

CHAPTER 5

RESULTS FROM ROCKALL TROUGH

5.1 The general pattern of arrivals from stacked records

This chapter deals with the analysis of shots fired in the Rockall Trough which were recorded at the temporary recording sites in Scotland and Northern Ireland. Figures 5.1 and 5.2 show stacked record sections of the K shots recorded at St. Kilda (DU15) and Glencassley (GS5). Other shots are included in these diagrams but these have already been discussed in Chapter 4. The K shots have been included in other stacked record sections in Chapter 4 and Appendix B.

Two distinct phases of correlated arrivals can be recognised and traced from record to record, the first, with an apparent velocity of about 5.7 km sec^{-1} will be called P_1, and the second, with an average apparent velocity of about 8.3 km sec^{-1} will be called P_n.

P_1 occurs as a first arrival only on recordings of shots K1, K2 and K3 at St. Kilda (DU15) but can be seen as a late arrival for shots K4, K5 and K6 at St. Kilda (Figure 5.1) and for shots K1 to K6 recorded at Laxay (MD1) and Husinish (DU10) (Figures 4.39, 4.40, 4.43 and 4.44). The correlation of this refraction shows quite large deviations from a straight line which are probably due to changing sedimentary delays in Rockall Trough. Seismic reflection profiles across the Trough show some large changes in depth to 'basement' (e.g. Figure 1.3).

The P_n headwave occurs as a first arrival for all

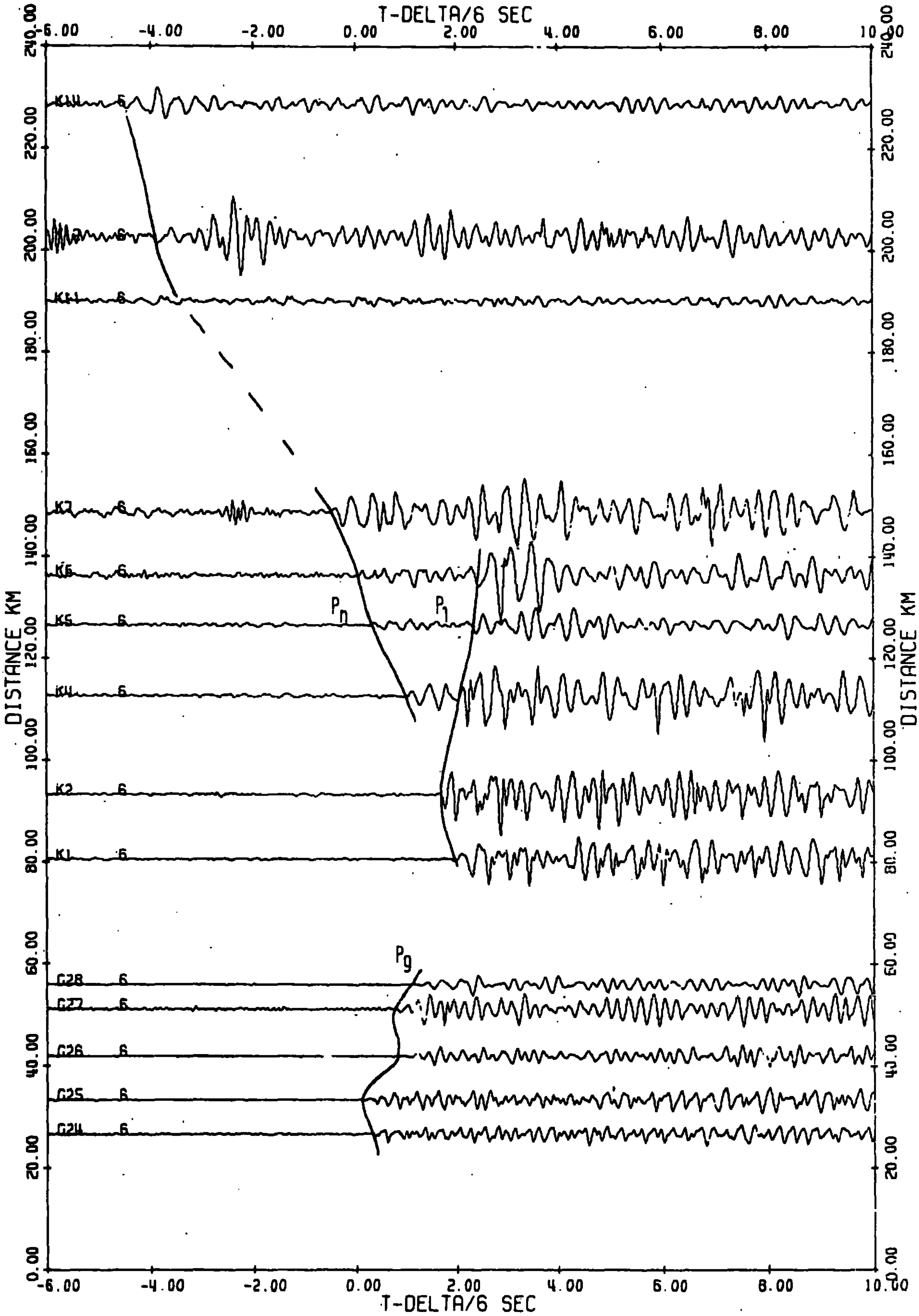

Figure 5.1 Computer drawn stacked record section of the G and K shots recorded at St. Kilda (DU15). Filtered vertical seismometer.

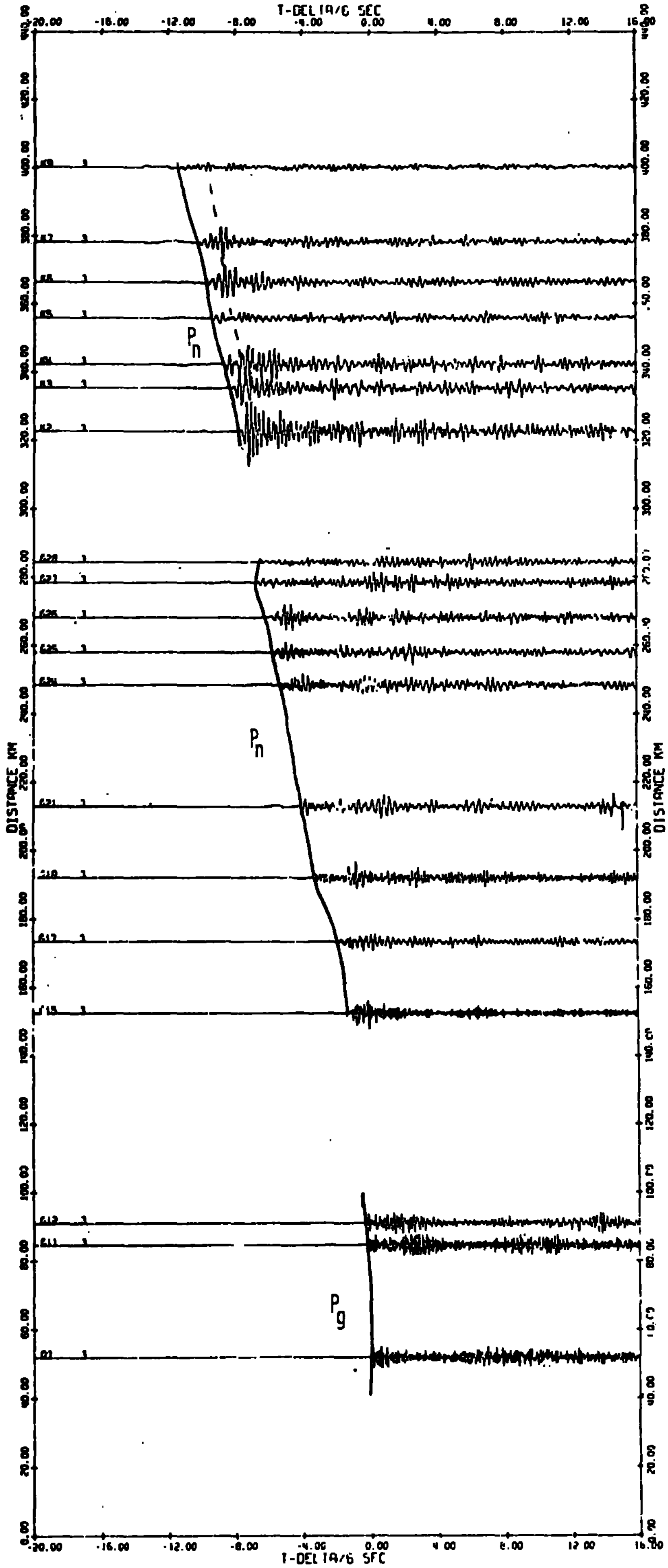

Figure 5.2 Computer drawn stacked record section of G and K shots recorded at Glencassley (GS5). Unfiltered vertical seismometer. Note the large amplitudes for K shots in Rockall Trough.

recordings above about 110 km range and the arrival times also show large and regular deviations from a straight line correlation. Varying sedimentary delay is the most probable explanation although changes in Moho depth will probably make some contribution. At quiet stations the phase can be recognised out to very large ranges where it still has impulsive onsets (Figure 5.2).

The amplitude of the first arrival shows a prominent peak in the distance range 310 to 330 km and it is possible that such a distance range marks the critical distance of a sub-Moho reflection. Alternatively, this phenomenon could indicate the development of large energy from a wave continuously refracted in a layer of increasing velocity below the Moho. If this second phase has a velocity only slightly greater than that of P_n it will be difficult to detect.

Most of the recordings of the K shots show large amplitude arrivals within about 2 seconds of the first arrival (Figures 5.2 and 4.2). These arrivals are probably not simple sea-water multiples of the first arrival since their amplitude is so large. The arrivals are P-waves (Figure 4.43) and so an origin from simple P to S conversions is ruled out. Phase correlation of the arrivals from record to record is difficult but there is a slight indication that, for ranges below about 310 km, a correlated arrival with a velocity slightly greater than that of the first arrival can be recognised. At ranges above about 330 km any correlated phase has a velocity slightly less than that of the first arrival. If this is so it may suggest that the more distant first arrival segment is formed from a deeper and faster interface than the Moho.

The dominant frequency of the recordings of these shots is generally lower than those made for the shots on the shallow shelf area and the signals contain a narrower band of frequencies. The signal characteristics generated by the dispersed charge system used for the K shots should be the same as those generated by a single charge (Section 2.2.2). The effect of the selective attenuation of the higher frequencies and the large ranges over which most of the recordings were made is probably responsible for the observed differences. When these shots are recorded at low ranges they contain a much broader band of frequencies and have a higher dominant frequency (Figure 5.1). Figure 5.3 shows the amplitude spectra of both signal-plus-noise and noise only for one of the shots. Clearly, there is a large low frequency component of noise below about 1 hz which can be removed by frequency filtering, as shown in Figure 5.4 which is a plot of the same signals filtered between 2 and 15 hz. Fortunately, the frequencies of signal and noise are distinctly different and thus this type of frequency filtering is effective.

5.2 Travel-time graphs

Since the stations and shots were sited on opposite sides of a continental margin and were believed to be sampling two different structures, two sets of travel-time graphs were drawn. The apparent velocity at the shot end of the line is shown by a graph of arrival times of all the

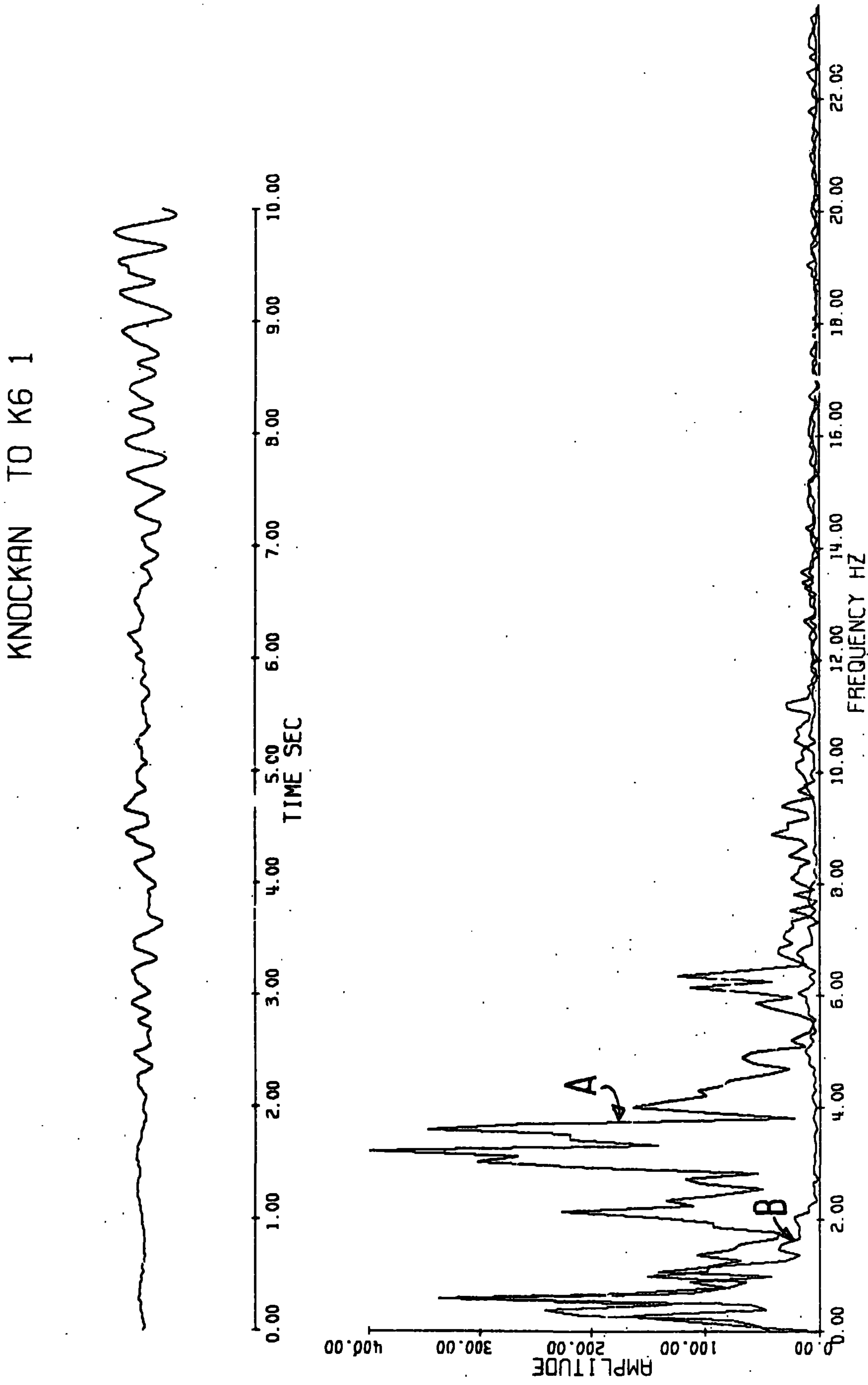

Figure 5.3 Computer drawn amplitude/frequency plot for shot K6 recorded at Knockan (GS3). Amplitude scale in arbitrary units. A is spectrum of signal-plus-noise and B is noise only.

Figure 5.4 Computer drawn amplitude/frequency plot for shot K6 recorded at Knockan and filtered between 2 and 15 hz. Conventions as in Figure 5.3. Note removal of low-frequency noise.

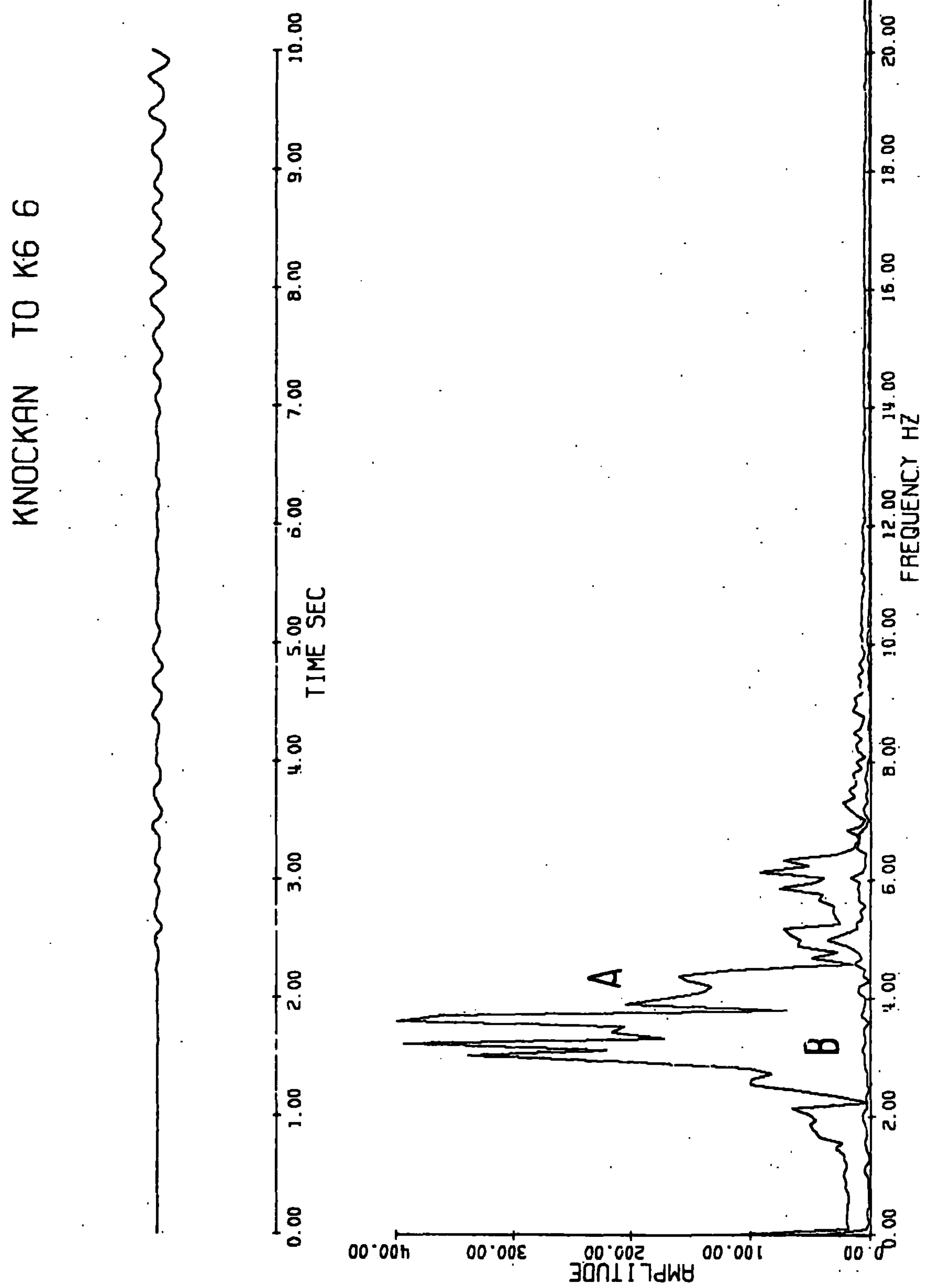

shots at one station (Figures 5.5 to 5.7). Figures 5.8 and 5.9 show graphs of the arrival times for one shot recorded at all the stations and is used to estimate the apparent velocity at the station end of the line. Other travel-time graphs for these shots are shown in Figures 4.10 to 4.12 and in Appendix B. Tables 5.1 and 5.2 summarise the results of fitting the best straight lines to the two data sets.

The arrival times of the P_1 phase were picked from the Laxay array records with the help of velocity filtering (Figures 4.39 and 4.40) and from the Husinish records with the help of particle motion processing (Figures 4.43 and 4.44). The accuracy of these picks is less than that for the picks of first arrivals but, nevertheless, reasonable least-squares velocities were found. Figure 5.5 shows that the P_1 phase has an apparent velocity between the shots of about 5.7 ± 0.8 km sec^{-1} whilst the apparent velocity between the stations is about 6.2 ± 1.0 km sec^{-1} (Table 5.2). Such values of apparent velocity neglect the effects of changing sedimentary delay which is a reasonable assumption for the stations but may be quite invalid for the shots since large sedimentary delay changes are shown on reflection profiles from this area. However, a phase change at the continental margin may be expected, as such an observation has been made between the Iceland-Faeroe Ridge and the Faeroes Plateau by Bott, Nielsen and Sunderland (1975).

In order to test whether first arrivals beyond about 310 km range correspond to a deep refractor beneath the Moho, recordings of all the shots at all the stations were

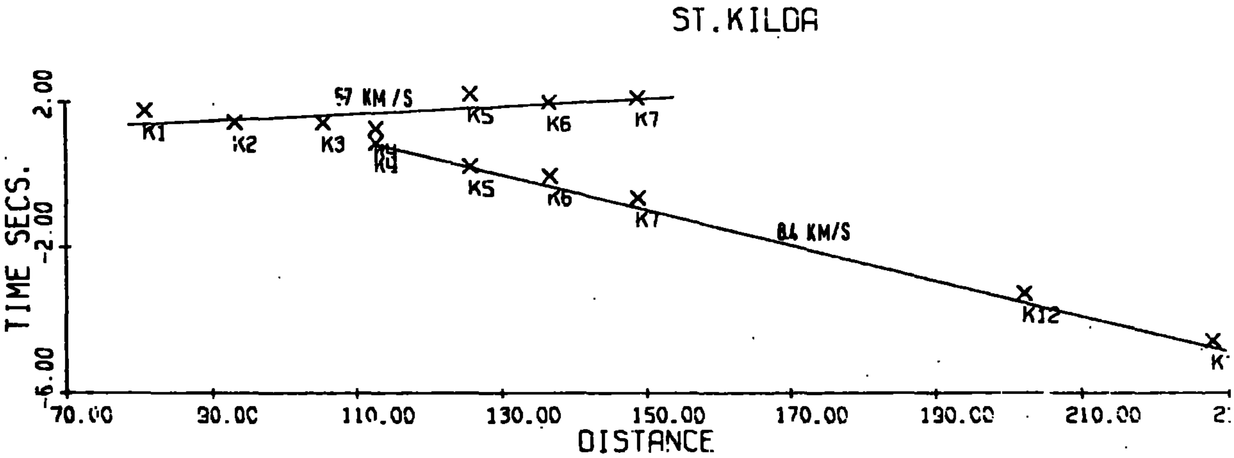

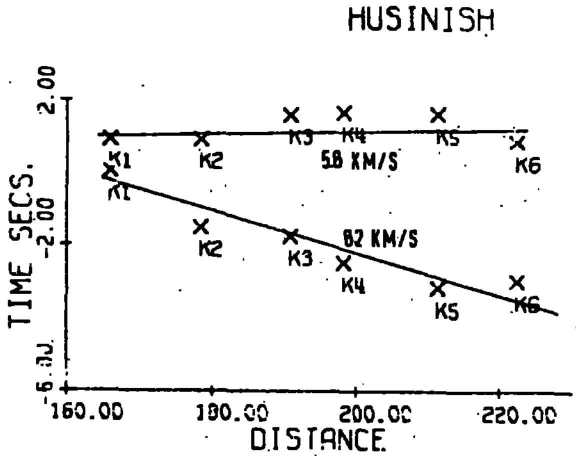

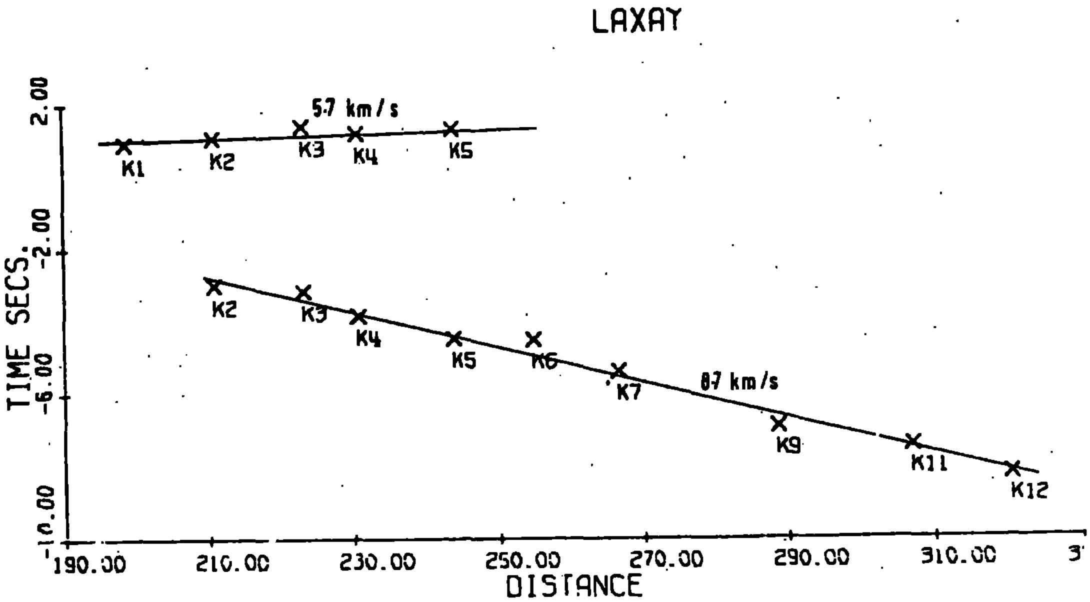

Figure 5.5 Reduced travel-time graphs at St. Kilda, Husinish and Laxay. Reduction velocity is 6.0 km sec^{-1}.

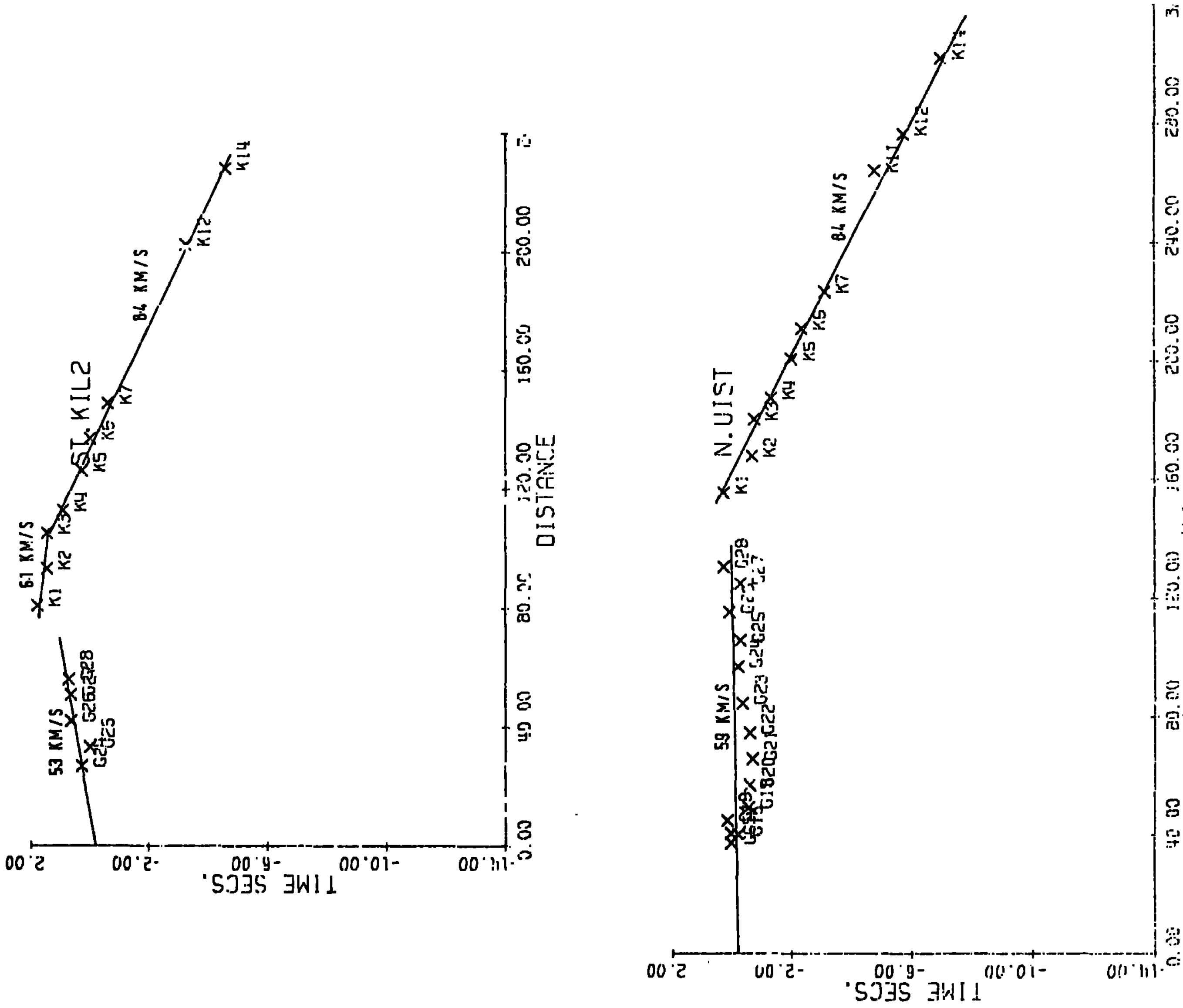

Figure 5.6 **Reduced travel-time graphs at St. Kilda and North Uist. Reduction velocity is 6.0 km sec^{-1}.**

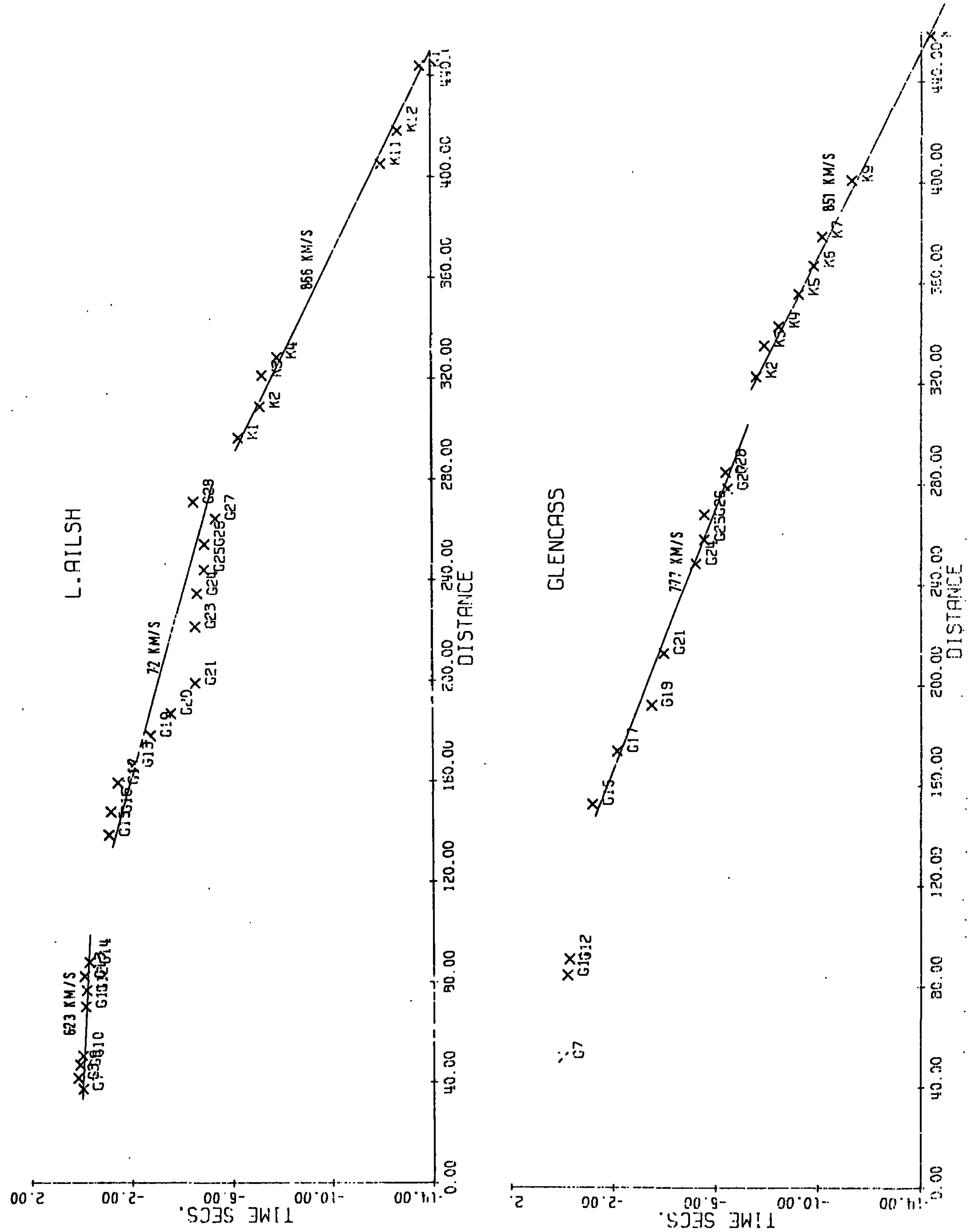

Figure 5.7 **Reduced travel-time graphs at Loch Ailsh and Glencassley. Reduction velocity is 6.0 km sec^{-1}.**

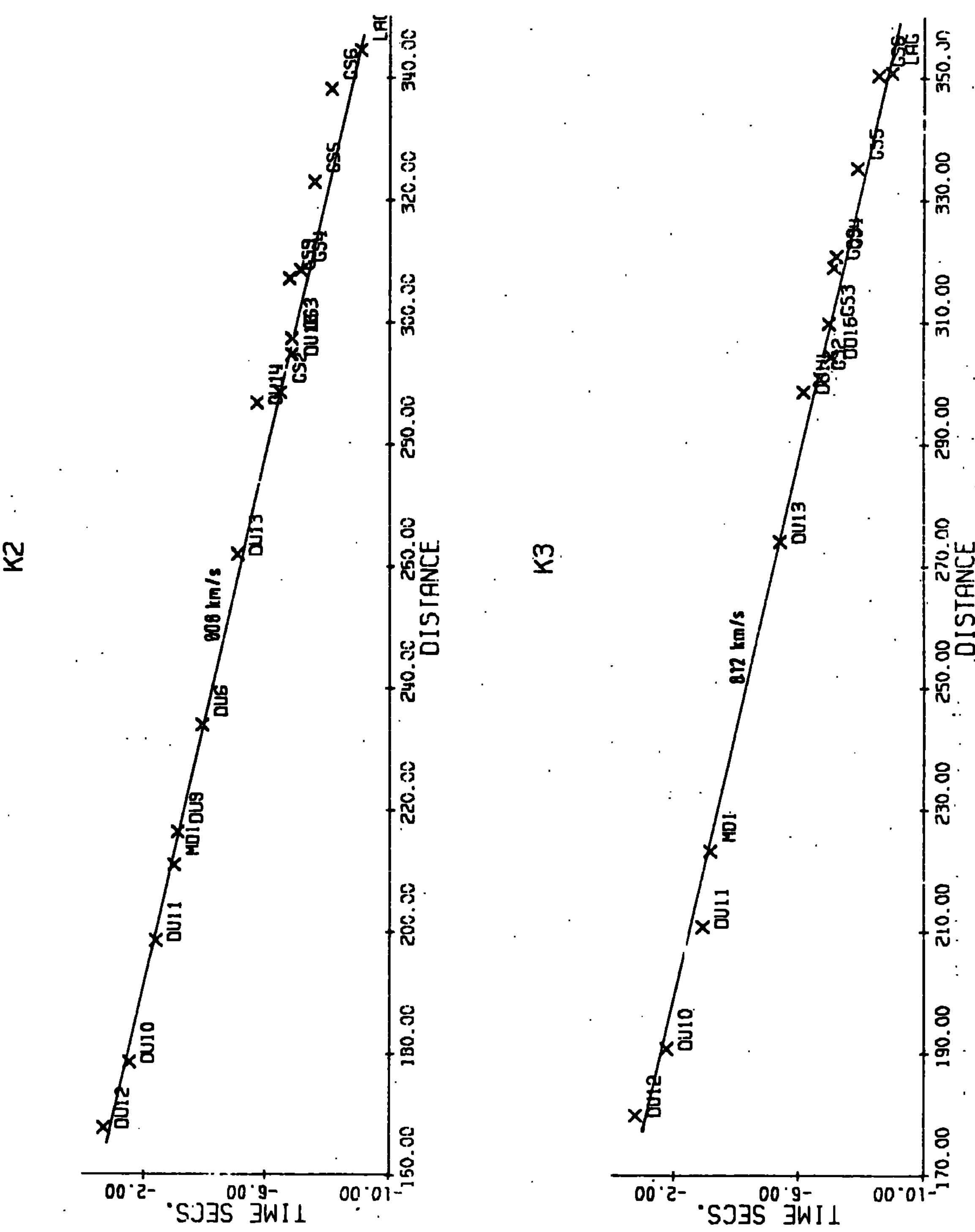

Figure 5.8 Reduced travel-time graphs for first arrival travel-times of shots K2 and K3 recorded at all the stations. Reduction velocity is 6.0 km sec^{-1}.

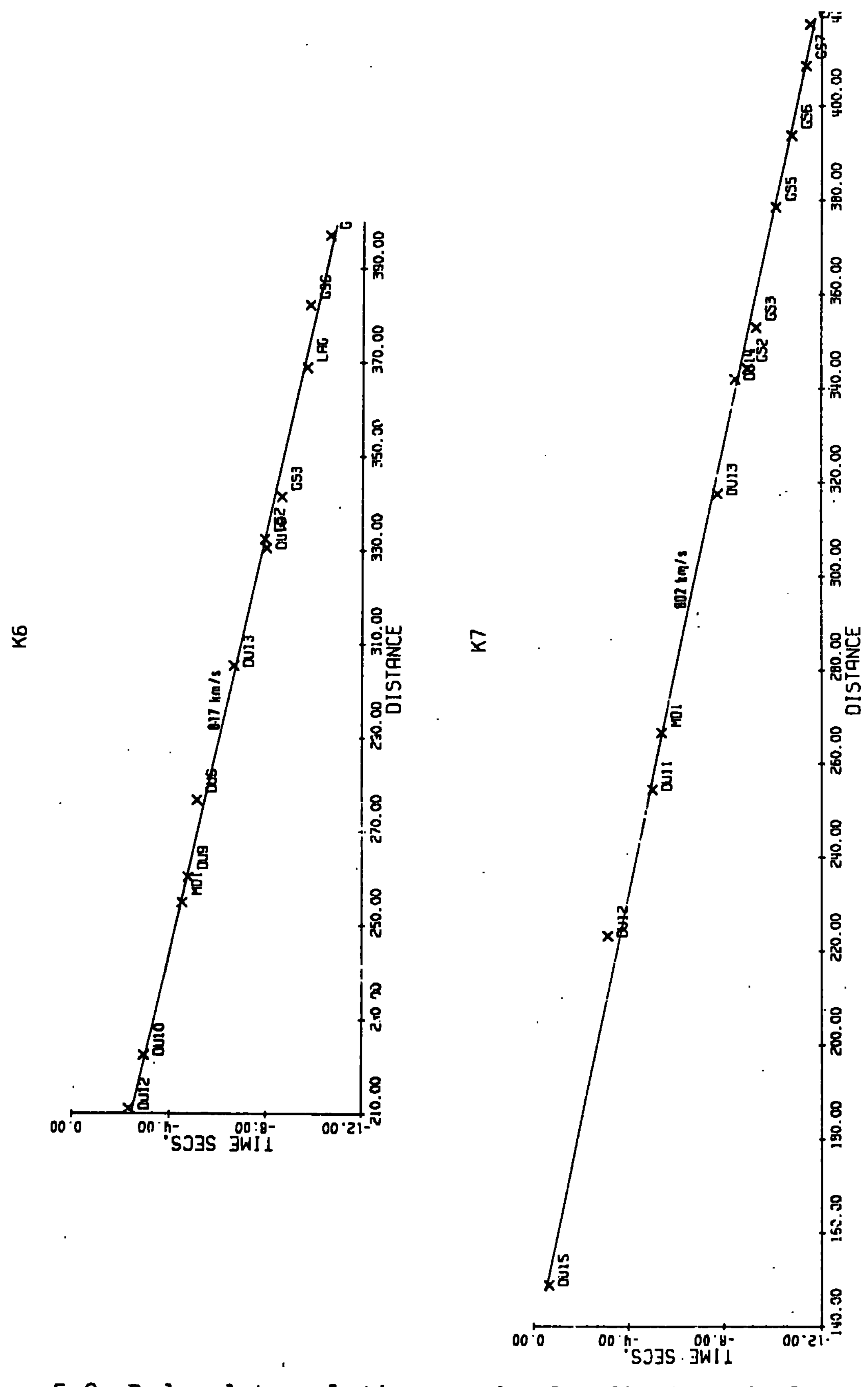

Figure 5.9 Reduced travel-time graphs for first arrival travel-times of shots K6 and K7 recorded at all the stations. Reduction velocity is 6.0 km sec^{-1}.

Station	Code	Phase	Average distance and direction (km)	Velocity ($km\ sec^{-1}$)	Int. time (sec)	No. of shots
Stac Pollaidh	GS2	P_n	323E	8.55	8.24	7
Knockan	GS3	P_n	330E	8.48	7.87	8
Loch Ailsh	GS4	P_n	360E	8.66	8.94	7
Glencassley	GS5	P_n	357E	8.51	8.40	7
Lairg	GS6	P_n	385E	8.46	8.43	10
Cape Wrath	GS9	P_n	311E	8.54	8.53	4
Butt of Lewis	DU6	P_n	257E	7.08	1.98	4
Husinish	DU10	P_n	207E	8.23	6.86	7
Husinish	DU10	P_1	194E	5.82	0.30	6
Maaruig	DU11	P_n	225E	7.59	4.56	6
North Uist	DU12	P_n	216E	8.43	7.67	10
Loch Torridon	DU13	P_n	294E	8.53	8.12	7
Loch Carron	DU14	P_n	317E	8.95	10.17	7
St. Kilda	DU15	P_n	159E	8.38	6.31	6
St. Kilda	DU15	P_1	114E	5.67	0.64	7
Mull	DU16	P_n	307E	7.75	4.33	6
Laxay	MD1	P_n	254E	8.72	8.39	10
Laxay	MD1	P_1	221E	5.70	-0.72	5
Lagg	LAGG	P_n	376SE	8.09	6.15	9

Weighted Average P_n = 8.37 km sec^{-1}

Weighted Average P_1 = 5.73 km sec^{-1}

Table 5.1 Summary of least-squares fitting of first and second arrival travel-time segments for K shots at each station.

Table 5.2 Summary of least-squares fitting of first and second arrival travel-time segments for each shot at all recording stations.

Shot	Phase	Average distance and direction (km)	Velocity ($km\ sec^{-1}$)	Intercept time (sec)	Number of stations
K1	P_n	269W	8.16	7.02	8
K1	P_1	148W	6.29	2.37	3
K2	P_n	260W	8.08	6.19	15
K2	P_1	160W	6.13	1.73	3
K3	P_n	278W	8.12	6.60	13
K3	P_1	173W	6.00	1.48	3
K4	P_n	271W	8.02	5.88	15
K4	P_1	180W	5.98	1.32	3
K5	P_n	280W	8.05	5.91	10
K5	P_1	193W	6.29	3.23	3
K6	P_n	301W	8.17	6.88	11
K7	P_n	320W	8.02	5.78	12
K9	P_n	368W	7.87	4.54	3
K11	P_n	326W	8.23	6.88	3
K12	P_n	355W	8.09	5.68	8
K14	P_n	389W	8.04	5.37	6
L10	P_n	327W	7.71	4.98	5
L11	P_n	329W	7.59	4.34	3

Weighted Average P_n = 8.09 km sec^{-1}

Weighted Average P_1 = 6.14 km sec^{-1}

included in a straight line fitting routine. The aim was to test if a two layer travel-time curve fitted the data more closely than a single layer curve. The data set was split into two sets above and below a certain distance and the least-squares velocities of the two segments found. If a two layer travel-time curve is present the velocities and fits of the two curves should show systematic variations as the splitting distance is varied. The shorter range set should give a constant velocity until, as the splitting distance is increased, arrivals from the deeper layer are included, whereupon the velocity estimate should rise slowly towards a mean value. Similarly, for the larger range set a stable estimate of the velocity in the lower layer should be observed until, as the splitting distance is decreased, arrivals from the upper layer are included. No clear systematic variations of velocity or fit, which might suggest the presence of a two layer travel-time curve, were found; although, as the data included delay-times at shots and receivers, a small change in gradient would probably not be observed. It was therefore felt valid to include all the P_n data in the time-term analysis of Section 5.6.

The apparent velocity of the P_n headwave between the shots varies between about 8.1 and 8.7 km sec^{-1} with an average value of about 8.37 km sec^{-1}. Observations at Lagg give a lower apparent surface velocity of 8.09$\pm$0.6 km sec^{-1} and the significance of this observation is discussed in Section 5.6. Apparent surface velocity measurements at the stations of north-west Scotland give values of about

8.09 ± 0.5 km sec^{-1} which should be compared with a value of 8.01 ± 0.04 km sec^{-1} shown by time-term analysis of shots fired on the shelf. The slight difference may be due to a small increase of P_n time-term towards the east and is probably not significant. It is therefore assumed that arrivals from the K shots in Rockall Trough travel as a normal P_n headwave beneath the Hebridean shelf area and the Scottish Mainland.

5.3 Results of velocity filtering

Figure 5.10 shows the computer output from the velocity filtering program for the shot K1 recorded at the Laxay array (MD1). The stacking velocity for each correlator function is given along the bottom of each trace. The compiled results of the velocity filtering of these shots have been included in Figures 4.39 and 4.40. The very small first arrival (A) in Figure 5.10 is P_n and is just shown on the correlator functions to have an apparent velocity of about 8.1 ± 0.2 km sec^{-1}. A strong late arrival (B) is the P_1 phase and is shown to have an apparent velocity of 6.5 ± 0.2 km sec^{-1}. Several later arrivals have large amplitudes and strong correlations, particularly the arrival C which has an apparent velocity of 6.7 ± 0.2 km sec^{-1}. The shot K1 is peculiar in that these strong late phases are recorded at all stations. This group of arrivals does not contain any characteristic phase which can be correlated from station to station, e.g. Figures 4.1 and 4.2, and therefore an origin as a complex reverberation or a focusing effect of the nearby continental margin is probable.

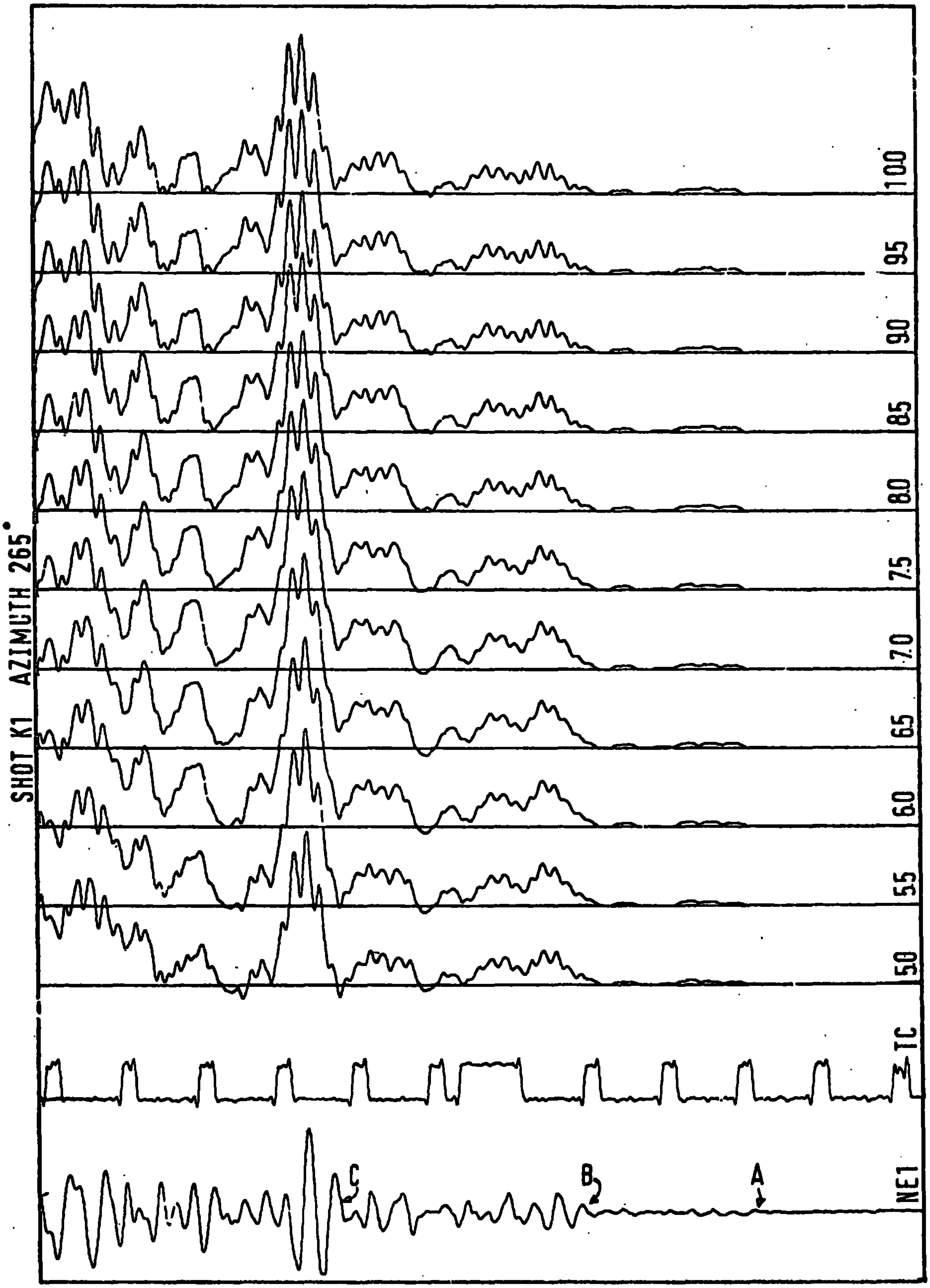

Figure 5.10 Computer drawn output from velocity filter program for shot K1. Signal marked A is P_n, B is P_1 phase and C is a very strong phase discussed in text.

The large amplitude arrivals following within 1 to 2 seconds behind P_n are shown in Figure 4.39 to have apparent velocities of between 8.7 and 7.5 km sec^{-1}. This large spread in velocities is probably more a function of inaccurate velocity determinations than of a real variation. In any case no confident phase correlations can be made for these arrivals.

5.4 Results of particle motion processing

Figures 4.43 and 4.44 include the K shots recorded at Husinish (DU10) as well as the G shots. The strong phases within 1 to 2 seconds behind P_n (marked A in Figure 4.43) are shown to give good positive correlations and a phase correlation of these arrivals is possible. An apparent velocity slightly lower than that of P_n is indicated which argues against their origin as a refraction from a faster interface beneath the Moho since their ranges are less than 310 km. A multiple reflection within the sediments, or water, should have the same apparent velocity as P_n unless there is a systematic thickening of sediments, or water, towards the west. A slight increase in sedimentary thickness from K2 towards K6 is suggested in Figure 5.11 but the large amplitude of these arrivals cannot be explained as a sedimentary multiple. The P_1 phase gives good positive correlations which were of great help in picking the onset times of these arrivals. Few negative S correlations are visible in the first part of these records.

5.5 Time-term analysis of P_1

If the identification of the P_1 phase as a wave refracted along the top of the basement refractor in Rockall Trough and converted to a direct crustal arrival at the continental margin is correct, it should be possible to derive a set of time-terms for it. The solution will be poorly behaved since these arrivals were identified at three stations only which were all sited in-line and to one side of the shot line. The suspected difference in structure beneath shots and stations will also cause problems, particularly in determining a least-squares velocity in Rockall Trough. The aim of the time-term analysis was to try to determine the change in sediment thicknesses rather than the absolute value of the sedimentary thickness in the Trough. Using seismic reflection data, Roberts (1975b) has presented a smoothed contour map of two-way travel-time for a basement reflector which he identifies as the base of the sediments in the Trough. This can be used to constrain the value of one of the shot time-terms and, coupled with the known time-terms for the stations, enables a least-squares velocity to be found. A velocity of 6.2 ± 0.18 km sec^{-1} is found but the time-terms are subject to rather large 95 per cent confidence limits.

This value of velocity is weighted heavily in favour of the continental part of the path, which has already been shown to have a velocity of about 6.2 km sec^{-1}. Using this value gives a slight increase of time-term towards the centre of Rockall Trough, the effect of which is shown in Figure 5.11 to be comparable with the sediment structure

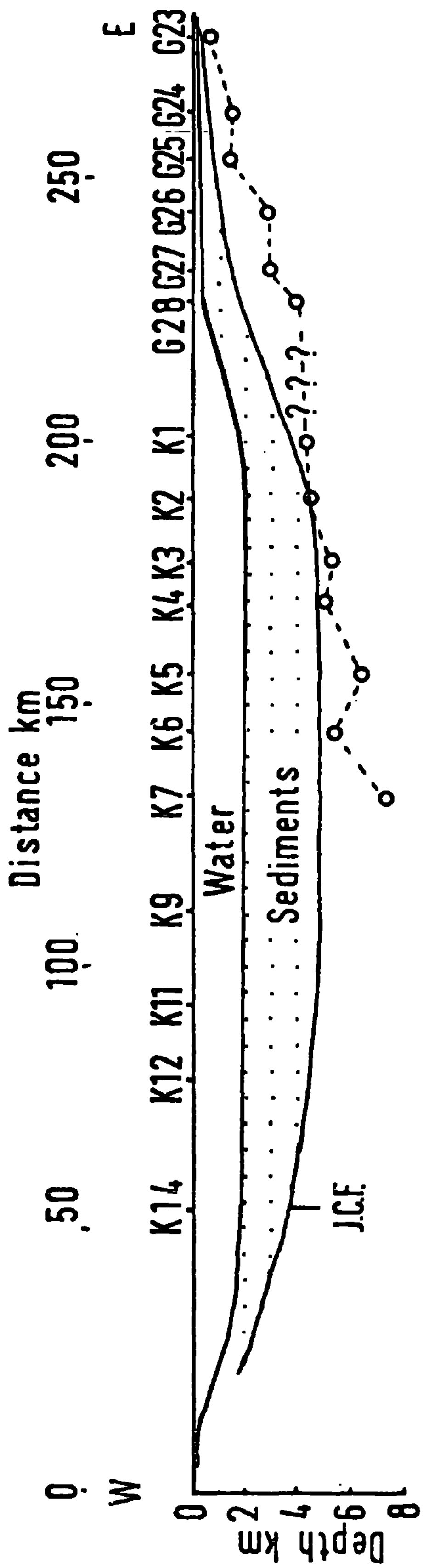

Figure 5.11 Sediment structure from seismic reflection profiles and interpretation of P_1 time-terms in Rockall Trough. JCF is Jean Charcot Fault zone and may mark continent - ocean boundary on west side of Rockall Trough.

derived from seismic reflection profiles. Table 5.3 gives the P_1 time-terms corrected for water delay and converted to a thickness of sediments of assumed velocity of 3.0 km sec^{-1}. Figure 5.12 shows the P_1 time-terms with 95 per cent confidence limits and points out the danger of taking the calculated value too literally. In general terms, the P_1 time-terms show a similar structure to the already known structure but highlight large changes of sedimentary thickness not evident from a smoothed contour map. Such changes are, however, indicated on the reflection profiles themselves (Figure 1.3).

The estimates of sediment thickness, derived from seismic reflection profiling by Roberts (1975b), are minimum estimates as it is possible that more sediments lie beneath the deepest identified reflector. For example, the structure determined by an unreversed refraction line, E11, reported by Ewing and Ewing (1959), would have a two-way travel-time for the base of sediments reflection of 2.6 seconds, whereas the smoothed contour map of Roberts shows about 2 seconds of sediments. Similarly, further south in the Trough the structure determined from an unreversed refraction experiment reported by Scrutton (1971) would give a sediment two-way travel-time of about 3.4 seconds, but the contoured thickness map shows only about 2.5 seconds of sediments. Exactly how much confidence should be placed in structures determined from unreversed refraction profiles is doubtful, but it is possible that Roberts' thickness map underestimates the true thickness of sediments.

Shot	Number of Observations	P_1 time-term observed (sec)	95% conf.	Water and shot depth correction (sec)	Corrected P_1 time-term (sec)	Sediment thickness $V = 3.0\ km\ sec^{-1}$ (km)
K1	3	1.82	0.48	1.12	0.70	2.40
K2	3	1.83	0.48	1.20	0.63	2.16
K3	3	2.22	0.48	1.27	0.95	3.26
K4	3	2.16	0.39	1.28	0.88	3.02
K5	3	2.57	0.48	1.29	1.28	4.39
K6	2	2.25	0.92	1.28	0.97	3.33

Table 5.3 P_1 time-terms, sedimentary delays and interpreted sedimentary thicknesses.

5.6 Time-term analysis of P_n

The aim of the time-term analysis of the P_n data from Rockall Trough is to establish the velocity beneath the Moho in this region and define a depth to the Moho. The sedimentary delay effect of the sediments in Rockall Trough can be estimated from the reflection profiles, or P_1 time-terms, and its effect subtracted from the observed P_n time-terms. The estimation of the true sub-Moho velocity proves difficult because the distribution of shots and stations did not provide either true reversal or good offset stations. Nevertheless, estimates of the maximum and minimum thicknesses of the crust were possible.

All data recorded above ranges of 110 km was included in the time-term analysis. The aerial distribution of the data set is poor and the requirements of the time-term method are only partially met. Unlike the G shots on the shelf, the K shots have a significantly large range variation to the station at Lagg in Northern Ireland. It was therefore impossible to make the simplifying assumption that all the observed variation in travel-times at Lagg were due solely to changes of shot time-terms and independent of refractor velocity. However, the Lagg recordings are useful in that they are more sensitive to time-term changes than to velocity changes and do enable a least-squares velocity to be found.

A second complication with the shot - station layout was that stations and shots were on areas of differing structures and,, in particular, it was apparent that the

Moho velocity in Rockall Trough was probably higher than that on the shelf. However, the shelf part of the path could be reasonably estimated from results obtained from shots fired on the shelf, and discussed in Chapter 4. The travel-times and distances of the Trough shots were therefore corrected for the fixed parts of their paths by subtracting the distance from the station to the supposed continental margin and the time taken to travel such a distance, at a velocity of 8.01 km sec^{-1}, from each observed distance and travel-time.

The continent ocean boundary was assumed to lie at the foot of the slope in Rockall Trough, as evidenced in reflection work by Roberts (1975b) and others. The shot K1 was fired close to the foot of the slope and therefore the corrected distance was quite small and the corrected travel-time effectively fixed the time-term for K1 independently of the velocity beneath the Moho.

The least-squares velocity of 8.20 ± 0.17 km sec^{-1} is poorly defined and for this reason sets of time-terms for three different sub-Moho velocities are tabulated in Table 5.4 and interpreted in Figure 5.12. It is important to note the small size of the 95 per cent confidence limits in Table 5.4 and Figure 5.12 as they show the degree of internal consistency of the data and confirm that the changes of time-terms from shot to shot are quite real and not functions of large errors.

The significance of the least-squares velocity for the upper mantle is difficult to assess. The determination of the velocity is itself subject to large confidence limits

Table 5.4 P_n time-terms for the least-squares velocity of 8.2 km sec^{-1} and two constrained velocities.

Shot	N	Time-term			95% conf.
		V = 8.0	V = 8.2	V = 8.4	
K1	8	3.97	3.97	3.98	0.09
K2	16	3.51	3.53	3.57	0.05
K3	14	3.79	3.83	3.91	0.06
K4	16	3.50	3.55	3.65	0.05
K5	11	3.43	3.50	3.64	0.06
K6	12	3.80	3.89	4.06	0.06
K7	12	3.41	3.52	3.73	0.06
K9	3	3.05	3.19	3.46	0.24
K11	3	3.49	3.66	4.00	0.23
K12	8	3.04	3.23	3.59	0.08
K14	6	3.01	3.24	3.69	0.11
L9	2	3.54	3.61	3.76	0.48
L10	5	4.22	4.30	4.45	0.14
L11	3	4.28	4.39	4.61	0.25
Av. K2 - K14		3.40	3.51	3.73	
Av. L9 - L11		4.01	4.10	4.27	

N is the number of observations of each time-term.

but if the value of 8.2 km sec^{-1} is accepted, it can be explained in several ways. Firstly, normal upper mantle material of 8.0 km sec^{-1} velocity may underlie the Moho which is dipping at a few degrees to the east. Secondly, high velocities for the upper mantle might be quite normal for this area since Smith (1974) determined a reversed velocity of 8.27 km sec^{-1} beneath the Faeroe-Shetland Channel and Scrutton (1971) has reported an unreversed velocity of 8.2 km sec^{-1} beneath Rockall Plateau. Finally, if Rockall Trough is oceanic, and similar in structure to other oceanic areas, a degree of anisotropy of the upper mantle velocity might be expected (Raitt et al., 1969; Bamford and Crampin, 1977). The observation scheme of HMSP is broadly at right angles to the postulated spreading axis in the Trough and would probably show velocities a few per cent greater than those along the Trough. Although not a well controlled experiment, the refraction line E10 of Ewing and Ewing (1959) can be interpreted as a Moho at 14 km depth and an upper mantle velocity of 8.0 km sec^{-1} which may suggest lower velocities along the axis of the Trough.

The lack of reversal and poor offset stations make a choice between these alternatives difficult. The K shots observed at Lagg have an apparent velocity of 8.09$\pm$0.06 km sec^{-1} (Figure 4.12) which is significantly lower than the apparent velocities observed by the in-line stations, and probably precludes the second alternative of simply high velocity upper mantle. The observed minus calculated residuals derived from the time-term solution show systematic variations with distance only for the Lagg recordings which supports the inference that the apparent velocity beneath the Trough is lower in the south-easterly direction than in the easterly direction.

Before the time-terms can be interpreted in terms of the thickness of a crustal layer they must be corrected for the delaying effects of the layers above such a layer and the advancing effect of being fired below sea level. The velocity contrast between the water and the sub-Moho material is large and the size of the delay in the water is very close to the one-way travel-time through the water. This is also true, to a large extent, for sediments of a velocity of less than about 3 km sec^{-1}. This means that the delay caused by sediments can be estimated directly from the two-way travel-time on adjacent reflection profiles without the need to assume a velocity for the sediments. Table 5.5 gives the water and shot depth corrections and the one-way travel-time to the base of sediments given in the contour map of Roberts (1975b) and the total correction to be applied to the P_n time-terms. For reasonable values of sub-Moho and sedimentary velocities the size of the correction to the P_n time-terms is almost independent of the exact values chosen.

Small scale refraction observations in Rockall Trough and the Faeroe-Shetland Channel, reviewed in Chapter 1, have revealed two 'basement' refractors with velocities of 4.9 and 6.2 km sec^{-1} (Hill, 1952; Ewing and Ewing, 1959; Smith, 1974). The 4.9 km sec^{-1} layer has a thickness of between about 2 and 4 km and may represent oceanic layer 2 basalts.

Table 5.5 Corrections to P_n time-terms for water and sedimentary delay.

Shot	Water depth (km)	Water 1-way time (sec)	Sediment 1-way time (sec)	Sediment thickness at 3 km sec^{-1} (km)	Total P_n correction for sediments (sec)
K1	1.82	1.21	0.65	1.95	1.80
K2	1.95	1.30	0.80	2.40	2.04
K3	2.05	1.37	0.90	2.70	2.21
K4	2.07	1.38	0.90	2.70	2.22
K5	2.08	1.39	0.92	2.76	2.25
K6	2.07	1.38	0.95	2.85	2.27
K7	2.01	1.34	0.95	2.85	2.23
K9	1.96	1.31	0.95	2.85	2.20
K11	1.87	1.25	0.92	2.76	2.11
K12	1.71	1.14	0.90	2.70	1.98
K14	1.70	1.13	0.65	1.95	1.72
L9	1.46	0.97	0.75	2.25	1.66
L10	1.41	0.94	0.75	2.25	1.63
L11	1.36	0.91	0.75	2.25	1.60

This velocity could also represent consolidated sedimentary rocks but in either case the P_n time-terms will need correcting for their delaying effect.

The corrected time-terms can then be interpreted in terms of the thickness of a crustal layer assuming the velocity of such a layer is known. In this experiment no direct estimate of the average crustal velocity was possible and so a range of suitable values was chosen from previous work. A velocity of 6.2 km sec^{-1} is observed for the Rockall Trough 'basement' in Section 5.5 and this was used as a minimum estimate for the crustal velocity. A velocity of about 6.5 km sec^{-1} may be considered as a more realistic estimate for the whole crust and was used as a maximum estimate. These two values of average crustal velocity were used to obtain estimates of crustal thicknesses for a variety of upper crustal structures.

Figure 5.12 shows the time-terms obtained from the least-squares velocities of P_1 and P_n, together with their 95 per cent confidence limits. Also shown is a set of crustal models derived from the seismic reflection data of Roberts (1975b) and an interpretation of the three sets of time-terms of Table 5.4. The average crustal velocity used in this Figure is 6.2 km sec^{-1}. Using a higher value of 6.5 km sec^{-1} would increase the estimates of crustal thickness by about 2 km.

The thicknesses calculated from the shot time-terms have been plotted beneath the shots in Figure 5.12 but, in fact, the time-terms apply to points on the refractor offset some 20 to 30 km to the east of the shots. This presents

Figure 5.12 P and P time-terms and interpreted crustal structure in Rockall Trough. Error bars are 95% confidence limits. Model A uses 8.0, B uses 8.2 and C uses 8.4 km sec^{-1} for the sub-Moho velocity.

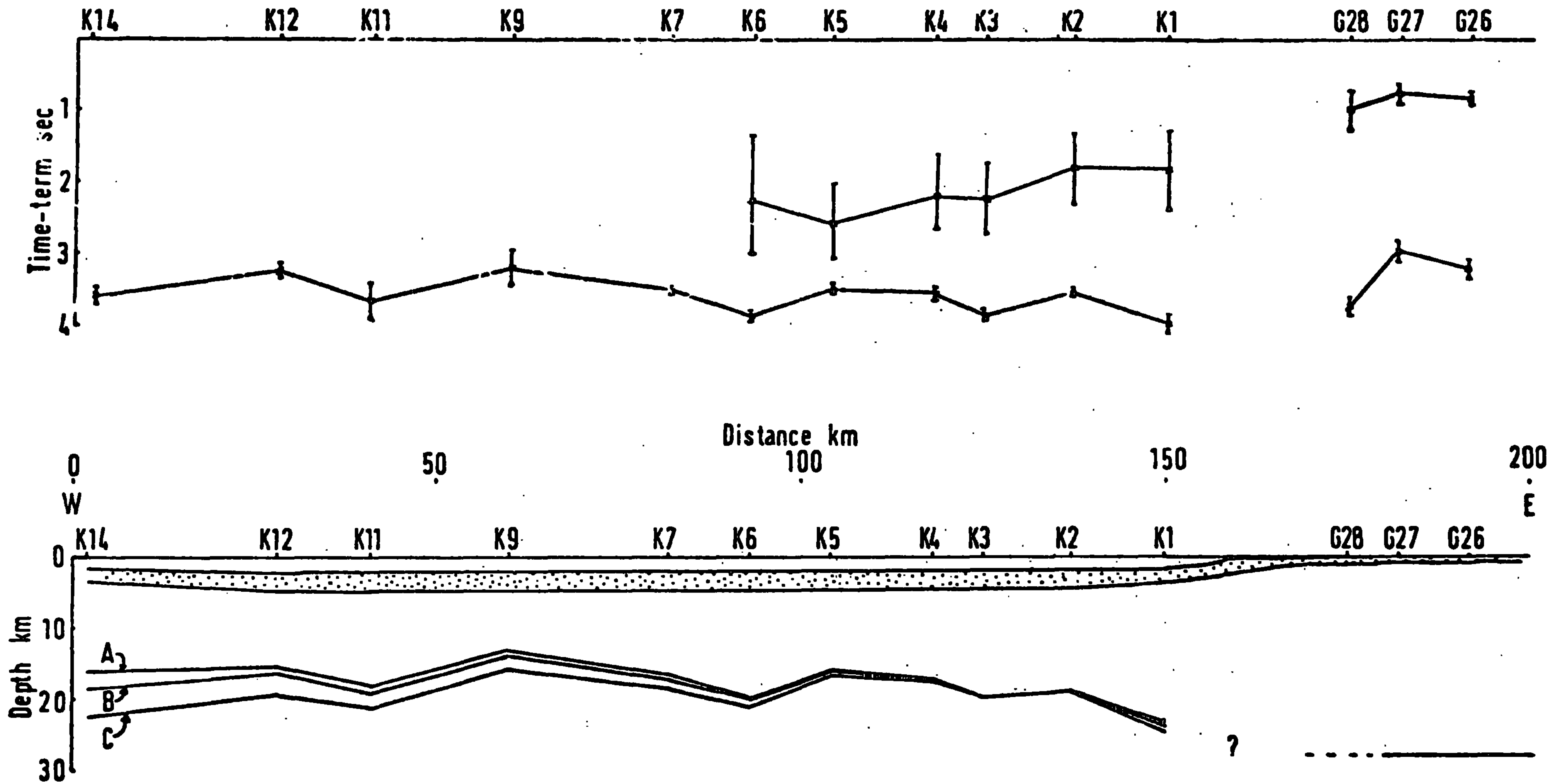

a possible explanation for the large value of the K1 time-term since this shot is so close to the continental margin.

The variability of the P_n time-term has been shown to be a well defined feature and in Figure 5.12 has been assumed to be caused by variations in Moho depth. It is most unlikely that this is strictly true and a more probable explanation lies in a variation of the sediment thickness hinted at in the P_1 time-term analysis of Section 5.5. However, because of the poor definition of the P_1 time-terms it was not felt reasonable to try to correct the P_n time-terms for anything other than a smooth sediment/basement interface.

Figure 5.13 shows three models of the average crustal structure for the region of Rockall Trough at 58° N and, for comparison, a typical oceanic crustal structure is shown. The model (a) is derived from the sedimentary structure shown on reflection profiles and gives an absolute maximum estimate of Moho depth of 20.4 km. Model (b) includes a 2 km thick layer of velocity 5.0 km sec^{-1} beneath the sediments which is introduced on the basis of the small scale refraction evidence. Model (c) is derived using the sediment and upper crustal structure shown by the refraction line E11 of Ewing and Ewing (1959). This model gives a smaller depth to Moho of about 13.6 km with the thickness of the main crustal layer about 7.0 km. Each model includes the Moho depth calculated for a crustal layer with a lower velocity of 6.2 km sec^{-1}. Models (b) and (c) are probably the best approximations and show a crustal layer between $1\frac{1}{2}$ and 2 times thicker than the average oceanic crustal layer.

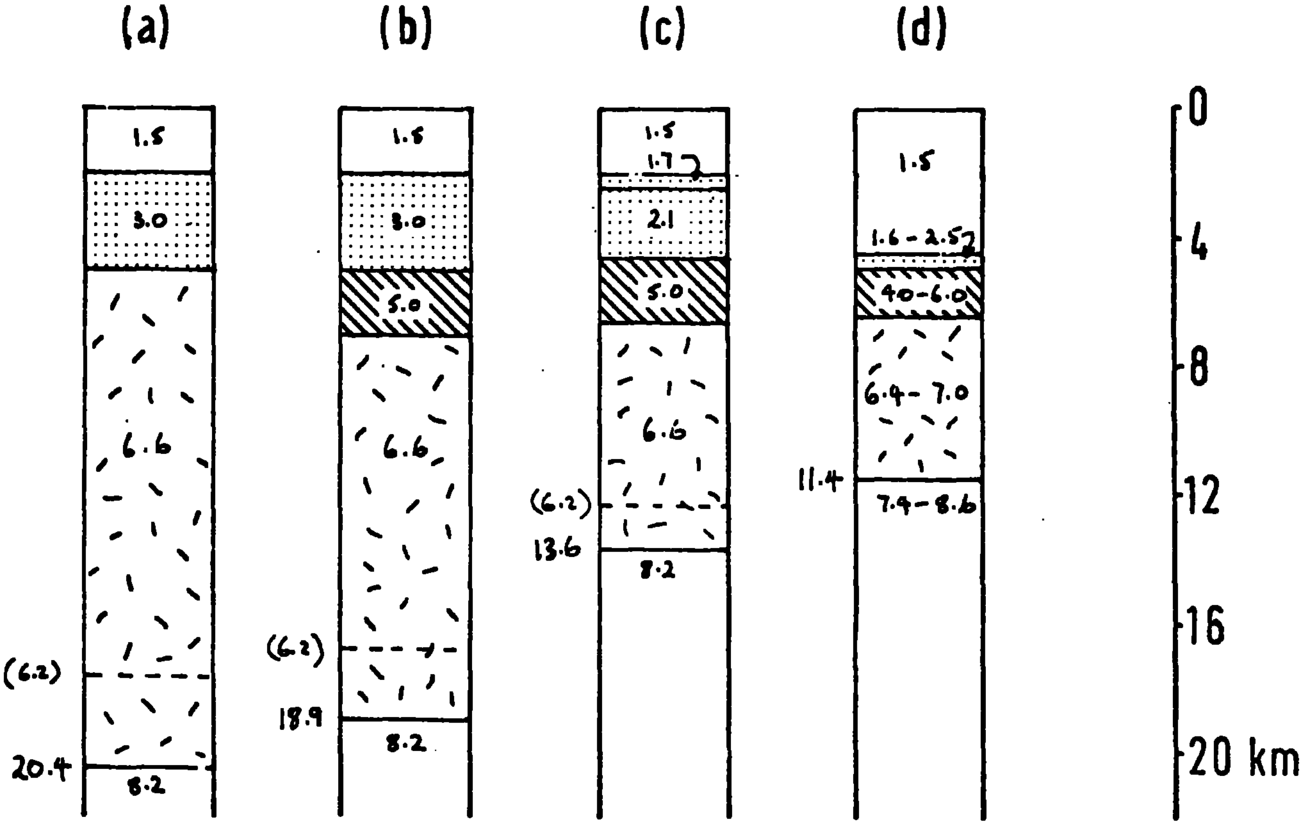

Figure 5.13 Three models of crustal structure in Rockall Trough at 58° N for average of K2 to K14 time-terms, in comparison with typical oceanic structure. Model (a) uses sediment structure from seismic reflection profiles, (b) includes 2 km of 5.0 km sec^{-1} material (oceanic layer 2?), (c) uses sediment and upper crustal structure of line E11 of Ewing and Ewing (1959), (d) is an average oceanic crustal structure. The Moho depth for a 6.2 km sec^{-1} crustal layer is shown as a dashed line.

The Trough is also different in the large thickness of sediments deposited since spreading, but this may be accounted for by the proximity of a ready supply of terrigenous sediments from the British Isles.

The values of the three time-terms in the north Rockall Trough, near Rosemary Bank (L9, L10 and L11) are considerably higher than those of the 58° N shots. Unfortunately, control of the sedimentary delay to the north-east of Rosemary Bank is poor and a value of about 1.5 seconds has been chosen as a best estimate of the travel-time. The water depth is also less beneath these shots and therefore a substantially smaller correction to the P_n time-term for sediment and water delay is required. Figure 5.14 shows four models of the crustal structure derived from the average of the three time-terms and using differing upper crustal constraints. Model (a) uses the observed sediment plus a layer of 5.0 km sec^{-1} material 2 km thick (representing oceanic layer 2?) and gives a Moho depth of 29.5 km. Model (b) uses the sedimentary structure of Ewing and Ewing (1959) E11 plus 2 km of 5.0 km sec^{-1} material and gives an estimate of 23.8 km for the depth to Moho. It has been suggested that a lava sequence may form the observed acoustic basement in the northern parts of the Trough and may mask an underlying sedimentary succession (H. Peacock, personal communication). Model (c) shows this possibility and gives a Moho depth of 19.7 km. Finally, the time-term of L9 is about 0.7 seconds less than those for L10 and L11 and it seems likely that changing sedimentary thicknesses are responsible for such a large

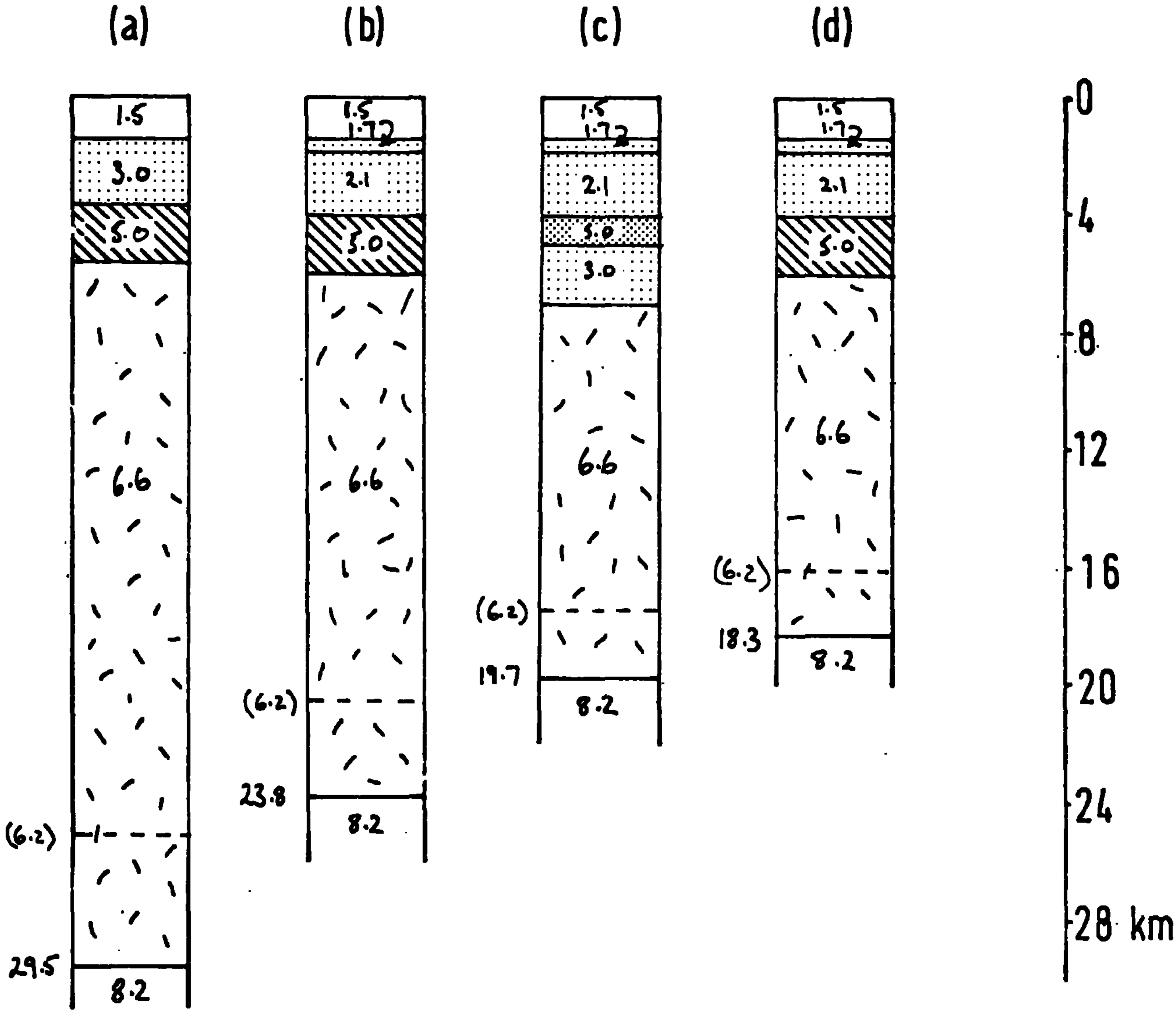

Figure 5.14 Four models of crustal structure in Rockall Trough north-east of Rosemary Bank. Models (a), (b) and (c) are for average of L9, L10 and L11 time-terms and model (d) interprets L9 time-term only. Model (a) uses sediment structure from seismic reflection profiles and 2 km of 5.0 km sec material. Model (b) uses sediment and upper crustal structure of line E11 of Ewing and Ewing (1959). Model (c) assumes 2 km of sediment beneath a masking layer of lavas. Model (d) uses Ewing and Ewing (1959) E11 structure for L9 time-term. The Moho depth for a 6.2 km sec^{-1} crustal layer is shown as a dashed line.

change over a small distance. Model (d) shows this possibility and interprets the L9 time-term, using the E11 sedimentary and upper crustal structure, as a Moho depth of 18.3 km. A depth to Moho of between about 18 and 24 km is most probable with the crustal layer being about 12 to 18 km thick.

Gravity interpretations by Himsworth (1973) were used to suggest a northward crustal thickening in the Trough from 11 km Moho depth at 58° N to 20 km at 59° $30'$ N. Such a magnitude for the thickening agrees well with the values presented here of about 13 km for the K shots and 21 km for the L shots.

Results from NASP in the Faeroes-Shetland Channel have shown a crustal layer of 6.5 km sec^{-1} thickening from 15 km in the northern part of the channel to 21 km in the southern part (Smith, 1974). This is of the same order and scale as the crustal thickening suggested for Rockall Trough by both seismic and gravity evidence and confirms the tendency for thickened crust towards the Wyville-Thompson Ridge.

5.7 Summary

The foregoing analysis has, of necessity, made certain assumptions about the upper crustal structure of the Rockall Trough area in order that estimates of the Moho depth could be made. The following limits can be placed on the structure:

(1) The "basement" in the Trough has a velocity of about 6.2 km sec^{-1} and lies beneath a variable layer of sediments, about 3 km thick near 58° N, and a 4.9 km sec^{-1} layer, not observed in this experiment but

shown to be present in earlier refraction profiles. The "basement" topography, or sediment thickness, changes by the order of 1.5 km over a distance of 10 km. Further north, near the L shots, a similar variation is probable.

(2) The Moho beneath the Trough is probably at a depth of between 13.6 and 18.9 km at 58^{o} N with the minimum value possibly being more likely. The sub-Moho velocity is 8.2 ± 0.17 km sec^{-1} when measured at right angles to the axis of the Trough and when measured in a more southerly direction, at Lagg, is about 8.09 ± 0.6 km sec^{-1}. Such observations are consistent with the existence of upper mantle anisotropy but cannot serve to demonstrate that this is the case.

(3) The crustal thickness, further north in the Trough, beneath the L shots is considerably larger than that at 58^{o} N. A depth to Moho of between about 18 and 24 km is possible although the lower value may be more likely as it has been calculated using a more realistic estimate of the sedimentary delay effect.

CHAPTER 6

SUMMARY AND DISCUSSION OF THE REGIONAL STRUCTURE OF THE HEBRIDEAN MARGIN

6.1 Introduction

An outline of the current state of the understanding of the structure of the Hebridean Margin and adjacent areas has been given in Chapter 1. The aims of HMSP were stated and the subsequent chapters presented details of the results. The following sections discuss the relevance of these results to hypotheses concerning the structure and formation of the Hebridean Margin, and the adjacent shelf and Scottish Mainland.

6.2 The north Scottish Mainland and continental shelf

The results of long range seismic observations on the shallow shelf areas complement gravity and magnetic anomaly measurements and the results of seismic reflection and small scale refraction work already performed. A generally thin, but variable, sediment cover is shown in the sea areas with several sedimentary basins developed. The largest of these basins is the South Minch Basin which contains at least three km of Permo-Triassic and Jurassic rocks deposited in an actively subsiding basin bounded to the north-west and north-east by normal faults (Smythe et al., 1972; Hall and Smythe, 1973; Steel, Nicholson and Kalander, 1975). The Minch fault forms the north-west margin of this basin and is also a bounding fault for the North Minch Basin. The

G line in the Minch was fired along a north-westerly trending ridge of Torridonian which separates the two Minch basins. The depth to the basement along this line is about 2 km but shows local variations which correlate well with the short wavelength component of the Bouguer gravity anomalies.

The sediments in the smaller Outer Hebrides Basin are between about 1 and 3 km thick, depending on the assumptions made concerning the density and velocity of the fill, and it is probably bounded to east and west by north-north-easterly trending normal faults. Each of the three basins shows alignment in a north-north-easterly direction, with their bounding faults trending sub-parallel to the Rockall Trough margin. The genetic relationship between these basins and the Rockall Trough is unclear since, firstly, similar basins closer to Rockall Trough appear to be absent, except for the 20 km adjacent to the shelf break where there is evidence of thickening sediments. Secondly, some of the basins, noteably the South Minch Basin, have important north-westerly trending faulted margins (Hall and Smythe, 1973), a direction at right angles to the trend of the north-easterly faults and Rockall Trough. Detailed, good quality seismic reflection data close to the margin is needed to clarify the sub-Tertiary structure in this area.

The velocities of the Lewisian gneiss are everywhere about 6.1 km sec^{-1} even over the areas of outcropping or subcropping Scourian granulites, where velocities of about 6.5 km sec^{-1} might be expected if these rocks represent lower crustal material as suggested by Smith and Bott (1975). Even more suprising is the lack of evidence for a mid-crustal refractor, comparable to the 6.5 km sec^{-1} refractor observed to the north of the present area during NASP (Smith, 1974), within the top 10 km of the crust. There is slim evidence for a deep reflector on the outer shelf west of Lewis at a depth of about 18 km but refractions from this interface were not observed.

The suggested velocity increase with depth, in the upper parts of the crust, can be shown to be of a comparable magnitude to the observed changes of velocity with pressure of some granulites reported by Christensen and Fountain (1975). The rapid increase of velocity at shallow depth is caused by crack closure and expulsion of pore water as the pressure increases. At greater depths and pressures, the rate of velocity increase dies away and the velocity may even decrease as the effects of elevated temperature outweigh the effects of increasing pressure. The velocities observed over the granulite terrains of this part of Scotland are at the lower end of the range of possible values for granulites (Hall and Al-Haddad, 1976).

Lateral variations of the velocity of the Lewisian basement rocks are important in this area. On the outer shelf, between the Outer Hebrides Basin and St. Kilda, a region of high velocity material, which shows up strongly on the gravity and magnetic maps, causes negative P_g time-terms and low values of the observed P_n time-terms. Variations of the proportion of granitic material in the Lewisian gneiss across Lewis primarily affect the Bouguer anomaly (McQuillin and Watson, 1973) but also possibly cause large values of the observed P_n time-terms on the west coast of Lewis. Variations of the basement velocity beneath the South Minch Basin were recognised but cannot be adequately defined due to the large spacing of the shots compared to the size of the anomalous zones and lead to some apparent contradictions

The crustal structure beneath the Hebrides and the Hebridean shelf is fairly uniform with thickness of about 25 km maintained to within 20 km of Rockall Trough. Closer to the margin the interpretation of the P_n time-terms is ambiguous but does not seem to show any evidence of thinning. Steady values of the Bouguer anomaly until very close to the margin support the inference of a uniform crustal thickness across most of this region (Himsworth, 1973). Coupled with the observed thin sediments, this observation has important implications for the mode of formation of the Rockall Trough margin, for most continental margins exhibit thick sedimentary wedges and some degree of crustal thinning over a distance of the order of about 150 km.

The crust of the outer shelf region has a low average crustal velocity of about 6.2 km sec^{-1} thus suggesting a lower than average crustal density. This value for average crustal velocity is derived from an analysis of the Moho wide-angle reflection and is well defined since the reflection can be traced over a large distance range and its curvature measured accurately. The mainland region has more normal values of average crustal velocity of about 6.6 km sec^{-1} and thicknesses of about 30 km. At 58° N there is little difference found between the stations sited to the east and west sides of the Moine thrust. Caledonian foreland crust is likely to underlie a zone about 50 km wide to the east of the Moine thrust and it is possible that true Caledonian fold belt crust has not been sampled at 58° N. Further south, in the Grampian Highlands at Blair Atholl, the crust is about 10 km thicker than beneath the shelf area and the residual root of the Caledonides can be identified.

Several lines of evidence point towards an anomalous crustal structure beneath the Minch. Firstly, a Moho deepening, of the size suggested by a simple interpretation of the time-terms, is incompatible with the observed Bouguer anomaly, is opposite to the normally observed crustal thinning beneath sedimentary basins and would result in isostatic inequilibrium. Secondly, velocity anomalies in the upper parts of the basement are shown beneath the South Minch Basin by plus-minus analysis of the H line shots. Although the plus-minus analysis of the G line shots in the Minch showed a single velocity refractor, the waves descending to the Moho to be recorded at stations to the south, traverse the area of velocity anomalies. Thirdly, the agreement of the values of the P_n time-terms at GS1 and GS3 when measured in opposite directions, suggests that the time-terms cannot faithfully represent crustal thickness, but instead represent crustal velocity anomalies, for there should be large azimuthal variations in a region of such rapidly changing crustal thickness. It seems quite probable that most of the increase in the values of the time-terms towards the centre of the Minch can be attributed to a localised reduction of crustal velocity in the South Minch region. when the poor quality of the wide-angle reflection results in this region is taken into account.

Figure 6.1 shows a composite crustal structure profile derived from the known geology and the studies presented in this thesis.

Figure 6.1 Summary of geological structure across north-west Scotlanddand Hebridean Shelf. Figures are velocities in km sec^{-1}. OIT - Outer Isles Thrust, MT - Moine Thrust, GGF - Great Glen Fault.

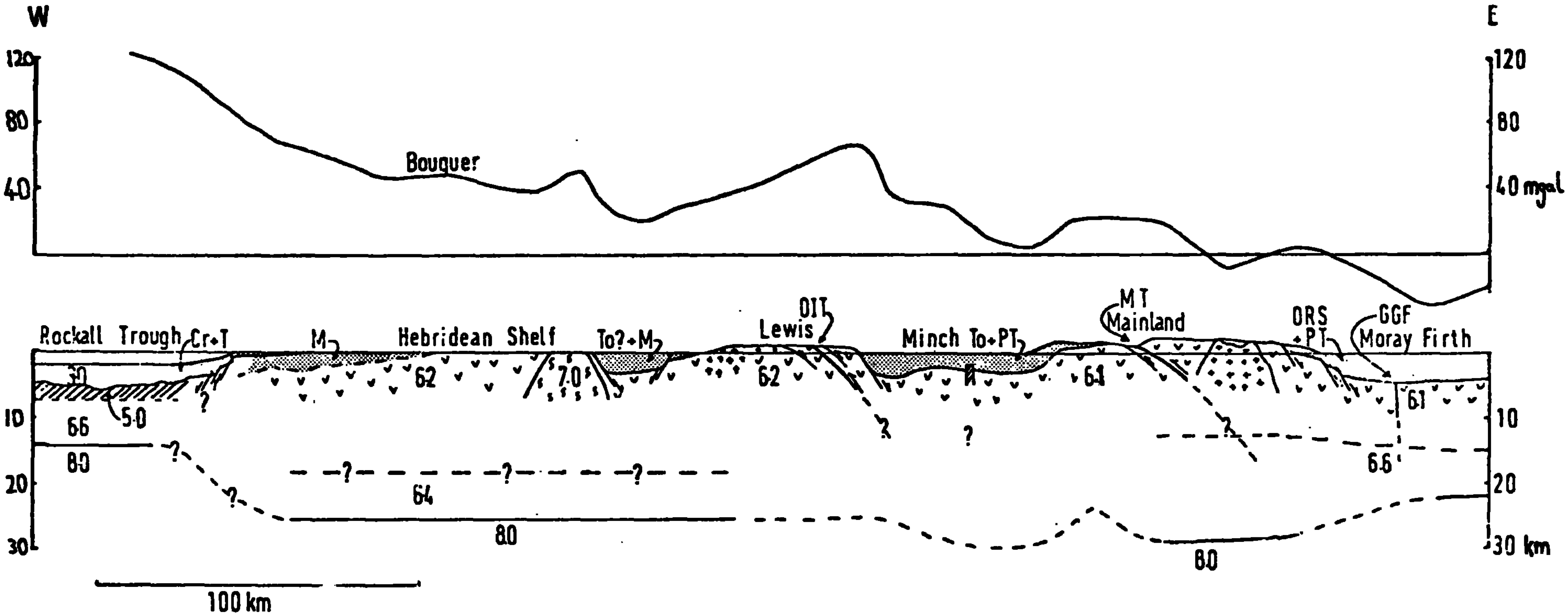

6.3 Rockall Trough

At 58° N, Rockall Trough contains at least 3 km of sediments beneath about 2 km of water. The 'basement', identified on reflection profiles, is extremely rough and gives rise to a series of parabolic reflections. Small scale refraction profiles give a velocity for this basement layer of about 4.9 km sec^{-1} (Hill, 1952; Ewing and Ewing, 1959; Scrutton, 1971; Smith, 1974) but the large scale observations reported in this thesis detect only a layer of velocity of about 6.2 km sec^{-1}. The thickness of the 4.9 km sec^{-1} layer is about 2 to 3 km in the southern part of Rockall Trough (Hill, 1952) and about 4 km in the Faeroes-Shetland Channel (Smith, 1974). It is possible that a layer of such a velocity corresponds to oceanic layer 2 basalts but the velocity is also compatible with consolidated sediments. Large changes of P_1 time-term reflect the rapidly varying thickness of sediments and possibly changing thickness of the 4.9 km sec^{-1} layer.

Estimates of Moho depth depend critically upon the assumed upper crustal structure in Rockall Trough. A minimum estimate of Moho depth, derived from the upper crustal structure of Ewing and Ewing (1959) line E11 and assuming 2 km of 4.9 km sec^{-1} material, is 13.6 km. A maximum depth to the Moho, assuming only the sediment structure seen on reflection profiles, is 20 km. The estimates of crustal thickness for the L shots to the north-east of Rosemary Bank are even more ambiguous, with a minimum depth to Moho of 18 km and a maximum of 31 km possible. The observed deepening northwards towards the Wyville-

Thompson Ridge supports the gravity interpretations by Himsworth (1973) which suggested a northward thickening from 11 to 19 km with an inferred depth to Moho of 25 km beneath the Wyville-Thompson Ridge itself. The Wyville-Thompson Ridge is an anomalous zone possibly formed in a similar manner to the Iceland-Faeroe Ridge during the splitting of Rockall Trough, or as a line of volcanic vents extruding lavas after the formation of the Trough (Himsworth, 1973).

6.4 The margins of Rockall Trough

The crustal structure of a zone 20 to 30 km wide on each side of the margin was difficult to determine due to the complicating effects of the margin itself. The transition from foreland type continental crust to oceanic crust takes place over this narrow zone of about 50 km width. Thin sediments on the continental side show that little subsidence has occured since spreading began.

Figure 6.2 shows a comparison of the Rockall Trough margin structure determined from this study with a more normal passive margin off the east coast of North America. The North American example is redrawn from Sheridan (1975) who presents a series of cross-sections compiled from a variety of sources. The major differences relate to the relative thickness of crust and sediments and the relative width of the transition zone from oceanic to continental crustal structure.

Any mechanism proposed for the formation of the

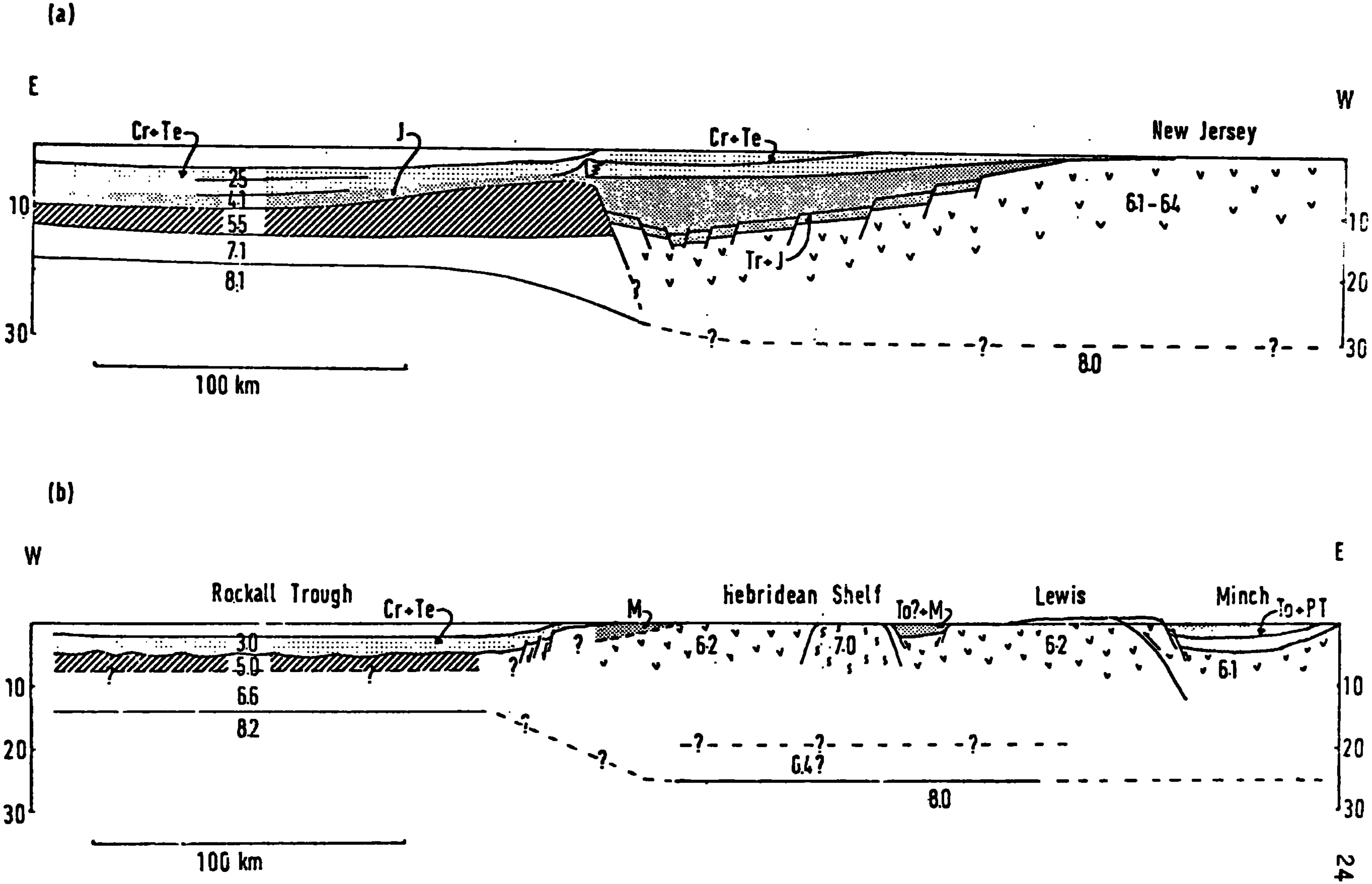

Figure 6.2 Comparison of Rockall Trough margin with a more typical Atlantic type continental margin off east coast of North America (redrawn from Sheridan, 1975). Figures are velocities in km sec^{-1}.

Rockall Trough margin must be able to account for the following unusual features:

(1) Uniform continental crustal thicknesses to within about 20 km of the margin.

(2) Oceanic crust in Rockall Trough slightly thicker than normal.

(3) An extremely strong attenuation of the continental crust which takes place beneath the slope. The slope itself shows some large normal faults (each of up to about 1 second two-way travel-time) downthrowing to the west, Tertiary, and probably Mesozoic strata (Stride et al., 1969; Roberts, 1975b).

(4) Lack of subsidence of the continental crust landward of the shelf break.

The three major hypotheses used to account for the subsidence history of a continental margin have been reviewed by Bott (1977b) who sets out the major points of each theory and suggests criticisms of each. The gravity loading hypothesis of Dietz (1963) and Walcott (1972) attributes subsidence to a load imposed by sediments and can account for sedimentary thicknesses of about 2 to 3 times the original water depth. However, large thicknesses of shallow water facies sediments exist on some shelves and on others subsidence has occurred without major sedimentation (Watts and Ryan, 1976; Montadert, 1977). This hypothesis can be successfully applied to the subsidence of original deep water areas, such as deltas, and can act as a secondary mechanism, amplifying subsidence generated by some other cause.

The thermal expansion hypothesis of Hsu (1965) and Sleep (1971) attributes uplift and subsidence to thermal events linked with the onset of splitting. Initial heating of the lithosphere in the region of the incipient split reduces crust and upper mantle densities with consequent isostatic uplift. As the split progresses, the continental margins move away from the heat source and cool, subsiding in an approximately exponential manner back to their original elevation, or deeper if erosion of the elevated region has taken place. However, such a mechanism can only explain broad regional subsidences and sediment thicknesses of 2 to 3 km and cannot explain the large local differential subsidence characteristic of some shelves. Metamorphism of the lower continental crust at the time of the split may increase its density and cause extra subsidence of the order of 3 to 4 km (Falvey, 1974).

The third hypotheses concerns the response of the continental crust to stress imposed by unequal loading across the margin. Bott and Dean (1972) have shown that the excess weight of the upper part of the continental crust, coupled with the bouyant effect of the lower parts of the crust, puts the continental crust into a state of horizontal tension perpendicular to the margin with large stresses concentrated in the top 15 km. They showed that stress differences of the order of about 400 bar can occur and may give rise to failure of the brittle upper crust by normal faulting and graben formation with oceanward flow, by steady-state creep, of the viscous lower crustal material (Bott, 1971). Such a mechanism accounts for crustal thinning close to the margin which can lead to broad isostatic subsidence amplified by sediment loading. The process is temperature dependent with higher temperatures enabling flow over a wider area and, consequently, the area affected by subsidence can vary in both horizontal and vertical extent.

The structure of the Rockall Trough margin, as determined in this study, cannot be unequivocally attributed to any of the three mechanisms. The narrow transition from continental to oceanic structure and the lack of subsidence of fault bounded basins on the continental side of the margin suggest that a narrow, cool zone was involved in the split. A large scale domal uplift, similar to the present-day East African domes, may not have occurred since any subsequent subsidence cannot be identified.

6.5 Outstanding problems and criticism of HMSP

HMSP was generally quite successful but its aims were not fully realised due to a reduction of the quantity of data recovered. The variety of azimuthal coverage on the shelf area and in Rockall Trough was severely limited by the withdrawal of the Royal Navy and inadequate performance of the receiving ship.

In modern explosion seismology the trend is towards very closely spaced observations which enable even short-lived phases to be traced accurately and their variation of amplitude and frequency to be well defined. In this way a model of crustal structure showing more detail than a one or two layer crust can be produced. In such studies care must be taken to minimise equipment variability and maintain as constant as possible the characteristics of the shots. This will mean careful selection of shot points and charge sizes to give the desired frequency content.

Obviously, the most outstanding problems relate to the crustal structure beneath the Minch and the exact details of structure at the Rockall Trough margin. The structure beneath the Minch is shown to be related to velocity anomalies within the crust and a wide azimuthal coverage at a variety of ranges is really required to finally resolve the difficult problem of the Moho structure. The importance of just one station offset at P_n range to the side of a shot line is clearly deomonstrated by this study. Small, closely spaced shots would be very helpful in determining the exact form of the lateral velocity variations beneath the South Minch and between St. Kilda and the Outer Hebrides Basin.

A good quality reflection profile across the continental margin at 58° N and into Rockall Trough would allow a more accurate sedimentary delay correction to be applied to the Rockall Trough data. Small scale reversed refraction lines in the Trough could provide better control on the upper crustal structure and larger scale observations along the axis of the Trough might produce convincing evidence of velocity anisotropy of the oceanic upper mantle in this area. The use of sonobuoys, or, preferably, seabed seismometers, would necessarily form a vital part of any such investigations.

The structural variation of the continental margin must be investigated using a set of reversed refraction profiles parallel to the margin as well as profiles at right angles to it. The proper understanding of margin structure is one of the most interesting geotectonic problems. This margin forms a good candidate for investigation because of the thin sediments. However, it must be realised that by its very ease of observation the Rockall Trough margin shows itself to be atypical of Atlantic-type continental margins.

REFERENCES

AGGER, H.E., & CARPENTER, E.W., 1965. A crustal study in the vicinity of the Eskdalemuir seismological array station. Geophys. J. R. astr. Soc. **9**, 69-83.

ALLERTON, H.A., 1968. An interpretation of the gravity of the North Minch, Scotland. M.Sc. thesis, University of Durham.

BAILEY, R.J., GRZYWACZ, J.M., & BUCKLEY, J.S., 1974. Seismic reflection profiles of the continental margin bordering the Rockall Trough. J. geol. Soc., Lond. **130**, 55-69.

BAMFORD, D., 1973. Refraction data in Western Germany; a time-term interpretation. J. Geophys.- Z. Geophys. **39**, 907-927.

BAMFORD, D., & BLUNDELL, D.J., 1971. South-west Britain continental margin experiment. In The geology of the East Atlantic continental margin (Ed DELANY, F.M.) **2**, Inst. geol. Sci. Rep. No. 70/14, 143-156.

BAMFORD, D., & CRAMPIN, S., 1977. Seismic anisotropy - the state of the art. Geophys. J. R. astr. Soc. **49**, 1-8.

BAMFORD, D., FABER, S., JACOB, B., KAMINSKI, W., NUNN, K., PRODEHL, C., FUCHS, K., KING, R., & WILLMORE, P., 1976. A Lithospheric Seismic Profile in Britain - I preliminary results. Geophys. J. R. astr. Soc. **44**, 145-160.

BERRY, M.J., & WEST, G.F., 1966. A time-term interpretation of the first-arrival data of the 1963 Lake Superior experiment. In The Earth beneath the continents (Eds STEINHART, J.S., & SMITH, T.J.) 166-180, American Geophysical Union.

BINNS, P.E., McQUILLIN, R., FANNIN, N.G.T., KENOLTY, N., & ARDUS, D.A., 1975. Structure and stratigraphy of sedimentary basins in the Sea of the Hebrides and the Minches. In Petroleum and the continental shelf of North-West Europe (Ed WOODLAND, A.W.) **1**, 93-102, Appl. Sci.

BIRTHILL, J.W., & WHITEWAY, F.E., 1965. The application of phased arrays to the analysis of seismic body waves. Phil. Trans. R. Soc. **A258**, 421-493.

BLUNDELL, D.J., & PARKS, R., 1969. A study of the crustal structure beneath the Irish Sea. Geophys. J. R. astr. Soc. **17**, 45-62.

BOMFORD, G., 1962. Geodesy, 2nd Ed, O.U.P., 561pp.

BOTT, M.H.P., 1971. Evolution of young continental margins and formation of shelf basins. Tectonophysics 11, 319-327.

BOTT, M.H.P., 1975. Structure and evolution of the North Scottish shelf, the Faeroe block and the intervening region. In Petroleum and the continental shelf of North-West Europe (Ed WOODLAND, A.W.) 1, 105-115, Appl. Sci.

BOTT, M.H.P., 1977. The origin and development of the continental margin between the British Isles and South-Eastern Greenland. Geol. J. (in the press).

BOTT, M.H.P., 1977b. Subsidence mechanisms at passive continental margins. Am. Ass. Petrol. Geol. Special Vol. (in the press).

BOTT, M.H.P., & DEAN, D.S., 1972. Stress systems at young continental margins. Nature (Phys. Sci.), Lond. 235, 23-25.

BOTT, M.H.P., BROWITT, C.W.A., & STACEY, A.P., 1971. The deep structure of the Iceland-Faeroe Ridge. Mar. Geophys. Res. 1, 328-351.

BOTT, M.H.P., HOLLAND, J.G., STORRY, P.G., & WATTS, A.B., 1972. Geophysical evidence concerning the structure of the Lewisian of Sutherland, N.W. Scotland. J. geol. Soc., Lond. 128, 599-612.

BOTT, M.H.P., NIELSEN, P.H., & SUNDERLAND, J., 1976. Converted p-waves originating at the continental margin between the Iceland-Faeroe ridge and the Faeroe block. Geophys. J. R. astr. Soc. 44, 229-238.

BOTT, M.H.P., SUNDERLAND, J., SMITH, P.J., CASTEN, U., & SAXON, S., 1974. Evidence for continental crust beneath the Faeroe Islands. Nature, Lond. 248, 202-204.

BOTT, M.H.P., & WATTS, A.B., 1971. Deep structure of the continental margin adjacent to the British Isles. In The geology of the East Atlantic continental margin (Ed DELANY, F.M.) 2, Inst. geol. Sci. Rep. No. 70/14, 89-109.

BOWES, D.R., 1968. An orogenic interpretation of the Lewisian of Scotland. In Report of the 23rd session of the International Geological Congress, Czechoslovakia, Proceedings of Section 4, Geology of Pre-Cambrian, 225-236.

BRAILE, L.W., & SMITH, R.B., 1974. Guide to the interpretation of crustal refraction profiles. Geophys. J. R. astr. Soc. 40, 145-176.

BROWITT, C.W.A., 1971. Seismic refraction investigation of deep sedimentary basin in the continental shelf west of Shetlands. Nature, Lond. 236, 161-163.

BULLARD, E., EVERETT, J.E., & SMITH, A.G., 1965. The fit of the continents around the Atlantic. Phil. Trans. R. Soc. A258, 41-51.

CASTEN, U., & NIELSEN, P.H., 1975. Faeroe Island - a microcontinental fragment? J. Geophys. 41, 357-366.

ČERVENÝ, V., 1966. On dynamic properties of reflected and head waves in the n-layered Earth's crust. Geophys. J. R. astr. Soc. 11, 139-147.

CHESHER, J.A., DEEGAN, C.E., ARDUS, D.A., BINNS, P.E., & FANNIN, N.G.T., 1972. IGS marine drilling with m.v.Whitethorn in Scottish waters 1970-1971. Inst. geol. Sci. Rep. No. 72/10.

CHRISTENSEN, N.I., & FOUNTAIN, D.M., 1975. Constitution of the lower continental crust based on experimental studies of seismic velocities in granulite. Bull. Geol. Soc. Am. 86, 227-236.

CLAERBOUT, J.F., 1976. Fundamentals of geophysical data processing, McGraw Hill, 352pp.

COLLETTE, B.J., 1968. On the subsidence of the North Sea area. In Geology of shelf seas (Ed DONOVAN, D.T.) 15-30, Oliver and Boyd,

COWARD, M.P., FRANCIS, P.W., GRAHAM, R.H., & WATSON, J., 1970. Large-scale Laxfordian structures of the Outer Hebrides in relation to those of the Scottish Mainland. Tectonophysics 10, 425-435.

CRAMPIN, S., JACOB, A.W.B., MILLER, A., & NEILSEN, G., 1970. The LOWNET radio-linked seismometer network in Scotland. Geophys. J. R. astr. Soc. 21, 207-216.

DAVYDOVA, N.I., 1972. Possibilities of the DSS technique in studying properties of deep-seated seismic interfaces. In Seismic properties of the Mohorovicic discontinuity (Ed DAVYDOVA, N.I.) 4-22, Israel Program for Scientific Translations.

DEARNLEY, R., 1962. An outline of the Lewisian complex of the Outer Hebrides in relation to that of the Scottish Mainland. Q. J. geol. Soc. Lond. 118, 143-176.

DEWEY, J.F., & BIRD, J.M., 1970. Mountain belts and the new global tectonics. J. geophys. Res. **75**, 2625-2647.

DIETRICH, G., & ULRICH, J., 1961. On the topography of the Anton Dohrn seamount. Kieler Meeresforsch. **17**, 3-7.

DIETZ, R.S., 1963. Collapsing continental rises: an actualistic concept of geosynclines and mountain building. J. Geol. **71**, 314-333.

DOBRIN, M.B., 1960. Introduction to geophysical prospecting, 2nd Ed, McGraw Hill, 446pp.

EWING, J., & EWING, M., 1959. Seismic-refraction measurements in the Atlantic Ocean basins, in the Mediterranean Sea, on the Mid-Atlantic ridge, and in the Norwegian Sea. Bull. Geol. Soc. Am. **70**, 291-318.

FALVEY, D.A., 1974. The development of continental margins in plate tectonic theory. J. Aust. Pet. Explor. Assoc. **14**, 95-106.

FUCHS, K., 1975. Synthetic seismograms of PS-reflections from transition zones computed with the reflectivity method. J. Geophys. **41**, 445-462.

HAGEDOORN, J.G., 1959. The plus-minus method of interpreting seismic refraction sections. Geophys. Prospect. **7**, 158-182.

HALL, J., & AL-HADDAD, F.M., 1976. Seismic velocities in the Lewisian metamorphic complex, northwest Britain - 'in situ' measurements. Scott. J. Geol. **12**, 305-314.

HALL, J., & SMYTHE, D.K., 1973. Discussion of the relation of Palaeogene ridge and basin structures of Britain to the North Atlantic. Earth planet. Sci. Lett. (Neth.) **19**, 54-60.

HEEZEN, B.C., & FORNARI, D.J., 1975. Geological map of the Pacific Ocean. In LAUGHTON, A.S., BERGGREN, W.A. et al., Initial reports of the deep sea drilling project **30**, U.S. Government Printing Office, Washington.

HEIRTZLER, J.R., DICKSON, G.O., HERRON, E.M., PITMAN, W.C., & Le PICHON, X., 1968. Marine magnetic anomalies, geomagnetic field reversals and the motions of the ocean floors and continents. J. geophys. Res. **73**, 2119-2136.

HILL, M.N., 1952. Seismic refraction shooting in an area of the Eastern Atlantic. Phil. Trans. R. Soc. **A244**, 561-594.

HIMSWORTH, E.M., 1973. Marine geophysical studies between Northwest Scotland and the Faeroe plateau. Ph.D. thesis, University of Durham.

HOLDER, A.P., & BOTT, M.H.P., 1971. Crustal structure in the vicinity of South-west England. Geophys. J. R. astr. Soc. 23, 465-489.

HOLLAND, J.G., & LAMBERT, R. St.J., 1973. Comparative major element geochemistry of the Lewisian of the mainland of Scotland. In The early Precambrian of Scotland and related rocks of Greenland (Eds PARK, R.G., & TARVEY, J.) 51-62, Univ. of Keele.

HSU, K.J., 1965. Isostasy, crustal thinning, mantle changes and the disappearance of ancient land masses. Am. J. Sci. 263, 97-109.

HUDSON, J.D., 1964. The petrology of the sandstones of the Great Estuarine Series, and the Jurassic palaeogeography of Scotland. Proc. geol. Ass. 75, 499-527.

HYDROGRAPHIC DEPARTMENT, 1973. Free-air gravity maps No. 016 9GC and 016 10GC of the Hebridean shelf and the Minches.

INSTITUTE OF GEOLOGICAL SCIENCES, 1968. Aeromagnetic map of part of Great Britain and Northern Ireland. Sheet 12.

INSTITUTE OF GEOLOGICAL SCIENCES, 1972. Map of the Sub-Pleistocene geology of the British Isles and the adjacent continental shelf.

IRVING, E., & RUNCORN, S.K., 1957. Analysis of the palaeomagnetism of the Torridonian Series of North-west Scotland. I. Phil. Trans. R. Soc. A250, 83-99.

JACOB, A.W.B., 1970. Long range observations of underwater explosions. Proc. geol. Soc., Lond. 1662, 82-83.

JACOB, A.W.B., 1975. Dispersed shots at optimum depth - an efficient seismic source for lithospheric studies. J. Geophys. 41, 63-70.

JACOB, A.W.B., & BOOTH, D.C., 1977. Observations of PS reflections from the Moho. Geophys. J. R. astr. Soc. 49, 285.

JAMES, F., & ROOS, M., 1969. Minuit. A program to minimise a function of n variables, compute the covariance matrix, and find the true errors. Long write up. CERN Computer 6,000 Series Program Library.

JONES, E.J.W., EWING, M., EWING, J.I., & EITTREIM, S.L., 1970. Influences of Norwegian Sea overflow water on sedimentation in the Northern North Atlantic and Labrador Sea. J. geophys. Res. 75, 1655-1680.

JONES, E.J.W., RAMSAY, A.T.S., PRESTON, N.J., & SMITH, A.C.S., 1974. A Cretaceous guyot in the Rockall Trough. Nature, Lond. 251, 129-131.

KAMINSKI, W., BAMFORD, D., FABER, S., JACOB, B., NUNN, K., & PRODEHL, C., 1976. A Lithospheric Seismic Profile in Britain - II preliminary report on the recording of a local earthquake. J. Geophys. 42, 103-110.

KENT, P.E., 1975. The tectonic development of Great Britain and the surrounding seas. In Petroleum and the continental shelf of North-West Europe (Ed WOODLAND, A.W.) 1, 3-28, Appl. Sci.

LAUGHTON, A.S., BERGGREN, W.A. et al., 1972. Sites 116 and 117. In LAUGHTON, A.S., BERGGREN, W.A. et al. Initial reports of the deep sea drilling project 12, 395-457, U.S. Government Printing Office, Washington.

LONG, R.E., 1974. A compact portable seismic recorder. Geophys. J. R. astr. Soc. 37, 91-98.

MAGUIRE, P.K.H., 1974. The crustal structure of East Africa through earthquake seismology. Ph.D. thesis, University of Durham.

McCAMY, K., & MEYER, R.P., 1964. A correlation method of apparent velocity measurement. J. geophys. Res. 69, 691-699.

McQUILLIN, R., BACON, M., & BINNS, P.E., 1973. The Blackstones Tertiary igneous centre. J. geol. Soc., Lond. 129, 317.

McQUILLIN, R., & BINNS, P.E., 1973. Geological structure in the Sea of the Hebrides. Nature (Phys. Sci.), Lond. 241, 2-4.

McQUILLIN, R., & WATSON, J., 1973. Large-scale basement structures of the Outer Hebrides in the light of geophysical evidence. Nature (Phys. Sci.), Lond. 245, 1-3.

MILLER, J.A., MATTHEWS, D.H., & ROBERTS, D.G., 1973. Rock of Grenville age from Rockall bank. Nature (Phys. Sci.), Lond. 246, 61.

MONTADERT, L., ROBERTS, D.G., AUFFRET, G.A., BOCK, W., Du PEUBLE, P.A., HAILWOOD, E.A., HARRISON, W., KAGAMI, H., LUMSDEN, D.N., MULLER, C., SCHNITKER, D., THOMPSON, R.W., THOMPSON, T.L., & TIMOFEEV, P. P., 1977. Rifting and subsidence on passive continental margins in the North East Atlantic. Nature, Lond. 268, 305-309.

MOORBATH, S., 1969. Evidence for the age of deposition of the Torridonian sediments of North-West Scotland. Scott. J. Geol. 5, 154-170.

MOORBATH, S., & WELKE, H., 1969. Isotopic evidence for the continental affinity of the Rockall Bank, North Atlantic. Earth planet. Sci. Lett. (Neth.) 5, 211-216.

NUTTLI, O., 1961. The effect of the Earth's surface on the S wave particle motion. Bull. Seis. Soc. Am. 51, 237-246.

PARK, R.G., 1970. Observations on Lewisian chronology. Scott. J. Geol. 6, 379-399.

PHILLIPS, W.E.A., STILLMAN, C.J., & MURPHY, T., 1976. A Caledonian plate tectonic model. J. geol. Soc., Lond. 132, 579-609.

RAITT, R.W., SHOR, G.G., FRANCIS, T.J.G., & MORRIS, G.B., 1969. Anisotropy of the Pacific upper mantle. J. geophys. Res. 74, 3095-3109.

RIDDIHOUGH, R.P., & MAX, M.D., 1976. A geological framework for the continental margin to the west of Ireland. Geol. J. 11, 109-120.

ROBERTS, D.G., 1975a. Tectonic and stratigraphic evolution of the Rockall Plateau and Trough. In Petroleum and the continental shelf of North-West Europe (Ed WOODLAND, A.W.) 1, 77-91, Appl. Sci.

ROBERTS, D,G,, 1975b. Marine geology of the Rockall Plateau and Trough. Phil. Trans. R. Soc. A278, 447-509.

ROBERTS, D.G., ARDUS, D.A., & DEARNLEY, R., 1973. Precambrian rocks drilled on the Rockall Bank. Nature (Phys. Sci.), Lond. 244, 21-23.

RUSSELL, M.J., 1976. A possible Lower Permian age for the onset of ocean floor spreading in the Northern North Atlantic. Scott. J. Geol. 12, 315-323.

SCRUTTON, R.A., 1971. Geophysical studies of Rockall microcontinent and adjacent features. Ph.D. thesis, University of Cambridge.

SCRUTTON, R.A., 1972. The crustal structure of Rockall Plateau microcontinent. Geophys. J. R. astr. Soc. 27, 259-275.

SCRUTTON, R.A., & ROBERTS, D.G., 1971. Structure of Rockall Plateau and Trough, North-East Atlantic. In The geology of the East Atlantic continental margin (Ed DELANY, F.M.) 2, Inst. geol. Sci. Rep. No. 70/14, 79-87.

SHERIDAN, R.E., 1974. Atlantic continental margin of North America. In The geology of continental margins (Eds BURK, C.A., & DRAKE, C.L.) 391-407, Springer-Verlag.

SHIMSHONI, M., & SMITH, S.W., 1964. Seismic signal enhancement with three-component detectors. Geophysics 29, 664-671.

SLEEP. N.H., 1971. Thermal effects of the formation of Atlantic type continental margins by continental break up. Geophys. J. R. astr. Soc. 24, 325-350.

SMITH, P.J., 1974. A seismic refraction study of crustal structure between the Faeroe Isles and Scotland. Ph.D. thesis, University of Durham.

SMITH, P.J., & BOTT, M.H.P., 1975. Structure of the crust beneath the Caledonian foreland and Caledonian belt of the North Scottish shelf region. Geophys. J. R. astr. Soc. 40, 187-205.

SMYTHE, D.K., SOWERBUTTS, W.T.C., BACON, M., & McQUILLIN, R., 1972. Deep sedimentary basin below Northern Skye and the Little Minch. Nature (Phys. Sci.), Lond. 236, 87-89.

STEEL, R.J., 1971. New Red Sandstone movement on the Minch fault. Nature (Phys. Sci.), Lond. 234, 158-159.

STEEL, R.J., 1974. New Red Sandstone floodplain and piedmont sedimentation in the Hebridean province, Scotland. J. Sed. Pet. 44, 336-357.

STEEL, R.J., NICHOLSON, R., & KALANDER, L., 1975. Triassic sedimentation and palaoegraphy in Central Skye. Scott. J. Geol. 11, 1-13.

STEWART, A.D., 1966. An unconformity in the Torridonian. Geol. Mag. 103, 462-465.

STEWART, A.D., & IRVING, E., 1974. Palaeomagnetism of Precambrian sedimentary rocks from NW Scotland and the apparent polar wandering path of Laurentia. Geophys. J. R. astr. Soc. 37, 51-72.

STEWART, M., 1933. Notes on the geology of Sula Sgeir and the Flannan Isles. Geol. Mag. 70, 110-116.

STRIDE, A.H., CURRAY, J.R., MOORE, D.G., & BELDERSON, R.H., 1969. Marine geology of the Atlantic continental margin of Europe. Phil. Trans. R. Soc. A264, 31-75.

SUTTON, J., & WATSON, J., 1951. The Pre-Torridonain metamorphic history of the Loch Torridon and Scourie areas in the North-West Highlands, and its bearing on the chronological classification of the Lewisian. Q. J. geol. Soc., Lond. 106, 241-307.

SWINBURN, P.M., 1975. The crustal structure of Northern England. Ph.D. thesis, University of Durham.

TALWANI, M., & ELDHOLM, O., 1972. Continental margin off Norway; a geophysical study. Bull. Geol. Soc. Am. 83, 3575-3606.

TUSON, J., 1959. A geophysical investigation of the Tertiary volcanic districts of Western Scotland. Ph.D. thesis, University of Durham.

WALCOTT, R.I., 1972. Gravity, flexure, and the growth of sedimentary basins at a continental edge. Bull. Geol. Soc. Am. 83, 1845-1848.

WATTS, A.B., 1971. Geophysical investigations on the continental shelf and slope north of Scotland. Scott. J. Geol. 7, 189-218.

WATTS, A.B., & RYAN, W.B.F., 1976. Flexure of the lithosphere and continental margin basins. Tectonophysics 36, 25-44.

WESTBROOK, G.K., 1974. The South Harris magnetic anomaly. Proc. geol. Ass. 85, 1-12.

WHITBREAD, D.R., 1975. Geology and petroleum possibilities west of the United Kingdom. In Petroleum and the continental shelf of North-West Europe (Ed WOODLAND, A.W.) 1, 45-59, Appl. Sci.

WHITE, J.E., 1964. Motion product seismograms. Geophysics 29, 288-298.

WHITEWAY, F.E., 1965. The recording and analysis of seismic body waves using linear cross arrays. Rad. Elec. Engr. 29, 33-46.

WHITMARSH, R.B., LONGFORD, J.J., BUCKLEY, J.S., BAILEY, R.J., & BLUNDELL, D.J., 1974. The crustal structure beneath Porcupine ridge as determined by explosion seismology. Earth planet. Sci. Lett. (Neth.) 22, 197-204.

WILLMORE, P.L., & BANCROFT, A.M., 1960. The time term approach to refraction seismology. Geophys. J. R. astr. Soc. 3, 419-432.

APPENDIX A

TRAVEL-TIME DATA

The following tables contain details of the shots recorded at each station. The first line gives the station name and code, its latitude and longitude, its elevation in meters and its elevation correction in seconds.

The columns are:

(1) The line number of the table.

(2) The shot number.

(3) Water depth in metres.

(4) Shot depth in metres.

(5) P_n depth correction in seconds.

(6) P* depth correction in seconds.

(7) P_g depth correction in seconds.

(8) Shot instant: Day, hour, minute and second. Dates in August continue on from July, i.e. Aug 1st is day 32.

(9) Internal clock error: If fast - positive, if slow - negative, if 0.00 - not available.

(10) Arrival time: Hour, minute, second. If second = 0.00 then not picked.

(11) Confidence level of pick: 1 - excellent.... 4 - very poor, 5 - impossible.

(12) Travel-time in seconds. Uncorrected for shot and water depth.

(13) Distance in kilometres.

(14)	Origin time plus distance/6: time at zero on a T - Δ/6 plot.
(15) and (16)	Type of east-west seismometer and its gain setting.
(17) and (18)	Type of north-south seismometer and its gain setting.
(19) and (20)	Type of vertical seismometer and its gain setting.
(21)	Number of zero line sample. Refers to digitised event on magnetic tape and is used in construction of stacked record sections.

STATION:POLBAIN   CODE:GS1   TYPE:GEOSTORE   LAT:53 2.45   LONG: 5 23.70   ELEV:160 M   PN CORR: 0.02 S

	SHOT	W.D	S.D	PNDC	PSDC	PGDC	DAY H+M SECS	CL.ER	H+M SECS	CONF	T.T	DIST	T-D/6	E.SEI	G	N.SEI	G	V.SEI	G	NOLS
		M	M	S	S	S		S			S	KM	S							
1	G7	45	45	-.02	-.02	-.02	29:1008:59.30	3.86	1109: 4.49	1	1.33	7.97	64.49	MKII	9	MKII	9	HS10	9	193
2	G8	102	91	-.03	-.03	-.03	29:1148:43.52	3.86	1249:49.63	1	2.25	11.59	49.31	MKII	9	MKII	9	HS10	9	184
3	G9	100	91	-.03	-.03	-.03	29:1308:21.83	3.86	1408:28.82	1	3.13	16.59	28.45	MKII	9	MKII	9	HS10	9	177
4	G10	110	91	-.03	-.03	-.03	29:1436:14.63	3.87	1536:22.15	1	3.65	20.37	21.89	MKII	9	MKII	9	HS10	9	177
5	G11	48	30	-.01	-.01	-.01	29:1706:19.96	3.87	1806:30.67	1	6.84	39.66	30.44	MKII	10	MKII	10	HS10	10	179
6	G12	63	45	-.01	-.01	-.01	29:1821:22.46	3.87	1921:34.20	1	7.87	46.03	34.00	MKII	10	MKII	10	HS10	10	175
7	G13	118	91	-.03	-.03	-.02	30: 805:46.96	3.90	905:59.66	1	8.80	51.43	59.43	MKII	10	MKII	10	HS10	10	137
8	G14	151	91	-.02	-.02	-.02	30: 942:55.52	3.90	1043: 9.02	1	9.60	57.05	68.93	MKII	10	MKII	10	HS10	10	145
9	G15	40	30	-.01	-.01	-.01	39:1622: 5.00	0.0	830: 0.0	5	0.0	107.69	22.95	MKII	9	MKII	9	HS10	9	0
10	G16	97	91	-.03	-.03	-.03	43:1021:14.04	-0.02	1121:32.93	3	18.91	116.72	33.47	MKII	9	MKII	9	HS10	9	209
11	G17	94	76	-.02	-.02	-.02	39:1419:25.42	0.0	628: 0.0	5	0.0	128.47	46.83	MKII	9	MKII	9	HS10	9	0
12	G18	98	90	-.03	-.03	-.03	43:1233:54.78	-0.02	1334:16.94	3	22.18	135.15	77.28	MKII	9	MKII	9	HS10	9	198
13	G19	70	45	-.01	-.01	-.01	39:1226:10.60	0.0	434: 0.0	5	0.0	146.99	35.10	MKII	9	MKII	9	HS10	9	0
14	G20	96	91	-.03	-.03	-.03	43:1441: 8.02	-0.02	1541:32.60	5	24.60	155.76	33.96	MKII	9	MKII	9	HS10	9	210
15	G21	143	91	-.02	-.02	-.02	39:1014:53.81	0.0	223: 0.0	5	0.0	168.00	81.81	MKII	9	MKII	9	HS10	9	0
16	G22	140	91	-.02	-.02	-.02	43:1705:40.99	-0.02	1806: 8.66	3	27.69	178.62	70.74	MKII	9	MKII	9	HS10	9	163
17	G23	153	91	-.02	-.02	-.01	43:1844:19.73	-0.02	1944:49.30	3	29.59	190.25	51.42	MKII	9	MKII	9	HS10	9	220
18	G24	164	91	-.01	-.01	-.01	46:1345:52.43	-0.11	1446:23.20	3	30.88	203.41	86.22	MKII	9	MKII	9	HS10	9	194
19	G25	172	91	-.01	-.01	-.01	46:1227:36.95	-0.11	1328: 0.0	5	0.0	212.93	72.33	MKII	9	MKII	9	HS10	9	214
20	G26	218	91	-.00	0.00	0.00	46:1028:24.04	-0.11	1128:57.71	3	33.78	223.16	61.12	MKII	9	MKII	9	HS10	9	212
21	G27	275	91	0.02	0.02	0.02	46: 905:31.91	-0.11	1006: 0.0	5	0.0	233.44	70.71	MKII	9	MKII	9	HS10	9	173
22	G28	364	91	0.04	0.04	0.05	46: 731:33.42	-0.11	832: 0.0	5	0.0	239.72	73.26	MKII	9	MKII	9	HS10	9	2364
23	H9	124	91	-.03	-.02	-.02	30:2205:45.76	-0.10	2305:55.14	2	9.48	56.99	55.16	MKII	8	MKII	8	HS10	8	389
24	H10	55	55	-.02	-.02	-.02	30:2039:48.51	-0.10	2139:57.11	2	8.70	56.12	57.76	MKII	8	MKII	8	HS10	8	286
25	H11	149	91	-.02	-.02	-.02	30:1911:32.66	-0.10	2011:42.04	3	9.48	56.80	42.03	MKII	8	MKII	8	HS10	8	362
26	H12	120	91	-.03	-.03	-.02	30:1740:51.81	-0.10	1841: 1.47	2	9.76	56.80	61.18	MKII	8	MKII	8	HS10	8	290
27	H13	74	55	-.02	-.02	-.01	30:1608:45.21	-0.10	1708:55.28	2	10.17	58.60	54.88	MKII	8	MKII	8	HS10	6	287
28	H14	75	60	-.02	-.02	-.02	30:1446:57.53	-0.10	1547: 8.19	2	10.76	61.48	67.68	MKII	8	MKII	8	HS10	8	286
29	H15	73	73	-.03	-.03	-.03	30:1313:45.40	-0.10	1413:56.58	2	11.28	65.04	56.14	MKII	8	MKII	8	HS10	8	346
30	H16	136	91	-.02	-.02	-.02	30:1206:27.09	-0.10	1306:38.49	2	11.50	66.98	38.15	MKII	8	MKII	8	HS10	8	338
31	J1	63	45	-.01	-.01	-.01	34: 739:17.77	-0.40	839:45.90	3	28.53	190.81	49.17	MKII	9	MKII	9	HS10	9	0
32	J2	118	91	-.03	-.03	-.02	47: 747:44.55	-0.12	848: 0.0	5	0.0	188.68	75.88	MKII	9	MKII	9	HS10	9	0
33	J3	151	91	-.02	-.02	-.02	47:1033:40.40	-0.12	1134:10.46	3	30.18	192.59	72.38	MKII	9	MKII	9	HS10	9	0
34	J4	134	91	-.02	-.02	-.02	47:1319:38.06	-0.12	1420: 0.0	5	0.0	207.21	72.47	MKII	9	MKII	9	HS10	9	0
35	J5	120	91	-.03	-.03	-.02	47:1606:27.28	-0.12	1707: 0.0	5	0.0	216.57	63.25	MKII	9	MKII	9	HS10	9	0
36	J7	90	76	-.03	-.02	-.02	48: 741:49.34	-0.12	842: 0.0	5	0.0	254.26	91.60	MKII	9	MKII	9	HS10	9	0
37	J8	132	91	-.02	-.02	-.02	48:1030:32.38	-0.12	1131: 0.0	5	0.0	277.55	78.52	MKII	9	MKII	9	HS10	9	0
38	K1	1824	91	0.43	0.45	0.47	44: 906:15.17	-0.02	1006: 0.0	5	0.0	265.45	59.39	MKII	9	MKII	9	HS10	9	131
39	K2	1950	91	0.47	0.49	0.51	45:1734:54.14	-0.10	1835:34.38	3	40.34	277.80	100.34	MKII	9	MKII	9	HS10	9	449
40	K3	2052	91	0.49	0.52	0.54	44:1330:39.05	-0.02	1431: 0.0	5	0.0	290.23	87.40	MKII	9	MKII	9	HS10	9	1076
41	K4	2070	91	0.50	0.52	0.54	45:1309:54.85	-0.10	1410:38.60	3	43.25	297.66	104.36	MKII	9	MKII	9	HS10	9	439
42	K5	2088	91	0.50	0.53	0.55	44:1736:41.83	-0.03	1837: 0.0	5	0.0	310.75	93.59	MKII	9	MKII	9	HS10	9	2372
43	K6	2076	91	0.50	0.52	0.54	45: 821:28.00	-0.08	922:14.74	3	46.82	321.87	81.56	MKII	9	MKII	9	HS10	9	1988
44	K7	2016	91	0.49	0.51	0.53	37:1446:39.42	-0.51	1547: 0.0	5	0.0	333.59	94.51	MKII	9	MKII	9	HS10	10	2594
45	K9	1968	91	0.47	0.49	0.51	37: 906:42.43	-0.50	1007: 0.0	5	0.0	355.56	101.21	MKII	9	MKII	9	HS10	10	469
46	K11	1872	91	0.45	0.47	0.48	36:1810:54.25	-0.49	1912: 0.0	5	0.0	374.24	116.13	MKII	9	MKII	9	HS10	10	411
47	K12	1710	91	0.40	0.42	0.44	36:1336:21.18	-0.48	1437: 0.0	5	0.0	387.53	85.29	MKII	9	MKII	9	HS10	9	716
48	K14	1704	91	0.40	0.42	0.44	35:1104:56.75	-0.43	1206: 0.0	5	0.0	413.27	125.20	MKII	9	MKII	9	HS10	9	2684

STATION:STAC POL CODE:GS2 TYPE:GEOSTORE LAT:58 1.95 LONG: 5 12.95 ELEV: 75 M PN CORR: 0.01 S

	SHOT	W.D	S.D	PNDC	PSDC	PGDC	DAY H+M SECS	CL.ER	H+M SECS	CONF	T.T	DIST	T-D/6	E.SEI	G	N.SEI	G	V.SEI	G	NOLS
		M	M	S	S	S		S			S	KM	S							
1	G7	45	45	-.02	-.02	-.02	29:1008:59.30	0.01	1109: 2.44	1	3.13	17.57	62.24	MKIII	7	MKIII	7	MKII	10	0
2	G9	100	91	-.03	-.03	-.03	29:1308:21.83	10.10	1408:36.69	1	4.76	26.82	36.40	MKIII	7	MKIII	7	MKII	10	82
3	G10	110	91	-.03	-.03	-.03	29:1436:14.63	10.10	1537:30.00	1	5.27	30.65	29.84	MKIII	7	MKIII	7	MKII	10	121
4	G11	48	30	-.01	-.01	-.01	29:1706:19.96	10.10	1807:38.48	1	8.42	50.11	38.41	MKIII	7	MKIII	7	MKII	10	186
5	G12	63	45	-.01	-.01	-.01	29:1821:22.46	10.10	1922:42.03	1	9.47	56.50	41.98	MKIII	7	MKIII	7	MKII	10	130
6	G13	118	91	-.03	-.03	-.02	30: 805:46.96	10.10	907: 7.46	1	10.40	61.94	67.38	MKIII	7	MKIII	7	MKII	10	187
7	G14	151	91	-.02	-.02	-.02	30: 942:55.52	10.10	1044:16.83	1	11.21	67.57	76.88	MKIII	7	MKIII	7	MKII	10	189
8	G15	40	30	-.01	-.01	-.01	39:1622: 5.00	-0.22	1722:23.58	2	18.80	118.21	24.48	HS10V	9	MKIII	9	MKII	10	239
9	G16	97	91	-.03	-.03	-.03	43:1021:14.04	-0.26	1121:34.20	2	20.42	127.30	35.00	HS10V	9	MKIII	9	MKII	10	232
10	G17	94	76	-.02	-.02	-.02	39:1419:25.42	-0.22	1519:47.29	2	22.09	139.03	48.37	HS10V	9	MKIII	9	MKII	10	238
11	G18	98	90	-.03	-.03	-.03	43:1233:54.78	-0.26	1334:17.42	3	22.90	145.73	78.81	HS10V	9	MKIII	9	MKII	10	213
12	G19	70	45	-.01	-.01	-.01	39:1226:10.60	-0.22	1326:34.20	2	23.82	157.56	36.64	HS10V	9	MKIII	9	MKII	10	277
13	G20	96	91	-.03	-.03	-.03	43:1441: 8.02	-0.26	1541:32.90	3	25.14	166.34	35.48	HS10V	9	MKIII	9	MKII	10	274
14	G21	143	91	-.02	-.02	-.02	39:1014:53.81	-0.22	1115:20.12	3	26.53	178.58	83.35	HS10V	9	MKIII	9	MKII	10	269
15	G22	140	91	-.02	-.02	-.02	43:1705:40.99	-0.27	1806: 0.0	5	0.0	189.20	72.25	HS10V	9	MKIII	9	MKII	10	314
16	G23	153	91	-.02	-.02	-.01	43:1844:19.73	-0.27	1944:49.22	3	29.76	200.83	52.93	HS10V	9	MKIII	9	MKII	10	256
17	G24	164	91	-.01	-.01	-.01	46:1345:52.43	-0.29	1446: 0.0	5	0.0	214.00	87.81	MKIII	9	MKIII	9	HS10	9	356
18	G25	172	91	-.01	-.01	-.01	46:1227:36.95	-0.29	1328: 0.0	5	0.0	223.52	73.91	MKIII	9	MKIII	9	HS10	9	350
19	G26	218	91	-.00	0.00	0.00	46:1028:24.04	-0.29	1128:58.61	3	34.86	233.76	62.71	MKIII	9	MKIII	9	HS10	9	394
20	G27	275	91	0.02	0.02	0.02	46: 905:31.91	-0.29	1006: 0.0	5	0.0	244.04	72.29	MKIII	9	MKIII	9	HS10	9	2066
21	G28	364	91	0.04	0.04	0.05	46: 731:33.42	-0.29	832: 0.0	5	0.0	250.31	74.85	MKIII	9	MKIII	9	HS10	9	134
22	H9	124	91	-.03	-.02	-.02	30:2205:45.76	10.10	2307: 6.12	1	10.26	62.41	66.26	MKIII	7	MKIII	7	MKII	8	204
23	H10	55	55	-.02	-.02	-.02	30:2039:48.51	10.10	2141: 8.61	1	10.00	62.48	69.02	MKIII	7	MKIII	7	MKII	8	211
24	H11	149	91	-.02	-.02	-.02	30:1911:32.66	10.10	2012:53.24	1	10.48	64.11	53.44	MKIII	7	MKIII	7	MKII	8	197
25	H12	120	91	-.03	-.03	-.02	30:1740:51.81	10.10	1842:12.68	1	10.77	64.99	72.74	MKIII	7	MKIII	7	MKII	8	174
26	H13	74	55	-.02	-.02	-.01	30:1608:45.21	10.10	1710: 6.61	2	11.30	67.52	66.56	MKIII	7	MKIII	7	MKII	8	94
27	H14	75	60	-.02	-.02	-.02	30:1446:57.53	10.10	1548:19.56	2	11.93	70.96	79.46	MKIII	7	MKIII	7	MKII	8	115
28	H15	73	73	-.03	-.03	-.03	30:1313:45.40	10.10	1415: 8.06	1	12.56	75.09	68.02	MKIII	7	MKIII	7	MKII	8	165
29	H16	136	91	-.02	-.02	-.02	30:1206:27.09	10.10	1307:49.92	1	12.73	77.17	50.05	MKIII	7	MKIII	7	MKII	8	138
30	J1	63	45	-.01	-.01	-.01	34: 739:17.77	-1.18	840:45.95	1	29.36	201.27	50.13	MKIII	9	MKIII	9	MKII	9	0
31	J2	118	91	-.03	-.03	-.02	47: 747:44.55	-0.29	848:13.65	3	29.39	198.66	77.37	MKIII	9	MKIII	9	HS10	9	0
32	J3	151	91	-.02	-.02	-.02	47:1033:40.40	-0.29	1134: 0.0	5	0.0	201.83	73.75	MKIII	9	MKIII	9	HS10	9	0
33	J4	134	91	-.02	-.02	-.02	47:1319:38.06	-0.29	1420: 8.86	3	31.09	215.32	73.66	MKIII	9	MKIII	9	HS10	9	0
34	J5	120	91	-.03	-.03	-.02	47:1536:27.28	-0.29	1707: 0.0	5	0.0	223.97	64.32	MKIII	9	MKIII	9	HS10	9	0
35	J7	90	76	-.03	-.02	-.02	48: 741:49.34	-0.29	842: 0.0	5	0.0	259.80	92.35	MKIII	9	MKIII	9	HS10	9	0
36	J8	132	91	-.02	-.02	-.02	48:1030:32.38	-0.27	1131: 0.0	5	0.0	282.22	79.13	MKIII	9	MKIII	9	HS10	9	0
37	I3	55	55	-.02	-.02	-.02	32:1905:35.01	10.10	2006:56.33	1	11.22	58.92	56.60	MKIII	9	MKIII	9	MKII	9	0
38	K1	1824	91	0.43	0.45	0.47	44: 906:15.17	-0.27	1006:55.30	3	40.48	276.05	60.91	MKIII	9	MKIII	9	HS10	9	0
39	K2	1950	91	0.47	0.49	0.51	45:1734:54.14	-0.29	1835:35.42	3	41.57	288.40	101.92	MKIII	9	MKIII	9	HS10	9	454
40	K3	2052	91	0.49	0.52	0.54	44:1330:39.05	-0.28	1331:22.22	3	43.45	3[illegible].83	88.91	MKIII	9	MKIII	9	HS10	9	829
41	K4	2070	91	0.50	0.52	0.54	45:1309:54.85	-0.29	1410: 0.0	5	0.0	308.26	105.94	MKIII	9	MKIII	9	HS10	9	1478
42	K5	2088	91	0.50	0.53	0.55	44:1735:41.83	-0.28	1837:27.60	3	46.05	321.35	95.11	MKIII	9	MKIII	9	HS10	9	2409
43	K6	2076	91	0.50	0.52	0.54	45: 821.28.00	-0.28	922:15.22	3	47.50	332.47	83.13	MKIII	9	MKIII	9	HS10	9	541
44	K7	2016	91	0.49	0.51	0.53	37:1446:39.42	-1.61	1547:26.22	4	48.41	344.19	95.18	MKIII	9	MKIII	9	MKII	10	632
45	K9	1969	91	0.47	0.49	0.51	37: 906:42.43	-1.61	1007: 0.0	5	0.0	366.27	101.86	MKIII	9	MKIII	9	MKII	10	545
46	K11	1872	91	0.45	0.47	0.48	36:1810:54.25	-1.61	1911: 0.0	5	0.0	384.85	116.78	MKIII	9	MKIII	9	MKII	10	629
47	K12	1710	91	0.40	0.42	0.44	36:1336:21.18	-1.61	1437:14.14	2	54.57	398.14	85.93	MKIII	9	MKIII	9	MKII	9	1278

STATION:KNOCKAN CODE:GS3 TYPE:GEOSTORE LAT:58 2.40 LONG: 5 3.89 ELEV:250 M PN CORR: 0.03 S

	SHOT	W.D M	S.D M	PNDC S	PSDC S	PGDC S	DAY H+M SECS	CL.ER S	H+M SECS	CONF	T.T S	DIST KM	T-D/6 S	E.SEI	G	N.SEI	G	V.SEI	G	NOLS
1	G7	45	45	-.02	-.02	-.02	29:1008:59.30	-0.10	1109: 7.57	4	4.47	26.50	63.62	MKIII	9	MKIII	9	HS10	9	184
2	G8	102	91	-.03	-.03	-.03	29:1148:43.52	-0.10	1248:48.82	1	5.40	30.63	48.53	MKIII	9	MKIII	9	HS10	9	178
3	G9	100	91	-.03	-.03	-.03	29:1308:21.83	-0.10	1408:27.94	1	6.21	35.77	27.69	MKIII	9	MKIII	9	HS10	9	171
4	G10	110	91	-.03	-.03	-.03	29:1436:14.63	-0.10	1536:21.24	1	6.71	39.61	21.13	MKIII	9	MKIII	9	HS10	9	176
5	G11	48	30	-.01	-.01	-.01	29:1706:19.96	-0.10	1806:29.71	1	9.85	59.06	29.70	MKIII	9	MKIII	9	HS10	9	178
6	G12	63	45	-.01	-.01	-.01	29:1821:22.46	-0.10	1921:33.25	1	10.89	65.46	33.27	MKIII	9	MKIII	9	HS10	9	168
7	G13	118	91	-.03	-.03	-.02	30: 805:46.96	-0.10	905:58.71	1	11.85	70.89	58.67	MKIII	9	MKIII	9	HS10	9	190
8	G14	151	91	-.02	-.02	-.02	30: 942:55.52	-0.10	1043: 8.06	1	12.64	76.51	68.17	MKIII	9	MKIII	9	HS10	9	185
9	G15	40	30	-.01	-.01	-.01	39:1622: 5.00	-0.27	1722:24.96	3	20.23	127.16	25.92	MKIII	10	MKIII	10	HS10	9	244
10	G16	97	91	-.03	-.03	-.03	43:1021:14.04	-0.39	1121:35.48	2	21.83	136.22	36.35	MKIII	10	MKIII	10	HS10	9	230
11	G17	94	76	-.02	-.02	-.02	39:1419:25.42	-0.27	1519:48.46	2	23.31	147.97	19.81	MKIII	10	MKIII	10	HS10	9	256
12	G18	98	90	-.03	-.03	-.03	43:1233:54.78	-0.39	1334:18.50	3	24.11	154.65	80.16	MKIII	10	MKIII	10	HS10	9	268
13	G19	70	45	-.01	-.01	-.01	39:1226:10.60	-0.27	1326:35.80	3	25.47	166.49	38.08	MKIII	10	MKIII	10	HS10	9	306
14	G20	96	91	-.03	-.03	-.03	43:1441: 8.02	-0.39	1541:34.00	2	26.37	175.26	36.84	MKIII	10	MKIII	10	HS10	9	279
15	G21	143	91	-.02	-.02	-.02	39:1014:53.81	-0.27	1115:21.50	2	27.96	187.50	84.79	MKIII	10	MKIII	10	HS10	9	358
16	G22	140	91	-.02	-.02	-.02	43:1705:40.99	-0.39	1806:10.00	3	29.40	198.12	73.62	MKIII	10	MKIII	10	HS10	9	315
17	G23	153	91	-.02	-.02	-.01	43:1844:19.73	-0.39	1944:50.21	3	30.87	209.75	54.30	MKIII	10	MKIII	10	HS10	9	335
18	G24	164	91	-.01	-.01	-.01	46:1345:52.43	-0.44	1446: 0.0	5	0.0	222.91	89.14	MKIII	10	MKIII	10	HS10	9	501
19	G25	172	91	-.01	-.01	-.01	46:1227:36.95	-0.44	1328:10.23	3	33.72	232.43	75.25	MKIII	10	MKIII	10	HS10	9	390
20	G26	218	91	-.00	0.00	0.00	46:1028:24.04	-0.44	1128:59.17	3	35.57	242.66	64.04	MKIII	10	MKIII	10	HS10	9	400
21	G27	275	91	0.02	0.02	0.02	46: 905:31.91	-0.44	1006: 8.54	3	37.07	252.94	73.63	MKIII	10	MKIII	10	HS10	9	419
22	G28	364	91	0.04	0.04	0.05	46: 731:33.42	-0.44	832:11.40	3	38.42	259.22	76.18	MKIII	10	MKIII	10	HS10	9	413
23	H9	124	91	-.03	-.02	-.02	30:2205:45.76	-0.10	2306:57.02	2	11.36	69.08	57.17	MKIII	9	MKIII	9	HS10	9	212
24	H10	55	55	-.02	-.02	-.02	30:2039:48.51	-0.10	2139:59.58	2	11.17	69.69	60.03	MKIII	9	MKIII	9	HS10	9	113
25	H11	149	91	-.02	-.02	-.02	30:1911:32.66	-0.10	2011:44.33	2	11.77	71.83	44.53	MKIII	9	MKIII	9	HS10	9	14
26	H12	120	91	-.03	-.03	-.02	30:1740:51.81	-0.10	1841: 3.90	2	12.19	73.14	63.90	MKIII	9	MKIII	9	HS10	9	186
27	H13	74	55	-.02	-.02	-.01	30:1608:45.21	-0.10	1708:57.77	2	12.66	76.01	57.78	MKIII	9	MKIII	9	HS10	9	109
28	H14	75	60	-.02	-.02	-.02	30:1446:57.53	-0.10	1547:10.72	2	13.29	79.67	70.71	MKIII	9	MKIII	9	HS10	9	127
29	H15	73	73	-.03	-.03	-.03	30:1313:45.40	-0.10	1413:59.35	3	14.05	83.99	59.30	MKIII	9	MKIII	9	HS10	9	130
30	H16	136	91	-.02	-.02	-.02	30:1206:27.09	-0.10	1306:41.31	3	14.32	86.11	41.34	MKIII	9	MKIII	9	HS10	9	148
31	J1	83	45	-.01	-.01	-.01	34: 739:17.77	-0.12	839:48.22	3	30.57	210.23	82.69	MKIII	9	MKIII	9	HS10	9	0
32	J2	118	91	-.03	-.03	-.02	47: 747:44.55	-0.46	0: 0.0	5	0.0	207.81	78.68	MKIII	10	MKIII	10	HS10	9	0
33	J3	151	91	-.02	-.02	-.02	47:1033:40.40	-0.46	0: 0.0	5	0.0	210.35	75.00	MKIII	10	MKIII	10	HS10	9	0
34	I3	55	55	-.02	-.02	-.02	32:1905:35.01	-0.11	2005:45.47	1	10.57	64.24	45.61	MKIII	9	MKIII	9	HS10	9	0
35	K1	1824	91	0.43	0.45	0.47	44: 906:15.17	-0.41	1006:56.48	3	41.72	284.95	62.25	MKIII	10	MKIII	10	HS10	9	448
36	K2	1950	91	0.47	0.49	0.51	45:1734:54.14	-0.43	1835:36.41	3	42.70	297.30	103.26	MKIII	10	MKIII	10	HS10	9	504
37	K3	2052	91	0.49	0.52	0.54	44:1330:39.05	-0.41	1431:23.30	3	44.66	309.72	90.26	MKIII	10	MKIII	10	HS10	9	810
38	K4	2070	91	0.50	0.52	0.54	45:1309:54.95	-0.43	1410:39.34	3	4[illegible].92	317.16	107.28	MKIII	10	MKIII	10	HS10	9	2056
39	K5	2088	91	0.50	0.53	0.55	44:1736:41.83	-0.41	1835:28.06	3	46.64	330.24	96.46	MKIII	10	MKIII	10	HS10	9	461
40	K6	2076	91	0.50	0.52	0.54	45: 821:28.00	-0.42	922:15.85	3	48.27	341.36	84.47	MKIII	10	MKIII	10	HS10	9	576
41	K7	2016	91	0.49	0.51	0.53	37:1446:39.42	-0.21	1547:28.75	4	49.54	353.07	98.06	MKIII	10	MKIII	10	HS10	9	583
42	K9	1968	91	0.47	0.49	0.51	37: 906:42.43	-0.20	1007: 0.0	5	0.0	375.14	104.75	MKIII	10	MKIII	10	HS10	9	2448
43	K11	1872	91	0.45	0.47	0.48	36:1810:54.25	-0.18	1911: 0.0	5	0.0	393.72	119.69	MKIII	10	MKIII	10	HS10	9	1638
44	K12	1710	91	0.40	0.42	0.44	36:1336:21.18	-0.18	1431:16.89	3	55.89	407.01	88.84	MKIII	10	MKIII	10	HS10	9	754
45	K14	1704	91	0.40	0.42	0.44	35:1104:56.75	-0.14	1206: 0.0	5	0.0	432.75	128.73	MKIII	9	MKIII	9	HS10	9	760
46	L9	1464	91	0.34	0.35	0.37	27:1820: 8.86	-0.10	1920:52.11	4	43.35	305.66	59.70	MKIII	9	MKIII	9	MKIII	9	0
47	L10	1416	91	0.32	0.34	0.35	27:1010:24.07	-0.10	1111:10.00	4	46.03	318.05	76.98	MKIII	9	MKIII	9	MKIII	9	0

STATION:L.AILSH CODE:GS4 TYPE:GEOSTORE LAT:58 2.30 LONG: 4 52.70 ELEV:200 M PN CORR: 0.02 S

	SHOT	W.D	S.D	PNDC	PSDC	PGDC	DAY H+M SECS	CL.ER	H+M SECS	CONF	T.T	DIST	T-D/6	E.SEI	G	N.SEI	G	V.SEI	G	NOLS
		M	M	S	S	S		S			S	KM	S							
1	G7	45	45	-.02	-.02	-.02	29:1008:59.30	-0.67	1109: 4.82	2	6.19	37.39	64.86	MKII	9	MKII	9	HS10	9	102
2	G8	102	91	-.03	-.03	-.03	29:1148:43.52	-0.68	1248:49.92	1	7.08	41.57	49.77	MKII	9	MKII	9	HS10	9	86
3	G9	106	91	-.03	-.03	-.03	29:1308:21.83	-0.68	1408:29.00	2	7.85	46.72	28.94	MKII	9	MKII	9	HS10	9	90
4	G10	110	91	-.03	-.03	-.03	29:1436:14.63	-0.68	1536:22.34	2	8.39	50.56	22.38	MKII	9	MKII	9	HS10	9	94
5	G11	48	30	-.01	-.01	-.01	29:1706:19.96	-0.68	1806:30.78	2	11.50	70.04	30.95	MKII	9	MKII	9	HS10	9	106
6	G12	63	45	-.01	-.01	-.01	29:1821:22.46	-0.68	1921:34.32	1	12.54	76.44	34.52	MKII	9	MKII	9	HS10	9	111
7	G13	118	91	-.03	-.03	-.02	30: 805:46.96	-0.70	905:59.80	2	13.54	81.88	59.91	MKII	9	MKII	9	HS10	9	112
8	G14	151	91	-.02	-.02	-.02	30: 942:55.52	-0.70	1043: 9.10	2	14.28	87.51	69.41	MKII	9	MKII	9	HS10	9	87
9	G15	40	30	-.01	-.01	-.01	39:1622: 5.00	-0.58	1722:26.32	1	21.90	138.16	27.45	MKII	9	MKII	9	HS10	9	249
10	G16	97	91	-.03	-.03	-.03	43:1021:14.04	-0.21	1121:37.19	1	23.36	147.24	36.37	MKII	9	MKII	9	HS10	9	253
11	G17	94	76	-.02	-.02	-.02	39:1419:25.42	-0.58	1519:49.85	3	25.01	158.98	51.34	MKII	9	MKII	9	HS10	9	255
12	G18	98	90	-.03	-.03	-.03	43:1233:54.78	-0.21	1334:20.15	2	25.58	155.66	82.18	MKII	9	MKII	9	HS10	9	281
13	G19	70	45	-.01	-.01	-.01	39:1226:10.60	-0.58	1326:36.60	3	26.82	177.50	39.60	MKII	9	MKII	9	HS10	9	303
14	G20	90	91	-.03	-.03	-.03	43:1441: 8.02	-0.22	1541:35.29	2	27.49	186.28	38.85	MKII	9	MKII	9	HS10	9	273
15	G21	143	91	-.02	-.02	-.02	39:1014:53.81	-0.57	1115:21.80	3	28.56	190.51	86.33	MKII	9	MKII	9	HS10	9	355
16	G22	140	91	-.02	-.02	-.02	43:1705:40.99	-0.22	1805: 0.0	5	0.0	209.13	75.63	MKII	9	MKII	9	HS10	9	239
17	G23	153	91	-.02	-.02	-.01	43:1844:19.73	-0.22	1944:51.78	3	32.27	220.77	56.30	MKII	9	MKII	9	HS10	9	311
18	G24	164	91	-.01	-.01	-.01	46:1345:52.43	-0.56	1446:26.24	3	34.37	233.92	90.86	MKII	9	MKII	9	HS10	9	258
19	G25	172	91	-.01	-.01	-.01	46:1227:36.95	-0.56	1328:12.08	2	35.69	243.44	76.96	MKII	9	MKII	9	HS10	9	412
20	G26	218	91	-.00	0.00	0.00	46:1028:24.04	-0.56	1129: 0.90	3	37.42	253.68	65.76	MKII	9	MKII	9	HS10	9	470
21	G27	275	91	0.02	0.02	0.02	46: 905:31.91	-0.56	1006:10.02	3	38.67	263.96	75.34	MKII	9	MKII	9	HS10	9	304
22	G28	364	91	0.04	0.04	0.05	46: 731:33.42	-0.56	832:13.44	3	40.58	270.23	77.90	MKII	9	MKII	9	HS10	9	425
23	H9	124	91	-.03	-.02	-.02	30:2205:45.76	-0.71	2305:57.68	2	12.63	77.20	57.92	MKII	9	MKII	9	HS10	9	0
24	H10	55	55	-.02	-.02	-.02	30:2039:48.51	-0.71	2140: 0.39	4	12.59	78.42	60.87	MKII	9	MKII	9	HS10	9	0
25	H11	149	91	-.02	-.02	-.02	30:1911:32.66	-0.71	2011:45.16	2	13.21	81.12	45.47	MKII	9	MKII	9	HS10	9	0
26	H12	120	91	-.03	-.03	-.02	30:1740:51.81	-0.71	1841: 4.80	2	13.70	82.94	64.92	MKII	9	MKII	9	HS10	9	0
27	H13	74	55	-.02	-.02	-.01	30:1608:45.21	-0.70	1708:58.80	4	14.29	86.21	58.88	MKII	9	MKII	9	HS10	9	0
28	H14	75	60	-.02	-.02	-.02	30:1446:57.53	-0.70	1547:11.83	3	15.00	90.17	71.86	MKII	9	MKII	9	HS10	9	0
29	H15	73	73	-.03	-.03	-.03	30:1313:45.40	-0.70	1414: 0.42	3	15.72	94.78	60.50	MKII	9	MKII	9	HS10	9	0
30	H16	136	91	-.02	-.02	-.02	30:1206:27.09	-0.70	1306:42.23	3	15.84	96.97	42.55	MKII	9	MKII	9	HS10	9	0
31	J1	63	45	-.01	-.01	-.01	34: 739:17.77	-5.59	834:44.44	3	32.26	221.19	49.05	MKII	9	MKII	9	HS10	9	0
32	I3	55	55	-.02	-.02	-.02	32:1905:35.01	-5.59	2000:39.44	2	10.02	60.98	39.58	MKII	9	MKII	9	HS10	9	0
33	K1	1824	91	0.43	0.45	0.47	44: 906:15.17	-0.23	1006:58.03	3	43.09	295.97	64.27	MKII	7	MKII	7	HS10	8	1403
34	K2	1950	91	0.47	0.49	0.51	45:1734:54.14	-0.56	1835:37.86	3	44.28	308.31	104.97	MKII	9	MKII	9	HS10	9	522
35	K3	2052	91	0.49	0.52	0.54	44:1330:39.05	-0.23	1431:25.08	3	46.26	320.74	92.28	MKII	9	MKII	9	HS10	9	541
36	K4	2070	91	0.50	0.52	0.54	45:1309:54.85	-0.56	1410:41.18	3	46.89	328.17	108.98	MKII	9	MKII	9	HS10	9	526
37	K5	2088	91	0.50	0.53	0.55	44:1736:41.83	-0.23	0: 0.0	5	0.0	341.25	98.47	MKII	9	MKII	9	HS10	9	719
38	K6	2076	91	0.50	0.52	0.54	45: 821:28.00	-0.56	922: 0.0	5	0.0	352.37	86.17	MKII	9	MKII	9	HS10	9	594
39	K7	2016	91	0.49	0.51	0.53	37:1446:39.42	-0.54	0: 0.0	5	0.0	364.08	99.56	MKII	9	MKII	9	HS10	10	2008
40	K9	1968	91	0.47	0.49	0.51	37: 906:42.43	-0.54	1007: 0.0	5	0.0	386.15	106.25	MKII	9	MKII	9	HS10	10	658
41	K11	1872	91	0.45	0.47	0.48	36:1810:54.25	-0.53	1911:49.18	4	55.46	404.72	121.17	MKII	9	MKII	9	HS10	10	823
42	K12	1710	91	0.40	0.42	0.44	36:1336:21.18	-0.53	1437:17.66	4	57.01	418.02	90.32	MKII	9	MKII	9	HS10	10	737
43	K14	1704	91	0.40	0.42	0.44	35:1104:56.75	-0.52	1206:56.62	4	60.39	443.75	130.19	MKII	9	MKII	9	HS10	10	3236

STATION:GLENCASS CODE:GS5 TYPE:GEOSTORE LAT:58 1.80 LONG: 4 38.00 ELEV:180 M PN CORR: 0.02 S

	SHOT	W.D	S.D	PNDC	PSDC	PGDC	DAY H+M SECS	CL.ER	H+M SECS	CONF	T.T	DIST	T-D/6	E.SEI	G	N.SEI	G	V.SEI	G	NOLS
		M	M	S	S	S		S			S	KM	S							
1	G7	45	45	-.02	-.02	-.02	29:1008:59.30	-0.16	1109: 7.71	1	8.57	51.75	67.76	MKII	9	MKII	9	HS10	10	196
2	G11	48	33	-.01	-.01	-.01	29:1706:19.96	-0.16	1806:33.67	1	13.87	84.46	33.88	MKII	9	MKII	9	HS10	10	164
3	G12	63	45	-.01	-.01	-.01	29:1821:22.46	-0.16	1921:37.18	1	14.88	90.87	37.44	MKII	9	MKII	9	HS10	10	206
4	G15	40	30	-.01	-.01	-.01	39:1622: 5.00	-0.70	1722:28.59	2	24.29	152.59	29.73	MKII	9	MKII	9	HS10	9	239
5	G17	94	76	-.02	-.02	-.02	39:1419:25.42	-0.70	1519:51.50	2	26.78	173.44	53.63	MKII	9	MKII	9	HS10	9	192
6	G19	70	45	-.01	-.01	-.01	39:1226:10.60	-0.70	1326:38.43	2	28.53	191.97	41.90	MKII	9	MKII	9	HS10	9	264
7	G21	143	91	-.02	-.02	-.02	39:1014:53.81	-0.70	1115:24.63	1	31.52	212.99	98.61	MKII	10	MKII	10	HS10	10	374
8	G24	164	91	-.01	-.01	-.01	46:1345:52.43	-0.08	1446:28.55	2	36.20	248.41	93.75	MKII	9	MKII	9	HS10	9	376
9	G25	172	91	-.01	-.01	-.01	46:1227:36.95	-0.08	1326:14.33	2	37.46	257.93	79.86	MKII	9	MKII	9	HS10	9	443
10	G26	218	91	-.00	0.00	0.00	46:1028:24.04	-0.08	1129: 3.12	2	39.16	258.16	68.65	MKII	9	MKII	9	HS10	9	448
11	G27	275	91	0.02	0.02	0.02	46: 905:31.91	-0.08	1006:11.31	2	39.98	278.44	78.24	MKII	9	MKII	9	HS10	9	510
12	G28	364	91	0.04	0.04	0.05	46: 731:33.42	-0.08	832:14.44	2	41.10	284.71	80.79	MKII	9	MKII	9	HS10	9	393
13	H9	124	91	-.03	-.02	-.02	30:2205:45.76	-0.48	2305:59.74	1	14.46	88.48	60.03	MKII	9	MKII	9	HS10	10	197
14	H10	55	55	-.02	-.02	-.02	30:2039:48.51	-0.48	2140: 2.52	2	14.49	90.34	63.09	MKII	9	MKII	9	HS10	10	88
15	H11	149	91	-.02	-.02	-.02	30:1911:32.66	-0.48	2011:47.44	1	15.26	93.63	47.79	MKII	9	MKII	9	HS10	10	200
16	J1	63	45	-.01	-.01	-.01	34: 739:17.77	-0.57	839:51.34	1	34.14	235.57	56.46	MKII	9	MKII	9	HS10	9	0
17	J2	118	91	-.03	-.03	-.02	47: 747:44.55	-0.08	848:18.35	2	33.88	232.12	83.16	MKII	9	MKII	9	HS10	9	0
18	J3	151	91	-.02	-.02	-.02	47:1033:40.40	-0.08	1134:14.67	3	34.35	233.69	79.27	MKII	9	MKII	9	HS10	9	0
19	I3	55	55	-.02	-.02	-.02	32:1905:35.01	-0.52	2005:44.48	1	9.99	60.22	44.53	MKII	9	MKII	9	HS10	9	0
20	K2	1950	91	0.47	0.49	0.51	45:1734:54.14	-0.07	1835:40.30	2	46.23	322.80	107.87	MKII	9	MKII	9	HS10	9	561
21	K3	2052	91	0.49	0.52	0.54	44:1330:39.05	-0.04	1431:27.01	2	48.00	335.23	94.88	MKII	9	MKII	9	HS10	9	584
22	K4	2070	91	0.50	0.52	0.54	45:1309:54.85	-0.07	1409:43.45	2	48.67	342.66	111.89	MKII	9	MKII	9	HS10	9	613
23	K5	2088	91	0.50	0.53	0.55	44:1736:41.83	-0.04	1837:31.87	2	50.08	355.74	101.08	MKII	9	MKII	9	HS10	9	635
24	K6	2076	91	0.50	0.52	0.54	45: 821:28.00	-0.07	922:19.29	2	51.36	366.86	89.07	MKII	9	MKII	9	HS10	9	646
25	K7	2016	91	0.49	0.51	0.53	37:1446:39.42	-0.68	1547:31.71	3	52.97	378.58	101.84	MKII	10	MKII	10	HS10	10	691
26	K9	1968	91	0.47	0.49	0.51	37: 906:42.43	-0.68	1007:37.24	2	55.49	400.65	108.52	MKII	10	MKII	10	HS10	10	678
27	K14	1704	91	0.40	0.42	0.44	35:1104:56.75	-0.61	1206:58.13	3	61.99	458.25	132.51	MKII	10	MKII	10	HS10	10	828

STATION:LAIRG CODE:GS6 TYPE:GEOSTORE LAT:58 0.40 LONG: 4 22.60 ELEV:180 M PN CORR: 0.02 S

	SHOT	W.D	S.D	PNDC	PSDC	PGDC	DAY H+M SECS	CL.ER	H+M SECS	CONF	T.T	DIST	T-D/6	E.SEI	G	N.SEI	G	V.SEI	G	NOLS
		M	M	S	S	S		S			S	KM	S							
1	G15	40	30	-.01	-.01	-.01	39:1622: 5.00	-0.67	1722:30.50	2	26.17	167.73	32.28	MKII	9	MKII	9	HS10	9	0
2	G16	97	91	-.03	-.03	-.03	43:1021:14.04	0.18	1121:41.55	2	27.33	176.91	43.71	MKII	9	MKII	9	HS10	9	0
3	G17	94	76	-.02	-.02	-.02	39:1419:25.42	-0.67	1519:53.24	3	28.49	188.63	56.19	MKII	9	MKII	9	HS10	9	0
4	G18	98	90	-.03	-.03	-.03	43:1233:54.78	0.17	1334:24.65	2	29.73	195.55	87.51	MKII	9	MKII	9	HS10	9	0
5	G19	70	45	-.01	-.01	-.01	39:1226:10.60	-0.67	1326:40.38	4	30.45	207.16	44.46	MKII	9	MKII	9	HS10	9	0
6	G20	96	91	-.03	-.03	-.03	43:1441: 8.02	0.17	1541:40.17	3	31.98	215.97	44.18	MKII	9	MKII	9	HS10	9	0
7	G21	143	91	-.02	-.02	-.02	39:1014:53.81	-0.66	1115:26.29	3	33.14	228.20	91.18	MKII	9	MKII	9	HS10	9	0
8	G22	140	91	-.02	-.02	-.02	43:1705:40.99	0.15	1806:16.12	4	34.98	238.83	80.94	MKII	9	MKII	9	HS10	9	0
9	G23	153	91	-.02	-.02	-.01	43:1844:19.73	0.15	1944:56.06	4	36.18	250.46	61.62	MKII	9	MKII	9	HS10	9	0
10	G24	164	91	-.01	-.01	-.01	46:1345:52.43	-0.01	1446:30.79	3	38.37	263.63	96.36	MKII	9	MKII	9	HS10	9	0
11	G25	172	91	-.01	-.01	-.01	46:1227:36.95	-0.01	1328:16.44	4	39.50	273.16	82.47	MKII	9	MKII	9	HS10	9	0
12	G26	218	91	-.00	0.00	0.00	46:1028:24.04	-0.01	1129: 4.96	4	40.93	283.40	71.26	MKII	9	MKII	9	HS10	9	0
13	G27	275	91	0.02	0.02	0.02	46: 925:31.91	-0.01	1006:14.16	4	42.26	293.68	80.85	MKII	9	MKII	9	HS10	9	0
14	G28	364	91	0.04	0.04	0.05	46: 731:33.42	0.01	832:16.96	4	43.53	299.94	83.42	MKII	8	MKII	8	HS10	8	0
15	J1	63	45	-.01	-.01	-.01	34: 739:17.77	-0.45	839:53.70	2	36.39	250.57	59.07	MKII	9	MKII	9	HS10	9	6
16	J2	118	91	-.03	-.03	-.02	47: 747:44.55	0.09	848:20.48	4	35.84	246.51	85.73	MKII	9	MKII	9	HS10	9	0
17	J3	151	91	-.02	-.02	-.02	47:1033:40.40	0.09	1134:16.71	4	36.22	247.21	81.69	MKII	9	MKII	9	HS10	9	0
18	J4	134	91	-.02	-.02	-.02	47:1319:38.06	0.09	1420:14.36	3	36.21	256.64	80.92	MKII	9	MKII	9	HS10	9	0
19	J5	120	91	-.03	-.03	-.02	47:1606:27.28	0.09	1737: 4.94	4	37.57	262.62	71.14	MKII	9	MKII	9	HS10	9	0
20	J7	90	76	-.03	-.02	-.02	48: 741:49.34	0.11	842:30.91	4	41.46	290.93	97.93	MKII	9	MKII	9	HS10	9	0
21	J8	132	91	-.02	-.02	-.02	48:1030:32.38	0.11	0: 0.0	5	0.0	309.51	84.07	MKII	9	MKII	9	HS10	9	0
22	I3	55	55	-.02	-.02	-.02	32:1905:35.01	-0.39	2005:45.20	1	10.58	64.63	45.39	MKII	9	MKII	9	HS10	9	0
23	K1	1824	91	0.43	0.45	0.47	44: 906:15.17	0.12	1007: 2.56	4	47.27	325.68	69.57	MKII	9	MKII	9	HS10	9	0
24	K2	1950	91	0.47	0.49	0.51	45:1734:54.14	0.05	1835:42.40	4	48.21	338.04	110.53	MKII	9	MKII	9	HS10	9	0
25	K3	2052	91	0.49	0.52	0.54	44:1330:39.05	0.11	1431:29.00	4	49.84	350.47	97.57	MKII	9	MKII	9	HS10	9	0
26	[illegible]	2070	91	0.50	0.52	0.54	45:1309:54.85	0.06	1410:45.54	4	50.63	357.91	114.56	MKII	9	MKII	9	HS10	9	0
27	K5	2088	91	0.50	0.53	0.55	44:1736:41.83	0.10	1837:33.88	4	51.95	371.00	103.76	MKII	9	MKII	9	HS10	9	0
28	K6	2076	91	0.50	0.52	0.54	45: 821:28.00	0.07	922:21.94	4	53.87	382.11	91.76	MKII	9	MKII	9	HS10	9	0
29	K7	2016	91	0.49	0.51	0.53	37:1446:39.42	-0.60	1547:33.70	3	54.88	393.85	104.46	MKII	10	MKII	10	HS10	10	0
30	K9	1968	91	0.47	0.49	0.51	37: 906:42.43	-0.60	1007:39.08	3	57.25	415.92	111.15	MKII	10	MKII	10	HS10	10	0
31	K11	1672	91	0.45	0.47	0.48	36:1810:54.25	-0.57	0: 0.0	5	0.0	434.51	126.10	MKII	10	MKII	10	HS10	10	0
32	K12	1718	91	0.40	0.42	0.44	36:1336:21.18	-0.56	1437:22.02	3	61.40	447.79	95.25	MKII	10	MKII	10	HS10	10	0
33	K14	1704	91	0.40	0.42	0.44	36:1104:56.75	-0.50	1207: 0.76	3	64.53	473.52	135.17	MKII	10	MKII	10	HS10	10	0

STATION:ROGART CODE:GS7 TYPE:GEOSTORE LAT:58 0.45 LONG: 4 7.50 ELEV:210 PN CORR: 0.02

	SHOT	W.D	S.D	PNDC	PSDC	PGDC	DAY H+M SECS	CL.ER	H+M SECS	CONF	T.T	DIST	T-D/6	E.SEI	G	N.SEI	G	V.SEI	G	NOLS
		M	H	S	S	S		S			S	KM	S							
1	G10	110	91	-.03	-.03	-.03	29:1436:14.63	-0.05	1536:30.37	1	15.79	94.93	30.40	MKII	9	MKII	9	HS10	8	178
2	G11	48	30	-.01	-.01	-.01	29:1706:19.96	-0.05	1806:38.76	1	18.85	114.47	38.99	MKII	9	MKII	9	HS10	8	161
3	G12	53	45	-.01	-.01	-.01	29:1821:22.46	-0.05	1921:42.28	1	19.87	120.87	42.56	MKII	9	MKII	9	HS10	8	208
4	G13	118	91	-.03	-.03	-.02	30: 805:46.96	-0.05	906: 7.72	1	20.81	126.35	67.97	MKII	9	MKII	9	HS10	8	169
5	G14	151	91	-.02	-.02	-.02	30: 942:55.52	-0.05	1043:17.02	2	21.55	131.99	77.47	MKII	9	MKII	9	HS10	8	167
6	G15	40	30	-.01	-.01	-.01	39:1622: 5.60	-0.20	1722:32.41	4	27.61	182.60	35.23	MKII	9	MKII	9	HS10	8	314
7	G16	97	91	-.03	-.03	-.03	43:1021:14.04	-0.25	1121:42.98	2	29.19	191.78	45.75	MKII	8	MKII	8	HS10	8	332
8	G17	94	76	-.02	-.02	-.02	39:1419:25.42	-0.20	1519:55.84	4	30.62	203.50	59.14	MKII	9	MKII	9	HS10	8	337
9	G18	98	90	-.03	-.03	-.03	43:1233:54.78	-0.25	1334:25.94	4	31.41	210.22	89.57	MKII	9	MKII	9	HS10	9	343
10	G19	70	45	-.01	-.01	-.01	39:1226:10.60	-0.20	1326:42.80	4	32.40	222.03	47.41	MKII	9	MKII	9	HS10	8	383
11	G20	96	91	-.03	-.03	-.03	43:1441: 8.02	-0.25	1541:41.32	4	33.55	230.84	46.24	MKII	9	MKII	9	HS10	9	2271
12	G21	143	91	-.02	-.02	-.02	39:1014:53.81	-0.29	1115:28.25	4	34.64	243.07	94.12	MKII	9	MKII	9	HS10	8	385
13	G22	140	91	-.02	-.02	-.02	43:1705:40.99	-0.25	1806:17.64	3	36.86	253.70	83.02	MKII	9	MKII	9	HS10	9	786
14	G23	153	91	-.02	-.02	-.01	43:1844:19.73	-0.25	1944:57.63	4	38.15	265.33	63.70	MKII	9	MKII	9	HS10	9	0
15	H11	149	91	-.02	-.02	-.02	30:1911:32.66	-0.05	2011:52.48	1	19.87	120.92	52.76	MKII	9	MKII	9	HS10	8	0
16	H12	120	91	-.03	-.03	-.02	30:1740:51.81	-0.05	1841:12.29	1	20.53	124.04	72.43	MKII	9	MKII	9	HS10	8	0
17	H13	74	55	-.02	-.02	-.01	30:1608:45.21	-0.05	1709: 6.51	2	21.35	128.33	66.55	MKII	9	MKII	9	HS10	8	0
18	H14	75	60	-.02	-.02	-.02	30:1446:57.53	-0.05	1547:19.86	2	22.38	133.07	79.66	MKII	9	MKII	9	HS10	8	0
19	H15	73	73	-.03	-.03	-.03	30:1313:45.40	-0.05	1414: 8.19	1	22.84	138.51	68.43	MKII	9	MKII	9	HS10	8	0
20	H16	136	91	-.02	-.02	-.02	30:1206:27.09	-0.05	1306:50.44	1	23.40	140.92	50.53	MKII	9	MKII	9	HS10	8	0
21	J1	63	45	-.01	-.01	-.01	34: 739:17.77	-0.04	839:55.83	2	38.10	265.44	61.97	MKII	9	MKII	9	HS10	8	0
22	J2	118	91	-.03	-.03	-.02	47: 747:44.55	-0.0	848:22.90	2	38.35	261.18	88.08	MKII	10	MKII	10	HS10	10	0
23	J4	134	91	-.02	-.02	-.02	47:1319:38.06	-0.0	1420:16.58	2	38.52	270.05	83.07	MKII	10	MKII	10	HS10	9	0
24	J5	120	91	-.03	-.03	-.02	47:1606:27.28	-0.0	1806: 0.0	5	0.0	275.44	73.19	MKII	10	MKII	10	HS10	9	0
25	J7	90	76	-.03	-.02	-.02	48: 741:49.34	-0.0	842: 0.0	5	0.0	301.92	99.66	MKII	10	MKII	10	HS10	9	0
26	J8	132	91	-.02	-.02	-.02	48:1030:32.38	-0.0	1031: 0.0	5	0.0	319.54	85.64	MKII	10	MKII	10	HS10	9	0
27	I3	55	55	-.02	-.02	-.02	32:1905:35.01	-0.05	2005:46.32	1	11.36	69.51	46.55	MKII	9	MKII	9	HS10	8	0
28	K2	1950	91	0.47	0.49	0.51	45:1734:54.14	-0.28	1835: 0.0	5	0.0	352.90	112.68	MKII	10	MKII	10	HS10	9	0
29	K3	2052	91	0.49	0.52	0.54	44:1330:39.05	-0.26	1431:29.60	3	50.81	365.33	99.68	MKII	10	MKII	10	HS10	9	6
30	K4	2070	91	0.50	0.52	0.54	45:1309:54.85	-0.28	1410: 0.0	5	0.0	372.76	116.70	MKII	10	MKII	10	HS10	9	0
31	K5	2088	91	0.50	0.53	0.55	44:1736:41.03	-0.26	1837: 0.0	5	0.0	385.85	105.88	MKII	10	MKII	10	HS10	9	0
32	K6	2076	91	0.50	0.52	0.54	45: 821:28.00	-0.27	922:23.27	3	55.54	396.97	93.89	MKII	10	MKII	10	HS10	9	0
33	K7	2016	91	0.49	0.51	0.53	37:1446:39.42	-0.10	1547:36.06	3	56.74	408.69	107.44	MKII	9	MKII	9	HS10	8	0
34	K14	1704	91	0.40	0.42	0.44	35:1104:56.75	-0.06	0: 0.0	5	0.0	488.36	138.08	MKII	10	MKII	10	HS10	9	0
35	L10	1416	91	0.32	0.34	0.35	27:1010:24.07	-0.06	1111:16.40	4	52.39	364.24	84.72	MKII	9	MKII	9	HS06	8	0
36	L11	1365	91	0.31	0.32	0.34	26:1235:30.74	-0.06	0: 0.0	5	0.0	374.40	93.08	MKII	9	MKII	9	HS10	8	0

STATION:BACKIES CODE:GS8 TYPE:GEOSTORE LAT:58 0.17 LONG: 3 58.75 ELEV:260 M PN CORR: 0.03 S

	SHOT	W.D M	S.D M	PNDC S	PSDC S	PGDC S	DAY H+M SECS	CL.ER S	H+M SECS	CONF	T.T S	DIST KM	T-D/6 S	E.SEI	G	N.SEI	G	V.SEI	G	NOLS
1	G7	45	45	-.02	-.02	-.02	29:1008:59.30	-0.33	1109:14.07	2	15.10	90.35	74.03	MKII	9	MKII	9	HS10	9	182
2	G8	102	91	-.03	-.03	-.03	29:1148:43.52	-0.33	1248:59.14	4	15.95	94.56	58.95	MKII	9	MKII	9	HS10	9	233
3	G9	100	91	-.03	-.03	-.03	29:1308:21.83	-0.33	1408:38.20	1	16.70	99.73	38.12	MKII	9	MKII	9	HS10	9	181
4	G10	110	91	-.03	-.03	-.03	29:1436:14.63	-0.33	1536:31.52	1	17.22	103.56	31.56	MKII	9	MKII	9	HS10	9	190
5	G11	48	30	-.01	-.01	-.01	29:1706:19.96	-0.34	1806:39.91	1	20.29	123.09	40.14	MKII	9	MKII	9	HS10	9	195
6	G12	63	45	-.01	-.01	-.01	29:1821:22.46	-0.34	1921:43.40	1	21.28	129.50	43.70	MKII	9	MKII	9	HS10	9	195
7	G13	118	91	-.03	-.03	-.02	30: 805:46.96	-0.36	906: 8.74	1	22.14	134.98	69.10	MKII	9	MKII	9	HS10	9	195
8	G14	151	91	-.02	-.02	-.02	30: 942:55.52	-0.36	1043:18.16	1	23.00	140.62	78.60	MKII	9	MKII	9	HS10	9	138
9	G15	40	30	-.01	-.01	-.01	39:1622: 5.00	-0.01	1722:33.70	3	28.71	191.23	36.86	MKII	9	MKII	9	HS10	9	350
10	G16	97	91	-.03	-.03	-.03	43:1021:14.04	-0.08	1121: 0.0	5	0.0	200.42	47.36	MKII	8	MKII	8	HS10	8	244
11	G17	94	76	-.02	-.02	-.02	39:1419:25.42	-0.01	1519: 0.0	5	0.0	212.13	60.76	MKII	9	MKII	9	HS10	9	259
12	G18	98	90	-.03	-.03	-.03	43:1233:54.78	-0.08	1334: 0.0	5	0.0	218.85	91.18	MKII	8	MKII	8	HS10	8	233
13	G19	70	45	-.01	-.01	-.01	39:1226:10.60	-0.01	1326: 0.0	5	0.0	230.56	49.03	MKII	10	MKII	10	HS10	10	396
14	G20	96	91	-.03	-.03	-.03	43:1441: 8.02	-0.08	1541: 0.0	5	0.0	239.47	47.85	MKII	9	MKII	9	HS10	9	297
15	G21	143	91	-.02	-.02	-.02	39:1014:53.81	-0.01	1115: 0.0	5	0.0	251.70	95.75	MKII	10	MKII	10	HS10	10	0
16	G22	140	91	-.02	-.02	-.02	43:1705:40.99	-0.09	1806: 0.0	5	0.0	262.33	84.62	MKII	9	MKII	9	HS10	9	241
17	G23	153	91	-.02	-.02	-.01	43:1844:19.73	-0.09	1944: 0.0	5	0.0	273.96	65.30	MKII	9	MKII	9	HS10	9	274
18	G24	164	91	-.01	-.01	-.01	46:1345:52.43	-0.14	0: 0.0	5	0.0	287.13	100.15	MKII	10	MKII	10	HS10	10	1088
19	G25	172	91	-.01	-.01	-.01	46:1227:36.95	-0.14	0: 0.0	5	0.0	296.65	86.25	MKII	10	MKII	10	HS10	10	1818
20	G26	218	91	-.00	0.00	0.00	46:1028:24.04	-0.14	0: 0.0	5	0.0	306.89	75.05	MKII	10	MKII	10	HS10	10	0
21	G27	275	91	0.02	0.02	0.02	46: 905:31.91	-0.14	0: 0.0	5	0.0	317.17	84.63	MKII	10	MKII	10	HS10	10	3613
22	G28	364	91	0.04	0.04	0.05	46: 731:33.42	-0.14	0: 0.0	5	0.0	323.43	87.19	MKII	10	MKII	10	HS10	10	252
23	H9	124	91	-.03	-.02	-.02	30:2205:45.76	-0.37	2306: 5.38	1	19.99	121.92	65.71	MKII	9	MKII	9	HS10	9	0
24	H10	55	55	-.02	-.02	-.02	30:2039:48.51	-0.37	2140: 8.29	2	20.15	124.83	68.94	MKII	9	MKII	9	HS10	9	0
25	H11	149	91	-.02	-.02	-.02	30:1911:32.66	-0.37	2011:53.44	2	21.15	129.05	53.80	MKII	9	MKII	9	HS10	9	0
26	H12	120	91	-.03	-.03	-.02	30:1740:51.81	-0.37	1841:13.35	2	21.91	132.32	73.49	MKII	9	MKII	9	HS10	9	0
27	H13	74	55	-.02	-.02	-.01	30:1608:45.21	-0.36	1709: 7.42	2	22.57	136.71	67.64	MKII	9	MKII	9	HS10	9	0
28	H14	75	60	-.02	-.02	-.02	30:1446:57.53	-0.36	1547:20.45	1	23.28	141.53	80.76	MKII	9	MKII	9	HS10	9	0
29	H15	73	73	-.03	-.03	-.03	30:1313:45.40	-0.36	1414: 9.19	1	24.15	147.06	69.55	MKII	9	MKII	9	HS10	9	0
30	H16	136	91	-.02	-.02	-.02	30:1206:27.09	-0.36	1306:51.12	1	24.39	149.50	51.65	MKII	9	MKII	9	HS10	9	0
31	J1	63	45	-.01	-.01	-.01	34: 739:17.77	-0.15	839:57.06	3	39.44	274.03	63.29	MKII	9	MKII	9	HS10	9	0
32	J2	118	91	-.03	-.03	-.02	47: 747:44.55	-0.15	0: 0.0	5	0.0	269.61	89.34	MKII	10	MKII	10	HS10	10	0
33	J3	151	91	-.02	-.02	-.02	47:1033:40.40	-0.15	0: 0.0	5	0.0	269.57	85.18	MKII	10	MKII	10	HS10	10	0
34	J4	134	91	-.02	-.02	-.02	47:1319:38.06	-0.15	0: 0.0	5	0.0	277.66	84.19	MKII	10	MKII	10	HS10	10	0
35	J7	90	76	-.03	-.02	-.02	48: 741:49.34	-0.07	0: 0.0	5	0.0	308.10	100.62	MKII	10	MKII	10	HS10	10	0
36	J8	132	91	-.02	-.02	-.02	48:1030:32.38	-0.07	0: 0.0	5	0.0	325.13	86.50	MKII	10	MKII	10	HS10	10	0
37	I3	55	55	-.02	-.02	-.02	32:1905:35.01	-0.45	2005:46.69	2	12.13	74.05	46.90	MKII	9	MKII	9	HS10	9	0
38	K1	1824	91	0.43	0.45	0.47	44: 906:15.17	-0.12	0: 0.0	5	0.0	349.18	73.25	MKII	9	MKII	9	HS10	9	203
39	K2	1950	91	0.47	0.49	0.51	45:1734:54.14	-0.13	1835:44.47	4	50.46	361.54	114.27	MKII	10	MKII	10	HS10	10	535
40	K3	2052	91	0.49	0.52	0.54	44:1330:39.05	-0.12	1431:32.44	3	53.51	373.96	101.26	MKII	10	MKII	10	HS10	10	606
41	K4	2070	91	0.50	0.52	0.54	45:1309:54.85	-0.13	0: 0.0	5	0.0	381.40	118.29	MKII	10	MKII	10	HS10	10	558
42	K5	2088	91	0.50	0.53	0.55	44:1736:41.83	-0.12	0: 0.0	5	0.0	394.48	107.46	MKII	10	MKII	10	HS10	10	636
43	K6	2076	91	0.50	0.52	0.54	45: 821:28.00	-0.13	0: 0.0	5	0.0	405.60	95.47	MKII	10	MKII	10	HS10	10	593
44	K7	2016	91	0.49	0.51	0.53	37:1446:39.42	0.05	1547:37.50	3	58.03	417.33	109.02	MKII	10	MKII	10	HS10	10	767
45	K9	1968	91	0.47	0.49	0.51	37: 906:42.43	0.05	0: 0.0	5	0.0	439.40	115.71	MKII	10	MKII	10	HS10	10	3591
46	K11	1872	91	0.45	0.47	0.48	36:1810:54.25	0.07	0: 0.0	5	0.0	457.97	130.65	MKII	10	MKII	10	HS10	10	1378
47	K12	1710	91	0.40	0.42	0.44	36:1336:21.18	0.07	0: 0.0	5	0.0	471.26	99.79	MKII	10	MKII	10	HS10	10	470
48	K14	1704	91	0.40	0.42	0.44	35:1104:56.75	0.10	0: 0.0	5	0.0	496.99	139.68	MKII	10	MKII	10	HS10	10	2253
49	L9	1464	91	0.34	0.35	0.37	27:1820: 8.86	-0.46	1920:59.48	3	51.03	359.83	68.37	MKII	9	MKII	9	HS10	9	0
50	L10	1416	91	0.32	0.34	0.35	27:1010:24.07	-0.50	1111:16.74	3	53.17	371.58	85.50	MKII	9	MKII	9	HS10	9	0
51	L11	1365	91	0.31	0.32	0.34	26:1235:30.74	-0.56	1336:25.14	3	54.96	381.69	93.80	MKII	9	MKII	9	HS10	9	0

STATION:CAPEWRAT CODE:GS9 TYPE:GEOSTORE LAT:58 37.45 LONG: 4 59.77 ELEV:140 M PN CORR: 0.02 S

	SHOT	W.D	S.D	PNDC	PSDC	PGDC	DAY H+M SECS	CL.ER	H+M SECS	CONF	T.T	DIST	T-D/G	E.SEI	G	N.SEI	G	V.SEI	G	NOLS
		M	M	S	S	S		S			S	KM	S							
1	G15	40	30	-.01	-.01	-.01	39:1622: 5.00	-1.67	1722:26.64	4	23.31	148.90	28.15	HS10	9	HS10	9	MKII	9	219
2	G16	97	91	-.03	-.03	-.03	43:1021:14.04	-1.77	1121:36.66	4	24.39	155.12	38.12	HS10	9	HS10	9	MKII	9	253
3	G17	94	76	-.02	-.02	-.02	39:1419:25.42	-1.67	1519:50.08	4	26.33	166.36	51.48	HS10	9	HS10	9	MKII	9	214
4	G18	98	90	-.03	-.03	-.03	43:1233:54.78	-1.77	1334:19.90	4	26.89	171.69	81.63	HS10	9	HS10	9	MKII	9	829
5	G19	70	45	-.01	-.01	-.01	39:1226:10.60	-1.67	1326:36.54	2	27.61	183.30	39.48	HS10	9	HS10	9	MKII	9	253
6	G20	95	91	-.03	-.03	-.03	43:1441: 8.02	-1.77	1541:34.78	4	28.53	190.77	38.05	HS10	9	HS10	9	MKII	9	243
7	G22	140	91	-.02	-.02	-.02	43:1705:40.99	-1.77	0: 0.0	5	0.0	212.18	74.58	HS10	9	HS10	9	MKII	9	258
8	G23	153	91	-.02	-.02	-.01	43:1844:19.73	-1.77	1944:50.70	3	32.74	223.22	55.16	HS10	9	HS10	9	MKII	9	390
9	G24	164	91	-.01	-.01	-.01	46:1345:52.43	-1.77	1446:25.16	4	34.50	235.46	89.90	HS10	9	HS10	9	MKII	9	431
10	G25	172	91	-.01	-.01	-.01	45:1227:36.95	-1.77	1227: 0.0	5	0.0	244.57	75.94	HS10	9	HS10	9	MKII	9	446
11	G26	218	91	-.00	0.00	0.00	46:1028:24.04	-1.77	1128:59.66	4	37.39	254.27	64.65	HS10	9	HS10	9	MKII	9	449
12	G27	275	91	0.02	0.02	0.02	46: 905:31.91	-1.77	1006: 0.0	5	0.0	264.16	74.17	HS10	9	HS10	9	MKII	9	452
13	G28	364	91	0.04	0.04	0.05	46: 731:33.42	-1.77	832:11.50	3	39.85	270.60	76.75	HS10	9	HS10	9	MKII	9	324
14	J1	63	45	-.01	-.01	-.01	34: 739:17.77	-1.67	0: 0.0	5	0.0	228.85	54.24	HS10	9	HS10	9	MKII	9	0
15	J2	118	91	-.03	-.03	-.02	47: 747:44.55	-1.81	848:17.08	3	34.34	235.36	81.97	HS10	9	HS10	9	MKII	9	0
16	J3	151	91	-.02	-.02	-.02	47:1033:40.40	-1.82	0: 0.0	5	0.0	246.31	79.63	HS10	9	HS10	9	MKII	9	0
17	J5	120	91	-.03	-.03	-.02	47:1606:27.28	-1.83	0: 0.0	5	0.0	279.20	71.98	HS10	9	HS10	9	MKII	9	0
18	I3	55	55	-.02	-.02	-.02	32:1905:35.01	-1.67	0: 0.0	5	0.0	21.79	36.97	HS10	9	HS10	9	MKII	9	0
19	K1	1824	91	0.43	0.45	0.47	44: 906:15.17	-1.77	1005:56.48	3	43.08	295.26	62.61	HS10	9	HS10	9	MKII	9	0
20	K2	1950	91	0.47	0.49	0.51	45:1734:54.14	-1.77	1835:36.78	3	44.41	306.92	103.52	HS10	9	HS10	9	MKII	9	457
21	K3	2052	91	0.49	0.52	0.54	44:1330:39.05	-1.77	1431:23.34	3	46.06	318.97	90.44	HS10	9	HS10	9	MKII	9	523
22	K4	2070	91	0.50	0.52	0.54	45:1309:54.85	-1.77	1410:39.66	3	46.58	326.14	107.44	HS10	9	HS10	9	MKII	9	516
23	K5	2088	91	0.50	0.53	0.55	44:1736:41.83	-1.77	0: 0.0	5	0.0	339.64	96.50	HS10	9	HS10	9	MKII	9	566
24	K6	2076	91	0.50	0.52	0.54	45: 821:28.00	-1.77	0: 0.0	5	0.0	349.72	84.52	HS10	9	HS10	9	MKII	9	2840
25	K7	2016	91	0.49	0.51	0.53	37:1446:39.42	-1.67	0: 0.0	5	0.0	360.56	97.84	HS10	9	HS10	9	MKII	9	618

STATION:BUTT CODE:DU6 TYPE:DURM II LAT:58 28.34 LONG: 6 13.23 ELEV: 60 M PN CORR: 0.01 S

	SHOT	W.D	S.D	PNDC	PSDC	PGDC	DAY H+M SECS	CL.ER	H+M SECS	CONF	T.T	DIST	T-D/6	E.SEI	G	N.SEI	G	V.SEI	G
		M	M	S	S	S		S			S	KM	S						
1	G7	45	45	-.02	-.02	-.02	29:1008:59.30	-0.77	1008:10.12	4	11.59	67.16	69.72	MKII	6	MKII	6	MKII	6
2	G8	162	91	-.03	-.03	-.03	29:1148:43.52	-0.82	1248:53.98	4	11.28	64.31	53.42	MKII	6	MKII	6	MKII	6
3	G9	100	91	-.03	-.03	-.03	29:1308:21.83	-0.83	1407:31.88	4	10.88	61.72	31.29	MKII	6	MKII	6	MKII	6
4	G10	110	91	-.03	-.03	-.03	29:1436:14.63	-0.83	1535:24.12	4	10.32	60.07	23.81	MKII	6	MKII	6	MKII	6
5	G11	48	30	-.01	-.01	-.01	29:1706:19.96	-0.92	1805:28.00	3	8.96	53.80	28.01	MKII	6	MKII	6	MKII	6
6	G12	63	45	-.01	-.01	-.01	29:1821:22.46	-0.98	1920:30.41	2	8.93	53.20	30.35	MKII	6	MKII	6	MKII	6
7	G13	118	91	-.03	-.03	-.02	30: 805:46.96	-1.21	904:54.86	3	9.11	52.59	54.52	MKII	6	MKII	6	MKII	6
8	G14	151	91	-.02	-.02	-.02	30: 942:55.52	-1.21	1042: 3.00	2	8.69	53.06	63.15	MKII	6	MKII	6	MKII	6
9	G16	97	91	-.03	-.03	-.03	43:1021:14.04	-7.70	1120:20.17	2	13.83	85.06	20.52	MKII	6	MKII	6	MKII	6
10	G18	98	90	-.03	-.03	-.03	43:1233:54.78	-7.84	1333: 3.20	3	16.26	100.20	63.64	MKII	6	MKII	6	MKII	6
11	G20	96	91	-.03	-.03	-.03	43:1441: 8.02	-7.84	1540:19.12	4	18.94	118.43	19.92	MKII	6	MKII	6	MKII	6
12	G22	140	91	-.02	-.02	-.02	43:1705:40.99	-7.88	1804:55.38	3	22.27	139.31	56.33	MKII	6	MKII	6	MKII	6
13	G23	153	91	-.02	-.02	-.01	43:1844:19.73	-7.91	1943:36.00	3	24.18	150.21	36.85	MKII	6	MKII	6	MKII	6
14	G24	164	91	-.01	-.01	-.01	46:1345:52.43	-9.58	1445: 8.56	3	25.71	162.31	69.90	MKII	6	MKII	6	MKII	6
15	G25	172	91	-.01	-.01	-.01	46:1227:36.95	-9.56	1326:54.14	4	26.75	171.37	55.95	MKII	6	MKII	6	MKII	6
16	G26	218	91	-.00	0.00	0.00	46:1028:24.04	-9.49	1127:42.97	4	28.42	181.03	44.72	MKII	6	MKII	6	MKII	6
17	G27	275	91	0.02	0.02	0.02	46: 905:31.91	-9.44	1004:52.12	4	29.65	190.91	54.29	MKII	6	MKII	6	MKII	6
18	G28	364	91	0.04	0.04	0.05	46: 731:33.42	-9.44	830:55.19	4	31.21	197.35	56.87	MKII	6	MKII	6	MKII	6
19	H9	124	91	-.03	-.02	-.02	30:2205:45.76	-1.46	2305: 0.69	3	16.59	98.95	60.79	MKII	6	MKII	6	MKII	6
20	H10	55	55	-.02	-.02	-.02	30:2039:48.51	-1.41	2139: 2.09	3	14.99	93.96	62.76	MKII	6	MKII	6	MKII	6
21	H11	149	91	-.02	-.02	-.02	30:1911:32.66	-1.41	2010:45.71	3	14.46	89.16	46.11	MKII	6	MKII	6	MKII	6
22	H12	120	91	-.03	-.03	-.02	30:1740:51.81	-1.41	1840: 4.18	3	13.78	83.35	64.29	MKII	6	MKII	6	MKII	6
23	H13	74	55	-.02	-.02	-.01	30:1608:45.21	-1.37	1707: 0.0	5	0.0	78.27	56.89	MKII	6	MKII	6	MKII	6
24	H14	75	60	-.02	-.02	-.02	30:1446:57.53	-1.33	1546: 8.41	5	12.21	73.83	68.50	MKII	6	MKII	6	MKII	6
25	H15	73	73	-.03	-.03	-.03	30:1313:45.40	-1.30	1412:55.32	3	11.22	67.27	55.31	MKII	6	MKII	6	MKII	6
26	H16	136	91	-.02	-.02	-.02	30:1206:27.09	-1.28	1305:36.60	3	10.79	65.22	36.68	MKII	6	MKII	6	MKII	6
27	J1	63	45	-.01	-.01	-.01	34: 739:17.77	-2.10	838:39.91	3	24.24	156.70	41.79	MKII	8	MKII	8	MKII	8
28	K1	1824	91	0.43	0.45	0.47	44: 906:15.17	-8.26	1005: 0.0	5	0.0	222.02	43.91	MKII	6	MKII	6	MKII	6
29	K2	1950	91	0.47	0.49	0.51	45:1734:54.14	-9.00	1834:20.16	4	35.02	233.72	84.09	MKII	8	MKII	8	MKII	8
30	K3	2052	91	0.49	0.52	0.54	44:1330:39.05	-8.33	1430: 0.0	5	0.0	245.80	71.69	MKII	8	MKII	8	MKII	8
31	K4	2070	91	0.50	0.52	0.54	45:1309:54.85	-8.86	1409:23.50	4	37.51	253.00	88.16	MKII	8	MKII	8	MKII	8
32	K5	2088	91	0.50	0.53	0.55	44:1736:41.83	-8.46	1836:13.00	4	39.63	265.56	77.63	MKII	8	MKII	8	MKII	8
33	K6	2076	91	0.50	0.52	0.54	45: 821:28.00	-8.75	921: 0.23	4	40.98	276.67	65.36	MKII	8	MKII	8	MKII	8
34	K12	1710	91	0.40	0.42	0.44	36:1336:21.18	-0.0	1436: 5.41	3	44.23	340.79	77.98	MKII	8	MKII	8	MKII	8

STATION:UIG   CODE:DU7   TYPE:DURH II   LAT:58 12.02   LONG: 7 0.69   ELEV: 50 M   PN CORR: 0.01 S

	SHOT	W.D	S.D	PNDC	PSDC	PGDC	DAY H+M SECS	CL.ER	H+M SECS	CONF	T.T	DIST	T-D/6	E.SEI	G	N.SEI	G	V.SEI	G
		M	M	S	S	S		S			S	KM	S						
1	G7	45	45	-.02	-.02	-.02	29:1008:59.30	-0.38	1009:14.13	1	15.21	91.43	74.16	MKII	7	MKII	7	MKII	7
2	G8	102	91	-.03	-.03	-.03	29:1148:43.52	-0.36	1249:57.07	1	14.51	87.24	57.70	MKII	1	MKII	6	MKII	6
3	G9	100	91	-.03	-.03	-.03	29:1308:21.83	-0.38	1408:35.07	1	13.62	82.37	35.18	MKII	6	MKII	6	MKII	6
4	G10	110	91	-.03	-.03	-.03	29:1436:14.63	-0.38	1536:27.17	1	12.92	78.79	27.38	MKII	6	MKII	6	MKII	6
5	G11	48	30	-.01	-.01	-.01	29:1706:19.96	-0.38	1806:29.50	6	9.92	60.47	29.66	MKII	6	MKII	6	MKII	6
6	G12	63	45	-.01	-.01	-.01	29:1821:22.46	-0.40	1921:31.00	1	8.94	54.65	31.17	MKII	6	MKII	6	MKII	6
7	G13	118	91	-.03	-.03	-.02	30: 805:46.96	-0.40	805:54.78	1	8.22	49.47	54.80	MKII	6	MKII	6	MKII	6
8	G14	151	91	-.02	-.02	-.02	30: 942:55.52	-0.40	1043: 2.41	1	7.29	44.46	62.53	MKII	6	MKII	6	MKII	6
9	G23	153	91	-.02	-.02	-.01	43:1844:19.73	5.45	1942:40.91	2	15.73	97.15	41.37	MKII	6	MKII	6	MKII	6
10	G24	164	91	-.01	-.01	-.01	46:1345:52.43	5.45	1444:15.96	2	18.08	109.85	76.19	MKII	6	MKII	6	MKII	6
11	G25	172	91	-.01	-.01	-.01	46:1227:36.95	5.45	1326: 1.91	2	19.51	119.22	62.27	MKII	6	MKII	6	MKII	6
12	G26	218	91	-.00	0.00	0.00	46:1028:24.04	5.45	1126:51.03	2	21.54	129.24	51.03	MKII	6	MKII	6	MKII	6
13	G27	275	91	0.02	0.02	0.02	46: 905:31.91	5.45	1004: 0.63	2	23.27	139.40	60.59	MKII	6	MKII	6	MKII	6
14	G28	354	91	0.04	0.04	0.05	46: 731:33.42	5.45	830: 3.70	2	24.83	145.81	63.17	MKII	6	MKII	6	MKII	6
15	H9	124	91	-.03	-.02	-.02	30:2205:45.76	-0.50	2206: 0.38	1	15.12	94.28	60.97	MKII	6	MKII	6	MKII	6
16	H10	55	55	-.02	-.02	-.02	30:2039:48.51	-0.50	2146: 3.00	3	14.99	87.96	62.67	MKII	6	MKII	6	MKII	6
17	H11	149	91	-.02	-.02	-.02	30:1911:32.66	-0.50	2012:46.00	2	13.84	80.98	45.66	MKII	6	MKII	6	MKII	6
18	H12	129	91	-.03	-.03	-.02	30:1740:51.81	-0.50	1841: 3.67	2	12.36	73.64	63.58	MKII	6	MKII	6	MKII	6
19	H13	74	55	-.02	-.02	-.01	30:1608:45.21	-0.50	1709:56.07	2	11.36	66.12	55.73	MKII	6	MKII	6	MKII	6
20	H14	75	60	-.02	-.02	-.02	30:1446:57.53	-0.50	1547: 7.07	2	10.04	58.68	66.81	MKII	6	MKII	6	MKII	6
21	H15	73	73	-.03	-.03	-.03	30:1313:45.40	-0.55	1414:53.06	3	8.21	48.57	52.95	MKII	6	MKII	6	MKII	6
22	H16	136	91	-.02	-.02	-.02	30:1206:27.09	-0.55	1306:33.95	3	7.41	44.72	33.99	MKII	6	MKII	6	MKII	6
23	J1	63	45	-.01	-.01	-.01	34: 739:17.77	-1.23	839:33.00	2	16.46	101.97	33.53	MKII	7	MKII	7	MKII	7
24	K1	1824	91	0.43	0.45	0.47	44: 906:15.17	0.0	1005:48.16	3	32.99	171.19	43.70	MKII	6	MKII	6	MKII	6
25	K2	1950	91	0.47	0.49	0.51	45:1734:54.14	-0.0	1835: 0.0	2	0.0	183.29	84.69	MKII	8	MKII	8	MKII	8
26	K3	2052	91	0.49	0.52	0.54	44:1330:39.05	-0.0	1429: 0.0	5	0.0	195.63	71.65	MKII	6	MKII	6	MKII	6
27	K4	2070	91	0.50	0.52	0.54	45:1309:54.85	0.0	1409:51.89	3	57.04	202.99	88.68	MKII	8	MKII	8	MKII	8
28	K5	2088	91	0.50	0.53	0.55	44:1736:41.83	-0.0	1835:40.60	3	58.77	215.90	77.81	MKII	8	MKII	8	MKII	8
29	K6	2076	91	0.50	0.52	0.54	45: 821:28.00	-0.0	920: 0.0	5	0.0	227.06	65.84	MKII	8	MKII	8	MKII	8
30	K11	1872	91	0.45	0.47	0.48	36:1810:54.25	-0.0	1911:32.57	2	38.32	278.82	100.72	MKII	8	MKII	8	MKII	8
31	K12	1710	91	0.40	0.42	0.44	36:1336:21.18	-0.0	1437: 1.05	2	39.87	292.29	69.89	MKII	8	MKII	8	MKII	8
32	K14	1704	91	0.40	0.42	0.44	35:1104:56.75	0.0	1206:39.71	2	42.96	317.96	109.74	MKII	7	MKII	7	MKII	7

STATION:LINSHADE CODE:DUB TYPE:DURH II LAT:58 8.51 LONG: 6 51.84 ELEV: 32 M PN CORR: 0.0 S

	SHOT	W.D M	S.D M	PNDC S	PSDC S	PSDC S	DAY H+M SECS	CL.ER S	H+M SECS	CONF	T.T S	DIST KM	T-D/6 S	E.SEI	G	N.SEI	G	V.SEI	G
.	G7	45	45	-.02	-.02	-.02	29:1008:59.30	2.83	1009:15.73	1	13.60	81.59	75.73	MKII	6	MKII	6	MKII	6
2	G8	102	91	-.03	-.03	-.03	29:1148:43.52	2.54	1249:58.95	1	12.89	77.37	58.95	MKII	6	MKII	6	MKII	6
3	G9	100	91	-.03	-.03	-.03	29:1308:21.83	2.27	1408:36.28	1	12.18	72.41	36.17	MKII	6	MKII	6	MKII	6
4	G10	110	91	-.03	-.03	-.03	29:1436:14.63	2.19	1536:28.15	1	11.33	68.76	28.28	MKII	6	MKII	7	MKII	7
5	G11	48	30	-.01	-.01	-.01	29:1705:19.96	1.75	1807:30.30	1	8.29	50.08	30.06	MKII	6	MKII	6	MKII	6
6	G12	63	45	-.01	-.01	-.01	29:1821:22.46	1.59	1921:31.33	1	7.28	44.13	31.40	MKII	6	MKII	6	MKII	6
6	G13	118	91	-.03	-.03	-.02	30: 805:46.96	-1.49	805:53.05	1	6.58	38.85	52.95	MKII	6	MKII	6	MKII	7
8	G14	151	91	-.02	-.02	-.02	30: 942:55.52	-0.73	1043: 0.51	1	5.72	33.73	60.41	MKII	6	MKII	6	MKII	6
9	H9	124	91	-.03	-.02	-.02	30:2205:45.76	-2.60	2205:56.71	1	13.55	83.54	57.08	MKII	6	MKII	6	MKII	6
10	H10	55	55	-.02	-.02	-.02	30:2039:48.51	-2.40	2039: 0.0	5	0.0	77.23	58.98	MKII	6	MKII	6	MKII	6
11	H11	149	91	-.02	-.02	-.02	30:1911:32.66	-2.17	1911:42.05	1	11.56	70.29	42.20	MKII	6	MKII	6	MKII	6
12	H12	120	91	-.03	-.03	-.02	30:1740:51.81	-1.95	1741: 0.66	1	10.80	62.94	60.35	MKII	6	MKII	6	MKII	6
13	H13	74	55	-.02	-.02	-.01	30:1608:45.21	-1.70	1608:53.24	1	9.73	55.45	52.75	MKII	6	MKII	6	MKII	6
14	H14	75	60	-.02	-.02	-.02	30:1446:57.53	-1.51	1446: 4.44	1	8.42	48.04	64.03	MKII	6	MKII	6	MKII	6
15	H15	73	73	-.03	-.03	-.03	30:1313:45.40	-1.26	1313:50.66	1	6.62	37.94	50.46	MKII	6	MKII	6	MKII	6
16	H16	136	91	-.02	-.02	-.02	30:1206:27.09	-1.08	1206:31.79	1	5.78	34.10	31.69	MKII	6	MKII	6	MKII	6

STATION:LEMREWAY CODE:DU9 TYPE:DURH II LAT:58 1.30 LONG: 6 26.33 ELEV: 50 M PN CORR: 0.01 S

	SHOT	W.D	S.D	PNDC	PSDC	PCDC	DAY H+M SECS	CL.ER	H+M SECS	CONF	T.T	DIST	T-D/6	E.SEI	G	N.SEI	G	V.SEI	G
		M	M	S	S	S		S			S	KM	S						
1	G8	102	91	-.03	-.03	-.03	29:1148:43.52	1.00	1249:53.08	1	8.56	50.87	53.00	MKII	7	MKII	7	MKII	7
2	G9	100	91	-.03	-.03	-.03	29:1308:21.83	1.00	1408:30.61	1	7.78	45.75	30.45	MKII	7	MKII	7	MKII	7
3	G10	110	91	-.03	-.03	-.03	29:1436:14.63	1.00	1536:22.71	1	7.08	41.95	22.62	MKII	7	MKII	7	MKII	7
4	G11	48	30	-.01	-.01	-.01	29:1706:19.96	1.00	1807:24.71	1	3.75	22.52	24.71	MKII	7	MKII	7	MKII	7
5	G12	63	45	-.01	-.01	-.01	29:1821:22.46	1.00	1921:26.14	1	2.69	16.21	26.16	MKII	7	MKII	7	MKII	7
6	G13	118	91	-.03	-.03	-.02	30: 805:46.96	1.00	805:49.77	1	1.81	10.71	49.75	MKII	7	MKII	7	MKII	7
7	G14	151	91	-.02	-.02	-.02	30: 942:55.52	1.00	1042:57.40	1	0.88	5.31	57.40	MKII	7	MKII	7	MKII	7
8	G15	40	30	-.01	-.01	-.01	39:1622: 5.00	-0.0	1722:14.26	2	9.26	46.05	12.68	MKII	6	MKII	6	MKII	6
9	G16	97	91	-.03	-.03	-.03	43:1021:14.04	-0.0	1121:24.61	2	10.57	55.02	23.21	MKII	6	MKII	6	MKII	6
10	G17	94	76	-.02	-.02	-.02	39:1419:25.42	-0.0	1519:38.35	2	12.93	66.77	36.55	MKII	6	MKII	6	MKII	6
11	G18	98	90	-.03	-.03	-.03	43:1233:54.78	-0.0	1334: 8.64	2	13.86	73.46	67.02	MKII	6	MKII	6	MKII	6
12	G19	70	45	-.01	-.01	-.01	39:1226:10.60	-0.0	1326: 0.0	5	0.0	85.29	24.82	MKII	6	MKII	6	MKII	6
13	G20	96	91	-.03	-.03	-.03	43:1441: 8.02	-0.0	1541:24.59	2	16.57	94.08	23.70	MKII	6	MKII	6	MKII	6
14	G21	143	91	-.02	-.02	-.02	39:1014:53.81	-0.0	1115: 0.0	5	0.0	106.31	71.53	MKII	6	MKII	6	MKII	6
15	G22	140	91	-.02	-.02	-.02	43:1705:40.99	-0.0	1806: 1.25	3	20.26	116.94	60.48	MKII	6	MKII	6	MKII	6
16	G23	153	91	-.02	-.02	-.01	43:1844:19.73	-0.0	1944:42.24	3	22.51	128.58	41.16	MKII	6	MKII	6	MKII	6
17	G24	164	91	-.01	-.01	-.01	46:1345:52.43	1.45	1446:16.06	3	22.98	141.75	77.50	MKII	8	MKII	8	MKII	8
18	G25	172	91	-.01	-.01	-.01	46:1227:36.95	1.45	1328: 0.0	5	0.0	151.27	63.61	MKII	8	MKII	8	MKII	8
19	G27	275	91	0.02	0.02	0.02	46: 905:31.91	1.45	1006: 0.0	5	0.0	171.88	61.99	MKII	8	MKII	8	MKII	8
20	G28	364	91	0.04	0.04	0.05	46: 731:33.42	1.45	832: 0.0	5	0.0	178.06	64.55	MKII	8	MKII	8	MKII	8
21	H9	124	91	-.03	-.02	-.02	30:2205:45.76	0.94	2205:56.00	2	9.30	57.13	56.22	MKII	6	MKII	6	MKII	6
22	H10	55	55	-.02	-.02	-.02	30:2039:48.51	0.94	2039: 0.0	5	0.0	50.99	57.95	MKII	6	MKII	6	MKII	6
23	H11	149	91	-.02	-.02	-.02	30:1911:32.66	0.94	1911:41.20	1	7.60	44.46	41.01	MKII	6	MKII	6	MKII	6
24	H12	122	91	-.03	-.03	-.02	30:1740:51.81	0.94	1740:59.33	1	6.58	37.31	58.97	MKII	6	MKII	6	MKII	6
25	H13	74	55	-.02	-.02	-.01	30:1608:45.21	0.96	1708:51.44	1	5.27	30.40	51.24	MKII	7	MKII	7	MKII	7
26	H14	75	60	-.02	-.02	-.02	30:1446:57.53	0.96	1547: 2.90	1	4.41	24.02	62.49	MKII	7	MKII	7	MKII	7
27	H15	73	73	-.03	-.03	-.03	30:1313:45.40	0.98	1413:49.13	1	2.75	15.70	49.00	MKII	7	MKII	7	MKII	7
28	H16	136	91	-.02	-.02	-.02	30:1206:27.09	0.98	1306:30.31	1	2.24	13.42	30.31	MKII	7	MKII	7	MKII	7
29	J1	63	45	-.01	-.01	-.01	34: 739:17.77	0.0	845:32.23	1	14.46	129.33	39.33	MKII	8	MKII	8	MKII	8
30	J2	118	91	-.03	-.03	-.02	47: 747:44.55	1.41	848: 6.69	3	20.73	129.70	67.58	MKII	7	MKII	7	MKII	7
31	J3	151	91	-.02	-.02	-.02	47:1033:40.40	0.0	1134: 3.79	2	23.39	138.44	53.47	MKII	7	MKII	7	MKII	7
32	J4	134	91	-.02	-.02	-.02	47:1319:38.06	0.0	1419: 0.0	5	0.0	160.39	64.79	MKII	7	MKII	7	MKII	7
33	J5	120	91	-.03	-.03	-.02	47:1606:27.28	-0.0	1706: 0.0	5	0.0	174.21	56.31	MKII	7	MKII	7	MKII	7
34	I3	55	55	-.02	-.02	-.02	32:1905:35.01	-0.0	2305:56.00	1	20.95	122.15	55.37	MKII	6	MKII	6	MKII	6
35	K1	1874	91	0.43	0.45	0.47	44: 906:15.17	1.57	1006: 0.0	5	0.0	203.81	50.71	MKII	6	MKII	6	MKII	6
36	K2	1950	91	0.47	0.49	0.51	45:1734:54.14	1.45	1839:28.52	2	32.93	216.18	91.62	MKII	8	MKII	8	MKII	8
37	K3	2052	91	0.49	0.52	0.54	44:1330:39.05	1.47	1431: 0.0	5	0.0	228.62	78.62	MKII	8	MKII	8	MKII	8
38	K4	2070	91	0.50	0.52	0.54	45:1309:54.85	1.45	1410: 0.0	5	0.0	236.05	95.64	MKII	8	MKII	8	MKII	8
39	K5	2088	91	0.50	0.53	0.55	44:1736:41.83	1.47	1837: 0.0	5	0.0	249.16	84.83	MKII	8	MKII	8	MKII	8
40	K6	2076	91	0.50	0.52	0.54	45: 821:28.00	1.45	922: 8.07	3	38.62	260.27	72.83	MKII	8	MKII	8	MKII	8
41	L9	1464	91	0.34	0.35	0.37	27:1820: 8.86	-0.0	1920: 0.0	5	0.0	248.74	50.32	MKII	7	MKII	7	MKII	7
42	L10	1416	91	0.32	0.34	0.35	27:1010:24.07	-0.0	1011: 0.0	5	0.0	261.99	67.73	MKII	7	MKII	7	MKII	7

STATION:HUSINISH CODE:DU10 TYPE:DURH II LAT:57 59.31 LONG: 7 4.78 ELEV: 0 M PN CORR: 0.0 S

	SHOT	W.D	S.D	PNDC	PSDC	PGDC	DAY H+M SECS	CL.ER	H+M SECS	CONF	T.T	DIST	T-D/6	E.SEI	G	N.SEI	G	V.SEI	G	NOLS
		M	M	S	S	S		S			S	KM	S							
1	G15	40	30	-.01	-.01	-.01	39:1622: 5.00	-0.17	1722: 6.03	1	1.20	8.05	6.17	MKII	5	MKII	5	MKII	5	1147
2	G16	97	91	-.03	-.03	-.03	43:1021:14.04	-0.61	1121:16.32	1	2.89	17.26	16.31	MKII	6	MKII	6	MKII	6	464
3	G17	94	76	-.02	-.02	-.02	39:1419:25.42	-0.15	1519:30.24	3	4.97	28.81	30.07	MKII	5	MKII	5	MKII	5	704
4	G18	98	90	-.03	-.03	-.03	43:1233:54.78	-0.64	1334: 0.39	1	6.25	35.64	60.08	MKII	6	MKII	6	MKII	6	607
6	G19	70	45	-.01	-.21	-.01	39:1226:10.60	-0.15	1326:18.00	1	7.55	47.34	18.34	MKII	6	MKII	6	MKII	6	2322
6	G20	96	91	-.03	-.03	-.03	43:1441: 8.02	-0.67	1546:16.38	2	9.03	56.23	16.72	MKII	6	MKII	6	MKII	6	336
7	G21	143	91	-.02	-.02	-.02	39:1014:53.81	-0.15	1115: 4.43	2	10.77	68.44	65.07	MKII	6	MKII	6	MKII	6	1084
6	G22	140	91	-.02	-.02	-.02	43:1705:40.99	-0.68	1805:53.16	2	12.85	79.08	53.49	MKII	6	MKII	6	MKII	6	1297
9	G23	153	91	-.02	-.02	-.01	43:1844:19.73	-0.67	1944:34.07	3	15.01	90.71	34.18	MKII	6	MKII	6	MKII	6	1259
10	G24	164	91	-.01	-.01	-.01	46:1345:52.43	-1.17	1446: 8.54	3	17.28	103.92	68.58	MKII	6	MKII	6	MKII	6	1752
11	G25	172	91	-.01	-.01	-.01	46:1227:36.95	-1.16	1327:54.61	3	18.82	113.44	54.70	MKII	6	MKII	6	MKII	6	2147
12	G26	218	91	-.00	0.00	0.00	46:1028:24.04	-1.16	1128:43.81	3	20.93	123.70	43.50	MKII	6	MKII	6	MKII	6	1259
13	G27	275	91	0.02	0.02	0.02	46: 905:31.91	-1.15	1005:53.06	3	22.30	133.98	53.09	MKII	6	MKII	6	MKII	6	1382
14	G28	364	91	0.04	0.04	0.05	46: 731:33.42	-1.15	831:56.43	3	24.16	140.19	55.64	MKII	6	MKII	6	MKII	6	1242
15	J2	118	91	-.03	-.03	-.02	47: 747:44.55	-1.30	847:58.90	3	15.65	94.20	58.95	MKII	6	MKII	6	MKII	6	0
16	J3	151	91	-.02	-.02	-.02	47:1033:40.40	-1.31	0: 0.0	5	0.0	107.79	57.06	MKII	6	MKII	6	MKII	6	0
17	J4	134	91	-.02	-.02	-.02	47:1319:38.06	-1.32	1419:57.52	2	20.78	135.89	59.39	MKII	6	MKII	6	MKII	8	0
18	J5	120	91	-.03	-.03	-.02	47:1606:27.28	-1.32	1707:50.89	2	24.93	153.00	51.46	MKII	6	MKII	6	MKII	6	0
19	J7	90	76	-.03	-.02	-.02	48: 741:49.34	-1.44	0: 0.0	5	0.0	208.17	82.60	MKII	6	MKII	6	MKII	6	0
20	J8	132	91	-.02	-.02	-.02	49:1030:32.38	-1.46	0: 0.0	6	0.0	238.69	70.73	MKII	6	MKII	6	MKII	6	0
21	K1	1824	91	0.43	0.45	0.47	44: 905:15.17	-0.82	1006:42.07	3	27.72	165.97	42.01	MKII	6	MKII	6	MKII	6	1538
22	K2	1950	91	0.47	0.49	0.51	45:1734:54.14	-1.09	1835:21.27	3	28.22	178.38	82.78	MKII	8	MKII	8	MKII	8	4680
23	K3	2052	91	0.49	0.52	0.54	44:1330:39.05	-0.85	1431: 8.24	3	30.04	190.82	70.00	MKII	8	MKII	8	MKII	8	2079
24	K4	2070	91	0.50	0.52	0.54	45:1309:54.85	-1.06	1410:24.36	3	30.57	198.26	86.83	MKII	8	MKII	8	MKII	8	1846
25	K5	2088	91	0.50	0.53	0.55	44:1736:41.83	-0.88	1837:13.03	3	32.08	211.40	76.18	MKII	8	MKII	8	MKII	8	1459
26	K6	2076	91	0.50	0.52	0.54	45: 821:28.00	-1.00	922: 1.10	2	34.10	222.48	64.08	MKII	8	MKII	8	MKII	8	1812
27	K11	1872	91	0.45	0.47	0.48	36:1810:54.25	-3.38	1911: 0.0	5	0.0	275.12	96.72	MKII	8	MKII	8	MKII	8	914
28	K12	1710	91	0.40	0.42	0.44	36:1336:21.18	-3.38	1436:59.86	3	42.06	288.28	65.85	MKII	8	MKII	8	MKII	8	1508

STATION:MAARUIG CODE:DU11 TYPE:DURH II LAT:57 57.18 LONG: 6 44.62 ELEV: 20 M PN CORR: 0.0 S

	SHOT	W.D	S.D	PNDC	PSDC	PGDC	DAY H+M SECS	CL.ER	H+M SECS	CONF	T.T	DIST	T-D/6	E.SEI	G	N.SEI	G	V.SEI	G
		M	M	S	S	S		S			S	KM	S						
1	G15	40	30	-.01	-.01	-.01	39:1622: 5.00	-2.42	1722: 6.83	1	4.25	2[illegible].77	7.21	MKII	6	MKII	6	MKII	6
2	G16	97	91	-.03	-.03	-.03	43:1021:14.04	-3.00	1121:17.04	1	6.00	37.51	17.29	MKII	6	MKII	6	MKII	6
3	G17	94	76	-.02	-.02	-.02	39:1419:25.42	-2.42	1519:30.94	1	7.94	48.89	31.15	MKII	6	MKII	6	MKII	6
4	G18	98	90	-.03	-.03	-.03	43:1233:54.78	-3.00	1334: 1.05	1	9.27	55.81	61.08	MKII	6	MKII	6	MKII	6
5	G19	70	45	-.01	-.01	-.01	39:1226:10.60	-2.44	1326:18.66	1	10.50	67.36	19.39	MKII	6	MKII	6	MKII	6
6	G20	96	91	-.03	-.03	-.03	43:1441: 8.02	-3.05	1547:17.04	1	12.07	76.32	17.69	MKII	6	MKII	6	MKII	6
7	G21	143	91	-.02	-.02	-.02	39:1014:53.81	-2.44	1115: 5.26	1	13.89	88.49	66.12	MKII	6	MKII	6	MKII	6
8	G22	140	91	-.02	-.02	-.02	43:1705:40.99	-3.05	1805:53.73	3	15.79	99.13	54.46	MKII	6	MKII	6	MKII	6
9	G23	153	91	-.02	-.02	-.01	43:1844:19.73	-3.15	1944:34.37	2	17.79	110.74	35.04	MKII	6	MKII	6	MKII	6
10	G24	164	91	-.01	-.01	-.01	46:1345:52.43	-3.35	1446: 9.47	2	20.39	123.96	69.74	MKII	6	MKII	6	MKII	6
11	G25	172	91	-.01	-.01	-.01	46:1227:36.95	-3.35	1327:55.36	2	21.76	133.47	55.85	MKII	8	MKII	8	MKII	8
12	G26	218	91	-.00	0.00	0.00	46:1028:24.04	-3.35	1128:43.97	2	23.28	143.73	44.65	MKII	8	MKII	8	MKII	8
13	G27	275	91	0.02	0.02	0.02	46: 905:31.91	-3.35	1005:53.73	2	25.17	154.00	54.23	MKII	8	MKII	8	MKII	8
14	G28	364	91	0.04	0.04	0.05	46: 731:33.42	-3.35	831:56.43	2	26.36	160.18	56.77	MKII	8	MKII	8	MKII	8
15	H9	124	91	-.03	-.02	-.02	30:2205:45.76	0.09	2305:56.33	1	10.48	64.25	56.56	MKII	7	MKII	7	MKII	7
16	H10	55	55	-.02	-.02	-.02	30:2039:48.51	0.10	2139:58.32	1	9.71	57.93	58.27	MKII	7	MKII	7	MKII	7
17	H11	149	91	-.02	-.02	-.02	30:1911:32.66	0.10	2011:41.51	1	8.75	50.83	41.23	MKII	7	MKII	7	MKII	7
18	H12	120	91	-.03	-.03	-.02	30:1740:51.81	0.10	1840:59.66	1	7.75	43.62	59.18	MKII	7	MKII	7	MKII	7
19	H13	74	55	-.02	-.02	-.01	30:1608:45.21	0.11	1708:51.92	1	6.60	36.11	51.34	MKII	7	MKII	7	MKII	7
20	H14	75	60	-.02	-.02	-.02	30:1446:57.53	0.12	1547: 2.89	1	5.24	28.62	62.42	MKII	7	MKII	7	MKII	7
21	H15	73	73	-.03	-.03	-.03	30:1313:45.40	0.15	1413:49.03	1	3.48	19.08	48.73	MKII	7	MKII	7	MKII	7
22	H16	136	91	-.02	-.02	-.02	30:1206:27.09	0.15	1306:29.98	1	2.74	15.51	29.83	MKII	7	MKII	7	MKII	7
23	J1	63	45	-.01	-.01	-.01	34: 739:17.77	-0.20	839:35.35	1	17.78	110.48	35.98	MKII	8	MKII	8	MKII	8
24	J2	118	91	-.03	-.03	-.02	47: 747:44.55	-3.43	847:58.98	1	17.86	110.12	59.47	MKII	6	MKII	6	MKII	6
25	J3	151	91	-.02	-.02	-.02	47:1033:40.40	-3.43	0: 0.0	5	0.0	119.52	56.89	MKII	6	MKII	6	MKII	6
26	J4	134	91	-.02	-.02	-.02	47:1319:38.06	-3.44	1419:56.38	1	21.76	143.21	58.49	MKII	6	MKII	6	MKII	6
27	J5	120	91	-.03	-.03	-.02	47:1606:27.28	-3.46	1706:49.27	1	25.45	158.18	50.18	MKII	6	MKII	6	MKII	6
28	J7	90	76	-.03	-.02	-.02	48: 741:49.34	-3.50	842:17.00	4	31.16	209.41	80.74	MKII	6	MKII	6	MKII	6
29	J8	132	91	-.02	-.02	-.02	48:1030:32.38	-3.51	1000: 0.0	5	0.0	238.68	68.65	MKII	6	MKII	6	MKII	6
30	K1	1824	91	0.43	0.45	0.47	44: 906:15.17	-3.16	1006: 0.0	5	0.0	185.97	43.00	MKII	6	MKII	6	MKII	6
31	K2	1950	91	0.47	0.49	0.51	45:1734:54.14	-3.28	1835:21.51	2	30.65	198.40	83.93	MKII	8	MKII	8	MKII	8
32	K3	2052	91	0.49	0.52	0.54	44:1330:39.05	-3.16	1431: 8.12	2	32.23	210.83	71.03	MKII	8	MKII	8	MKII	8
33	K4	2070	91	0.50	0.52	0.54	45:1309:54.85	-3.26	1410:24.48	3	32.89	218.28	87.97	MKII	8	MKII	8	MKII	8
34	K5	2088	91	0.50	0.53	0.55	44:1736:41.83	-3.20	1837:14.12	2	35.49	231.43	77.20	MKII	8	MKII	8	MKII	8
35	K6	2076	91	0.50	0.52	0.54	45: 821:28.00	-3.25	922: 1.91	3	37.16	242.50	65.17	MKII	8	MKII	8	MKII	8
36	K7	2016	91	0.49	0.51	0.53	37:1446:39.42	-1.86	1547:14.94	2	37.38	254.38	79.96	MKII	6	MKII	6	MKII	6
37	L9	1464	91	0.34	0.35	0.37	27:1820: 8.86	-0.11	1919:46.00	2	37.25	243.61	49.35	MKII	7	MKII	7	MKII	7
38	L10	1416	91	0.32	0.34	0.35	27:1010:24.07	-0.12	1110: 2.40	3	38.45	257.03	66.79	MKII	6	MKII	6	MKII	6
39	L11	1365	91	0.31	0.32	0.34	26:1235:30.74	-0.09	1335:10.49	2	39.84	267.85	75.29	MKII	6	MKII	6	MKII	6

STATION:N.UIST CODE:DU12 TYPE:DURH III LAT:57 38.80 LONG: 7 21.06 ELEV: 20 M PN CORR: 0.0 S

	SHOT	W.D M	S.D M	PNDC S	PSDC S	PGDC S	DAY H+M SECS	CL.ER S	H+M SECS	CONF	T.T S	DIST KM	T-D/6 S	E.SEI	G	N.SEI	G	V.SEI	G
1	G7	45	45	-.02	-.02	-.02	29:1008:59.30	-0.0	1109: 0.0	5	0.0	116.46	78.71	MKIII	6	MKIII	6	MKIII	6
2	G8	102	91	-.03	-.03	-.03	29:1148:43.52	-0.0	1248: 0.0	5	0.0	112.59	62.28	MKIII	6	MKIII	6	MKIII	6
3	G9	100	91	-.03	-.03	-.03	29:1308:21.83	-0.0	1408: 0.0	5	0.0	107.66	39.77	MKIII	6	MKIII	6	MKIII	6
4	G10	110	91	-.03	-.03	-.03	29:1436:14.63	-0.0	1536: 0.0	5	0.0	103.98	31.96	MKIII	6	MKIII	6	MKIII	6
5	G11	48	30	-.01	-.01	-.01	29:1706:19.96	-0.0	1806: 0.0	5	0.0	86.01	34.29	MKIII	6	MKIII	6	MKIII	6
6	G12	63	45	-.01	-.01	-.01	29:1821:22.46	-0.0	1921: 0.0	5	0.0	80.26	35.84	MKIII	6	MKIII	6	MKIII	6
7	G13	118	91	-.03	-.03	-.02	30: 805:46.96	-0.0	905: 0.0	5	0.0	75.78	59.59	MKIII	6	MKIII	6	MKIII	6
8	G14	151	91	-.02	-.02	-.02	30: 942:55.52	-0.0	1043: 0.0	5	0.0	71.04	67.36	MKIII	6	MKIII	6	MKIII	6
9	G15	40	30	-.01	-.01	-.01	39:1622: 5.00	0.35	1722:11.56	1	6.21	37.04	11.52	MKIII	6	MKIII	6	MKIII	6
10	G16	97	91	-.03	-.03	-.03	43:1021:14.04	0.60	1121:21.14	1	6.50	40.18	21.34	MKIII	8	MKIII	8	MKIII	8
11	G17	94	76	-.02	-.02	-.02	39:1419:25.42	0.35	1419:32.54	1	6.77	40.45	32.51	MKIII	6	MKIII	6	MKIII	6
12	G18	98	90	-.03	-.03	-.03	43:1233:54.78	0.60	1334: 2.98	1	7.60	44.74	62.84	MKIII	8	MKIII	8	MKIII	8
13	G19	70	45	-.01	-.01	-.01	39:1226:10.60	0.35	1326:18.63	1	7.68	49.33	19.17	MKIII	6	MKIII	6	MKIII	6
14	G20	96	91	-.03	-.03	-.03	43:1441: 8.02	0.61	1541:17.48	1	8.85	56.62	18.07	MKIII	8	MKIII	8	MKIII	8
15	G21	143	91	-.02	-.02	-.02	39:1014:53.81	0.35	1115: 4.40	1	10.24	65.61	65.09	MKIII	6	MKIII	6	MKIII	6
16	G22	140	91	-.02	-.02	-.02	43:1705:40.99	0.61	1805:53.43	1	11.83	74.56	54.03	MKIII	8	MKIII	8	MKIII	8
17	G23	153	91	-.02	-.02	-.01	43:1844:19.73	0.62	1944:34.10	1	13.75	84.54	34.44	MKIII	8	MKIII	8	MKIII	8
18	G24	164	91	-.01	-.01	-.01	46:1345:52.43	0.78	1446: 9.14	2	15.93	96.78	69.34	MKIII	6	MKIII	6	MKIII	6
19	G25	172	91	-.01	-.01	-.01	46:1227:36.95	0.79	1327:55.03	3	17.29	105.49	55.32	MKIII	6	MKIII	6	MKIII	6
20	G26	218	91	-.00	0.00	0.00	46:1028:24.04	0.76	1128:44.08	2	19.28	115.19	44.00	MKIII	6	MKIII	6	MKIII	6
21	G27	275	91	0.02	0.02	0.02	46: 905:31.91	0.76	1005:53.20	2	20.53	124.85	53.48	MKIII	6	MKIII	6	MKIII	6
22	G28	364	91	0.04	0.04	0.05	46: 731:33.42	0.76	832:56.16	2	21.98	130.26	55.89	MKIII	6	MKIII	6	MKIII	6
23	H9	124	91	-.03	-.02	-.02	30:2205:45.76	0.26	2306: 0.37	2	14.35	87.61	60.62	MKIII	5	MKIII	5	MKIII	5
24	H11	149	91	-.02	-.02	-.02	30:1911:32.66	0.20	2011:45.87	2	13.01	76.90	45.68	MKIII	5	MKIII	5	MKIII	5
25	H12	120	91	-.03	-.03	-.02	30:1740:51.81	0.19	1841: 4.37	2	12.37	72.37	64.06	MKIII	5	MKIII	5	MKIII	5
26	H14	75	60	-.02	-.02	-.02	30:1446:57.53	0.17	1547: 8.53	3	10.83	63.02	68.20	MKIII	5	MKIII	5	MKIII	5
27	H15	73	73	-.03	-.03	-.03	30:1313:45.40	0.16	1413:55.59	2	10.03	59.55	55.48	MKIII	5	MKIII	5	MKIII	5
28	H16	136	91	-.02	-.02	-.02	30:1206:27.09	0.16	1306:36.96	1	9.71	58.38	36.98	MKIII	5	MKIII	5	MKIII	5
29	J1	63	45	-.01	-.01	-.01	34: 739:17.77	0.03	839:30.24	1	12.44	76.91	30.62	MKIII	7	MKIII	7	MKIII	7
30	J2	118	91	-.03	-.03	-.02	47: 747:44.55	0.84	847:56.30	1	10.91	65.49	56.31	MKIII	6	MKIII	6	MKIII	6
31	J3	151	91	-.02	-.02	-.02	47:1033:40.40	0.83	1133:52.42	2	11.19	70.03	52.90	MKIII	6	MKIII	6	MKIII	6
32	J4	134	91	-.02	-.02	-.02	47:1319:38.06	0.84	1419:52.99	2	14.09	94.79	54.70	MKIII	6	MKIII	6	MKIII	6
33	J5	120	91	-.03	-.03	-.02	47:1606:27.28	0.87	1706:46.24	3	18.09	111.66	46.76	MKIII	6	MKIII	6	MKIII	6
34	J7	90	76	-.03	-.02	-.02	48: 741:49.34	0.89	842:16.24	3	26.01	167.82	78.20	MKIII	6	MKIII	6	MKIII	6
35	J8	132	91	-.02	-.02	-.02	48:1030:32.38	0.92	1131: 3.79	3	30.49	194.24	66.51	MKIII	6	MKIII	6	MKIII	6
36	I3	55	55	-.02	-.02	-.02	32:1905:35.01	-0.0	2005: 0.0	5	0.0	190.28	66.72	MKIII	5	MKIII	5	MKIII	5
37	K1	1824	91	0.43	0.45	0.47	44: 906:15.17	0.66	1006:41.98	2	26.15	155.30	41.71	MKIII	8	MKIII	8	MKIII	8
38	K2	1950	91	0.47	0.49	0.51	45:1734:54.14	0.73	1835:22.12	2	27.25	167.68	82.82	MKIII	8	MKIII	8	MKIII	8
39	K3	2052	91	0.49	0.52	0.54	44:1330:39.05	0.66	1431: 8.91	1	29.20	179.82	69.68	MKIII	8	MKIII	8	MKIII	8
40	K4	2070	91	0.50	0.52	0.54	45:1309:54.85	0.72	1410:25.44	2	29.87	187.16	86.76	MKIII	8	MKIII	8	MKIII	8
41	K5	2088	91	0.50	0.53	0.55	44:1736:41.83	0.63	1837:13.82	2	31.36	200.28	75.84	MKIII	8	MKIII	8	MKIII	8
42	K6	2076	91	0.50	0.52	0.54	45: 821:28.00	0.72	922: 1.50	2	32.78	210.93	63.88	MKIII	8	MKIII	8	MKIII	8
43	K7	2016	91	0.49	0.51	0.53	37:1446:39.42	0.24	1547:13.75	1	34.09	223.16	76.85	MKIII	8	MKIII	8	MKIII	8
44	K11	1872	91	0.45	0.47	0.48	36:1810:54.25	0.19	1911:33.69	2	39.25	263.96	98.43	MKIII	8	MKIII	8	MKIII	8
45	K12	1710	91	0.40	0.42	0.44	36:1336:21.18	0.18	1436: 1.69	1	40.33	276.38	67.42	MKIII	7	MKIII	7	MKIII	7
46	K14	1704	91	0.40	0.42	0.44	35:1104:56.75	0.12	1206:40.23	1	43.36	301.92	107.19	MKIII	7	MKIII	7	MKIII	7
47	L9	1464	91	0.34	0.35	0.37	27:1820: 8.86	-0.0	0: 0.0	5	0.0	254.52	51.28	MKIII	6	MKIII	6	MKIII	6
48	L10	1416	91	0.32	0.34	0.35	27:1010:24.07	-0.0	0: 0.0	5	0.0	268.04	68.74	MKIII	6	MKIII	6	MKIII	6
49	L11	1365	91	0.31	0.32	0.34	26:1235:30.74	-0.0	0: 0.0	5	0.0	278.66	77.18	MKIII	6	MKIII	6	MKIII	6

STATION:L.TORRID CODE:DU13 TYPE:DURH III LAT:57 33.60 LONG: 5 46.30 ELEV:130 M PN CORR: 0.01 S

	SHOT	W.D	S.D	PNDC	PSDC	PGDC	DAY H+M SECS	CL.ER	H+M SECS	CONF	T.T	DIST	T-D/6	E.SEI	G	N.SEI	G	V.SEI	G
		M	M	S	S	S		S			S	KM	S						
1	G7	45	45	-.02	-.02	-.02	29:1008:59.30	-0.09	1109: 7.93	1	8.72	51.59	67.81	MKII	7	MKII	7	MKII	7
2	G8	102	91	-.03	-.03	-.03	29:1148:43.52	-0.09	1248:52.19	1	8.76	50.82	51.90	MKII	7	MKII	7	MKII	7
3	G9	100	91	-.03	-.03	-.03	29:1308:21.83	-0.10	1408:30.34	1	8.61	49.59	30.00	MKII	7	MKII	7	MKII	7
4	G10	110	91	-.03	-.03	-.03	29:1436:14.63	-0.10	1536:23.04	1	8.51	48.95	22.69	MKII	7	MKII	7	MKII	7
5	G11	48	30	-.01	-.01	-.01	29:1706:19.96	-0.10	1806:28.50	1	8.64	51.59	28.46	MKII	7	MKII	7	MKII	7
6	G12	63	45	-.01	-.01	-.01	29:1821:22.46	-0.10	1921:31.46	1	9.10	53.96	31.35	MKII	7	MKII	7	MKII	7
7	G13	118	91	-.03	-.03	-.02	30: 805:46.96	-0.11	905:56.50	1	9.65	57.09	56.37	MKII	7	MKII	7	MKII	7
8	G14	151	91	-.02	-.02	-.02	30: 942:55.52	-0.11	1043: 5.56	1	10.15	60.27	65.46	MKII	7	MKII	7	MKII	7
9	G15	40	30	-.01	-.01	-.01	39:1622: 5.00	-5.59	1722: 0.0	5	0.0	97.15	15.60	MKII	5	MKII	5	MKII	5
10	G16	97	91	-.03	-.03	-.03	43:1021:14.04	-5.60	1121: 0.0	5	0.0	107.31	26.32	MKII	5	MKII	5	MKII	5
11	G17	94	76	-.02	-.02	-.02	39:1419:25.42	-5.60	0: 0.0	5	0.0	117.10	39.34	MKII	5	MKII	5	MKII	5
12	G18	98	90	-.03	-.03	-.03	43:1233:54.78	-5.61	1334: 9.61	4	20.44	124.06	69.85	MKII	5	MKII	5	MKII	5
13	G19	70	45	-.01	-.01	-.01	39:1226:10.60	-5.61	1326:26.41	2	21.42	134.20	27.36	MKII	5	MKII	5	MKII	5
14	G20	96	91	-.03	-.03	-.03	43:1441: 8.02	-5.55	1541:24.72	3	22.25	143.13	26.32	MKII	5	MKII	5	MKII	5
15	G21	143	91	-.02	-.02	-.02	39:1014:53.81	-5.61	1115:12.17	1	23.97	154.56	73.96	MKII	6	MKII	6	MKII	6
16	G22	140	91	-.02	-.02	-.02	43:1705:40.99	-5.55	1806: 0.69	3	25.25	164.80	62.91	MKII	6	MKII	6	MKII	6
17	G23	153	91	-.02	-.02	-.01	43:1844:19.73	-5.62	1944:40.86	3	26.75	175.91	43.43	MKII	6	MKII	6	MKII	6
18	G24	164	91	-.01	-.01	-.01	46:1345:52.43	-5.64	1446:15.40	2	28.61	188.87	78.27	MKII	6	MKII	6	MKII	6
19	G25	172	91	-.01	-.01	-.01	46:1227:36.95	-5.67	1328: 0.0	5	0.0	198.08	64.29	MKII	6	MKII	6	MKII	6
20	G26	218	91	-.00	0.00	0.00	46:1028:24.04	-5.65	1128:50.35	3	31.96	208.13	53.08	MKII	6	MKII	6	MKII	6
21	G27	275	91	0.02	0.02	0.02	46: 905:31.91	-5.67	1006: 0.0	5	0.0	218.13	62.60	MKII	7	MKII	7	MKII	7
22	G28	364	91	0.04	0.04	0.05	46: 731:33.42	-5.65	832: 1.81	3	34.04	223.87	65.08	MKII	7	MKII	7	MKII	7
23	H9	124	91	-.03	-.02	-.02	30:2205:45.76	-0.13	2305:47.18	1	1.55	8.32	47.02	MKII	7	MKII	7	MKII	7
24	H10	55	55	-.02	-.02	-.02	30:2039:48.51	-0.13	2139:50.85	1	2.47	14.62	50.82	MKII	7	MKII	7	MKII	7
25	H11	149	91	-.02	-.02	-.02	30:1911:32.66	-0.12	2011:36.45	1	3.91	21.73	36.16	MKII	7	MKII	7	MKII	7
26	H12	120	91	-.03	-.03	-.02	30:1740:51.81	-0.12	1840:56.93	1	5.24	29.97	56.52	MKII	7	MKII	7	MKII	7
27	H13	74	55	-.02	-.02	-.01	30:1608:45.21	-0.12	1708:51.54	1	6.45	36.51	51.18	MKII	7	MKII	7	MKII	7
28	H14	75	60	-.02	-.02	-.02	30:1446:57.53	-0.12	1547: 5.10	1	7.69	44.03	64.75	MKII	7	MKII	7	MKII	7
29	H15	73	73	-.03	-.03	-.03	30:1313:45.40	-0.11	1413:54.66	1	9.37	54.03	54.29	MKII	5	MKII	5	MKII	5
30	H16	136	91	-.02	-.02	-.02	30:1206:27.09	-0.11	1206:36.91	1	9.93	57.88	36.63	MKII	6	MKII	6	MKII	6
31	J1	63	45	-.01	-.01	-.01	34: 739:17.77	-5.55	839:38.94	3	26.72	171.01	40.72	MKII	6	MKII	6	MKII	6
32	J2	118	91	-.03	-.03	-.02	47: 747:44.55	-5.69	848: 3.66	2	24.80	159.18	65.39	MKII	6	MKII	6	MKII	6
33	J3	151	91	-.02	-.02	-.02	47:1033:40.40	-5.69	1133:59.72	1	25.01	154.18	60.41	MKII	6	MKII	6	MKII	6
34	J4	134	91	-.02	-.02	-.02	47:1319:38.06	-5.70	1419:57.35	2	24.99	160.19	59.06	MKII	6	MKII	6	MKII	6
35	J5	120	91	-.03	-.03	-.02	47:1606:27.28	-5.70	1706:47.75	2	26.17	165.92	49.23	MKII	6	MKII	6	MKII	6
36	J7	90	76	-.03	-.02	-.02	48: 741:49.34	-5.70	841: 0.0	5	0.0	198.01	76.64	MKII	5	MKII	5	MKII	5
37	J8	152	91	-.02	-.02	-.02	48:1030:32.38	-5.70	1131: 0.0	5	0.0	220.09	63.36	MKII	7	MKII	7	MKII	7
38	I3	55	55	-.02	-.02	-.02	32:1905:35.01	-5.43	2005:50.83	2	21.25	131.02	51.42	MKII	7	MKII	7	MKII	7
39	K1	1824	91	0.43	0.45	0.47	44: 906:15.17	-5.63	1006:47.00	3	37.46	249.31	51.09	MKII	7	MKII	7	MKII	7
40	K2	1950	91	0.47	0.49	0.51	45:1734:54.14	-5.65	1835:27.03	2	38.54	261.76	92.12	MKII	7	MKII	7	MKII	7
41	K3	2052	91	0.49	0.52	0.54	44:1330:39.05	-5.64	1431:13.67	2	40.26	274.03	79.08	MKII	7	MKII	7	MKII	7
42	K4	2070	91	0.50	0.52	0.54	45:1309:54.85	-5.65	1410:30.12	2	40.92	281.43	96.10	MKII	7	MKII	7	MKII	7
43	K5	2088	91	0.50	0.53	0.55	44:1736:41.83	-5.65	0: 0.0	5	0.0	294.59	85.28	MKII	7	MKII	7	MKII	7
44	K6	2076	91	0.50	0.52	0.54	45: 821:28.00	-5.65	922: 6.61	3	44.26	305.37	73.24	MKII	7	MKII	7	MKII	7
45	K7	2016	91	0.49	0.51	0.53	37:1446:39.42	-5.54	1447:19.10	3	45.22	317.55	86.80	MKII	7	MKII	7	MKII	7
46	K9	1968	91	0.47	0.49	0.51	37: 906:42.43	-5.53	0: 0.0	5	0.0	339.52	93.49	MKII	7	MKII	7	MKII	7
47	K11	1872	91	0.45	0.47	0.48	36:1810:54.25	-5.51	0: 0.0	5	0.0	358.43	108.48	MKII	7	MKII	7	MKII	7
48	K12	1710	91	0.40	0.42	0.44	36:1336:21.18	-5.50	1437: 7.19	3	51.51	370.99	77.51	MKII	7	MKII	7	MKII	7
49	K14	1704	91	0.40	0.42	0.44	35:1104:56.75	-5.50	0: 0.0	5	0.0	396.59	117.35	MKII	7	MKII	7	MKII	7
50	L9	1464	91	0.34	0.35	0.37	27:1820: 8.86	-0.05	1920:53.78	4	44.97	313.63	61.08	MKII	7	MKII	7	MKII	7
51	L10	1416	91	0.32	0.34	0.35	27:1010:24.07	-0.05	1011:11.04	3	47.02	326.90	78.50	MKII	7	MKII	7	MKII	7
52	L11	1365	91	0.31	0.32	0.34	26:1235:30.74	-0.03	1336:18.96	4	48.25	337.70	86.99	MKII	7	MKII	7	MKII	7

STATION:L.CARRON CODE:DU14 TYPE:DURH III LAT:57 23.19 LONG: 5 25.60 ELEV: 60 M PN CORR: 0.01 S

	SHOT	W.D	S.D	PNDC	PSDC	PGDC	DAY H+M SECS	CL.ER	H+M SECS	CONF	T.T	DIST	T-D/6	E.SEI	G	N.SEI	G	V.SEI	G
		M	M	S	S	S		S			S	KM	S						
1	G7	45	45	-.02	-.02	-.02	29:1008:59.30	-0.11	835:10.63	1	11.44	68.63	70.63	MKII	6	MKII	6	MKII	6
2	G8	102	91	-.03	-.03	-.03	29:1140:43.52	-0.11	1248:55.11	1	11.70	69.42	54.98	MKII	6	MKII	6	MKII	6
3	G9	100	91	-.03	-.03	-.03	29:1308:21.83	-0.11	1408:33.42	1	11.70	69.98	33.38	MKII	6	MKII	6	MKII	6
4	G10	110	91	-.03	-.03	-.03	29:1436:14.63	-0.11	1536:26.38	1	11.86	70.58	26.28	MKII	6	MKII	6	MKII	6
5	G11	48	30	-.01	-.01	-.01	29:1706:19.96	-0.11	1806: 0.0	5	0.0	77.77	32.81	MKII	5	MKII	5	MKII	5
6	G12	63	45	-.01	-.01	-.01	29:1821:22.46	-0.11	1921:35.78	3	13.43	81.00	35.85	MKII	5	MKII	5	MKII	5
7	G13	118	91	-.03	-.03	-.02	30: 805:46.96	-0.15	906: 1.08	2	14.27	84.62	60.91	MKII	5	MKII	5	MKII	5
8	G14	151	91	-.02	-.02	-.02	30: 942:55.52	-0.18	1042:10.00	2	14.66	88.16	70.03	MKII	5	MKII	5	MKII	5
9	G15	40	30	-.01	-.01	-.01	39:1622: 5.00	-0.18	1722:24.58	2	19.76	124.80	25.62	MKII	5	MKII	5	MKII	5
10	G16	97	91	-.03	-.03	-.03	43:1021:14.04	-1.40	1120:34.46	2	21.82	134.90	35.12	MKII	5	MKII	5	MKII	5
11	G17	94	76	-.02	-.02	-.02	39:1419:25.42	0.0	1520:47.60	2	22.18	144.31	49.47	MKII	5	MKII	5	MKII	5
12	G18	98	90	-.03	-.03	-.03	43:1233:54.78	-1.42	1333:17.32	2	23.96	151.19	78.56	MKII	5	MKII	5	MKII	5
13	G19	70	45	-.01	-.01	-.01	39:1226:10.60	-1.00	1327:34.25	2	24.65	160.93	36.42	MKII	5	MKII	5	MKII	5
14	G20	96	91	-.03	-.03	-.03	43:1441: 8.02	-1.42	1540: 0.0	5	0.0	169.75	34.89	MKII	5	MKII	5	MKII	5
15	G21	143	91	-.02	-.02	-.02	39:1014:53.81	0.0	0: 0.0	5	0.0	180.89	83.96	MKII	5	MKII	5	MKII	5
16	G22	140	91	-.02	-.02	-.02	43:1705:40.99	-1.42	1804: 0.0	5	0.0	190.93	71.39	MKII	5	MKII	5	MKII	5
17	G23	153	91	-.02	-.02	-.01	43:1844:19.73	-1.44	1943:48.54	2	30.25	201.81	51.92	MKII	5	MKII	5	MKII	5
18	G24	164	91	-.01	-.01	-.01	46:1345:52.43	-1.66	1446:22.76	3	31.99	214.59	86.54	MKII	6	MKII	6	MKII	6
19	G25	172	91	-.01	-.01	-.01	46:1227:36.95	-1.70	1328: 0.0	5	0.0	223.64	72.52	MKII	6	MKII	6	MKII	6
20	G26	218	91	-.00	0.00	0.00	46:1028:24.04	-1.70	1128:57.43	3	35.69	233.56	61.27	MKII	6	MKII	6	MKII	6
21	G27	275	91	0.02	0.02	0.02	46: 905:31.91	-1.70	1006: 5.92	3	35.71	243.41	70.78	MKII	7	MKII	7	MKII	7
22	G28	364	91	0.04	0.04	0.05	46: 731:33.42	-1.64	832: 9.06	3	37.28	248.97	73.28	MKII	7	MKII	7	MKII	7
23	H9	124	91	-.03	-.02	-.02	30:2205:45.76	-0.21	2305:51.77	3	6.22	30.56	51.64	MKII	8	MKII	8	MKII	8
24	H10	55	55	-.02	-.02	-.02	30:2030:48.51	-0.22	2139:55.40	2	7.11	42.90	55.44	MKII	8	MKII	8	MKII	8
25	H11	149	91	-.02	-.02	-.02	30:1911:32.66	-0.21	2011:40.97	2	8.52	49.98	40.78	MKII	8	MKII	8	MKII	8
26	H12	120	91	-.03	-.03	-.02	30:1740:51.81	-0.21	1841: 1.41	3	9.81	57.26	61.14	MKII	8	MKII	8	MKII	8
27	H13	74	55	-.02	-.02	-.01	30:1608:45.21	-0.20	1708:56.03	2	11.02	64.81	55.81	MKII	5	MKII	5	MKII	5
28	H14	75	60	-.02	-.02	-.02	30:1446:57.53	-0.20	1547: 9.60	3	12.27	72.33	69.38	MKII	5	MKII	5	MKII	5
29	H15	73	73	-.03	-.03	-.03	30:1313:45.40	-0.20	1413:59.19	3	13.99	82.34	58.92	MKII	5	MKII	5	MKII	5
30	H16	136	91	-.02	-.02	-.02	30:1206:27.09	-0.20	1306:41.40	3	14.51	86.19	41.26	MKII	5	MKII	5	MKII	5
31	J1	63	45	-.01	-.01	-.01	34: 739:17.77	-0.43	839: 0.0	5	0.0	195.74	49.96	MKII	6	MKII	6	MKII	6
32	J2	118	91	-.03	-.03	-.02	47: 747:44.55	0.0	834:12.28	3	27.73	181.14	74.74	MKII	6	MKII	6	MKII	6
33	J3	151	91	-.02	-.02	-.02	47:1033:40.40	-1.78	1134: 6.46	3	27.84	172.31	67.34	MKII	6	MKII	6	MKII	6
34	J4	134	91	-.02	-.02	-.02	47:1319:38.06	-1.76	1419: 3.43	3	27.16	172.49	65.05	MKII	6	MKII	6	MKII	6
35	J5	120	91	-.03	-.03	-.02	47:1606:27.28	-1.86	0: 0.0	5	0.0	174.69	54.54	MKII	6	MKII	6	MKII	6
36	J7	90	76	-.03	-.02	-.02	48: 741:49.34	0.0	0: 0.0	5	0.0	197.99	82.34	MKII	5	MKII	5	MKII	5
37	J8	132	91	-.02	-.02	-.02	48:1030:32.38	0.0	0: 0.0	5	0.0	216.36	68.44	MKII	5	MKII	5	MKII	5
38	I3	55	55	-.02	-.02	-.02	32:1905:35.01	-0.46	2005:57.35	2	22.80	139.94	57.87	MKII	5	MKII	5	MKII	5
39	K1	1824	91	0.43	0.45	0.47	44: 906:15.17	-1.50	1006:54.62	3	40.95	274.15	59.36	MKII	7	MKII	7	MKII	7
40	K2	1950	91	0.47	0.49	0.51	45:1734:54.14	-1.66	1839:34.51	2	42.03	286.54	100.24	MKII	7	MKII	7	MKII	7
41	K3	2052	91	0.49	0.52	0.54	44:1330:39.05	-1.52	1431:21.16	2	43.63	298.70	87.31	MKII	7	MKII	7	MKII	7
42	K4	2070	91	0.50	0.52	0.54	45:1309:54.85	-1.60	1410:37.36	2	44.11	306.04	104.26	MKII	7	MKII	7	MKII	7
43	K5	2088	91	0.50	0.53	0.55	44:1736:41.83	-1.55	1837:26.00	3	45.72	319.15	93.47	MKII	7	MKII	7	MKII	7
44	K6	2076	91	0.50	0.52	0.54	45: 821:28.00	0.0	0: 0.0	5	0.0	329.79	82.96	MKII	7	MKII	7	MKII	7
45	K7	2016	91	0.49	0.51	0.53	37:1446:39.42	-0.83	1547:27.14	3	48.55	342.02	95.59	MKII	7	MKII	7	MKII	7
46	K9	1968	91	0.47	0.49	0.51	37: 906:42.43	-0.84	1007: 0.0	5	0.0	363.87	102.24	MKII	7	MKII	7	MKII	7
47	K11	1872	91	0.45	0.47	0.48	36:1810:54.25	-0.74	1912: 0.0	5	0.0	382.79	117.31	MKII	7	MKII	7	MKII	7
48	K12	1710	91	0.40	0.42	0.44	36:1336:21.18	-0.74	1437:14.70	2	54.26	395.12	86.29	MKII	7	MKII	7	MKII	7
49	K14	1704	91	0.40	0.42	0.44	35:1104:56.75	-0.66	1206: 0.0	5	0.0	420.59	126.19	MKII	7	MKII	7	MKII	7

STATION:ST.KILD2 CODE:DU15 TYPE:DURH III LAT:57 48.65 LONG: 8 33.75 ELEV: 12 M PN CORR: 0.0 S

	SHOT	W.D	S.D	PNDC	PSDC	PGDC	DAY H+M SECS	CL.ER	H+M SECS	CONF	T.T	DIST	T-D/6	V.SEI	G	NOLS
		M	M	S	S	S		S			S	KM	S			
1	G7	45	45	-.02	-.02	-.02	29:1008:59.30	0.0	0: 0.0	5	0.0	182.36	89.69	MKII	8	0
2	G8	102	91	-.03	-.03	-.03	29:1148:43.52	0.0	0: 0.0	5	0.0	178.18	73.22	MKII	8	0
3	G9	100	91	-.03	-.03	-.03	29:1308:21.83	0.0	0: 0.0	5	0.0	173.03	50.67	MKII	8	0
4	G10	110	91	-.03	-.03	-.03	29:1436:14.63	0.0	0: 0.0	5	0.0	169.20	42.83	MKII	8	0
5	G11	48	30	-.01	-.01	-.01	29:1706:19.96	0.0	0: 0.0	5	0.0	149.75	44.92	MKII	8	0
6	G12	63	45	-.01	-.01	-.01	29:1821:22.46	0.0	0: 0.0	5	0.0	143.38	46.38	MKII	6	0
7	G13	118	91	-.03	-.03	-.02	30: 805:46.96	0.0	0: 0.0	5	0.0	138.01	69.98	MKII	6	0
8	G14	151	91	-.02	-.02	-.02	30: 942:55.52	0.0	0: 0.0	5	0.0	132.44	77.59	MKII	8	664
9	G15	40	30	-.01	-.01	-.01	39:1622: 5.00	-0.01	0:18.25	1	13.26	82.08	18.57	MKII	8	0
10	G16	97	91	-.03	-.03	-.03	43:1021:14.04	-9.02	0:17.22	1	12.20	74.04	17.36	MKII	7	1340
11	G17	94	76	-.02	-.02	-.02	39:1419:25.42	0.01	0:35.70	1	10.27	62.37	35.83	MKII	6	1044
12	G18	98	91	-.03	-.03	-.03	43:1233:54.78	-9.08	0:55.08	1	9.38	56.65	55.14	MKII	7	1935
13	G19	70	45	-.01	-.01	-.01	39:1226:10.60	0.01	0:17.72	1	7.11	45.03	18.11	MKII	6	511
14	G20	96	91	-.03	-.03	-.03	43:1441: 8.02	-9.08	0: 5.37	1	6.43	38.16	5.30	MKII	7	1116
15	G21	143	91	-.02	-.02	-.02	39:1014:53.81	0.01	0:58.55	1	4.73	28.45	58.56	MKII	6	671
16	G22	140	91	-.02	-.02	-.02	43:1705:40.99	-9.08	0:35.68	1	3.77	22.78	35.71	MKII	6	1051
17	G23	153	91	-.02	-.02	-.01	43:1844:19.73	-9.08	0:14.28	1	3.63	20.92	14.14	MKII	6	1217
18	G24	164	91	-.01	-.01	-.01	46:1345:52.43	-9.14	0:48.00	1	4.71	26.86	47.77	MKII	7	397
19	G25	172	91	-.01	-.01	-.01	46:1227:36.95	-9.14	0:33.34	1	5.53	33.36	33.37	MKII	7	582
20	G26	218	91	-.00	0.00	0.00	46:1028:24.04	-9.14	0:22.50	2	7.60	41.93	21.89	MKII	7	1109
21	G27	275	91	0.02	0.02	0.02	46: 905:31.91	-9.14	0:31.88	2	9.11	50.95	31.26	MKII	7	1219
22	G28	364	91	0.04	0.04	0.05	46: 731:33.42	-9.14	0:34.30	2	10.02	56.03	33.62	MKII	7	1706
23	H9	124	91	-.03	-.02	-.02	30:2205:45.76	0.0	0: 0.0	5	0.0	161.17	72.62	MKII	8	0
24	H10	55	55	-.02	-.02	-.02	30:2039:48.51	0.0	0: 0.0	5	0.0	155.85	74.49	MKII	8	0
25	H11	149	91	-.02	-.02	-.02	30:1911:32.66	0.0	0: 0.0	5	0.0	149.55	57.59	MKII	8	0
25	H12	120	91	-.03	-.03	-.02	30:1740:51.81	0.0	0: 0.0	5	0.0	144.09	75.82	MKII	8	0
27	H13	74	55	-.02	-.02	-.01	30:1608:45.21	0.0	0: 0.0	5	0.0	138.09	68.22	MKII	8	0
28	H14	75	60	-.02	-.02	-.02	30:1446:57.53	0.0	0: 0.0	5	0.0	132.13	79.55	MKII	8	0
29	H15	73	73	-.03	-.03	-.03	30:1313:45.40	0.0	0: 0.0	5	0.0	125.59	66.33	MKII	8	0
30	H16	136	91	-.02	-.02	-.02	30:1206:27.09	0.0	0: 0.0	5	0.0	123.03	47.59	MKII	8	0
31	J1	63	45	-.01	-.01	-.01	34: 739:17.77	0.0	0: 0.0	5	0.0	3.26	18.31	MKII	7	0
32	J2	118	91	-.03	-.03	-.02	47: 747:44.55	-0.47	0:48.89	1	4.81	30.33	49.13	MKII	7	0
33	J3	151	91	-.02	-.02	-.02	47:1033:40.40	-0.47	0:49.76	2	9.83	63.11	50.45	MKII	7	0
34	J4	134	91	-.02	-.02	-.02	47:1319:38.06	-0.47	0:52.80	2	15.21	103.52	54.84	MKII	7	0
35	J5	120	91	-.03	-.03	-.02	47:1606:27.28	-0.47	0:47.52	1	20.71	126.38	47.87	MKII	7	0
36	J7	90	76	-.03	-.02	-.02	48: 741:49.34	-0.52	0: 0.0	5	0.0	190.44	80.56	MKII	7	0
37	J8	132	91	-.02	-.02	-.02	48:1030:32.38	0.0	0: 0.0	5	0.0	224.42	69.73	MKII	7	0
38	I3	55	55	-.02	-.02	-.02	32:1905:35.01	0.0	0: 0.0	5	0.0	245.93	76.00	MKII	8	0
39	K1	1824	91	0.43	0.45	0.47	44: 906:15.17	-9.07	0:21.35	1	15.25	80.85	19.57	MKII	7	750
40	K2	1950	91	0.47	0.49	0.51	45:1734:54.14	-9.12	0: 2.00	1	16.98	93.22	60.56	MKII	7	1253
41	K3	2052	91	0.49	0.52	0.54	44:1330:39.05	-9.09	0:48.97	1	19.01	105.39	47.52	MKII	7	1418
42	K4	2070	91	0.50	0.52	0.54	45:1309:54.85	-9.12	0: 5.40	2	19.67	112.75	64.52	MKII	7	1345
43	K5	2088	91	0.50	0.53	0.55	44:1736:41.83	-9.09	0:53.96	2	21.22	125.88	53.72	MKII	7	1444
44	K6	2076	91	0.50	0.52	0.54	45: 821:28.00	-9.10	0:41.64	2	22.74	136.62	41.67	MKII	7	303
45	K7	2016	91	0.49	0.51	0.53	37:1446:39.42	-3.66	0:59.93	3	24.17	148.82	60.56	MKII	7	305
46	K9	1968	91	0.47	0.49	0.51	37: 906:42.43	-3.80	0: 0.0	5	0.0	170.77	67.09	MKII	7	3
47	K11	1872	91	0.45	0.47	0.48	36:1810:54.25	-4.77	0: 0.0	5	0.0	189.68	81.09	MKII	7	1896
48	K12	1710	91	0.40	0.42	0.44	36:1336:21.18	-4.77	0:46.86	2	30.45	202.25	50.12	MKII	6	727
49	K14	1704	91	0.40	0.42	0.44	35:1104:56.75	-6.30	0:23.88	2	33.43	227.89	88.43	MKII	7	728

STATION:MULL   CODE:DU16 TYPE:DURH III LAT:56 19.20 LONG: 6 19.60 ELEV: 50 M PN CORR: 0.01 S

	SHOT	W.D	S.D	PNDC	PSDC	PGDC	DAY H+M SECS	CL.ER	H+M SECS	CONF	T.T	DIST	T-D/6	E.SEI	G	N.SEI	G	V.SEI	G
		M	M	S	S	S		S			S	KM	S						
1	G7	45	45	-.02	-.02	-.02	29:1008:59.30	-0.0	0: 0.0	5	0.0	193.67	91.53	MKIII	5	MKIII	5	MKIII	5
2	G8	102	91	-.03	-.03	-.03	29:1148:43.52	-0.0	0: 0.0	5	0.0	192.96	75.68	MKIII	5	MKIII	5	MKIII	5
3	G9	100	91	-.03	-.03	-.03	29:1308:21.83	-0.0	1407:51.64	3	29.81	191.49	53.74	MKIII	5	MKIII	5	MKIII	5
4	G10	110	91	-.03	-.03	-.03	29:1436:14.63	-0.0	0: 0.0	5	0.0	190.42	46.37	MKIII	5	MKIII	5	MKIII	5
5	G11	48	30	-.01	-.01	-.01	29:1706:19.96	-0.0	0: 0.0	5	0.0	187.40	51.19	MKIII	5	MKIII	5	MKIII	5
6	G12	63	45	-.01	-.01	-.01	29:1821:22.46	-0.0	0: 0.0	5	0.0	186.83	53.60	MKIII	6	MKIII	6	MKIII	6
7	G13	118	91	-.03	-.03	-.02	30: 805:46.96	-0.0	904:15.93	3	28.97	187.20	78.16	MKIII	6	MKIII	6	MKIII	6
8	G14	151	91	-.02	-.02	-.02	30: 942:55.52	-0.0	0: 0.0	5	0.0	187.26	86.73	MKIII	6	MKIII	6	MKIII	6
9	G16	40	30	-.01	-.01	-.01	39:1622:14.04	-0.32	1121:43.53	2	29.81	198.20	46.75	MKIII	6	MKIII	6	MKIII	6
10	G17	94	76	-.02	-.02	-.02	39:1419:25.42	-0.18	1519:55.45	3	30.21	200.65	58.68	MKIII	6	MKIII	6	MKIII	6
11	G18	98	90	-.03	-.03	-.03	43:1233:54.78	-0.30	1334:25.08	3	30.60	205.02	88.65	MKIII	6	MKIII	6	MKIII	6
12	G19	70	45	-.01	-.01	-.01	39:1226:10.60	-0.20	1326: 0.0	5	0.0	208.17	45.09	MKIII	6	MKIII	6	MKIII	6
13	G20	96	91	-.03	-.03	-.03	43:1441: 8.02	-0.30	1541:39.21	3	31.49	213.90	43.37	MKIII	6	MKIII	6	MKIII	6
14	G21	143	91	-.02	-.02	-.02	39:1014:53.81	-0.20	1115:25.77	3	32.16	219.72	90.23	MKIII	6	MKIII	6	MKIII	6
15	G22	140	91	-.02	-.02	-.02	43:1705:40.99	-0.30	1806:13.58	3	32.89	225.79	78.32	MKIII	6	MKIII	6	MKIII	6
16	G23	153	91	-.02	-.02	-.01	43:1844:19.73	-0.30	1944: 0.0	5	0.0	232.37	58.16	MKIII	6	MKIII	6	MKIII	6
17	G24	164	91	-.01	-.01	-.01	46:1345:52.43	-0.33	1446:27.19	3	35.09	241.18	92.30	MKIII	7	MKIII	7	MKIII	7
18	G25	172	91	-.01	-.01	-.01	46:1227:36.95	-0.33	1328:12.41	3	35.79	247.24	77.83	MKIII	7	MKIII	7	MKIII	7
19	G26	218	91	-.00	0.00	0.00	46:1028:24.04	-0.33	1128: 0.0	5	0.0	254.37	66.10	MKIII	7	MKIII	7	MKIII	7
20	G27	275	91	0.02	0.02	0.02	46: 905:31.91	-0.33	1006: 9.37	3	37.79	261.40	75.15	MKIII	7	MKIII	7	MKIII	7
21	G28	364	91	0.04	0.04	0.05	46: 731:33.42	-0.33	832:12.11	3	39.02	264.62	77.19	MKIII	7	MKIII	7	MKIII	7
22	H9	124	91	-.03	-.02	-.02	30:2205:45.76	-0.03	2305: 8.94	4	23.21	145.21	69.93	MKIII	6	MKIII	6	MKIII	6
23	H10	55	55	-.02	-.02	-.02	30:2039:48.51	-0.02	2146:12.31	4	23.82	141.56	73.25	MKIII	6	MKIII	6	MKIII	6
24	H11	149	91	-.02	-.02	-.02	30:1911:32.56	-0.02	2011:57.19	3	24.55	151.86	57.95	MKIII	6	MKIII	6	MKIII	6
25	H12	120	91	-.03	-.03	-.02	30:1740:51.81	-0.02	1849:17.15	3	25.36	156.84	77.93	MKIII	6	MKIII	6	MKIII	6
26	H13	74	55	-.02	-.02	-.01	30:1608:45.21	-0.01	1709:11.42	3	26.22	161.51	72.12	MKIII	6	MKIII	6	MKIII	6
27	H14	75	53	-.02	-.02	-.02	30:1446:57.53	-0.01	1547:24.29	3	26.77	166.21	85.22	MKIII	6	MKIII	6	MKIII	6
28	H15	73	73	-.03	-.03	-.03	30:1313:45.40	-0.01	1414:12.85	3	27.46	173.98	74.39	MKIII	6	MKIII	6	MKIII	6
29	H16	136	91	-.02	-.02	-.02	30:1206:27.09	-0.01	1306:54.56	3	27.48	176.85	56.55	MKIII	6	MKIII	6	MKIII	6
30	J2	118	91	-.03	-.03	-.02	47: 747:44.55	-0.39	848:12.57	3	28.41	187.33	75.38	MKIII	5	MKIII	5	MKIII	5
31	J3	151	91	-.02	-.0[illegible]	-.02	47:1033:40.40	-0.37	1134: 4.89	3	24.86	159.06	66.54	MKIII	5	MKIII	5	MKIII	5
32	J4	134	91	-.02	-.02	-.02	47:1319:38.06	-0.36	1419:59.44	3	21.74	129.18	59.23	MKIII	5	MKIII	5	MKIII	5
33	J7	90	76	-.03	-.02	-.02	48: 741:49.34	-0.0	841: 0.0	5	0.0	91.08	64.52	MKIII	4	MKIII	4	MKIII	4
34	J8	132	91	-.02	-.02	-.02	48:1030:32.38	-0.0	1131: 0.0	5	0.0	95.00	48.21	MKIII	4	MKIII	4	MKIII	4
35	I3	55	55	-.02	-.02	-.02	32:1905:35.01	-0.06	2006:13.82	3	38.8[illegible]	270.40	80.02	MKIII	6	MKIII	6	MKIII	6
36	K1	1824	91	0.43	0.45	0.47	44: 906:15.17	-0.32	1006:55.84	2	40.99	284.19	62.21	MKIII	6	MKIII	6	MKIII	6
37	K2	1950	91	0.47	0.49	0.51	45:1734:54.14	-0.33	1835:36.07	1	42.26	294.62	102.91	MKIII	7	MKIII	7	MKIII	7
38	K3	2052	91	0.49	0.52	0.54	44:1330:39.05	-0.32	1431:22.45	1	43.72	304.46	89.47	MKIII	8	MKIII	8	MKIII	8
39	K4	2070	91	0.50	0.52	0.54	45:1309:54.85	-0.32	1410:38.88	2	44.35	310.59	106.30	MKIII	8	MKIII	8	MKIII	8
40	K5	2088	91	0.50	0.53	0.55	44:1736:41.83	-0.32	1837:27.16	2	45.65	321.98	95.17	MKIII	8	MKIII	8	MKIII	8
41	K6	2076	91	0.50	0.52	0.54	45: 821:28.00	-0.32	922:14.74	2	47.06	330.44	82.75	MKIII	8	MKIII	8	MKIII	8

STATION:LAXAY CODE:MD1 TYPE:UKAEA LAT:58 6.50 LONG: 6 31.80 ELEV: 40 M PN CORR: 0.0 S

	SHOT	W.D	S.D	PNDC	PSDC	PGDC	DAY H+M SECS	CL.ER	H+M SECS	CONF	T.T	DIST	T-D/6	G	NOLS
		M	M	S	S	S		S			S	KM	S		
1	G7	45	45	-.02	-.02	-.02	29:1008:59.30	-0.09	1009: 9.80	1	10.59	61.56	69.47	1	510
2	G8	102	91	-.03	-.03	-.03	29:1148:43.52	-0.09	1148:53.33	1	9.90	57.34	52.59	1	437
3	G9	100	91	-.03	-.03	-.03	29:1308:21.83	-0.09	1308:30.86	1	9.12	52.39	30.47	1	590
4	G10	110	91	-.03	-.03	-.03	29:1436:14.63	-0.09	1436:22.92	1	8.38	48.75	22.67	1	689
5	G11	48	30	-.01	-.01	-.01	29:1706:19.96	-0.09	1706:25.19	1	5.32	30.37	24.93	1	512
6	G12	63	45	-.01	-.01	-.01	29:1821:22.46	-0.09	1821:26.76	1	4.39	24.74	26.49	1	331
7	G13	118	91	-.03	-.03	-.02	30: 805:46.96	-0.09	805:50.51	1	3.64	19.85	50.18	1	452
8	G14	151	91	-.02	-.02	-.02	30: 942:55.52	-0.09	942:58.33	1	2.90	15.66	58.04	1	591
9	G15	40	30	-.01	-.01	-.01	39:1622: 5.00	-0.11	1622:12.00	1	7.11	43.08	12.07	1	891
10	G16	97	91	-.03	-.03	-.03	43:1021:14.04	-0.12	1021:22.57	1	8.65	50.81	22.39	1	547
11	G17	94	76	-.02	-.02	-.02	39:1419:25.42	-0.11	1419:35.95	1	10.64	62.59	35.74	1	609
12	G18	98	90	-.03	-.03	-.03	43:1233:54.78	-0.12	1234: 6.48	1	11.82	68.89	66.14	1	365
13	G19	70	45	-.01	-.01	-.01	39:1226:10.60	-0.11	1226:23.57	1	13.08	80.84	23.96	1	945
14	G20	96	91	-.03	-.03	-.03	43:1441: 8.02	-0.12	1441:22.38	1	14.48	89.33	22.79	1	1250
15	G21	143	91	-.02	-.02	-.02	39:1014:53.81	-0.11	1015:10.14	1	16.44	101.51	70.62	1	562
16	G22	140	91	-.02	-.02	-.02	43:1705:40.99	-0.12	1705:59.00	1	18.13	112.04	59.54	1	1202
17	G23	153	91	-.02	-.02	-.01	43:1844:19.73	-0.12	1844:39.90	1	20.29	123.63	40.22	1	206
18	G24	164	91	-.01	-.01	-.01	46:1345:52.43	-0.12	1346:14.62	1	22.31	136.69	75.09	1	877
19	G25	172	91	-.01	-.01	-.01	46:1227:30.95	-0.12	1228: 0.28	1	23.45	146.18	61.19	1	694
20	G26	218	91	-.00	0.00	0.00	46:1028:24.04	-0.12	1028:49.17	2	25.25	156.37	49.98	1	741
21	G27	275	91	0.02	0.02	0.02	46: 905:31.91	-0.12	905:57.72	1	25.93	166.63	59.56	1	2003
22	G28	364	91	0.04	0.04	0.05	46: 731:33.42	-0.12	832: 0.59	1	27.29	172.97	62.13	1	700
23	H9	124	91	-.03	-.02	-.02	30:2205:45.76	-0.09	2205:57.00	1	11.33	68.12	57.02	1	567
24	H10	55	55	-.02	-.02	-.02	30:2039:48.51	-0.09	2039:58.73	1	10.31	62.01	58.76	1	654
25	H11	149	91	-.02	-.02	-.02	30:1911:32.66	-0.09	1911:42.35	1	9.78	55.51	41.82	1	435
26	H12	120	91	-.03	-.03	-.02	30:1740:51.81	-0.09	1741: 0.33	1	8.61	48.36	59.78	1	1059
27	H13	74	55	-.02	-.02	-.01	30:1608:45.21	-0.09	1608:52.79	1	7.67	41.40	52.02	1	76
28	H14	75	60	-.02	-.02	-.02	30:1446:57.53	-0.09	1446: 4.02	1	6.58	34.82	63.24	1	375
29	H15	73	73	-.03	-.03	-.03	30:1313:45.40	-0.09	1313:50.15	1	4.84	25.76	49.60	1	391
30	H16	136	91	-.02	-.02	-.02	30:1206:27.09	-0.09	1206:31.15	1	4.15	22.69	30.78	1	323
31	J1	63	45	-.01	-.01	-.01	34: 739:17.77	-0.10	839:38.20	3	20.53	125.84	38.64	1	0
32	J2	118	91	-.03	-.03	-.02	47: 747:44.55	-0.12	848: 5.62	2	21.19	129.03	65.93	1	0
33	J3	151	91	-.02	-.02	-.02	47:1033:40.40	-0.12	1034: 2.90	2	22.62	[illegible].33	63.67	1	0
34	J4	134	91	-.02	-.02	-.02	47:1319:38.06	-0.12	1320: 2.83	2	24.89	164.62	65.38	1	0
35	J5	120	91	-.03	-.03	-.02	47:1606:27.28	-0.12	1606:55.90	3	28.74	179.49	57.07	1	0
36	J7	90	76	-.03	-.02	-.02	48: 741:49.34	-0.12	741: 0.0	5	0.0	229.83	87.53	1	0
37	J8	132	91	-.02	-.02	-.02	48:1030:32.38	-0.12	1030: 0.0	5	0.0	258.55	75.35	1	0
38	I3	55	55	-.02	-.02	-.02	32:1905:35.01	-0.10	1905:55.27	2	20.36	122.32	55.30	1	0
39	K1	1924	91	0.43	0.45	0.47	44: 906:15.17	-0.12	906:46.66	1	31.61	198.61	48.15	10	311
40	K2	1950	91	0.47	0.49	0.51	45:1734:54.14	-0.12	1735:26.17	1	32.15	210.89	89.17	10	813
41	K3	2052	91	0.49	0.52	0.54	44:1330:39.05	-0.12	1331:13.00	1	34.07	223.30	76.15	10	764
42	K4	2070	91	0.50	0.52	0.54	45:1309:54.85	-0.12	1310:29.33	1	34.60	230.71	93.18	10	534
43	K5	2088	91	0.50	0.53	0.55	44:1736:41.83	-0.12	1737:17.86	1	36.15	243.75	82.33	10	930
44	K6	2076	91	0.50	0.52	0.54	45: 821:28.00	-0.12	822: 5.86	1	37.98	254.89	70.36	10	690
45	K7	2016	91	0.49	0.51	0.53	37:1446:39.42	-0.11	1547:18.33	2	39.02	266.52	83.73	10	969
46	K9	1968	91	0.47	0.49	0.51	37: 906:42.43	-0.11	907:23.48	3	41.16	288.57	90.41	10	1469
47	K11	1872	91	0.45	0.47	0.48	36:1810:54.25	-0.11	1811:37.90	2	43.76	307.09	105.32	10	1570
48	K12	1710	91	0.40	0.42	0.44	36:1336:21.18	-0.11	1337: 6.24	2	45.17	320.44	74.48	10	941
49	K14	1704	91	0.40	0.42	0.44	35:1104:56.75	-0.11	1106: 0.0	5	0.0	346.16	114.33	1	2353

STATION:BLAIRAT CODE:BLA TYPE:GS LAT:60 3.27 LONG:30 6.47 ELEV:514 M PN CORR: 0.06 S

	SHOT	W.D	S.D	PNDC	PSDC	PGDC	DAY H+M SECS	CL.ER	H+M SECS	CONF	T.T	DIST	T-D/6
		M	M	S	S	S		S			S	KM	S
1	G7	45	45	-.02	-.02	-.02	29:1008:59.30	0.78	1009:25.80	3	25.72	155.60	86.01
2	G8	102	91	-.03	-.03	-.03	29:1148:43.52	0.78	1149:10.49	3	26.19	158.53	70.72
3	G9	100	91	-.03	-.03	-.03	29:1308:21.83	0.78	1308:49.27	3	26.66	161.58	49.54
4	G10	110	91	-.03	-.03	-.03	29:1436:14.63	0.78	1436:42.39	3	26.98	163.87	42.72
5	G11	48	30	-.01	-.01	-.01	29:1706:19.96	0.78	1706:49.55	3	28.81	177.32	50.29
6	G12	63	45	-.01	-.01	-.01	29:1821:22.46	0.78	1810:52.40	3	29.16	181.96	53.57
7	G13	118	91	-.03	-.03	-.02	30: 805:46.96	0.80	811:17.00	3	29.24	186.47	78.84
8	G14	151	91	-.02	-.02	-.02	30: 942:55.52	0.80	943:26.03	3	29.71	190.85	88.13
9	H9	124	91	-.03	-.02	-.02	30:2205:45.76	0.82	2206:10.62	3	24.04	141.84	70.22
10	H10	55	55	-.02	-.02	-.02	30:2039:48.51	0.82	2040:14.41	3	25.08	145.11	74.02
11	H11	149	91	-.02	-.02	-.02	30:1911:32.66	0.82	1911:59.19	3	25.71	155.22	59.35
12	H12	120	91	-.03	-.03	-.02	30:1740:51.81	0.80	1741:19.31	3	26.70	162.35	79.67
13	H13	74	55	-.02	-.02	-.01	30:1608:45.21	0.80	1609:14.39	3	28.38	169.84	74.32
14	H14	75	60	-.02	-.02	-.02	30:1446:57.53	0.80	1447:27.29	3	28.96	177.33	87.88
15	H15	73	73	-.03	-.03	-.03	30:1313:45.40	0.80	1314:16.00	3	29.80	187.13	77.39
16	H16	136	91	-.02	-.02	-.02	30:1206:27.09	0.80	1206:58.21	3	30.32	190.94	59.71

STATION:DUNDEE CODE:DUN TYPE:LOWNET LAT:56 32.85 LONG: 3 0.85 ELEV: 50 M PN CORR: 0.01 S

	SHOT	W.D	S.D	PNDC	PSDC	PGDC	DAY H+M SECS	CL.ER	H+M SECS	CONF	T.T	DIST	T-D/6
		M	M	S	S	S		S			S	KM	S
1	G7	45	45	-.02	-.02	-.02	29:1008:59.30	0.20	1009:33.70	5	34.20	220.93	96.32
2	G8	102	91	-.03	-.03	-.03	29:1148:43.52	0.20	1149:18.23	3	34.51	224.15	81.08
3	G9	100	91	-.03	-.03	-.03	29:1308:21.83	0.20	1308:56.95	2	34.92	227.58	59.96
4	G10	110	91	-.03	-.03	-.03	29:1436:14.63	0.20	1436:49.81	2	34.98	230.13	53.19
5	G11	48	30	-.01	-.01	-.01	29:1706:19.96	0.20	1706:56.73	2	36.57	244.54	60.92
6	G12	63	45	-.01	-.01	-.01	29:1821:22.46	0.20	1810:59.78	2	37.12	249.41	64.23
7	G13	118	91	-.03	-.03	-.02	30: 805:46.96	0.34	811:24.55	2	37.25	254.06	89.64
8	G14	151	91	-.02	-.02	-.02	30: 942:55.52	0.35	943:33.58	2	37.71	258.58	98.97
9	H9	124	91	-.03	-.02	-.02	30:2205:45.76	0.44	2206:18.30	3	32.16	210.07	81.21
10	H10	55	55	-.02	-.02	-.02	30:2039:48.51	0.43	2040:21.87	3	32.93	216.33	85.00
11	H11	149	91	-.02	-.02	-.02	30:1911:32.66	0.40	1912: 6.30	3	33.24	223.43	70.30
12	H12	120	91	-.03	-.03	-.02	30:1740:51.81	0.40	1741:26.87	3	34.66	230.54	90.63
13	H13	74	55	-.02	-.02	-.01	30:1608:45.21	0.40	1609:21.40	3	35.79	238.02	85.28
14	H14	75	60	-.02	-.02	-.02	30:1446:57.53	0.35	1447:34.76	3	36.88	245.50	98.80
15	H15	73	73	-.03	-.03	-.03	30:1313:45.40	0.37	1314:23.63	3	37.86	255.26	88.31
16	H16	136	91	-.02	-.02	-.02	30:1206:27.09	0.37	1207: 5.70	3	38.24	259.05	70.63

STATION:ESKB4 CODE:ESB4 TYPE:UKAEA LAT:55 19.90 LONG: 3 9.58 ELEV:229 M PN CORR: 0.03 S

	SHOT	W.D	S.D	PNDC	PSDC	PGDC	DAY H+M SECS	CL.ER	H+M SECS	CONF	T.T	DIST	T-D/6
		M	M	S	S	S		S			S	KM	S
1	G7	45	45	-.02	-.02	-.02	29:1008:59.30	0.01	1009:46.55	2	47.24	330.19	114.34
2	G8	102	91	-.03	-.03	-.03	29:1148:43.52	0.01	1149:31.32	2	47.79	332.46	98.94
3	G9	100	91	-.03	-.03	-.03	29:1308:21.83	0.01	1309:10.14	1	48.30	334.59	77.60
4	G10	110	91	-.03	-.03	-.03	29:1436:14.63	0.01	1437: 3.38	1	48.74	336.16	70.67
5	G11	48	30	-.01	-.01	-.01	29:1706:19.96	0.01	1707: 8.92	1	48.95	345.88	77.62
6	G12	63	45	-.01	-.01	-.01	29:1821:22.46	0.01	1822:11.71	1	49.24	349.23	80.68
7	G13	118	91	-.03	-.03	-.02	30: 805:46.96	0.01	806:36.36	3	49.39	352.74	105.76
8	G14	151	91	-.02	-.02	-.02	30: 942:55.52	0.01	943:45.72	3	50.19	356.00	114.86
9	H9	124	91	-.03	-.02	-.02	30:2205:45.76	0.01	2206:29.58	2	43.81	303.49	96.35
10	H10	55	55	-.02	-.02	-.02	30:2039:48.51	0.01	2040:33.35	2	44.83	309.65	100.13
11	H11	149	91	-.02	-.02	-.02	30:1911:32.66	0.01	1912:18.53	2	45.86	316.35	85.39
12	H12	120	91	-.03	-.03	-.02	30:1740:51.81	0.01	1741:38.31	2	46.49	323.65	105.76
13	H13	74	55	-.02	-.02	-.01	30:1608:45.21	0.01	1609:33.50	2	48.28	331.01	100.39
14	H14	75	60	-.02	-.02	-.02	30:1445:57.53	0.01	1447:46.33	2	48.79	338.29	113.92
15	H15	73	73	-.03	-.03	-.03	30:1313:45.40	0.01	1314:34.92	2	49.51	348.37	103.47
16	H16	136	91	-.02	-.02	-.02	30:1206:27.09	0.01	1207:17.30	1	50.20	352.18	85.80
17	K1	1824	91	0.43	0.45	0.47	44: 906:15.17	0.01	0: 0.0	5	0.0	506.94	99.67
18	K2	1950	91	0.47	0.49	0.51	45:1734:54.14	0.01	1734: 4.24	3	70.09	518.04	140.49
19	K3	2052	91	0.49	0.52	0.54	44:1330:39.05	0.01	1332:50.76	3	71.70	528.54	127.15
20	K4	2070	91	0.50	0.52	0.54	45:1309:54.85	0.01	1311: 7.00	3	72.14	535.00	144.03

STATION:ESKB9 CODE:ESB9 TYPE:UKAEA LAT:55 22.11 LONG: 3 8.00 ELEV:230 M PN CORR:0.03 S

	SHOT	W.D	S.D	PNDC	PSDC	PGDC	DAY H+M SECS	CL.ER	H+M SECS	CONF	T.T	DIST	T-D/6
		M	M	S	S	S		S			S	KM	S
1	G7	45	45	-.02	-.02	-.02	29:1008:59.30	0.01	1009:46.26	2	46.95	327.19	113.84
2	G8	102	91	-.03	-.03	-.03	29:1148:43.52	0.01	1149:31.00	2	47.47	329.49	98.44
3	G9	100	91	-.03	-.03	-.03	29:1308:21.83	0.01	1309: 9.80	1	47.96	331.67	77.12
4	G10	110	91	-.03	-.03	-.03	29:1436:14.63	0.01	1437: 2.98	1	48.34	333.28	70.19
5	G11	48	30	-.01	-.01	-.01	29:1706:19.96	0.01	1707: 8.69	1	48.72	343.17	77.16
6	G12	63	45	-.01	-.01	-.01	29:1821:22.46	0.01	1822:11.71	1	49.24	346.57	80.23
7	G13	118	91	-.03	-.03	-.02	30: 805:46.96	0.01	806:36.36	3	49.39	350.13	105.32
8	G14	151	91	-.02	-.02	-.02	30: 942:55.52	0.01	943:45.36	3	49.83	353.43	114.44
9	H9	124	91	-.03	-.02	-.02	30:2205:45.76	0.01	2206:29.28	2	43.51	300.95	95.93
10	H10	55	55	-.02	-.02	-.02	30:2039:48.51	0.01	2040:33.00	2	44.48	307.13	99.71
11	H11	149	91	-.02	-.02	-.02	30:1911:32.66	0.01	1912:18.38	2	45.71	313.85	84.98
12	H12	120	91	-.03	-.03	-.02	30:1740:51.81	0.01	1741:37.97	2	46.15	321.16	105.35
13	H13	74	55	-.02	-.02	-.01	30:1608:45.21	0.01	1609:33.10	2	47.88	328.54	99.98
14	H14	75	60	-.02	-.02	-.02	30:1446:57.53	0.01	1447:46.00	2	48.46	335.84	113.51
15	H15	73	73	-.03	-.03	-.03	30:1313:45.46	0.01	1314:34.60	2	49.19	345.93	103.06
16	H16	136	91	-.02	-.02	-.02	30:1206:27.09	0.01	1207:16.94	1	49.84	349.75	65.39

APPENDIX B

STACKED RECORD SECTIONS AND TRAVEL-TIME PLOTS

The following Appendix contains a number of stacked record sections not included in the text. The name of the station is on the bottom of each diagram.

The second part of the Appendix contains reduced travel-time plots of first arrivals for a number of stations. First arrival travel-time data from the shots fired in the Moray Firth by Cambridge University are also presented. Each plot shows the name of the station and the shot numbers. The reduction velocity in each case in 6.0 km sec^{-1}.

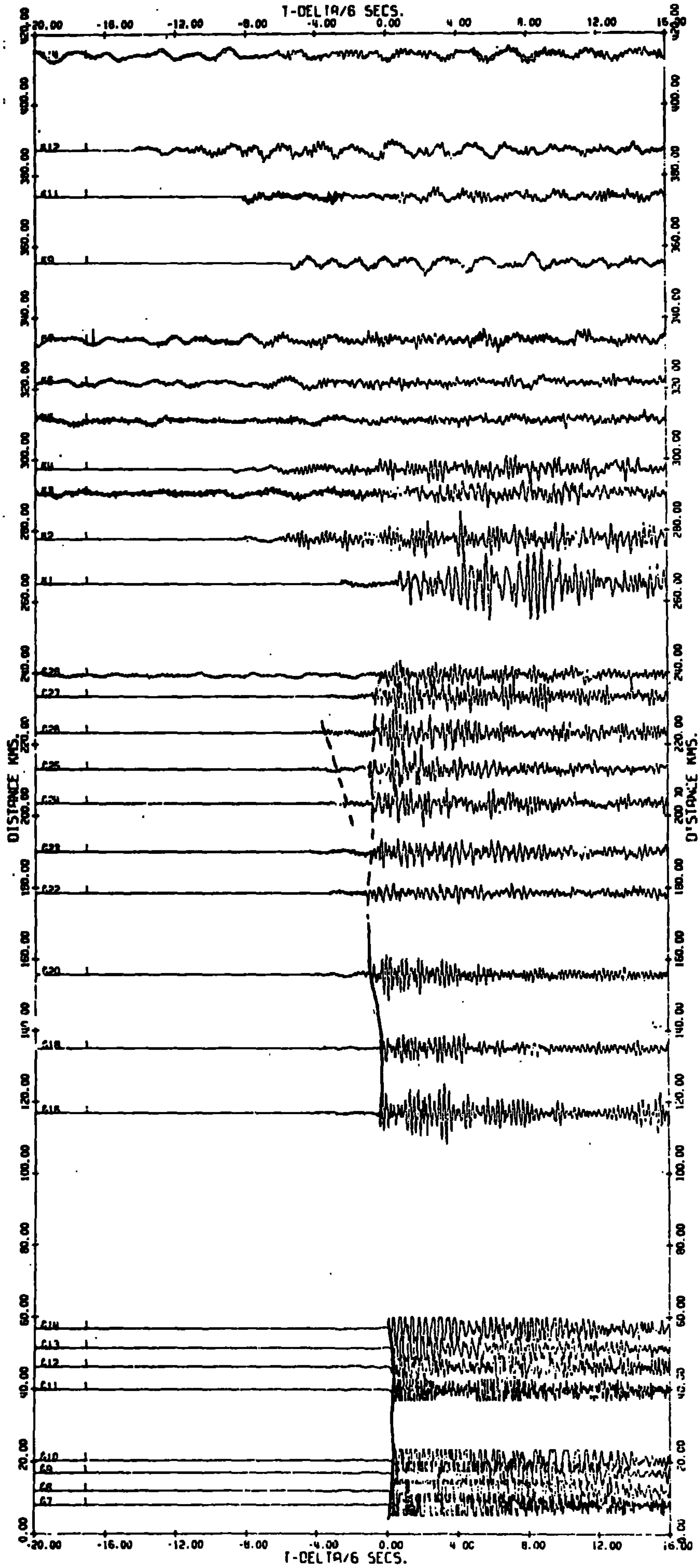

POLBAIN

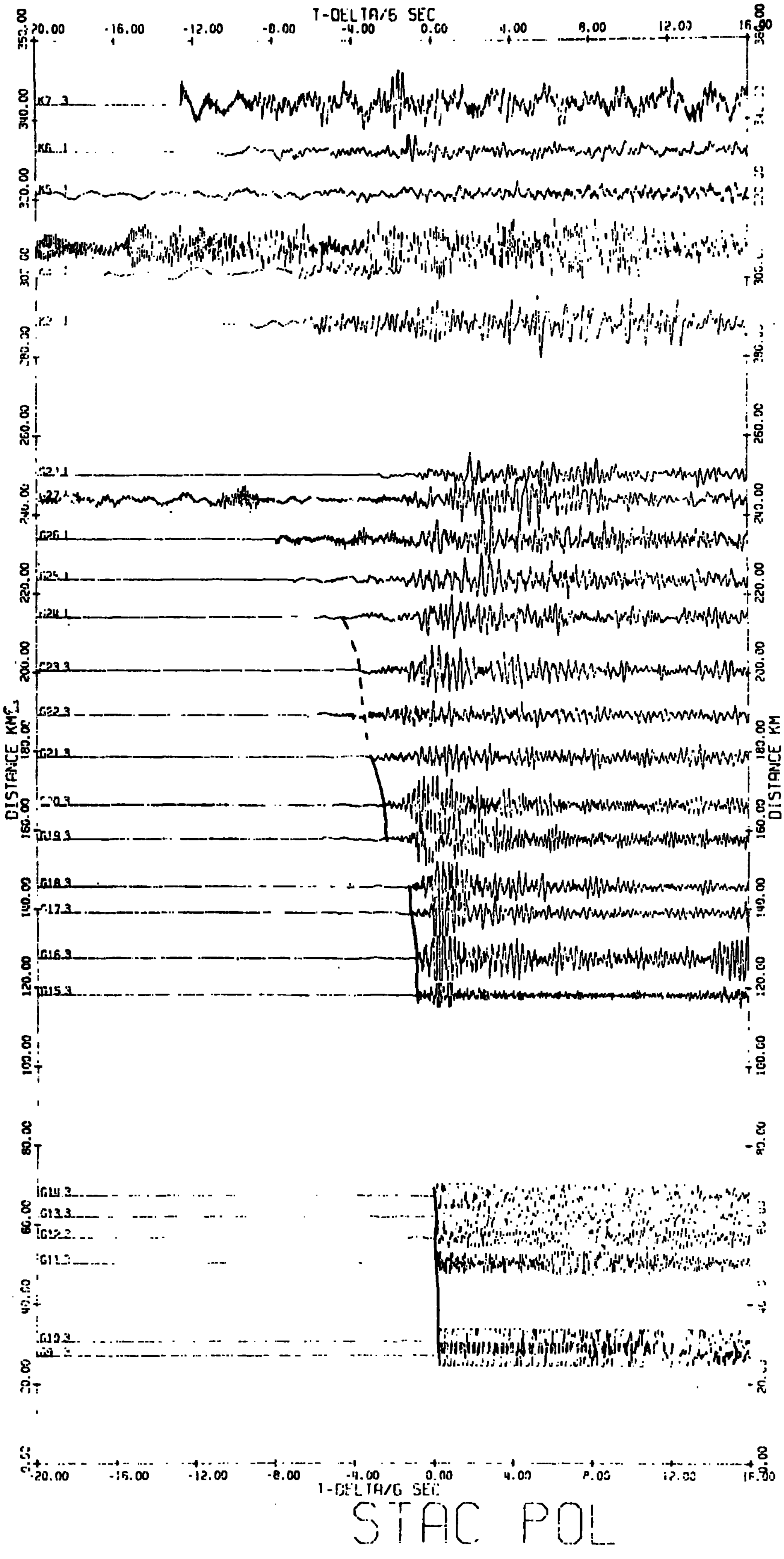
T-DELTA/6 SEC
DISTANCE KM
T-DELTA/6 SEC
STAC POL

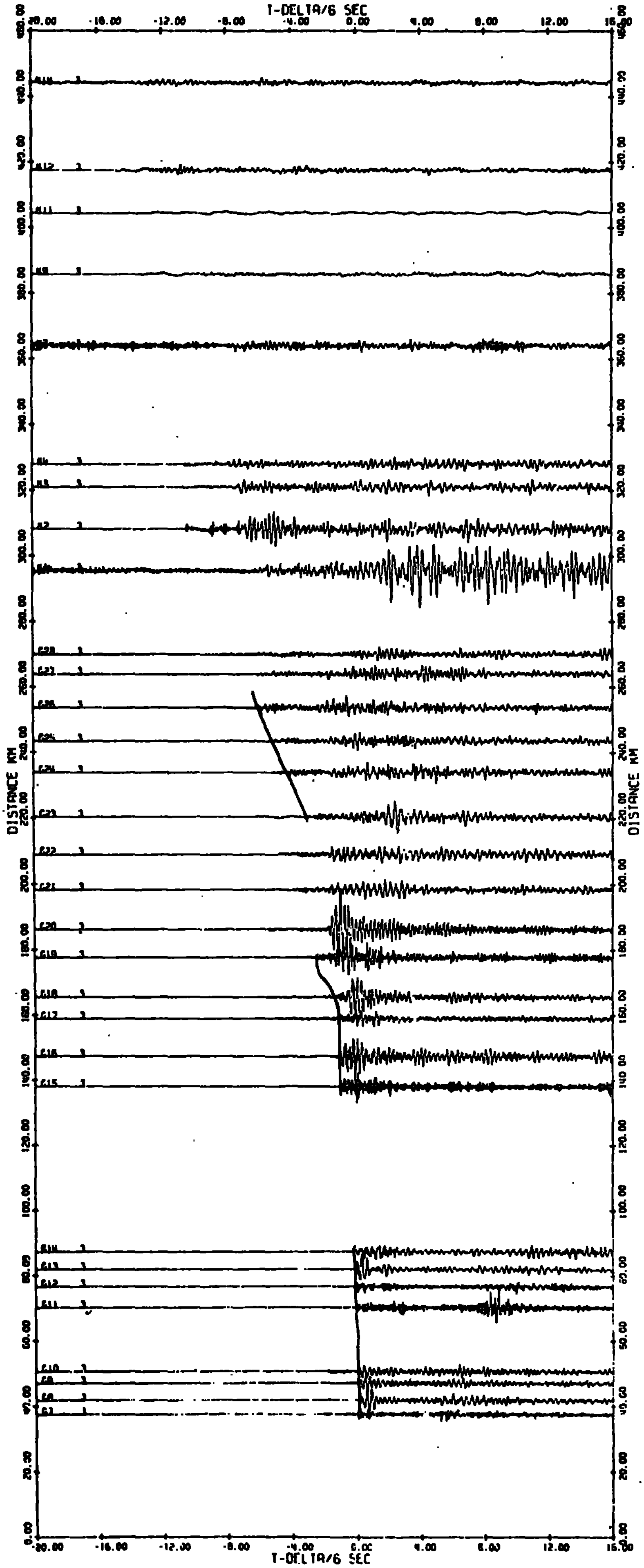

L.AILSH

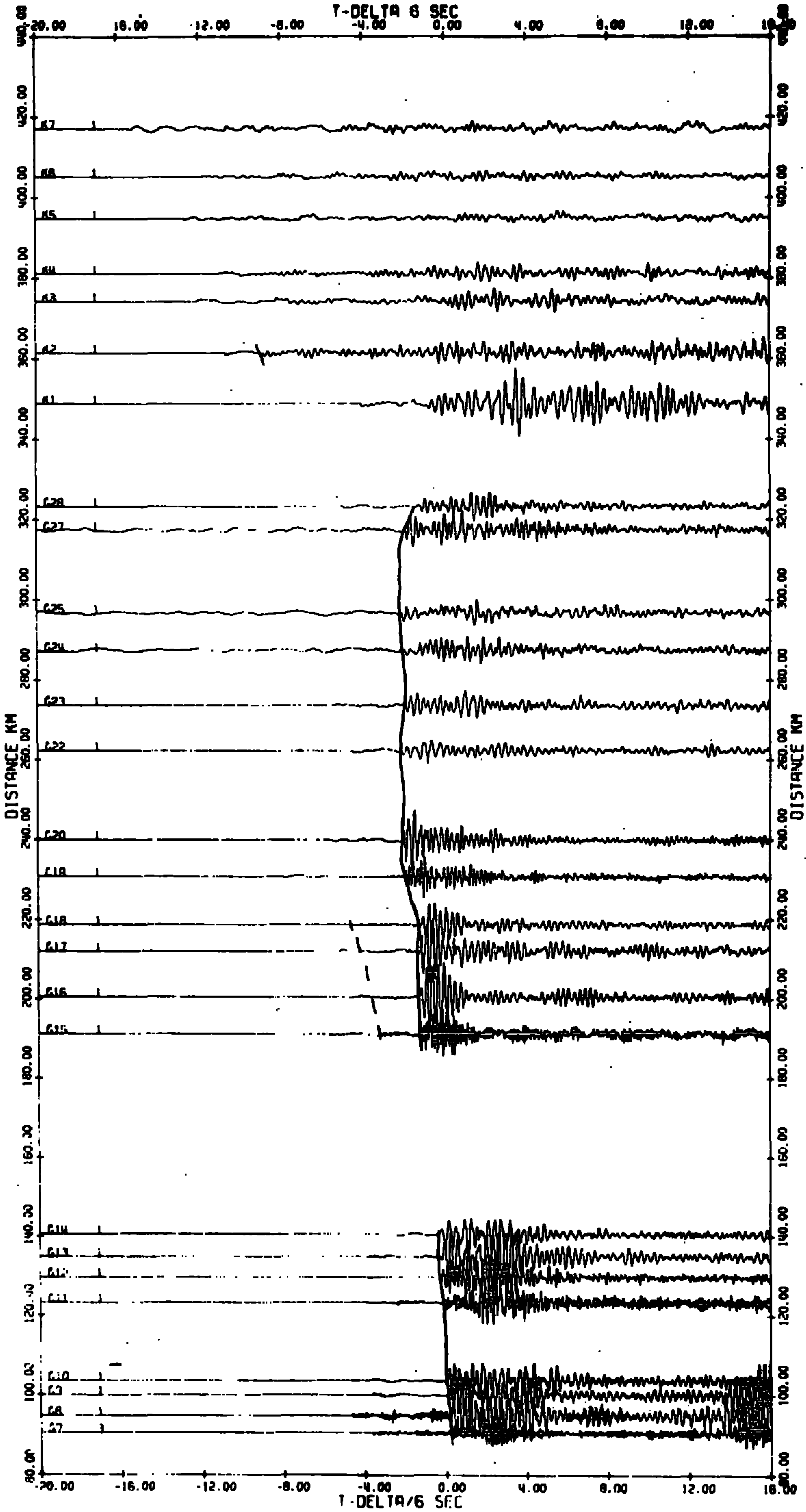

BACKIES

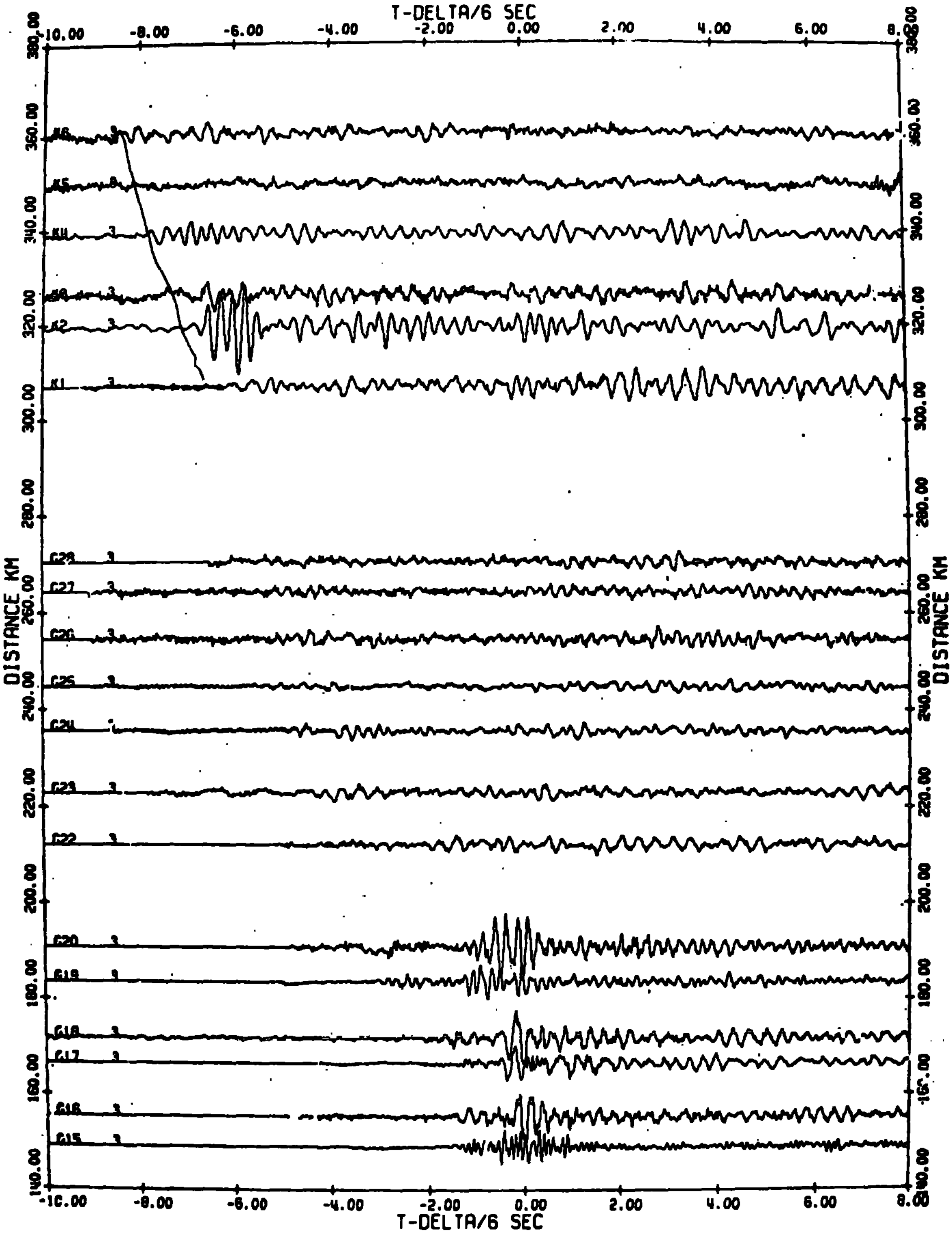
T-DELTA/6 SEC
DISTANCE KM
K6
K5
K4
K3
K2
K1
C28
C27
C26
C25
C24
C23
C22
C20
C19
C18
C17
C16
C15

CAPEWRAT

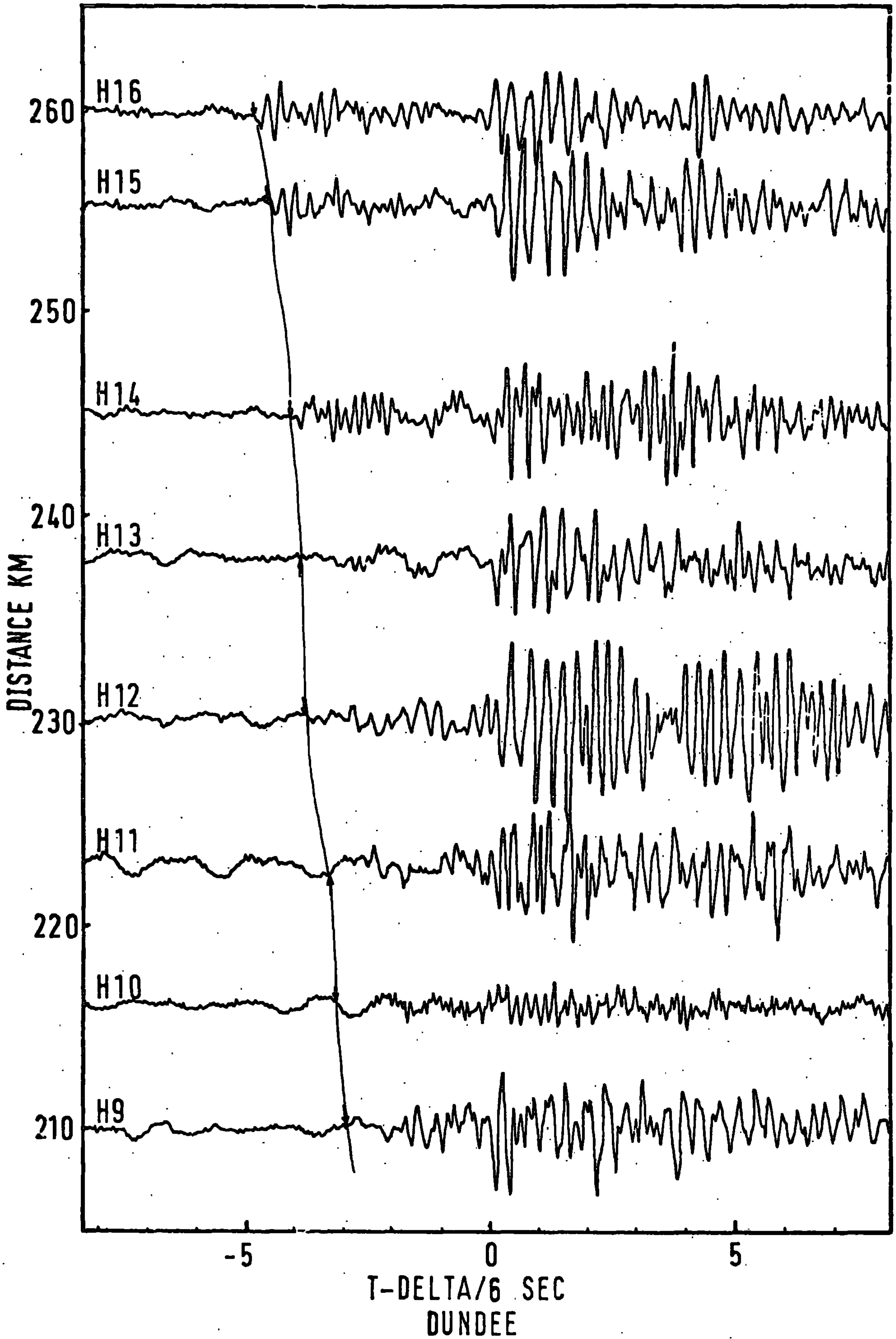
H16
H15
H14
H13
H12
H11
H10
H9
260
250
240
230
220
210
DISTANCE KM
-5
0
5
T-DELTA/6 SEC
DUNDEE

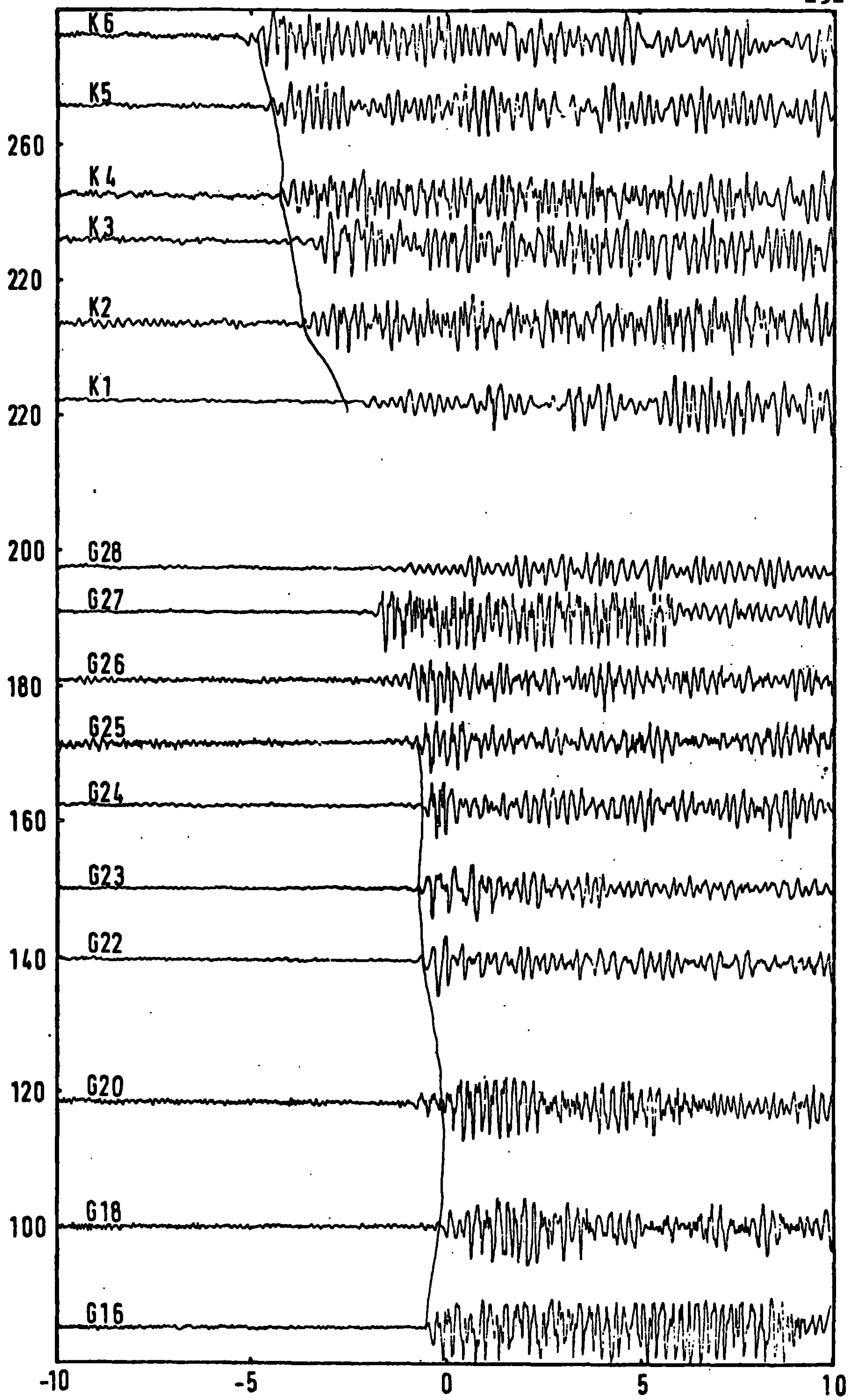
K6
K5
K4
K3
K2
K1
G28
G27
G26
G25
G24
G23
G22
G20
G18
G16
260
220
220
200
180
160
140
120
100
-10
-5
0
5
10

BUTT DU6

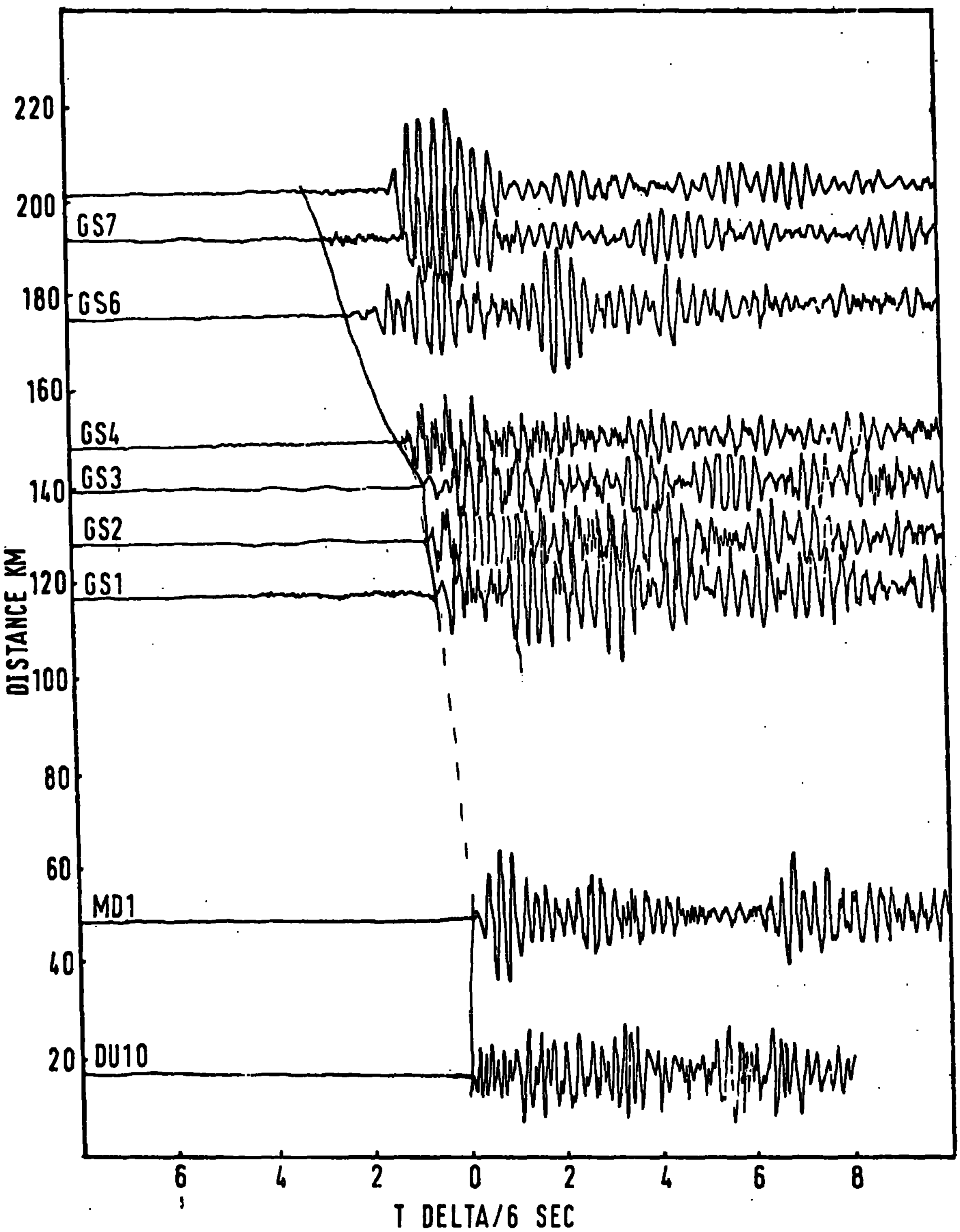
220
200
180
160
140
120
100
80
60
40
20
DISTANCE KM
GS7
GS6
GS4
GS3
GS2
GS1
MD1
DU10
6
4
2
0
2
4
6
8
T DELTA/6 SEC

G16

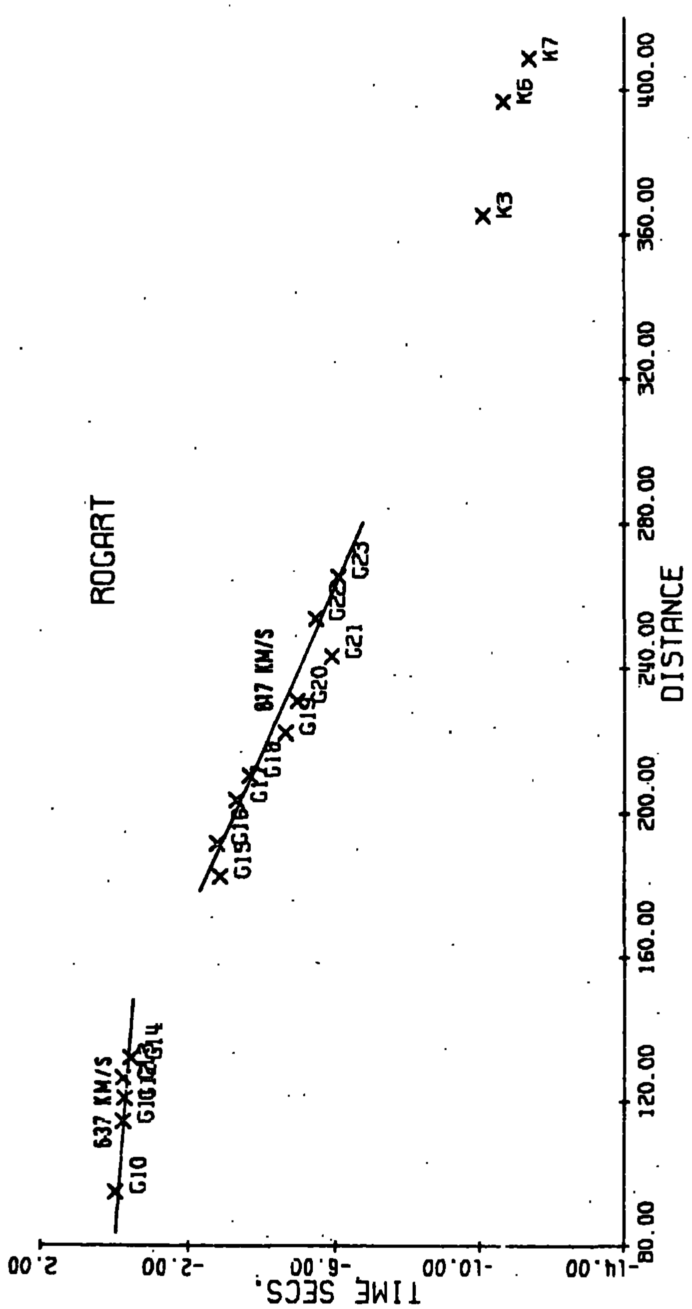
ROGART
637 KM/S
617 KM/S
G10
G11
G12
G14
G15
G16
G17
G18
G19
G20
G21
G22
G23
K3
K6
K7
TIME SECS.
2.00
-2.00
-6.00
-10.00
-14.00
DISTANCE
80.00
120.00
160.00
200.00
240.00
280.00
320.00
360.00
400.00

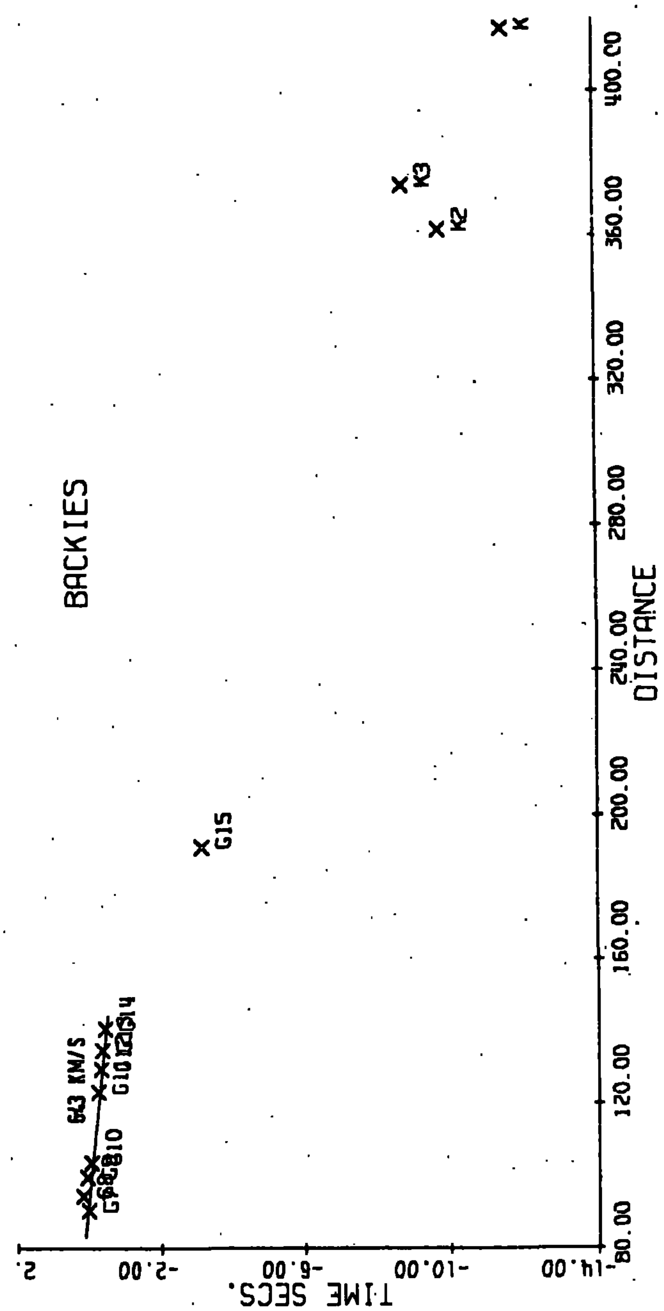
BACKIES
643 KM/S
G10
G12
G14
G15
K2
K3
TIME SECS.
-2.00
-6.00
-10.00
-14.00
DISTANCE
80.00
120.00
160.00
200.00
240.00
280.00
320.00
360.00
400.00

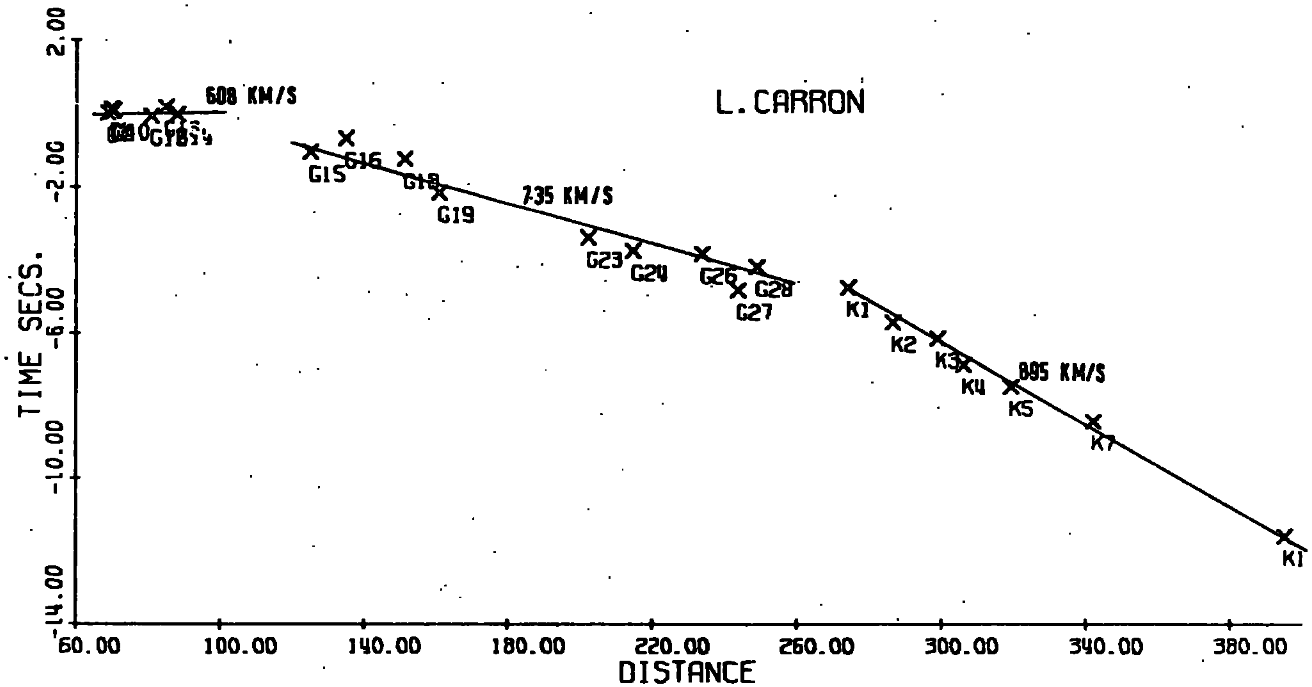
L.CARRON
6.08 KM/S
7.35 KM/S
8.95 KM/S
G15
G16
G18
G19
G23
G24
G26
G27
G28
K1
K2
K3
K4
K5
K7
TIME SECS.
2.00
-2.00
-6.00
-10.00
-14.00
60.00
100.00
140.00
180.00
220.00
260.00
300.00
340.00
380.00
DISTANCE

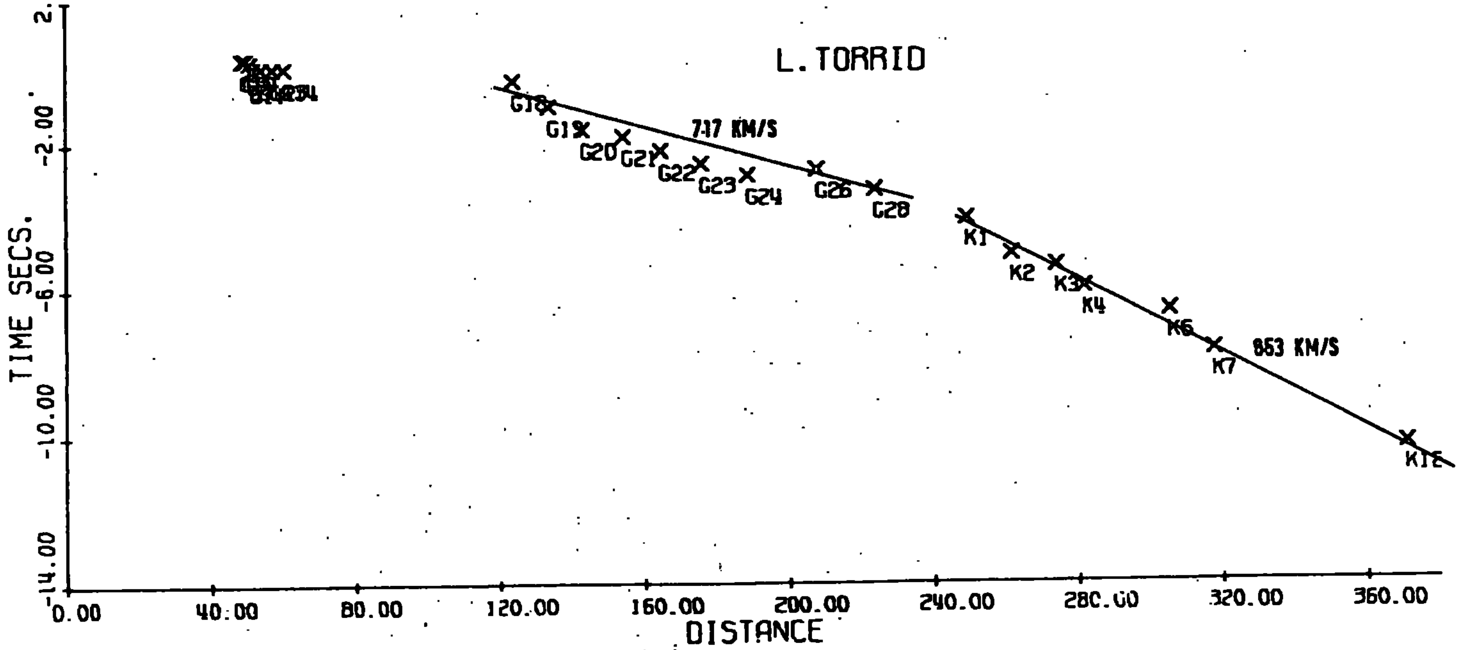
L.TORRID
7.17 KM/S
8.53 KM/S
G18
G19
G20
G21
G22
G23
G24
G26
G28
K1
K2
K3
K4
K6
K7
TIME SECS.
2.
-2.00
-6.00
-10.00
-14.00
0.00
40.00
80.00
120.00
160.00
200.00
240.00
280.00
320.00
360.00
DISTANCE

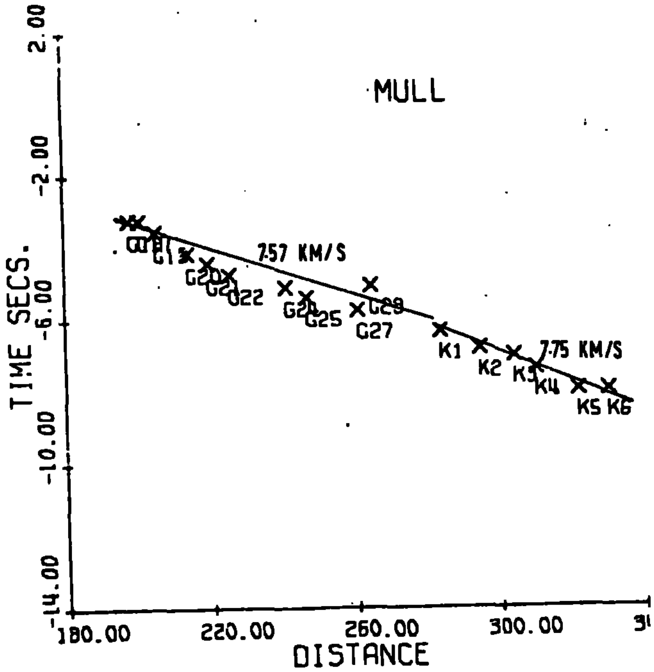
MULL
TIME SECS.
DISTANCE
7.57 KM/S
7.75 KM/S
G13
G20
G21
G22
G24
G25
G27
G29
K1
K2
K3
K4
K5
K6

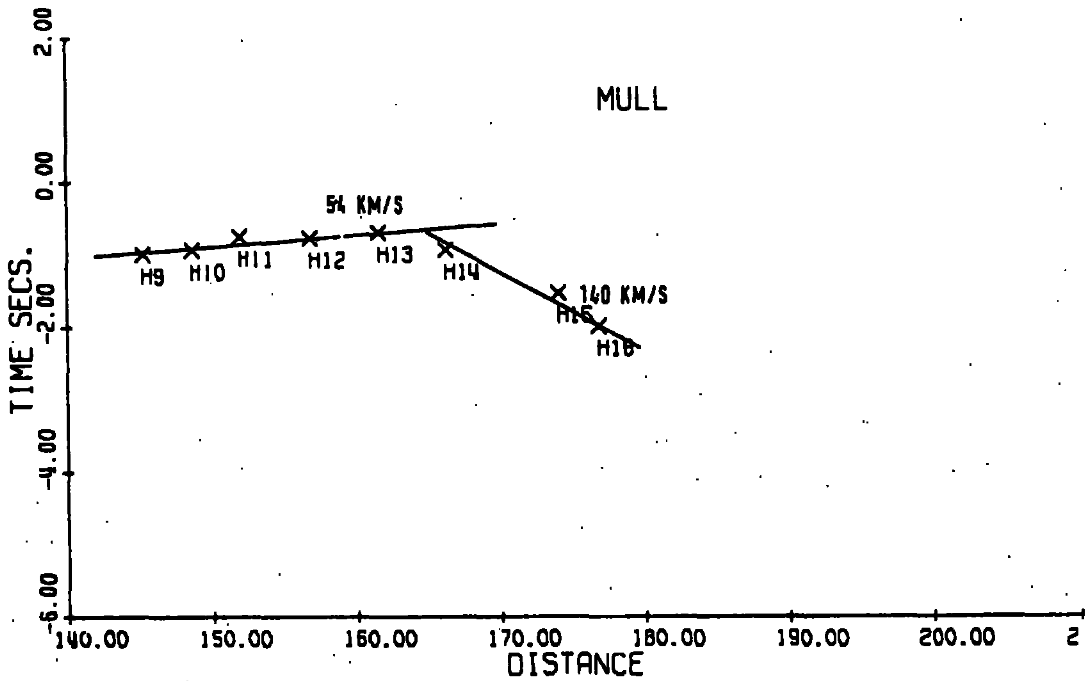
MULL
TIME SECS.
DISTANCE
5.4 KM/S
1.40 KM/S
H9
H10
H11
H12
H13
H14
H15
H16

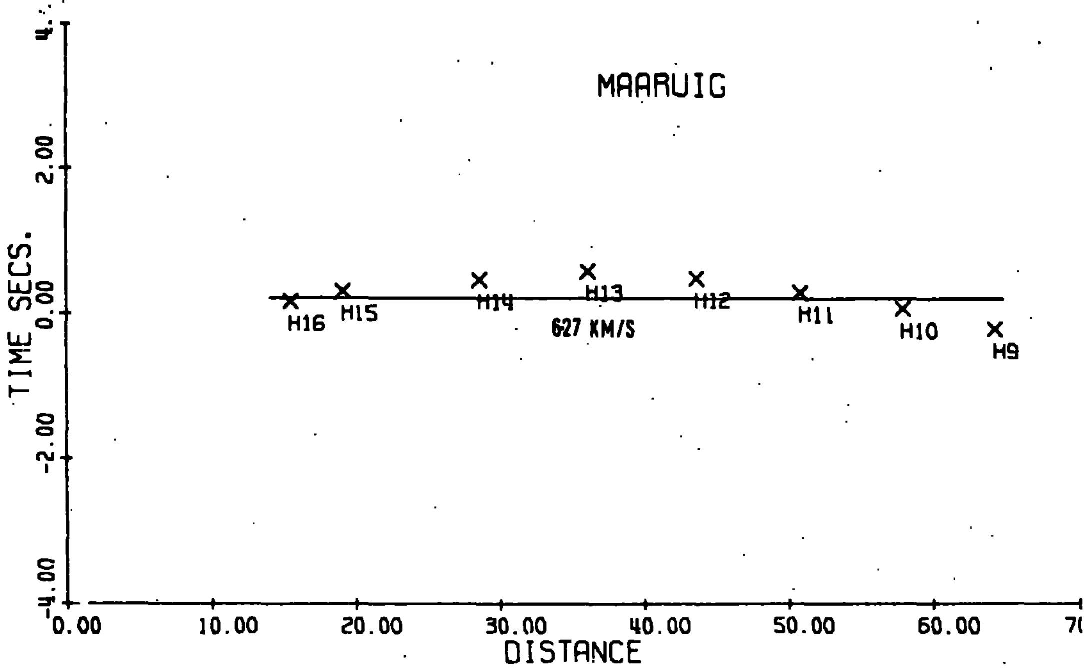
MAARUIG
TIME SECS.
DISTANCE
6.27 KM/S
H16
H15
H14
H13
H12
H11
H10
H9

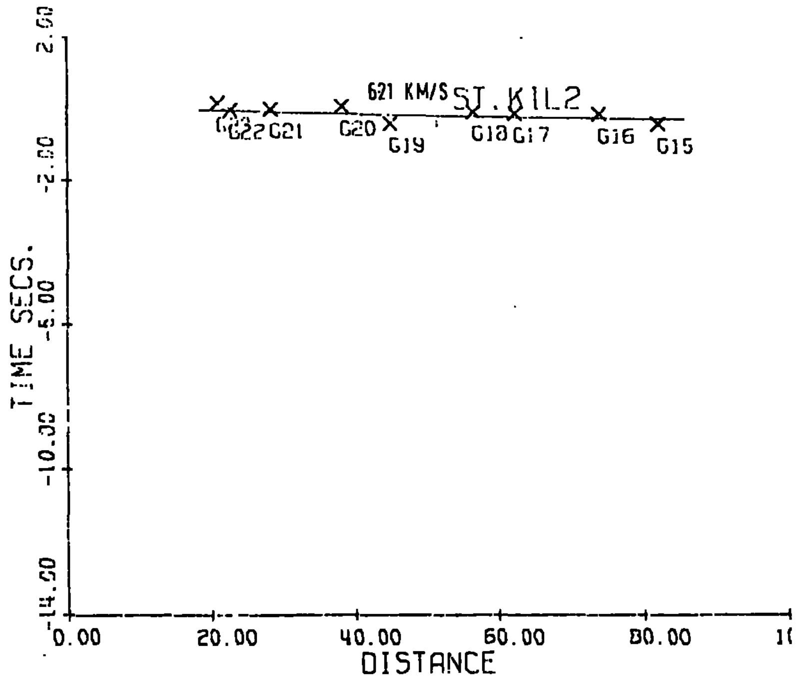
621 KM/S
ST.KIL2
G22 G21 G20 G19 G18 G17 G16 G15
TIME SECS.
DISTANCE

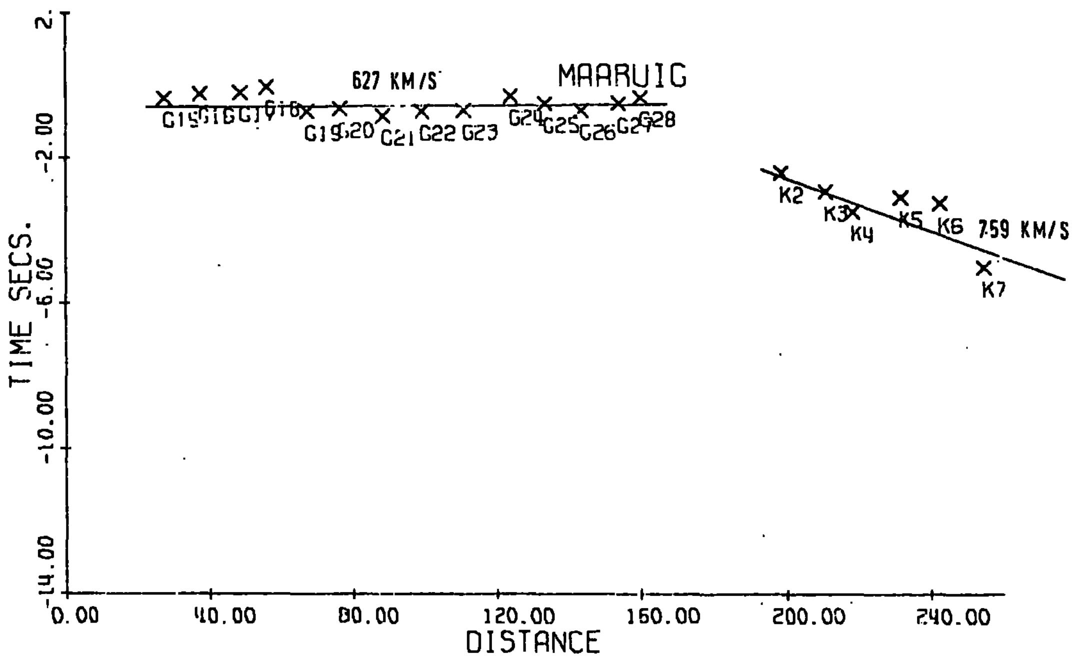
627 KM/S
MAARUIG
G19 G20 G21 G22 G23 G24 G25 G26 G27 G28
K2 K3 K4 K5 K6 K7
7.59 KM/S
TIME SECS.
DISTANCE

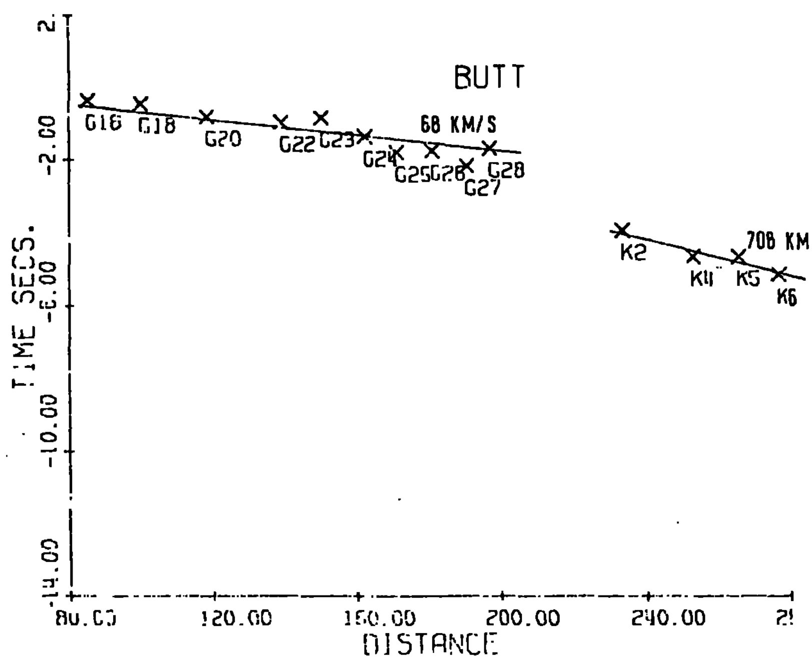
BUTT
G16 G18 G20 G22 G23 G24 G25 G26 G27 G28
68 KM/S
K2 K4 K5 K6
708 KM/S
TIME SECS.
DISTANCE

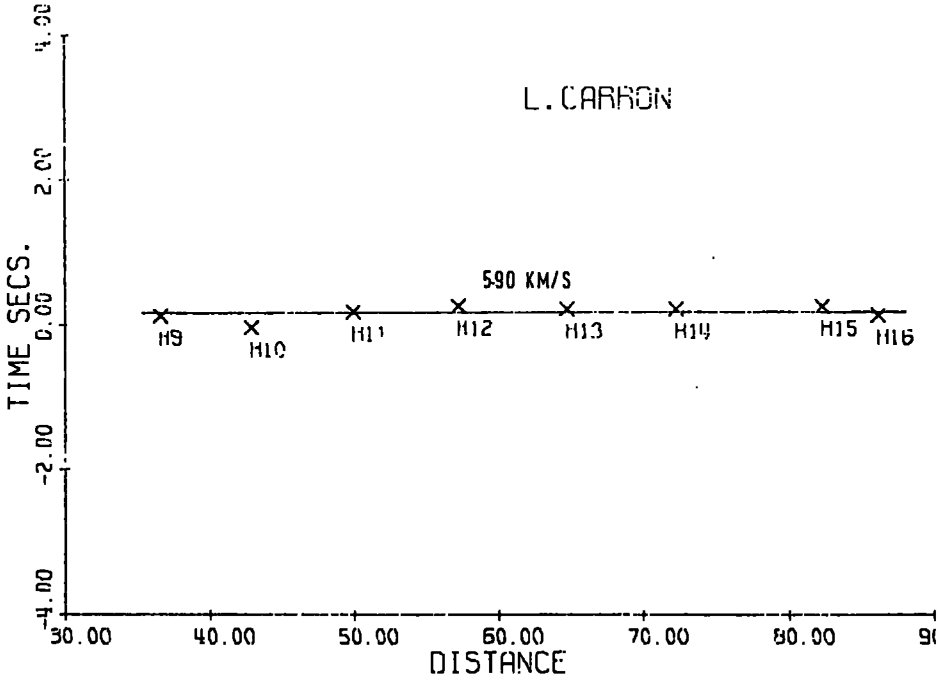
L. CARRON
5.90 KM/S
TIME SECS.
DISTANCE
H9
H10
H11
H12
H13
H14
H15
H16

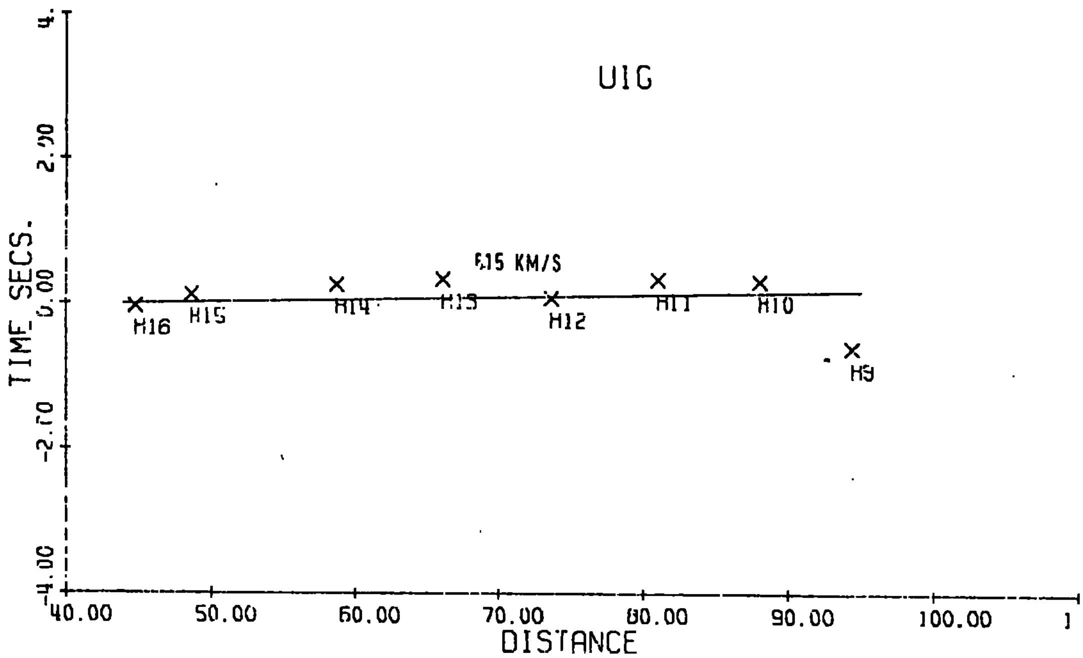
UIG
6.15 KM/S
TIME SECS.
DISTANCE
H16
H15
H14
H13
H12
H11
H10
H9

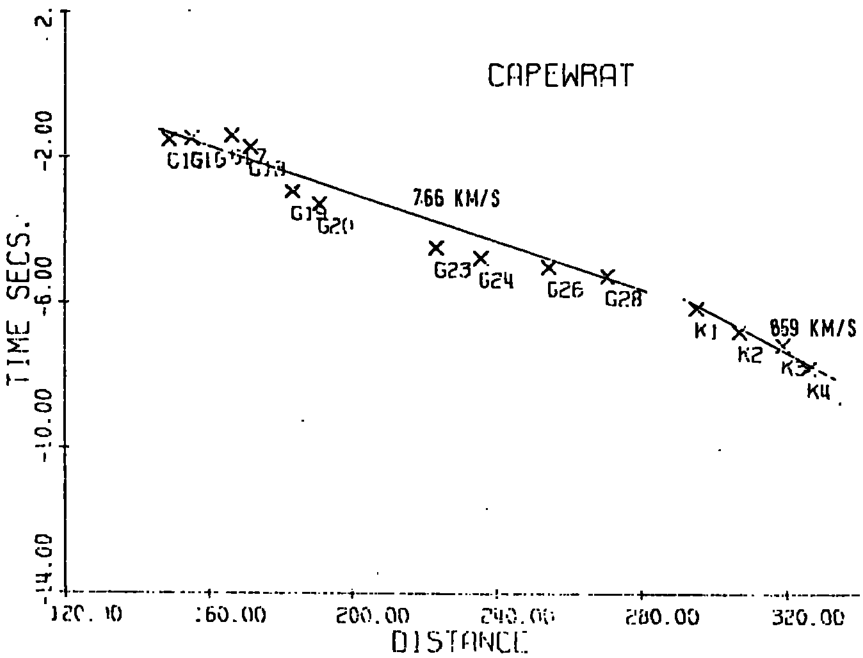
CAPEWRAT
7.66 KM/S
8.59 KM/S
TIME SECS.
DISTANCE
G19
G20
G23
G24
G26
G28
K1
K2
K3
K4

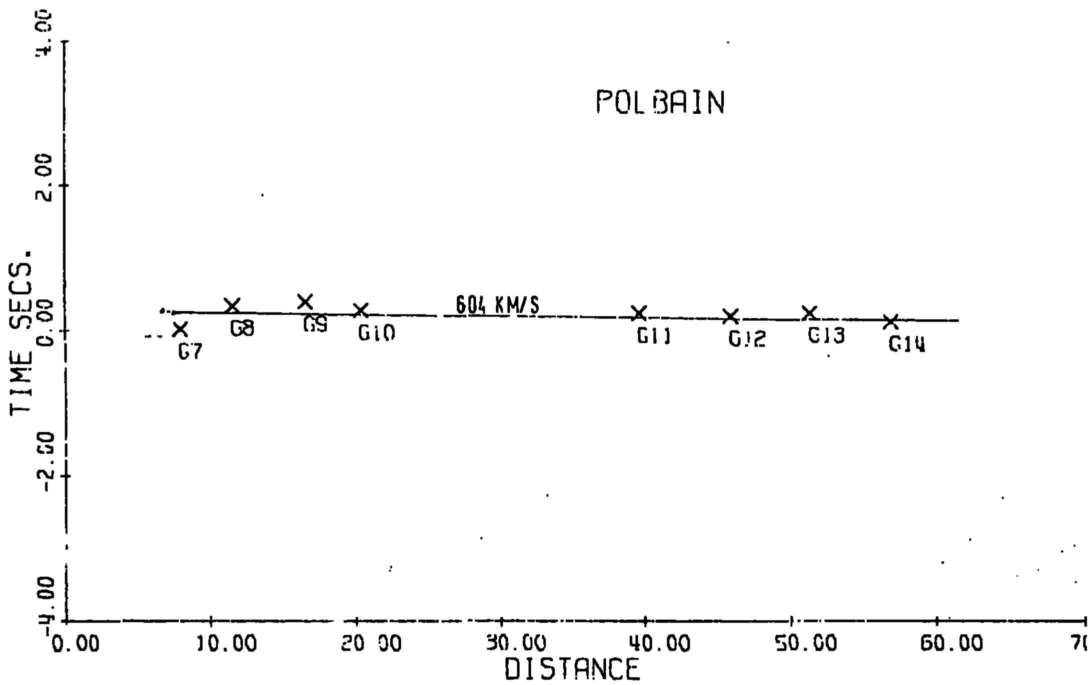
POLBAIN
TIME SECS.
604 KM/S
G7
G8
G9
G10
G11
G12
G13
G14
DISTANCE

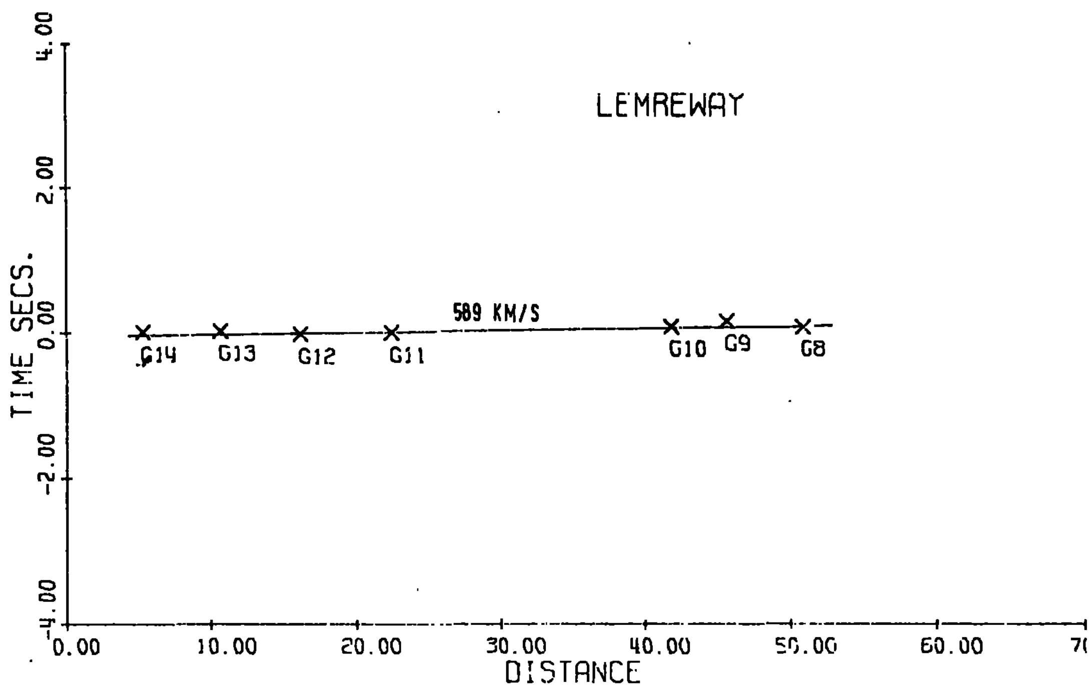
LEMREWAY
TIME SECS.
589 KM/S
G14
G13
G12
G11
G10
G9
G8
DISTANCE

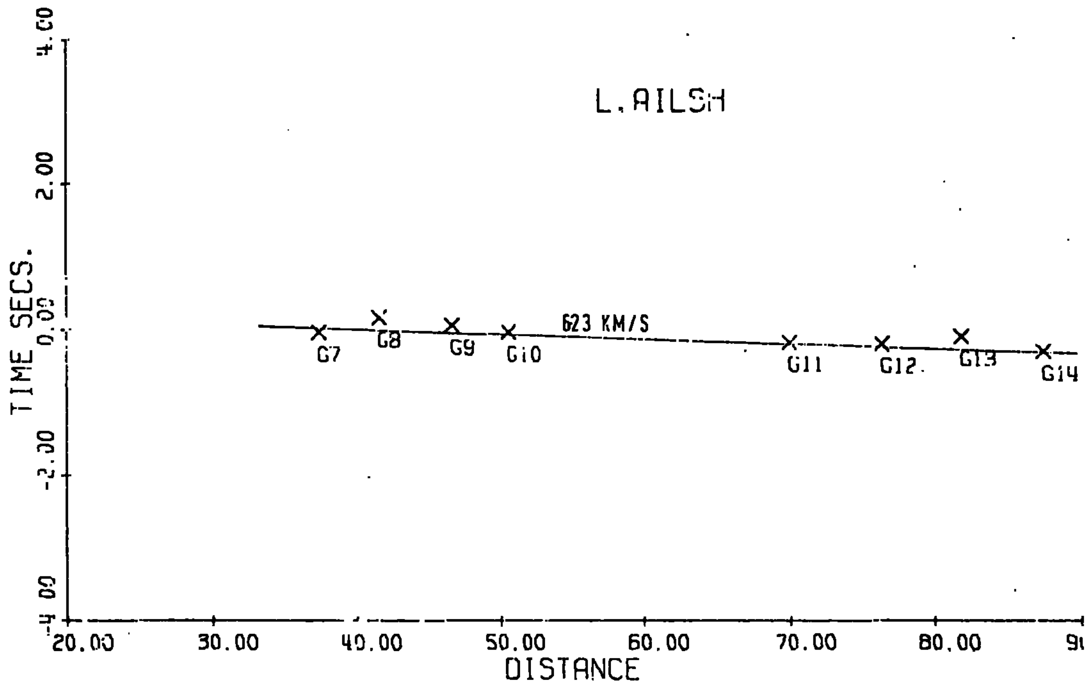
L.AILSH
623 KM/S
TIME SECS.
DISTANCE
G7
G8
G9
G10
G11
G12
G13
G14

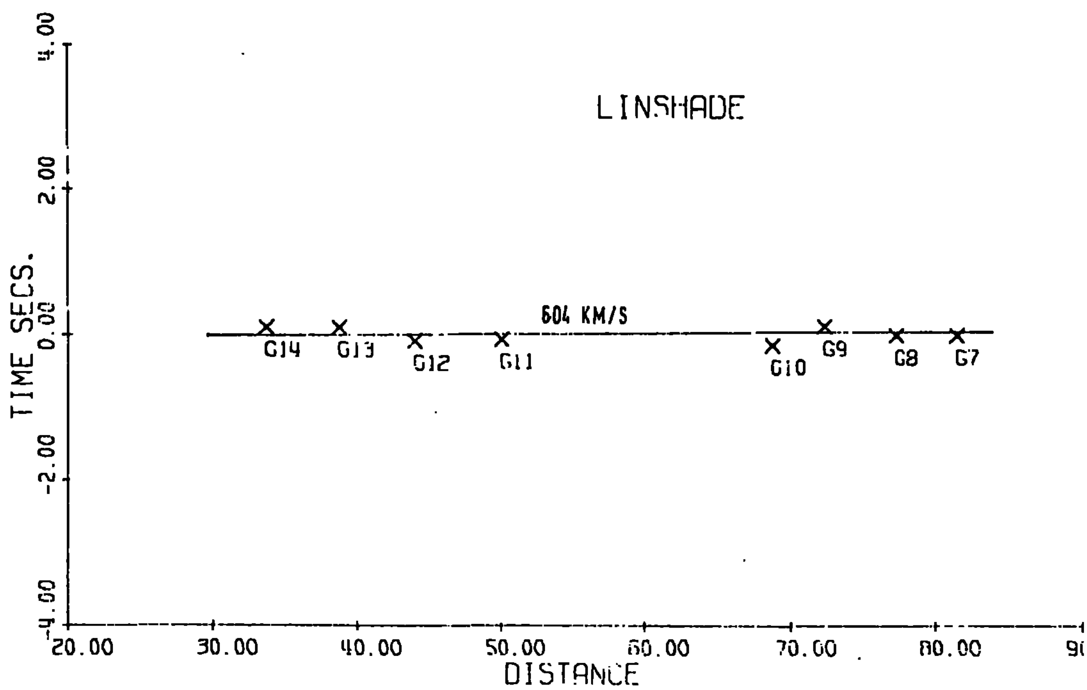
LINSHADE
604 KM/S
TIME SECS.
DISTANCE
G14
G13
G12
G11
G10
G9
G8
G7

K4

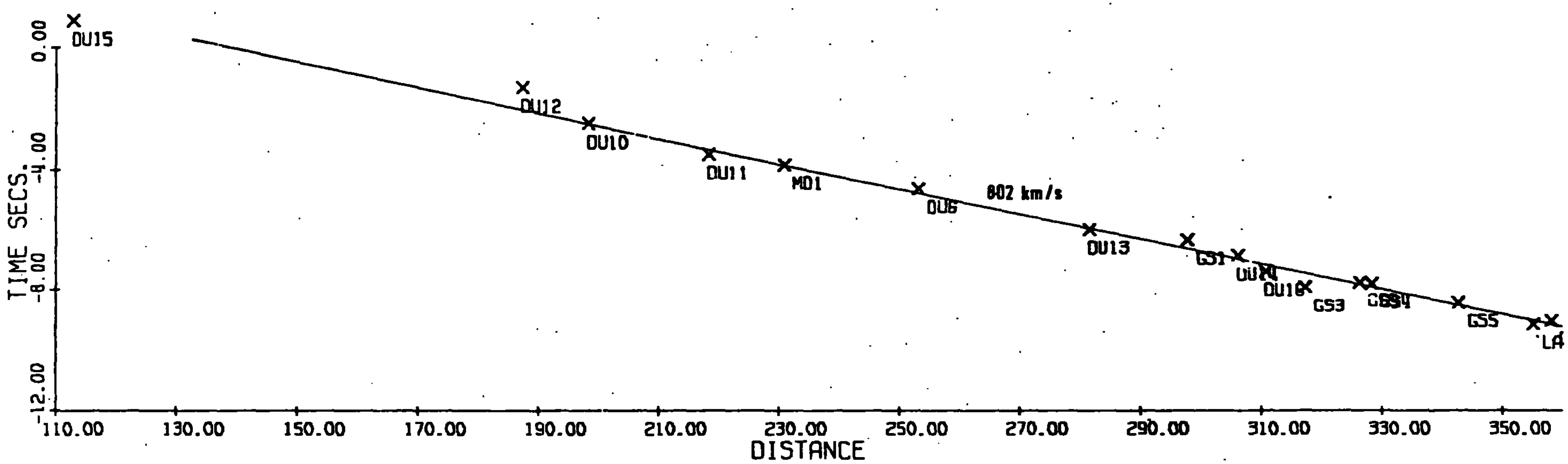
TIME SECS.
0.00
-4.00
-8.00
-12.00
110.00
130.00
150.00
170.00
190.00
210.00
230.00
250.00
270.00
290.00
310.00
330.00
350.00
DISTANCE
802 km/s
DU15
DU12
DU10
DU11
MD1
DU6
DU13
GS1
DU16
GS3
GS5

K5

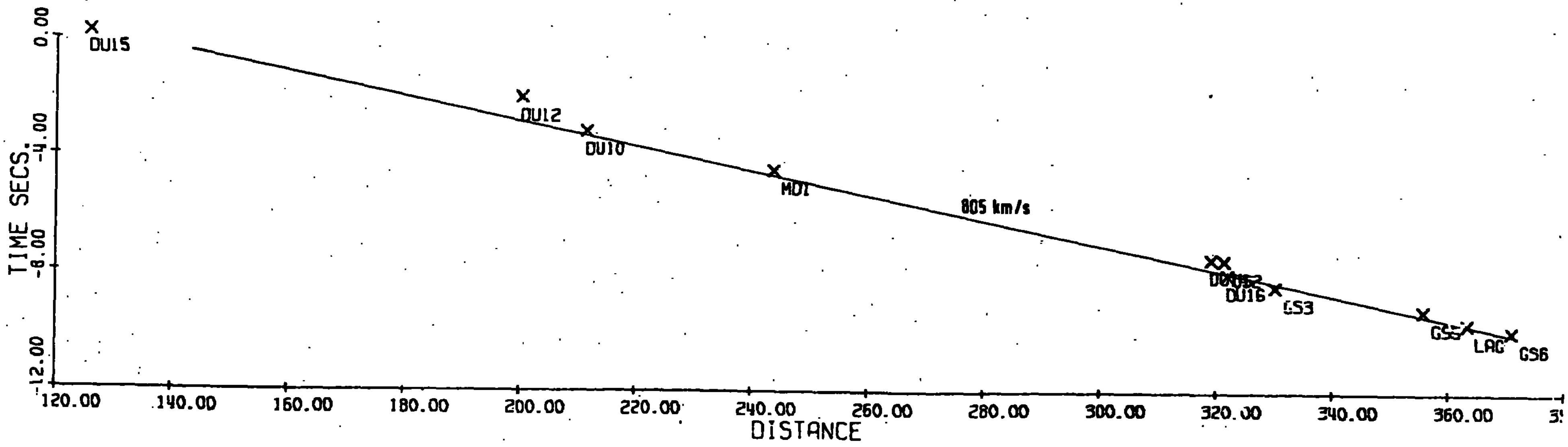
TIME SECS.
0.00
-4.00
-8.00
-12.00
120.00
140.00
160.00
180.00
200.00
220.00
240.00
260.00
280.00
300.00
320.00
340.00
360.00
DISTANCE
805 km/s
DU15
DU12
DU10
MDI
DU16
GS3
LAC
GS6

K4

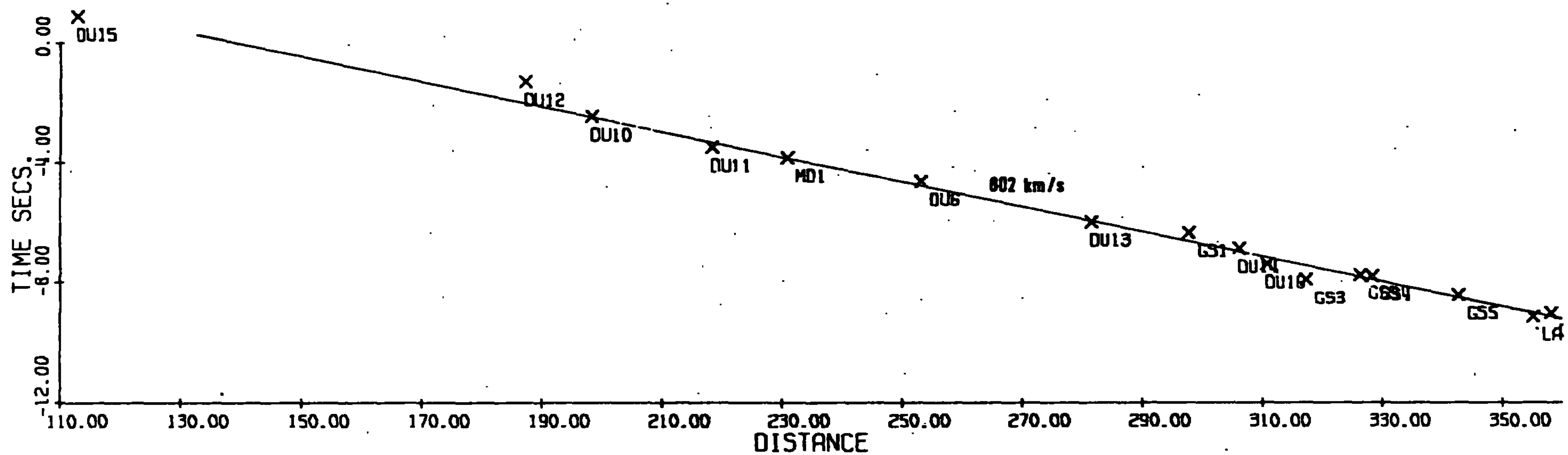
TIME SECS.
0.00
-4.00
-8.00
-12.00
DU15
DU12
DU10
DU11
MD1
DU6
802 km/s
DU13
GS1
DU18
GS3
GS5
LA
110.00
130.00
150.00
170.00
190.00
210.00
230.00
250.00
270.00
290.00
310.00
330.00
350.00
DISTANCE

K5

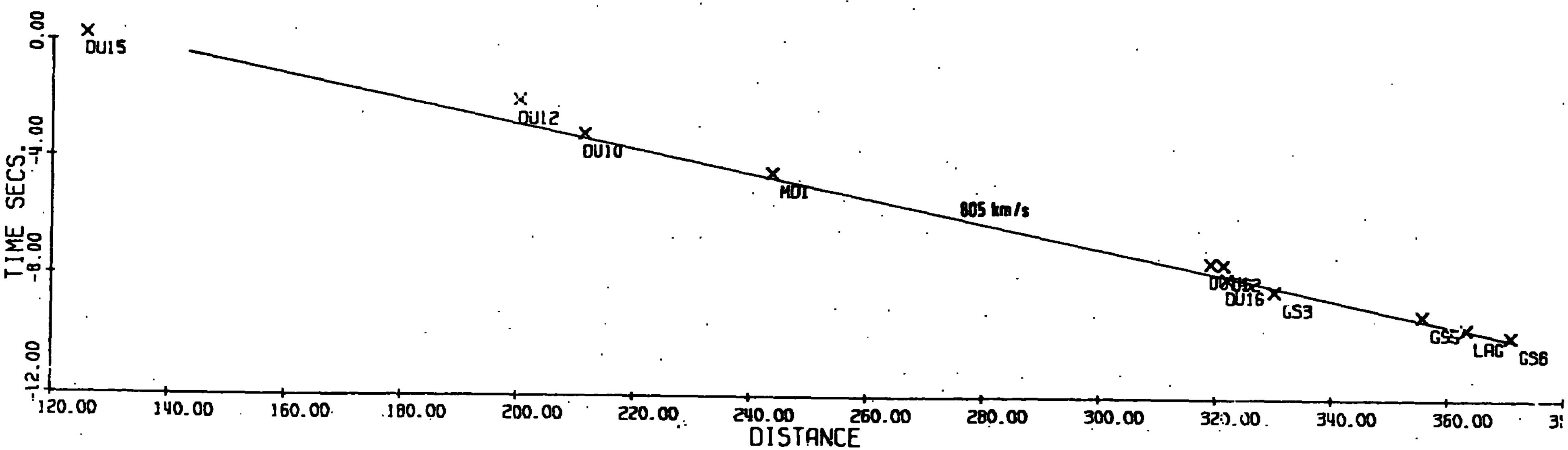
TIME SECS.
0.00
-4.00
-8.00
-12.00
DU15
DU12
DU10
MD1
805 km/s
DU16
GS3
GS5
LAG
GS6
120.00
140.00
160.00
180.00
200.00
220.00
240.00
260.00
280.00
300.00
340.00
360.00
DISTANCE

L10

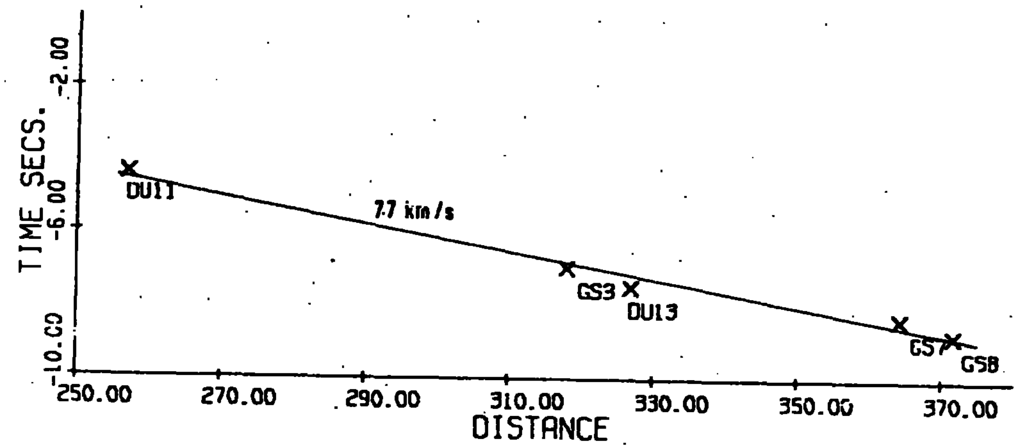

TIME SECS.
-2.00
-6.00
-10.00
DISTANCE
250.00
270.00
290.00
310.00
330.00
350.00
370.00
7.7 km/s
DU11
GS3
DU13
GS7
GS8

K12

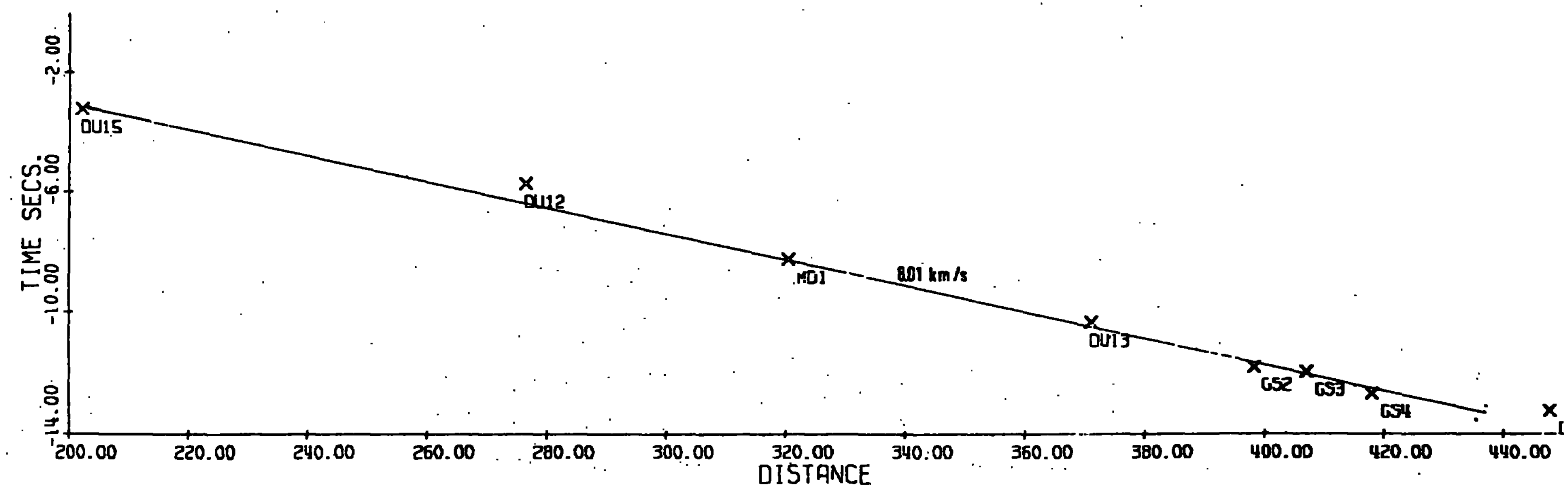

TIME SECS.
-2.00
-6.00
-10.00
-14.00
DISTANCE
200.00
220.00
240.00
260.00
280.00
300.00
320.00
340.00
360.00
380.00
400.00
420.00
440.00
8.01 km/s
DU15
DU12
MD1
DU13
GS2
GS3
GS4

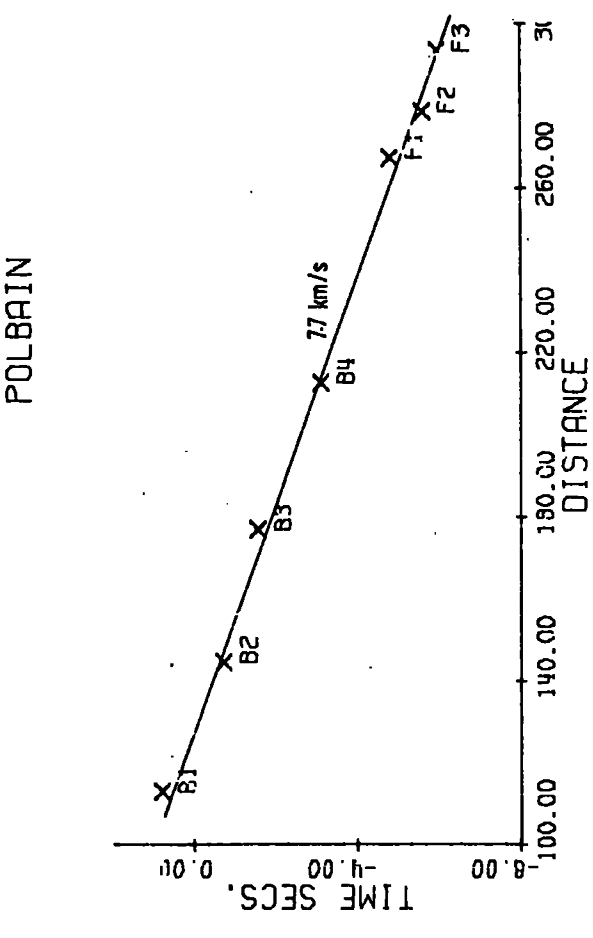
POLBAIN
7.7 km/s
B1
B2
B3
B4
F1
F2
F3
DISTANCE
TIME SECS.
100.00
140.00
180.00
220.00
260.00
0.00
-4.00
-8.00

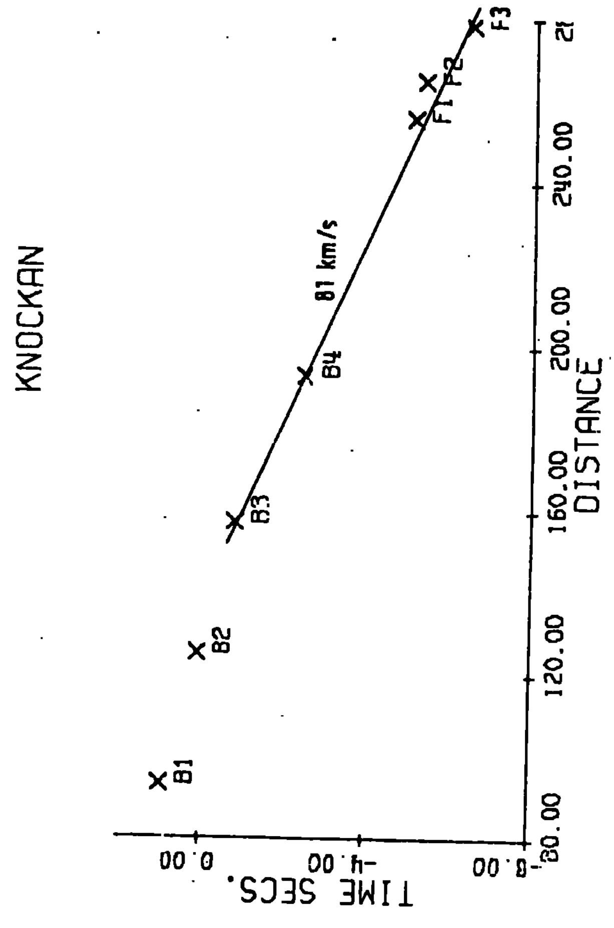
KNOCKAN
81 km/s
B1
B2
B3
B4
F1
F2
F3
DISTANCE
TIME SECS.
80.00
120.00
160.00
200.00
240.00
0.00
-4.00
-8.00

GLENCASS

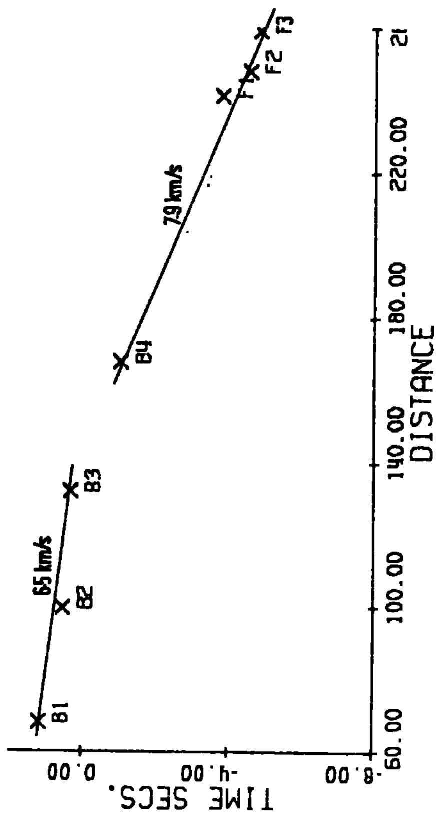

ROGART

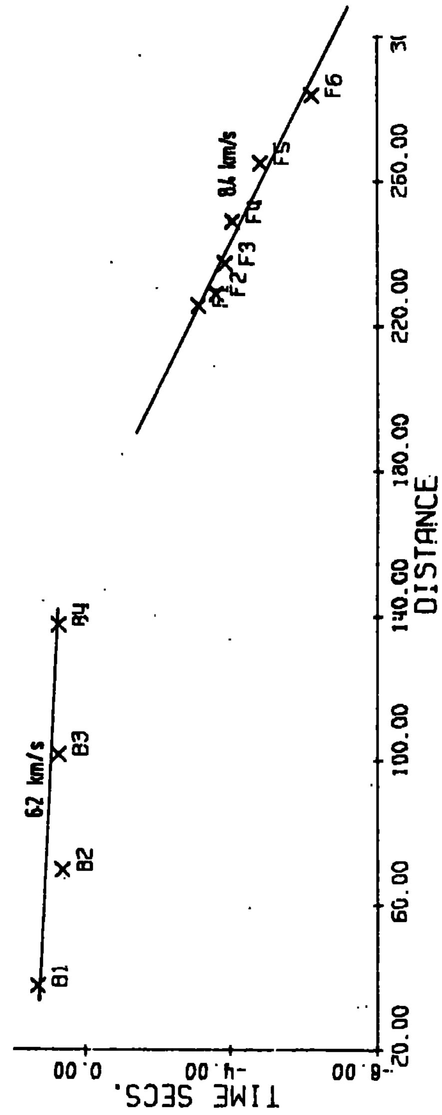

APPENDIX C

Stacking program FPLOT

The program takes events recorded on a 9-track digital magnetic tape produced on a CTL Modular 1 computer and forms a stacked record section, or "T $-\Delta/6$" plot. The program is written in FORTRAN IV, contains comments and is, hence, self explanatory. Access to the plotting subroutines held at Durham in the public file *PLOTSYS is required. A flow-diagram of the program is given in Figure C.1. A second version allows 16-track tapes to be plotted.

Input data

File 1: Plotter size, Plot name, Axes dimensions, Delay-time option.

File 2: Shot name, Data channel, Number of zero line sample (NOLS), Delay-time (optional), Range.

File 3: Seismometer gains.

File 4: Magnetic tape containing 8 tracks of time-series data.

Output data

File 6: Allows operator to see progress of program.

File 9: Data from plotting subroutines. This is ready for plot generation using *PLOTSEE (Tektronix oscilloscope) or *DURPLOT (Calcomp plotter).

Format of Modular 1 Magnetic Tapes

Modular 1 digital tapes take the form of a continuous string of digits multiplexed in blocks of 8 or 16. In most cases in this study 8 tracks were used and a diagram showing their arrangement on tape is given in Figure C.2. The Modular 1 tape-files contain additional header information and when used under MTS at NUMAC, these tape-files are referred to as "1 plus the Modular 1 number", e.g. the first file on tape is referred to as " *2* " in MTS.

For the first part of the processing in this thesis an automatic capture procedure was used to record events on to digital tape. The program used passes the signals through the store of the Modular 1 computer continuously and tests the most recently input value to see if it exceeds a previously set trigger level. If it does, the signals are copied to digital tape starting with the first value contained in store and continuing with the triggered event until a tape-file has been filled. The length of record in store at any one time is about 4 seconds worth, so that most tape-files start 4 seconds ahead of the trigger event on the file. Thus, many records do not have a long sample of noise preceding them. At a later stage in the processing automatic capture was abandoned in favour of "hand capturing" where transfer to a digital tape is started some 30 seconds before the event starts. This enables a sample of the noise immediately preceding the event to be obtained.

A listing of the program and a sample running sequence follows:

```
C     THIS PROGRAM IS CALLED EPLOT
C    THE PROGRAM TAKES EVENTS RECORDED ON 9 TRACK TAPE AS EIGHT
C    DATA CHANNELS AND PLOTS THEM ON THE CALCOMP 11INCH OR 30INCH
C    PLOTTER AS A T-DELTA/6 PLOT
C
      DIMENSION IX(4),ISAM(18000)
      INTEGER*2 JIM(256)
      REAL*8 STAT
      INTEGER *2 LEN
      INTEGER *4 RET(12)
      LEN=2
      WRITE(6,9)
    9 FORMAT('TYPE IN PLOTTER SIZE-11IN OR 30IN')
      READ(1,8) M
      WRITE(6,8) M
    8 FORMAT(1X,I2)
      WRITE(6,11)
   11 FORMAT('TYPE IN STATION NAME')
      READ(1,10) STAT
      WRITE(6,10) STAT
   10 FORMAT(A8)
C
C    THE FIRST SECTION ASKS FOR THE PLOT SIZE AND PLOTS AXES
C    INPUT:LENGTH OF TIME AXIS(SECS):SCALE OF TIME AXIS(SEC/IN):
C    START OF TIME AXIS(SECS):LENGTH OF DIST AXIS(KM):SCALE OF
C    DIST AXIS(KM/IN):START OF DIST AXIS(KM):
C
      WRITE(6,63)
   63 FORMAT('NOW TYPE IN AXES INFORMATION')
      READ(1,30) B,C,D,E,F,G
      WRITE(6,30) B,C,D,E,F,G
   30 FORMAT(6(F5.1,1X))
C
C    IF 10KM/IN IS USED SCALE DOWN NUMBERS ON PLOT
C
      IF (F.LE.10.0) GOTO 7
      Q=1.0
      P=-0.1
      Z=0.3
      GOTO 6
    7 Q=2.0
      P=-0.2
      Z=0.6
    6 R=E/F
      H=B/C
      S=1/(C*50.)
      IF (H.LE.9.5) GOTO 33
      WRITE(6,32)
   32 FORMAT('TIME AXIS TOO LONG FOR 11IN PLOTTER')
   33 CALL PLTYMX(R+4.0)
      CALL PSYMB(R+2.0,H/2,-Q/2.,STAT,90.0,8)
      CALL PAXIS(1.0,1.0,13HT-DELTA/6 SEC,13,H,90.0,D,C,Q)
      CALL PAXIS(1.0+R,1.0,13HT-DELTA/6 SEC,-13,H,90.0,D,C,Q)
      CALL PAXIS(1.0+R,1.0,11HDISTANCE KM,11,R,180.0,G,F,Q)
      CALL PAXIS(1.0+R,1.0+H,11HDISTANCE KM,-11,R,180.0,G,F,Q)
C
C    CONTROL DATA IS READ FROM 2 FILES-ONE LINE OF EACH FOR EACH RECORD
C
      WRITE(6,76)
   76 FORMAT('TYPE 01 IF DELAY TIMES ARE TO BE SUBTRACTED')
```

```
      READ(1,75) IFLAG
      WRITE(6,75) IFLAG
   75 FORMAT(1X,I2)
   31 READ(2,20,END=19) ANCM,J,NCLS,DT,DELTA
   20 FORMAT(A3,1X,I1,1X,I5,F5.2,1X,F6.2)
      IF(IFLAG.NE.1) GOTO 77
      NCLS=NCLS+(DT*50)
   77 IF(J.EQ.1) GOTO 21
      IF(J.EQ.6) GOTO 21
      IF(J.EQ.2) GOTO 24
      IF(J.EQ.7) GOTO 24
      READ(3,40) L
   40 FORMAT(28X,I2)
      GOTO 23
   21 READ(3,22) L
   22 FORMAT(6X,I2)
      GOTO 23
   24 READ(3,26) L
   26 FORMAT(17X,I2)
C
C  IF FILTERED CHANNELS ARE TO BE PLOTTED MULTIPLY BY 2
C
      IF(J.EQ.1) GOTO 23
      IF(J.EQ.2) GOTO 23
      IF(J.EQ.3) GOTO 23
      Z=Z*2.
   23 NOSAM=1
      NBLK=0
C
C  THIS SECTION WINDS TAPE ON TO NEXT FILE IF DISTANCE IS
C  TOO LARGE OR SMALL TO FIT ON PLOT OR IF CHANNEL 9 IS SPECIFIED
C
      IF (J.EQ.9) GOTO 36
      IF (DELTA-G.LT.0.0) GOTO 36
      IF (E+G-DELTA.LT.0.0) GOTO 36
      GOTO 13
   36 CALL CNTRL('FSF',LEN,5)
      GOTO 31
C
C  FOR EACH BLOCK EVERY SAMPLE IS READ INTO JIM(I)
C  DEPENDING ON THE DATA CHANNEL REQUIRED SELECTED SAMPLES ARE
C  TRANSFERRED FROM JIM(I) TO ISAM(I)
C
   13 READ(5,50,END=3)(JIM(I),I=1,256)
   50 FORMAT (128A2/,128A2)
C
C  THE FIRST 41 SAMPLES OF A RECORD ARE TAPE HEADER INFO AND ARE IGNORE
C  THE FIRST SAMPLE OF THE FIRST CHANNEL IS IN POSITION 42 ON TAPE
C  THE LAST SAMPLE OF THE EIGHTH CHANNEL WHICH IS EXPECTED TO APPEAR
C  AS THE LAST SAMPLE OF A BLOCK APPEARS AS THE FIRST SAMPLE ON THE NEX
C  BLOCK HENCE,FOR BLOCKS OTHER THAN THE FIRST,THE FIRST SAMPLE OF THE
C  FIRST CHANNEL APPEARS IN POSITION 2 ET CETERA
C  THIS IS THE REASON FOR THE COMPLEXITY OF THE FOLLOWING STATEMENTS
C
      NBLK=NBLK+1
      IF (J.NE.8) GOTO 91
      IF (NBLK.EQ.1) GOTO 25
      DO 14 I=1,255,8
      ISAM(NOSAM)=JIM(I)
      NOSAM=NOSAM+1
```

```
      14 CONTINUE
         GOTO 13
      25 DO 92 I=42,242,8
         ISAM(NOSAM)=JIM(I+J-1)
         NOSAM=NOSAM+1
      92 CONTINUE
         GOTO 13
      51 K=2
         IF(NBLK.EQ.1) K=42
      41 DO 12 I=K,256,8
         ISAM(NOSAM)=JIM(I+J-1)
         NOSAM=NOSAM+1
      12 CONTINUE
         GOTO 13
C
C   THIS SECTION CALCULATES THE D.C. OFFSET ON EACH RECORD
C
       3 N=0
         DO 15 M=1,150
      15 N=N+ISAM(M)
         N=N/150
C
C   THE SHOT NUMBER AND THE DATA CHANNEL USED ARE PLOTTED
C
         CALL PSYMB(1.0+R-(DELTA-G)/F,1.1,P,ANCM,90.0,3)
         CALL PNUMBR(1.0+R-(DELTA-G)/F,1.7,P,J,90.0,'I1*')
         CALL PENUP(1.0+R-(DELTA-G)/F,1.0)
C
C   THE X AND Y VALUES FOR THE PLOT ARE NOW FORMED
C   X VALUES ARE FORMED FROM ISAM. Y VALUES ARE CALCULATED USING NOLS
C
         FMUL=2.**(9-L)*DELTA/70.
         DELTA=P-(DELTA-G)/F
         DO 17 I=1,NOSAM
         ISAM(I)=ISAM(I)-N
         ISAM(I)=ISAM(I)*FMUL
         X=DELTA+Z*ISAM(I)/1000
         Y=-D/C+(I-NOLS)*S
         IF (Y.LE.0.0) GOTO 17
         X=X+1.0
         Y=Y+1.0
         IF (I.EQ.1) CALL PENUP(1.0+DELTA,1.0)
         IF (I.EQ.1) CALL PENDN(1.0+DELTA,Y)
         IF (Y.GE.H+1.0) GOTO 88
         CALL PENDN(X,Y)
      17 CONTINUE
      88 WRITE(6,60) ANCM
      60 FORMAT('THE SHOT',1X,A3,1X,'HAS BEEN PLOTTED')
         GOTO 31
      19 CALL PLTEND
         STOP
         END
END OF FILE
```

```
NO STATEMENTS FLAGGED IN THE ABOVE COMPILATIONS.
EXECUTION TERMINATED


$R -LOAD#+ PLOTSYS 5=*T* 9=-PLOT 2=GS4(1,P) 3=C(147)
EXECUTION BEGINS
TYPE IN PLOTTER SIZE-11IN OR 30IN
11
TYPE IN STATION NAME
L.WILSH
NOW TYPE IN AXES INFORMATION
16.0   2.0  -4.0  70.0   5.0  20.0


PDS: PLOT DESCRIPTION GENERATION BEGINS ***
TYPE 01 IF DELAY TIMES ARE TO BE SUBTRACTED
 0
THE SHOT G7  HAS BEEN PLOTTED
THE SHOT G8  HAS BEEN PLOTTED
THE SHOT G9  HAS BEEN PLOTTED
THE SHOT G10 HAS BEEN PLOTTED
THE SHOT G11 HAS BEEN PLOTTED
THE SHOT G12 HAS BEEN PLOTTED
THE SHOT G13 HAS BEEN PLOTTED
THE SHOT G14 HAS BEEN PLOTTED

 STOP      0
EXECUTION TERMINATED


$R *DURPLOT 1=-PLOT
******************************************************************************
*  NEW VERSION (07 FEB 77) ERROR REPORTS TO GAVIN EADIE (DURHAM SYSTEMS)  *
******************************************************************************
EXECUTION BEGINS


PDS: PLOT DESCRIPTION GENERATION BEGINS ***

GRAPHICS OUTPUT FOR JOB GPM9 ON APR 19, 1977 AT 18:12:13
OUTPUT DESTINED FOR THE  I.B.M. PLOTTER


*DURPLOT STATISTICS SUMMARY
       1 FRAME(S) GENERATED
     218 CARD RECORDS USED
    1950 X-MAX PLOTTER CO-ORDS
     986 Y-MAX PLOTTER CO-ORDS
    14.5 MINUTES ( 2.6% UP/DOWN)



$SET CPCUTF=DURH
$CP -PLOT# TO *PUNCH*
EXECUTION TERMINATED
$SIG $
TOC0      RELEASED.
```

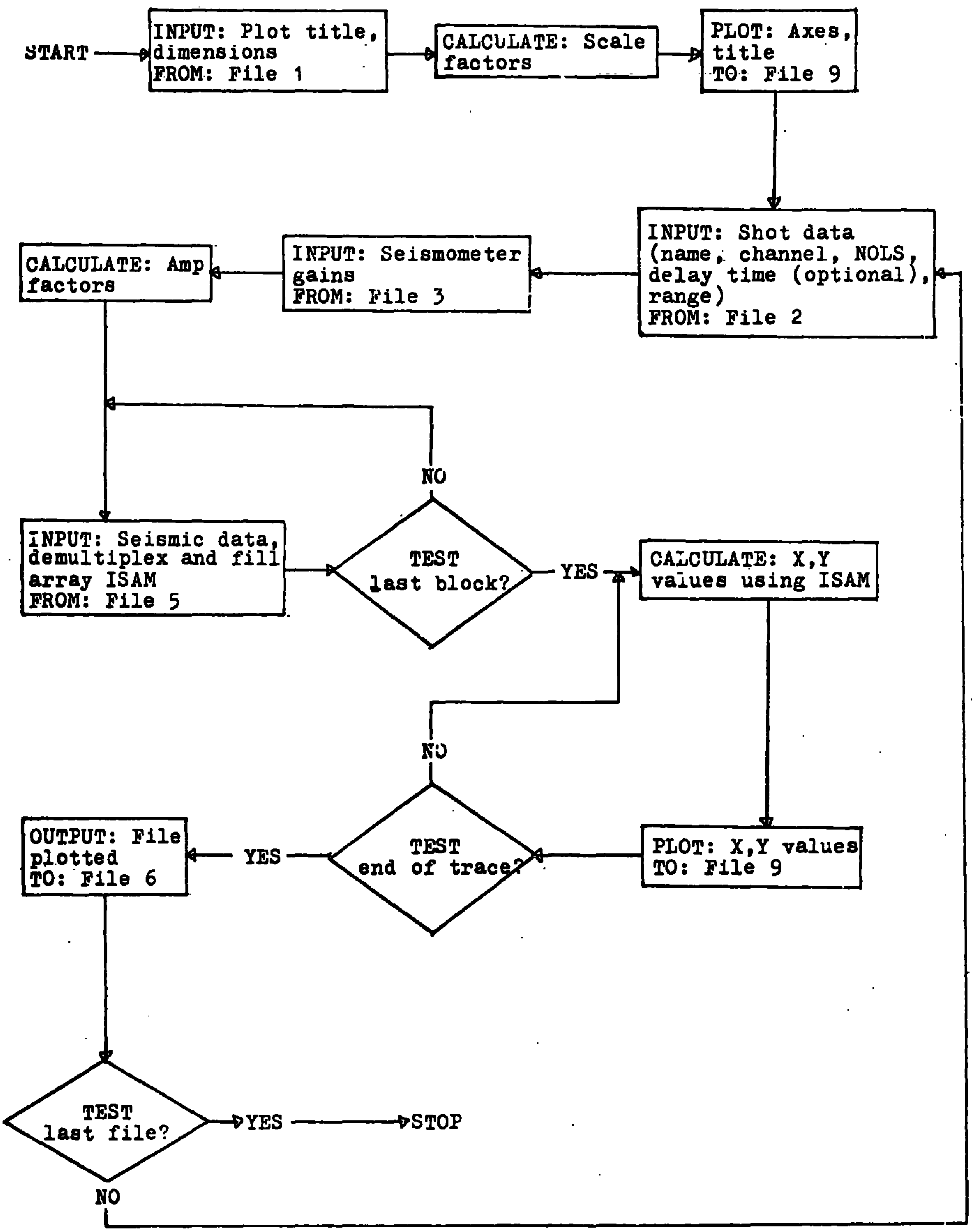

Figure C.1 Flow-diagram for program FPLOT.

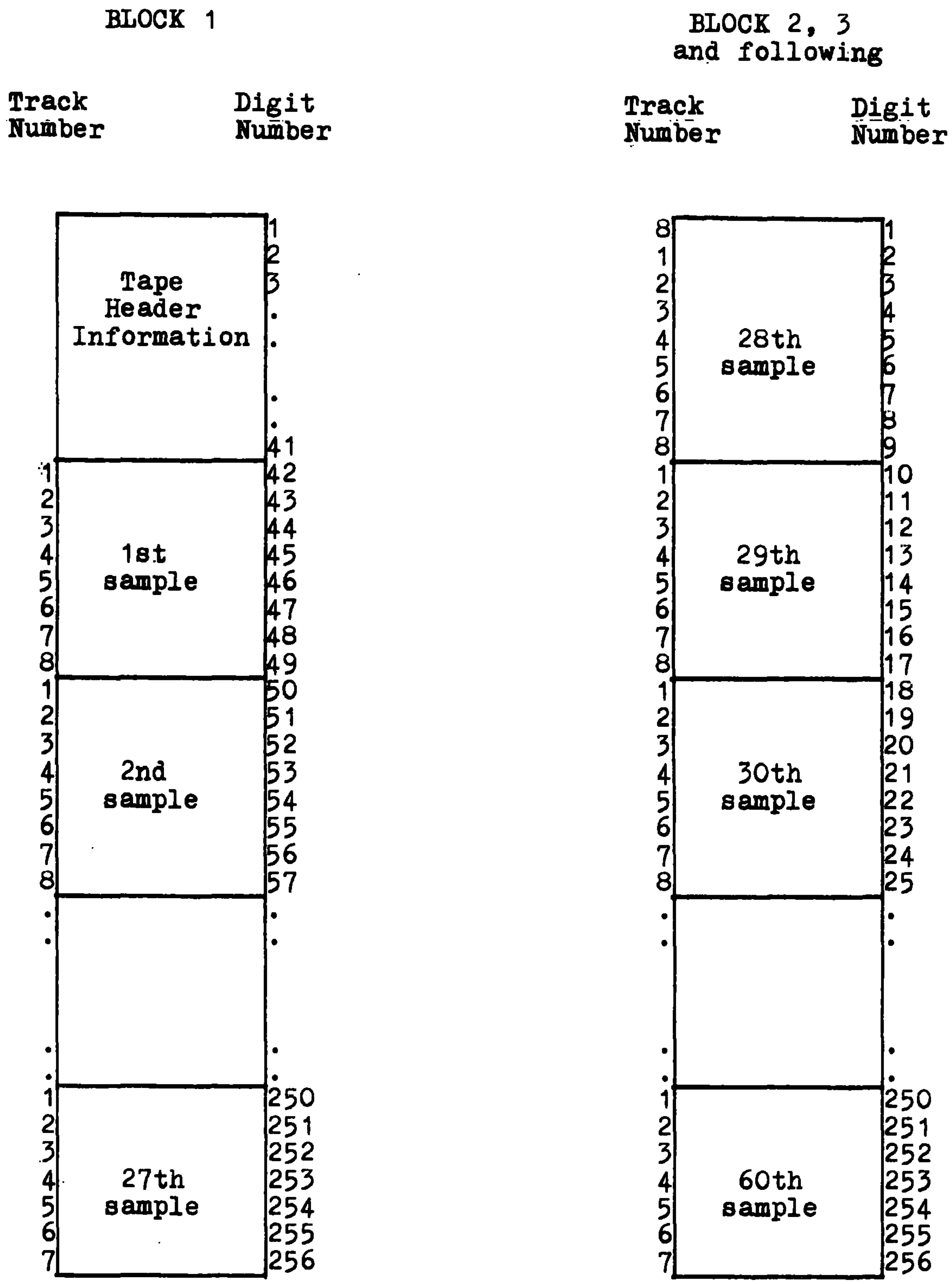

Figure C.2 Format of <u>Modular 1</u> magnetic tape files.

Program PLUSMIN

This program is written in FORTRAN IV and contains comment cards. Refractions from a single layer recorded at two ends of a line are used to form the minus-time curves. Offset of one of the stations from the end of the line is taken into account by calculating a theoretical minus-time curve for a single velocity refractor. The velocity of the theoretical refractor and the reduction velocity can be varied to maximise the fit between observed and calculated curves.

```
$L PLUSMIN
      C      PROGRAM PLUSMIN
      C      THE PROGRAM TAKES TRAVEL-TIMES (TT) FOR A LINE OF SHOTS RECORDED
      C      AT A PAIR OF STATIONS AT OPPOSITE ENDS OF THE SHOT LINE. ONE STATION NEED
      C      NOT BE EXACTLY IN LINE WITH THE SHOT LINE. USING AN INPUT VELOCITY
      C      AND IGNORING DELAY TIMES, THEORETICAL TT ARE CALCULATED FROM THE OBSERVATION
      C      DISTANCES. THE CALC REDUCED MINUS-TIME (RMT) IS COMPARED TO THE
      C      OBS RMT. IN PACTICE THE AVERAGE RMT FOR ALL SHOTS IS SUBTRACTED
      C      FROM EACH SHOT TO TAKE ACCOUNT OF THE CONSTANTS INTRODUCED BY
      C      THE DELAY TIMES.
      C
      C      INPUT NUMBER OF SHOTS IN LINE
      C
             READ(5,30) N
          30 FORMAT(I2)
             DIMENSION TT(8),TT1(8),TT2(8),DIST(8),DIST1(8),DIST2(8),TMI(8),DA(
            18),TAV(8),CTT(8),CTT1(8),CTT2(8),CMI(8),CAV(8),RES(8),RRES(8),PLUS
            2(8)
      C
      C      INPUT TITLE(ARBITRARY CHARACTER STRING)
      C
             READ(5,12) T1,T2,T3,T4,T5,T6,T7,T8,T9,T10
          12 FORMAT(10A4)
             WRITE(6,12) T1,T2,T3,T4,T5,T6,T7,T8,T9,T10
      C
      C      INPUT REFRACTOR VELOCITY
      C
             READ(5,5) V
           5 FORMAT(F5.2)
             WRITE(6,25) V
          25 FORMAT('REFRACTOR VELOCITY=',F5.2)
             WRITE(6,13)
          13 FORMAT(103HSHOT  DISTA   TTA    CTTA  DISTB  TTB    CTTB   MINUS
            1CMINUS  PLUS   2X/V  M-2X/V   -AV    -CAV   RES  )
             SUM=0.0
             CSUM=0.0
      C
      C      READ IN THE TT DATA FOR THE TWO STATIONS FROM TWO FILES
      C
             DO 99 I=1,N
             READ(4,10) DA(I),TT(I),DIST(I)
             READ(7,20) TT1(I),DIST1(I)
          10 FORMAT(26X,A3,22X,F5.2,5X,F6.2)
          20 FORMAT(51X,F5.2,5X,F6.2)
             CTT(I)=DIST(I)/V
             CTT1(I)=DIST1(I)/V
             DIST2(I)=2*DIST(I)/V
             TT2(I)=TT(I)-TT1(I)
             CTT2(I)=CTT(I)-CTT1(I)
             PLUS(I)=TT(I)+TT1(I)
             TMI(I)=TT2(I)-DIST2(I)
             CMI(I)=CTT2(I)-DIST2(I)
             SUM=SUM+TMI(I)
             CSUM=CSUM+CMI(I)
          99 CONTINUE
             SUM=SUM/N
             CSUM=CSUM/N
             SRES=0.0
             DO 101 I=1,N
             TAV(I)=SUM-TMI(I)
             CAV(I)=CSUM-CMI(I)
             RES(I)=TAV(I)-CAV(I)
             RRES(I)=RES(I)**2
             SRES=SRES+RRES(I)
      C
      C      OUTPUT CONSISTS OF: 1 SHOT NUMBER. 2+3+4+5+6+7 FOR BOTH STATIONS -
      C      OBS DIST,OBS TT,OBS DIST/INPUT VEL (=CALC TT). 8 OBS MINUS-TIME.
      C      9 CALC MINUS-TIME. 10 OBS PLUS-TIME. 11 REDUCTION FACTOR. 12 OBS
      C      RMT. 13 CALC RMT. 14 DIFF BETWEEN AVERAGE OBS RMT AND RMT. 14 DIFF
      C      BETWEEN AVERAGE CALC RMT AND RMT. 16 RESIDUAL (DIFF BETWEEN 14 AND 15
      C
             WRITE(6,15) DA(I),DIST(I),TT(I),CTT(I),DIST1(I),TT1(I),CTT1(I),
            1TT2(I),CTT2(I),PLUS(I),DIST2(I),TMI(I),TAV(I),CAV(I),RES(I)
          15 FORMAT(A3,3X,14(F6.2,1X))
         101 CONTINUE
      C
      C      THE SUM OF SQUARED RESIDUALS IS OUTPUT TO SHOW THE FIT BETWEEN
      C      OBS AND CALC FOR THIS VELOCITY
      C
             WRITE(6,16) SRES
          16 FORMAT('SUM OF SQUARED RESIDUALS IS',F6.3)
             STOP
             END
END OF FILE
```

Velocity filtering program

This program is written for the Modular 1 computer in a specialised language called SERAC. It is an adaptation of an original program written by Dr. P.A. Forth. The program takes array records of events recorded on 16-channel magnetic tapes and forms a plot, on an X-Y plotter, of a series of correlator functions for one azimuth and a range of velocities. The correlator function is the smoothed product of the delayed sum of the two arms of the array. Input data is the azimuth and source of the event (number of the tape- or disc-file containing the event) and 16-channel input from tape or disc. The output is the X coordinate of the pen (signal amplitudes), Y coordinate of the pen (time) and a penup/pendown command. About 1,000 samples length of data can be analysed in each plot and the source is usually a disc-file.

```
   90;                                                    Input data
;
SPR;
AZIMUTH;
ASK;
ADD;159;104;
SPR;
FILEN;
ASK;

CALL;73;                                                  Set up pen coordinates

LIN;;14;;                                                 Read and plot
INS;K;159;                                                time-code from
INP;K;;1,2,3,4,5,6,7,8,9;1,2,3,4,5,6,7,8,9;              channel 9
10WEI;9;.04;54;
OUT;;;1,2,3;54,61,62;
ADD;62,63;62;
IGOTO;9;

14SET;61;10;                                              Set up
OUT;;;2;61;                                               range of
16DO;A,B,D;5.0,5.0,1.0;0.5,0.5,0.8;10.0,10.0,9.0;        velocities
INS;C;159;                                                5.0 to
EVA;TBP=0;                                                10.0 km s-1
                                                          steps of
CALL;73;                                                  0.5

20INPUT;C;;1,2,3,4,5,6,7,8,9;                             Form delayed sum
1,2,3,4,5,6,7,8,9;                                        each arm
STACK;1,2,3,4;A;E;50;
STACK;5,6,7,8;B;E;51;
MUL;50,51,50;                                             Weight and
     60,60,51;                                            multiply
     50,51,71;                                            together
IF;C(.71,0)<0;                                            Take square-root
SUB;71;70;71;                                             (including -ve
SQRT;71;71;                                               numbers)
SUB;71;70;10;
GOTO;31;
ELSE;
SQRT;71;10;
31INT;10;.25;52;                                          Smooth, weight
32WEI;52;.1;53;                                           add D.C. level
ADD;53,103;54;                                            and output
ADD;62,63;62;
OUT;0;;1,2,3;54,61,62;
IF;TBP<11;
IGOTO;20;
ELSE;                                                     Lift pen
SET;61;10;
OUT;;;2;61;
SPR;                                                      Output velocity
;                                                         and azimuth to
CPR;100,104;                                              teletype
CONT;
```

Form correlator function and plot

```
CALL;73;

INS;F;159;
EVA;TBP=0;
SET;106;-1.0;
INP;F;;1,2,3,4,5,6,7,8,9;1,2,3,4,5,6,7,8,9;
49WEI;6;.04;53;
ADD;53,106;54;
OUT;;;1,2,3;54,61,62;
ADD;62,63;62;
IF;TBP<10;
IGOTO;48;
ELSE;
SET;61;10;
OUT;;;2;61;
```

Plot one seismic track

Lift pen

```
58DO;H;1.0;0.8;9.0;
```

Set up D.C. levels

```
CALL;73;

EVA;TBP=0;
INP;;;1;99;
ADD;62,63;62;
OUT;;;1,2,3;107,61,62;
IF;TBP<10;
IGOTO;61;
ELSE;
SET;61;10;
OUT;;;2;61;
SPR;
;
CPR;107;
CONT;
```

Plot zero line for each correlator function

Lift pen and output velocity to teletype

```
FGOTO;1;;
```

End

```
73SET;50,51,52,53,60,61,62,63,70;
      0,  0,  0, 0,.1,10,0,.01,0;

DO;90;0;.01;1;
SET;9,12;,;
SET;1,2,3,4,5,6,7,8;,,,,,,,;
INP;;;1;91;
OUT;;;1,2,3,4,5,6;50,51,53,54,61,62;
IGOTO;74;
CONT;

SET;61;-10;
RETURN;
END;
```

Subroutine to reset pen coordinates to zero and give pen time to get to start of trace before output begins again


12°
10°
8°
6°
4°
59°
58°
57°
56°
200m
L11
L10
L9
K14
K12
K11
K9
K7
K6
K5
K4
K3
K1
G28
G25
G20
G15
G14
G11
G10
G7
GS1
GS8
GS9
I3
DU6
DU7
DU8
MD1
DU9
DU10
DU11
H16
H9
DU12
DU13
DU14
DU15
DU16
J1
J2
J3
J4
J5
J7
J8
BLA
DUN
ESK
LAGG
Hebridean Margin Seismic Project 1975
University of Durham
Department of Geological Sciences
RRS Challenger Cruise 11/75
Shot Stations
1500 lbs (Minol)
300 lbs
Recording Station